The phylogenetic position of *Proconsul* and catarrhine ancestral morphotypes.

By

Ashley Bales

A dissertation submitted in partial fulfillment

of the requirements for the degree of

Doctor of Philosophy

Department of Anthropology

New York University

January, 2017

_____

Terry Harrison

ProQuest LLC.
789 East Eisenhower Parkway
P.O. Box 1346
Ann Arbor, MI 48106 – 1346

ACKNOWLEDGEMENTS

Completion of this dissertation would not have been possible without the extensive guidance, feedback and support of my graduate advisor Terry Harrison. I appreciate the time and energy he committed to my graduate career from my first days at NYU through completion of my masters and the early conception of this project. His aid in helping me polish my grant writing abilities allowed me to secure funding and progress through data collection and into the final stages of this process. I would particularly like to thank Terry for his detailed comments and patience as he worked with me in the final construction of this document. I would also like to thank the other members of my committee—Scott Williams, Todd Disotell, Kieran McNulty and Chris Gilbert—for their help and participation. In addition I would like to thank John Flynn and Ward Wheeler at the Richard Gilder Graduate School for additional instruction and guidance that proved essential to the development of the ideas presented in this dissertation.

Many institutions allowed me access to their collections and many individuals helped me navigate these collections. To begin with, I am grateful for access to the *Proconsul* material provided by Kenya's Ministry of Education, Science and Technology and the National Museum of Kenya (KNM). I thank Emma Mbua and Fredrick Kyalo Manthi for their time and assistance in accessing fossil specimens at the National Museum of Kenya. I also thank Brenda Benefit for allowing me access to *Victoriapithecus* material housed at the National Museum of Kenya. Additionally I must thank Keiran McNulty, Susan Cote, Caley Johnson and Ashley Hammond for their companionship and help while working in Kenya and Uganda. I would like to thank Rose Mwanja and Ezra Musiime for their assistance and allowing me to access the *Proconsul* material at the Uganda National Museum. I thank Robert Kruszynski at the Natural History

Museum, London for access to the *Proconsul* type specimens. Thank you to Salvador Moya-Sola for allowing me to access the *Pierolapithecus* material at the Catalan Institute of Paleontology and David Alba and Gretell Garcia for their help while working at the institute. I would also like to thank Loïc Costeur for allowing me to study and Martin Schneider for helping me access the *Oreopithecus* and *Epipliopithecus* material at the Naturhistorisches Museum, Basel. I thank Ursula Göhlich for allowing me access to *Epipliopithecus* fossils at the Naturhistorisches Museum, Vienna and Frank Emmanuel Zachos for access to the primate collections. I am grateful to the Naturhistorisches Museum, Vienna staff for providing housing during my stay. I would also like to thank Gregg Gunnell for allowing me to access the *Aegyptopithecus* material stored at the Duke Lemur Center. I thank Malcolm Harman for providing access to the skeletal collections at the Powell-Cotton Museum. I must particularly thank Frieder Mayer with the additional help of Nora Lange for being so welcoming and allowing me to work in the primate collections at the Humboldt-Universität zu Berlin, Museum für Naturkunde for such an extended period. I am also grateful for the support provided my while living in Berlin by NYU Berlin and my cohort of GRI Berlin students. I thank Caroline Lang for allowing me to access the primate collections at the Zoologische Staatssammlung, Munich. I thank Marcia Ponce De León for allowing me to access the primate collections at the Anthropological Institute and Museum, University of Zurich. I would also like to thank Jacques Cuisin for allowing me to work in the primate collections and Veronique Laborde for allowing me to work in the anthropology collections at the Muséum National d'Histoire Naturelle. Thank you to Darrin Lunde for helping me access the primate collections at the Smithsonian National Museum of Natural History. I must especially thank Eileen Westwig for her help in allowing me

to work in the primate collections at the American Museum of Natural History throughout my undergraduate and graduate career.

This dissertation would not have been possible without funding provided by a number of organizations: L.S.B. Leakey Foundation General Research Grant, The Evolving Earth Foundation, The Explorer's Club Exploration Fund, the NYU GSAS Margaret and Herman Sokol Award, The Ruggles-Gates Fund and the NYU Global Research Initiative.

I would like to thank Bill Kimbel for initially inspiring me to pursue a career in Biological Anthropology and additionally to Kaye Reed, Curtis Marean, Gary Schwartz and Harold Dibble for providing support, advice and opportunities during my undergraduate studies. I could not have completed this dissertation without the friendship and support of my community in New York. In particular, thank you to Isabelle Vea, Alejandro Grajales, John Denton, Ed Stanley, Scott Blumenthal, Su-Jen Roberts, Julia Zichello and Jen Parkinson for providing support through debate and companionship throughout my graduate career. A special thank you to Kieran McNulty for the encouraging and inspiring conversations. I would also like to thank Shara Bailey for establishing a supportive network of NYCEP women.

I am grateful to Andrew Bales for instilling an ambition and stubbornness without which I would not have completed this dissertation and to Jennifer Watkins for a curiosity and appreciation for scholarship without which I never would have begun. Thank you to Mike Rica for giving me tireless patience and encouragement. Finally, thank you to Isabelle Vea, Alejandro Grajales, Su-Jen Roberts, Jon McGough, Matt Jennings and Mike Rica for keeping me smiling and sane throughout this process.

ABSTRACT

There continues to be a lack of agreement concerning the precise phylogenetic placement of *Proconsul* despite a wealth of fossil material and extensive study. The difficulty in resolving the phylogenetic status of this important and well represented Miocene catarrhine is a consequence of its apparent basal position relative to crown catarrhines. This position complicates the inference of character polarities. This dissertation tests three previously proposed hypotheses concerning the phylogenetic position of *Proconsul*: (1) *Proconsul* is a stem catarrhine; (2) *Proconsul* is a stem hominoid; and (3) *Proconsul* is a basal hominid, most closely related to extant great apes and humans. A phylogenetic analysis based on 816 characters drawn from the skull, forelimb, pelvis and foot and sampling a diversity of extant anthropoid taxa, offers compelling support for a hominoid clade that including *Proconsul*. The origination of the hominoid and cercopithecoid lineages is inferred to occur nearly simultaneous with the origination of the *Proconsul* hypodigm. Further exploration of the data, by combining inferred ancestral morphotypes with phenetic visualizations of character evolution, demonstrated that and *Proconsul* is inferred to be phenetically similar to the inferred catarrhine most recent common ancestor (MRCA), however does not approximate the hominoid MRCA as closely as some platyrrhine taxa *Epipliopithecus*. This explains the difficulty in resolving the phylogenetic position of this taxon. While *Proconsul* does possess enough synapomorphies to confidently place it within the hominoid clade, it retains many symplesiomorphies shared with the earliest crown catarrhines that phenetically make it fall morphologically nearer the crown catarrhine ancestral morph than the hominoid ancestral morph, which is inferred to possess more symplesiomorphic similarities to basal catarrhines and platyrrhines. In addition to helping clarify the long-running debate concerning the phylogenetic status of *Proconsul*, these results offer fresh

insights into the early stages of hominoid evolution and demonstrate the importance of comprehensive phylogenetic analyses in helping to resolve the relationships of problematic stem taxa.

TABLE OF CONTENTS

LIST OF FIGURES

LIST OF TABLES

LIST OF APPENDICES

INTRODUCTION

The early Miocene is a crucial time period for understanding the evolutionary events and adaptive changes that led to the divergence of modern catarrhines. This period sees the diversification of the early cercopithecoids and hominoids, with both groups well-documented by a wealth of fossil specimens from Africa (Harrison, 2010, 2013; Jablonski and Frost, 2010). Stem catarrhines, found living contemporaneously with early cercopithecoids and hominoids, exhibit a range of primitive anthropoid features and varying degrees of more derived cercopithecoid and hominoid traits. This has made it challenging for researchers to resolve their phylogenetic relationships and perhaps most significantly problematizes determination of character polarities and the subsequent inference of hominoid synapomorphies. Distinguishing between basal hominoids and stem catarrhines is therefore difficult, given that uncertainty regarding the affinities of the earliest hominoids. Central to resolving this debate is *Proconsul* (here including *Ugandapithecus* and *Ekembo*, see discussion below), which is the best known of the Miocene East African catarrhines. It occupies a key position in the catarrhine fossil record, exhibiting few derived features of crown catarrhines, but clearly more derived than the Oligocene catarrhines. The consensus of the paleoanthropological community has been to identify *Proconsul* as a stem hominoid and subsequently use the suite of morphological features exhibited by *Proconsul* as a model for the earliest hominoids. All studies of hominoid evolution, particularly those focusing on the early stages in the Miocene, therefore begin with *Proconsul* as defining the hominoid archetype or ancestral morphotypic condition. In this way, *Proconsul* roots the hominoid clade and is used as a default outgroup defining character polarities among hominoids. Despite the significance attached to *Proconsul* in catarrhine and hominoid evolution,

the evolutionary relationships of this taxon have not been critically tested by a comprehensive phylogenetic analysis. As a result, conclusions regarding later catarrhine and hominoid evolution may rest on an uncertain interpretive framework.

This dissertation critically reconsiders the phylogenetic status of *Proconsul*—including the newly proposed genera *Ugandapithecus* (Senut, 2000; Pickford et al., 2009) and *Ekembo* (McNulty et al., 2015), regarde here as junior synonyms. Specifically, it tests whether *Proconsul* is a hominoid, a hominid, or a stem catarrhine – the three main competing hypotheses that have been proposed for its relationships (Harrison, 1982, 1987, 2010; Andrews, 1985; Andrews and Martin, 1987; Walker and Teaford, 1989; Rae, 1993, 1997; Begun, 1997; Walker, 1997; McNulty, 2015). In order to test these hypotheses, this dissertation employs the largest data set yet compiled to address questions of catarrhine and hominoid phylogeny, applies the latest systematic methods for handling morphological data and includes a broad range of fossil and extant anthropoids. A number of recent advances in phylogenetic methods have not been widely employed in paleoanthropology and this project is the first to apply them to investigating the phylogenetic relationships of *Proconsul*. As such, this study presents the most comprehensive phylogenetic analysis of this genus and the findings have broad implications for understanding early catarrhine and hominoid evolutionary history.

Methods for analyzing morphological data in systematic analyses are rapidly improving and are expanding the range of evolutionary questions that can be addressed (Egge et al., 2009; Magallon et al., 2010; Wiens, 2010; Lopardo et al., 2011; Pyron et al., 2011; Ronquist et al., 2012; Wood et al., 2013; Gavruyshkina et al., 2014; Arcila et al., 2015; Zhang et al., 2015). In addition to providing the basis for inferring cladistic relationships, morphological data can be combined with molecular clock estimates to investigate the adaptive divergence between taxa

and their rates of morphological evolution (Magallon et al., 2010; Pyron et al., 2011; Ronquist et al., 2012). By adding inferred ancestral morphotypes (Pagel, 1997, 1999) to the best-supported phylogenies, one can infer how phenetically similar or divergent taxa are compared to the ancestral morphotypes of the major catarrhine clades. This offers insight into the broader evolutionary scenarios deduced from placement of individual taxa and clades, including morphological differences between ancestral morphotypes and rates of evolutionary change. In particular, it documents complex evolutionary pathways involving character reversals and homoplasy; phenomena known to be common in catarrhine and hominoid evolution (Harrison, 1993; Pilbeam, 1996; Collard and Wood, 2001; Lycett and Collard, 2005).

The goal of this dissertation is to evaluate the phylogenetic position of *Proconsul* and to understand its significance in the broader picture of catarrhine evolutionary history. I attempt to achieve this goal first by sampling morphology across the cranium, pelvis, forelimb and foot. Comprehensive character sampling for included regions was prioritized in order to minimize bias. While this strategy limited the number of regions that could be practically included in the analysis, regions were chosen in order to cover multiple morphological complexes across the skeleton. A preliminary analysis was conducted summarizing the data set by portraying the phenetic distribution of variation among taxa (Chapter 3). I next test the three evolutionary hypotheses outlined above that have been proposed for the phylogenetic placement of *Proconsul* and infer rates of morphological change in catarrhine evolution (chapter 4). This section applies the phylogenetic methods that are the focus of this dissertation and the primary means of inferring the phylogenetic position of *Proconsul*. The final analysis (chapter 5) further explores the data set, inferring ancestral morphotypes given that each hypothesis, and describing three distinct evolutionary scenarios. These scenarios expand on the results of the phylogenetic

analysis presented in the previous chapter, describing the broader implications of each hypothesis. Finally, given that the results of the phylogenetic analyses and subsequent exploration of ancestral morphotypes, I assess whether a single hypothesis is best supported. The phylogenetic analyses will determine whether the available data are sufficient to confidently identify a single preferred hypothesis, while the final set of analyses will allow for a more detailed consideration of synapomorphic morphology and evolutionary implications of results.

CHAPTER 1: Phylogenetic relationships of *Proconsul*

1.1 MIOCENE CATARRHINES

The Miocene fossil record holds the key to understanding the early evolution of catarrhines. From among a diversity of stem catarrhines in Africa, the two crown clades emerged during the late Oligocene: cercopithecoids and hominoids (Szalay and Delson, 1979; Bernor, 1983; Andrews et al., 1996; Gebo et al., 1997; Harrison and Gu, 1999; MacLatchy, 2004; Harrison, 2005, 2010; Seiffert, 2007; Nakatsukasa, 2008; Jablonski and Frost, 2010; Stevens et al., 2013). Distinguishing members of the extant catarrhine superfamilies morphologically is straightforward. Hominoids (apes and humans) are relatively large bodied tail-less primates with bunodont cheek teeth, 5-cusped lower molars, upper molars with a crista obliqua, a reduction in the size of the m^3, an increase in size of the incisors relative to the molars, large brains, and postcranial adaptations for orthogrady, forelimb suspension and vertical climbing, with a broad thorax and a shortened thoraco-lumbar region (Schultz, 1930, 1936, 1938, 1960, 1961, 1969; Schultz and Straus, 1945; Evans and Krahl, 1945; Le Gros Clark, 1959; Napier and Davis, 1959; Ashton and Oxnard, 1963, 1964; Straus, 1963; Lewis, 1965, 1969, 1971, 1974; Lewis et al., 1970; Ankel, 1972; Groves, 1972; Corruccini, 1975, 1977, 1978; Corruccini et al.. 1975, 1976; Delson and Andrews, 1975; Rose, 1975, 1983; Andrews and Groves, 1975; Cartmill and Milton, 1977; Harrison, 1982, 1987; Andrews, 1985). Cercopithecoids (Old World monkeys) are dedicated pronograde quadrupeds with tails (at least primitively), elongate bilophodont upper and lower molars, and modification of the joints of the appendicular limbs to emphasize movements in the parasagittal plane (Gregory, 1920; Wood-Jones, 1929; Le Gros Clark, 1934; Napier and Davis, 1959; Jolly, 1967, 1972; Delson, 1975;

Szalay and Delson 1979; Harrison, 1982, 1987; Fleagle, 1983; Rose, 1983; Strasser and Delson, 1987; Gebo, 1993; Miller et al., 2009; Jablonski and Frost, 2010). The detailed list of cranio-dental and postcranial autapomorphies distinguishing these superfamilies is extensive (Schultz, 1930, 1936; Napier and Napier, 1967; Rose, 1973, 1987, 1994; Tuttle and Basmajian, 1974; Washburn and Moore, 1974; Andrews and Groves, 1975; Benton, 1976; Tuttle, 1977; Szalay and Delson, 1979; Rollinson and Martin, 1981; Walker and Pickford, 1983; Cant, 1987; Gebo, 1989; Lewis, 1989; Ward et al., 1993; Ward, 2007). Historically, researchers assumed, invoking an imperfect *scala naturae* paradigm, that cercopithecoids were more primitive than hominoids (Le Gros Clark, 1959; Delson and Andrews, 1975; Corruccini et al., 1976; Andrews, 1981; Pickford, 1982; Temerin and Cant, 1983). However, the fossil record offered little or no support for cercopithecoid-like features among stem catarrhines (Szalay and Delson, 1979; Fleagle and Kay, 1983; Gebo, 1993; Rose, 1994; Leakey et al., 2003; Ward, 2007; Jablonski and Frost, 2010) and in many respects Old World monkeys represent a highly derived clade (Gregory, 1920; Wood-Jones, 1929; Le Gros Clark, 1934; Von Koenigswald, 1968, 1969; Corruccini et al., 1976; Szalay and Delson, 1979; Rose, 1983; Strasser and Delson, 1987; Gebo, 1989; Jablonski and Frost, 2010).

As catarrhine fossils were discovered, researchers relied heavily on dental characters to place taxa either within Hominoidea or Cercopithecoidea, resulting in many 'dental apes' being placed within Hominoidea, often linked to specific extant lineages (Hofmann, 1893; Keith, 1915; Pilgrim, 1915; Schlosser and von Zittel, 1923; Gregory and Hellman, 1926; Hopwood, 1933; Gregory et al., 1934, 1938; Le Gros Clark, 1950; Leakey, 1951; Hürzeler, 1954; Zapfe, 1960; Napier and Davis, 1959; Simons and Pilbeam, 1965; Simons, 1965, 1967, 1972; Walker and Rose, 1968; Pilbeam, 1969, 1972; Simons and Fleagle, 1973; Corruccini et al., 1976). Early

catarrhine taxa, including the pliopithecoids and propliopithecoid*s,* with their mix of primitive anthropoid cranial (Hürzeler, 1954; Zapfe, 1960; Delson and Andrews, 1975; Szalay and Delson, 1979; Kay et al., 1981; Simons, 1984, 1985, 1987; Harrison, 1987) and postcranial characters (Le Gros Clark and Leakey, 1951; Napier and Davis, 1959; Napier, 1964, 1967; Preuschoft, 1973; Tuttle, 1967) all with dental similarities to extant apes (Pilgrim, 1915; Hopwood, 1933; Gregory, 1922; Gregory and Hellman, 1926; Gregory et al., 1938) challenged a simple dichotomous portrayal of catarrhine evolution. As researchers learned more about the distribution of variation, they were able to move beyond phenetic comparisons and make inferences concerning plesiomorphic versus apomorphic character states. This led to the recognition that many features, particularly in the dentition, that phenetically linked fossils with extant hominoids were in fact catarrhine symplesiomorphies and that the cercopithecoid dentition was highly derived (Gregory, 1922; Von Koenigswald, 1968, 1969; Szalay and Delson, 1979). The term 'dental apes' was coined referring to the taxa that possessed many primitive features in their cranium and postcranial morphology, but looked ape-like based on a suite of dental features including: bunodont dentition, 4-cusped upper molars possessing a crista obliqua, 5-cusped lower molars possessing a hypoconulid and a 'Y' shaped fissure pattern (Gregory, 1922; Von Koenigswald, 1968, 1969). Some researchers considered Hominoidea a paraphyletic 'wastebasket' taxon (Corruccini et al., 1976; Fleagle and Kay, 1983) that included all non-cercopithecoid catarrhines (i.e., stem catarrhines + hominoids). Other researchers accepted this pattern, referring all catarrhines to Hominoidea, with cercopithecoids nested within hominoids (Simons, 1965; Fleagle and Kay, 1983).

This gradistic interpretation led to retention of the dichotomous terminology of the crown catarrhines. In addition to recognizing that the hominoid dentition was more primitive and the

cercopithecoid dentition more derived, researchers also identified morphology of the ectotympanic (Cartmill et al., 1981; Harrison, 1987, 2013) distinguishing crown from stem catarrhine taxa, and further identified morphology in the cercopithecoid postcranium distinguishing cercopithecoids from stem catarrhines (Le Gros Clark, 1934; Szalay and Delson, 1979; Fleagle and Kay, 1983; Gebo, 1993; Rose, 1994; Leakey et al., 2003; Ward, 2007; Jablonski and Frost, 2010). The form of the ectotympanic clearly distinguishes all crown catarrhines from more basal taxa. Crown catarrhines all possess a fully enclosed tubular ectotympanic, differing from the annular form in platyrrhines and strepsirrhines (Cartmill et al., 1981; Harrison, 1987, 2013). Stem catarrhines are variable in expression of this feature, with *Aegyptopithecus* and other propliopithecoids possessing the primitive annular form (Cartmill et al., 1981; Fleagle and Kay 1987; Harrison 1987, 2013; Seiffert et al. 2010). *Epipliopithecus* and *Pliobates* both possess a partially enclosed bony tube (Harrison, 1987, 2013; Alba, et al., 2015). *Proconsul*, however, unambiguously groups with crown catarrhines for this feature, possessing a fully enclosed bony tube (Le Gros Clark and Leakey, 1951; Napier and Davis, 1959; Harrison, 2010).

In the postcranial skeleton, the forelimb in particular has played a central role in resolving relationships between stem and crown catarrhines. Two characters unambiguously distinguish early stem catarrhines from later catarrhines: presence of an entepicondylar foramen and an epitrochlear fossa in the distal humerus. The entepicondylar foramen is a primitive eutherian character shared by many strepsirrhines, fossil anthropoids and ceboids, but is lost in all crown catarrhines (Fleagle et al., 1982). The dorsal epitrochlear fossa is also present among many stem catarrhines and platyrrhines, but is absent in cercopithecoids and hominoids (Conroy,

1976; Fleagle and Kay, 1987; Harrison, 1987, 2013). *Proconsul,* similar to the crown catarrhines, lacks both of these features (Napier and Davis, 1959; Harrison, 1987, 2010).

Other features of the postcranial skeleton more directly linked to locomotor behaviors portray a more complicated evolutionary scenario. While hominoids present the most mobile shoulder, elbow and wrist joints—with the ability to fully extend the arm above the head at the shoulder, full extension at the elbow, abduction/adduction at the wrist, and a greater ability to pronate/supinate the hand and radius around the ulna (Schultz, 1930, 1969; Szalay and Delson, 1979; Fleagle, 1983; Rose, 1983, 1996; Ward, 2007)—cercopithecoids in general have a much more limited range of joint motion (to a lesser degree among colobines than in cercopithecines), holding the forelimb in a habitually flexed position at the elbow, limiting extension of the forelimb to ~90^0 at the shoulder and a stable wrist (Jolly, 1967; Delson, 1975; Rose, 1983, 1996; Jablonski and Frost, 2010). Platyrrhines and early catarrhines exhibit a range of variation from a limited range of motion to those , such as *Ateles* and *Epipliopithecus*, approaching the hominoid condition (Rose, 1983, 1996; Larson, 1998; Ward, 2007; Youlatos and Meldrum, 2011). In the hind limb, there is a similar morphology, with hominoids exhibiting a mobile hip and ankle—with greater range of extension at the hip and eversion at the ankle—associated with the ability to position the lower limb and foot around arboreal and particularly vertical supports (Rose, 1983, 1996; MacLatchy et al., 2000; Ward, 2007).

The *Epipliopithecus* skeleton exhibits mobile shoulder, hip and ankle joints, similar to the atelids and likely allowing for climbing, bridging and suspension in their locomotor repertoire (Zapfe, 1960; Ward, 2007). The presence of this morphology in stem catarrhines—with atelids also converging on this morphology—breaks down a dichotomous or gradistic interpretation of these features. Additionally, fossil hominoids exhibit adaptation to a range of locomotor modes,

not exclusively the derived climbing and suspensory adaptations indicative of extant hominoids (see chapter 2 discussion), but also variably expressing traits characteristic of arboreal quadrupeds (Sarmiento 1987; Rose, 1988, 1997; Pilbeam et al. 1990; Moyà-Solà and Kohler 1995; Begun et al. 1997; Richmond et al., 1998; Finarelli and Clyde 2004; Moyà-Solà et al. 2004; Larson, 2007; Ward, 2007; Alba et al., 2010, 2011, 2013; Rein et al., 2011).

The breakdown of this dichotomous framework has allowed many catarrhine fossils to be more confidently placed within the catarrhine phylogenetic tree (as with the pliopithecoids and propliopithecoids). Where uncertainty remains, it may be due to the difficulty in distinguishing between stem anthropoids and stem catarrhines (Simons, 1962; Szalay, 1970; Gingerich, 1977; Fleagle and Kay 1987; Harrison 1987, 2013; Rasmussen and Simons, 1988; Simons, 1992, 2001; Simons and Rasmussen, 1996; Kay et al., 1997, 2004; Ross et al., 1998; Beard, 2002; Rasmussen, 2002; Seiffert et al., 2005, 2010) and between stem catarrhines and stem hominoids (Andrews, 1978, 1985, 1992; Rose, 1983, 1992, 1997; Andrews and Martin, 1987; Begun et al., 1997, 2001; Kelley, 1997; Rae, 1997, 1999; Rose, 1997; Walker, 1997; Ward, 1997; Ward et al., 1997; Fleagle, 1998; Singleton, 2000; Harrison and Gu, 1999; Harrison 2002, 2010, 2013; Ward and Duren, 2002; Pickford and Kunimatsu, 2005). The following chapter will discuss the morphology used to define catarrhine clades, with particular emphasis placed on characters used to distinguish stem catarrhines and hominoids. Much of the difficulty in identifying catthine synapomorphies depends on how researchers parse out postcranial variation that may distinguish between the derived locomotor modes of cercopithecoids and hominoids versus a more primitive and generalized pattern. As discussed above, inferring primitive adaptations to a range of locomotor styles, versus derived adaptations to hominoid-like climbing and suspension is not

straight-forward (Corruccini et al., 1976; Gebo, 1989; Rose, 1994, 1996; McCrossin et al., 1998; MacLatchy et al., 2000; Ward, 2007; Nakatsukasa, 2012).

1.2 SUMMARY OF ALTERNATE HYPOTHESES

Here I outline the three hypotheses being tested in this dissertation. In order to fully explore each hypothesis I begin by outlining the set of morphological characters that has been used to support each. Only morphological characters drawn from the regions included in this thesis (i.e., cranium, forelimb, pelvis, pes) will be covered. I conclude each overview with a discussion of the broader evolutionary implications for the hypothesis across catarrhine evolution, predicting ancestral morphotypes based on this review of the evidence.

1.2.1 H1: *Proconsul* is a stem catarrhine

In order to establish that *Proconsul* is a stem catarrhine, a member of a lineage emerging before the origination of the cercopithecoid and hominoid clades, there must be synapomorphies linking cercopithecoids and hominoids to the exclusion of *Proconsul,* with *Proconsul* also expressing catarrhine synapomorphies shared by both crown and stem catarrhines. Given that both cercopithecoids and hominoids are highly distinctive relative to each other (Szalay and Delson, 1979; Ward, 2007; Harrison, 2010; Jablonski and Frost, 2010; Seiffert et al., 2010), few synapomorphies have been identified to support this hypothesis. The hominoid synapomorphies that are absent in *Proconsul* are inconsequential to supporting this hypothesis, as they are not able to reject the hypothesis that these evolved prior to the appearance of the early basal hominoids but after *Proconsul* diverged. Debate has been more focused on reevaluating synapomorphies proposed to support alternate hypotheses and examining the ways in which

crown hominoids are similar to the primitive catarrhine morphotype. There may be few characters to support this hypothesis, even if it is the biological reality.

The presence of ischial callosities in hylobatids and cercopithecoids (Pocock, 1925; Schultz, 1936; Miller, 1945; Wilson, 1970; Rose, 1974; Ward et al., 1989; Walker and Teaford, 1989; McCrossin and Benefit, 1992) may be the best evidence for a synapomorphy supporting this hypothesis. It leads to the argument that this feature evolved in the crown catarrhine ancestor prior to the diversification of cercopithecoids and hominoids. The absence of this feature in hominids has led to inference that this feature was lost in the large bodied apes (Washburn, 1957; Delson and Andrews, 1975; Walker and Teaford, 1989; Ward et al., 1993; Harrison and Sanders, 1999). In this scenario, the absence of ischial callosities in *Proconsul* (Ward et al., 1993) is inferred to indicate the *Proconsul* lineage evolved prior to the appearance of ischial callosities in cercopithecoids and hylobatids (Harrison and Sanders, 1999). This could also, however, support H3, linking *Proconsul* with the hominids. It has further been suggested to be independently derived in hylobatids and cercopithecids (Groves, 1968; Ward et al., 1989; McCrossin and Benefit, 1992).

1.2.1.1 H1 evolutionary implications

Overall, this hypothesis infers that *Proconsul* is primitive, with a monkey-like skeleton and fits well into an evolutionary scenario in which basal catarrhines exhibit a generalized, arboreal quadrupedal skeletal morphology (Le Gros Clark and Leakey, 1951; Napier and Davis, 1959; Andrews, 1978; Walker and Pickford, 1983; Andrews and Martin, 1987; Harrison, 1987; Ward et al., 1993), specialized for varying degrees of climbing and bridging behaviors (Cartmill and Milton, 1977; Rose, 1987, 1994, 1996; Ward et al., 1991; Nakatsukasa et al., 2003; Daver and Nakatsukasa, 2015). This pattern explains many of the similarities between *Proconsul* and extant

hominoids as compared to the more specialized cercopithecoid skeleton. In this scenario, the crown catarrhine ancestral morphotype would be expected to be similar to *Proconsul* (Harrison, 1987), with the addition of limited crown catarrhine synapomorphies, such as possession of ischial callosities. The hominoid morphotype would appear either quite close to this crown catarrhine morphotype or be closer to the derived morphology of hominoids or even hominids, given that hylobatids likely represent a highly specialized lineage (Cartmill, 1985; Shea, 1986; Gebo, 1997; Young, 2003; Young and MacLatchy, 2004).

1.2.2 H2: *Proconsul* is a stem hominoid

Current consensus supports placing *Proconsul* as an early member of the Hominoidea (Andrews, 1985; Kelley and Pilbeam, 1986; Andrews and Martin, 1987; Begun, 1997; McNulty et al., 2015) and this hypothesis has been supported with many purported synapomorphies that *Proconsul* shares with hominoids. This character list has been reevaluated with the understanding that in order to support this hypothesis characters must be confidently established as derived for hominoids. Difficulties in distinguishing hominoid synapomorphies from catarrhine symplesiomorphies is a source of confusion in inferring the phylogenetic position of *Proconsul*. Additionally, many characters discussed as supporting the position of *Proconsul* as a stem hominoid are the same characters that are similar between *Proconsul* and the hominids, working from the assumption that hylobatids do not express these traits due to being a highly derived lineage within Hominoidea. These features will be discussed under H3.

Few cranial characters have been advanced in support of this hypothesis. Andrews (1985) identified two cranial characters relevant to this study: a frontal bone wide at bregma and narrowing anteriorly forming a posteriorly convex frontal-parietal suture; and, a well-developed maxillary jugum. Harrison (1987) identified the frontal morphology as present in both

cercopithecoids and hominids suggesting it may be derived for catarrhines, though hylobatids retain the primitive condition. *Proconsul* and hominids express a higher degree of the posterior convexity described by this morphology (Harrison, 1987), however, possibly indicating a phylogenetically informative character polarity. The development of the maxillary jugum has been used as both a hominoid (Andrews, 1985; Zalmout, 2010) and hominid (Rae, 1999) synapomorphy. As hylobatids lack a well-developed maxillary jugum, it should be more accurately considered a hominid synapomorphy (Harrison, 1987) and is only considered a hominoid synapomorphy under the interpretative framework which excuses hylobatids as a derived lineage within the Hominoidea. Harrison (1987) further argued that the *Proconsul* maxillary jugum appears misleadingly large due to facial lengthening, but in fact, its maxillary jugum is more similar to the jugum of other stem catarrhines and platyrrhines than it is to the derived expression of the hominoids. Rae (1999) described the configuration of the premaxillary-nasal contact as a *Proconsul* + hominoid synapomorphy, indicating that in cercopithecoids the contact extends superiorly to the top of the nasals or even onto the frontal, whereas the hominoid and *Proconsul* premaxilla contacts the nasals inferiorly or not at all, terminating instead at the piriform aperture. Rae (1999) identifies the primitive catarrhine and platyrrhine condition as the premaxilla contacting the nasals near their midpoint. Rae (1999) goes on to suggest that the non-projecting nasals and inter-orbital region of hominoids is derived relative to the condition seen in cercopithecoids, stem catarrhines and platyrrhines, who all exhibit an anterior transverse arch between the orbits at the nasals. *Proconsul* shares a non-projecting morphology with the hominoids.

Postcranially, the forelimb provides the most evidence supporting this hypothesis. In particular, similarities between the *Proconsul* elbow and those of extant hominoids have led

some to suggest that the earliest adaptive changes in the hominoid skeleton occurred in the elbow (Gebo, 1996, 2009; Kelley, 1997; Fleagle, 1998; Larson and Stern, 2006; Nakatsukasa, 2009). Overall, the hominoid wrist allows for axial rotational movement and a range of both abduction and adduction, along with an increased ability to extend and hyperextend at the elbow. Cercopithecoids and platyrrhines on the other hand have a less flexible, more stable wrist, with limited ability to pronate and supinate, as their forelimb is typically carried in a habitually pronated position (Napier and Davis, 1959; O'Connor and Rarey, 1979; Fleagle, 1983; Sarmiento, 1988; Rose, 1988, 1993; McCrossin, 1994; Benefit and McCrossin, 1995; Gebo, 1996; Fleagle, 1998; Larson, 1998, 2006). Platyrrhines, however, practice a type of quadrupedalism distinct from cercopithecoids and express greater axial rotational abilities at the elbow, with elbows pointing more laterally than posteriorly and holding the forelimb in a habitually semi-flexed position (Grand, 1968; Rose, 1992, 1994; Youlatos and Meldrum, 2011).

Proconsul, along with extant apes and many of the middle and late Miocene hominoids, possesses a globular capitulum, lacking the antero-posterior flattening typical of platyrrhines and cercopithecoids and also lacking a proximo-lateral extension forming a tail and increasing the range of rotatory motion at the humero-radial joint (Fleagle, 1983; Rose, 1988, 1993; Rae, 1999; Larson and stern, 2006; Nakatsukasa, 2007). The lateral epicondyle of *Proconsul* and extant hominoids projects laterally beyond the level of the capitulum (Senut, 1989; Rose, 1997). *Proconsul,* similar to the hominoids, possesses a broad trochlea, with well-developed medial and lateral trochlear keels (Napier and Davis, 1959; Andrews, 1985; Harrison, 1987; Rose, 1988; McCrossin, 1994; Benefit and McCrossin, 1995; Walker, 1997; Fleagle, 1998; Larson, 1998, 2006; Rae, 1999; Gebo, 2009). The combination of these traits in hominoids forms the characteristic trochleiform trochlear implicated in maintaining stability during forelimb

pronation and supination necessary for forelimb suspension (Rose, 1988, 1993). In *Proconsul,* the form of the trochlea and medial and lateral keels is intermediate between the cylindrical platyrrhine and spool-shaped hominoid morphs (Harrison, 1987; Rose, 1988, 1994; Zylstra, 1999). The medial keel is intermediate between hominoids and other anthropoids (Harrison, 1987; Zylstra, 1999; Gebo, 2009). Extant hominoids possess a deep and narrow zona conoidea whereas this feature is shallower and wider in cercopithecoids and Oligocene and early Miocene catarrhines (Rose, 1988, 1993). The *Proconsul* zona conoidea is intermediate, though showing greater similarity to the hominoid condition (Fleagle, 1983; Walker, 1997; Rae, 1999; Gebo, 2009). This morphology increases stability at the radio-ulnar joint during pronation and supination (Jenkins, 1973; Sarmiento, 1985; Rose, 1988). Beveling of the radial head has also been related to stability, as it articulates with a deep zona conoidea and is seen in *Proconsul* and extant hominoids (Rose, 1992, 1997; Rae, 1999; Gebo, 2009). Harrison (1987) suggested that both medial and lateral keel development is related to an increase in body size. The well-developed lateral trochlear keel is even more pronounced in *Proconsul* than in hominoids, it being larger than in stem catarrhines and other anthropoids, suggesting a unique morphology that cannot be accommodated in a model of simple linear evolution in which basal taxa would expected to be morphologically intermediate between primitive and derived conditions (Kelley, 1997; Larson and Stern, 2006). This trait may not be homologous in *Proconsul* and extant hominoids or may be an exaptation to the form seen in the later hominoids as it is unlikely *Proconsul* was practicing large amounts of forelimb suspension (Rose, 1988, 1993; Kelley, 1997; Larson and Stern, 2006). A possible explanation may be related to a change in balancing mechanisms for a tail-less above branch arboreal quadruped, in which forelimb pronator and supinator muscles exert force against a stable elbow joint as they work to maintain balance

(Kelley, 1997; Larson and Stern, 2006). Working from the assumption that *Proconsul* is tail-less, others have highlighted the importance of unique adaptations to maintaining balance during arboreal quadrupedal locomotion as being prime drivers of the mix of skeleton adaptations in *Proconsul* (Cartmill and Milton, 1977; Ward et al., 1991; Nakatsukasa et al., 2003, 2007, 2009; Daver, 2015).

The *Proconsul* carpus has been the focus of much discussion, with some researchers recognizing a hominoid-like wrist in the configuration of the carpo-ulnar articulation while others see a more intermediate morphology (Napier and Davis, 1959; Lewis, 1971, 1972, 1989; O'Connor, 1975; Beard et al., 1986; Harrison, 1987; Rose, 1994; Youlatos, 1996; Daver and Nakatsukasa, 2015). In cercopithecoids, the ulna and carpus form a tight articulation with the ulnar styloid contacting the pisiform and triquetral. This articulation limits medio-lateral mobility and ulnar deviation in favor of stability at this weight-bearing joint (Lewis, 1971, 1972, 1974; Schon and Ziemer, 1973; Corruccini et at., 1975, 1976; Morbeck, 1975, 1977; O'Connor, 1975, 1976; Cartmill and Milton, 1977; O'Connor and Rarey, 1979; McHenry and Corruccini, 1983; Lewis, 1989; Sarmiento, 1995, 2002; Youlatos, 1996; Daver and Nakatsukasa, 2015). Hominoids have greatly reduced the ulnar styloid and, subsequently, reduced articulation between the ulna and carpus. Instead of direct contact, an inter-articular meniscus is present between the styloid, pisiform and triquetral. This increases mobility, allowing for ulnar deviation and axial rotation (Lewis, 1965, 1971, 1972, 1974, 1989; Conroy and Fleagle, 1972; O'Connor, 1975; Cartmill and Milton, 1977; Mendel, 1979; Sarmiento, 1987, 1988, 1995, 2002; Youlatos, 1996; Daver and Nakatsukasa, 2015). The degree of isolation between the ulna and carpus as measured by the extensiveness of the facet for the interarticular meniscus varies among hominoids. Hylobatids exhibit the least ulno-carpal contact, resulting in the greatest degree of

mobility, while the knuckle-walking apes must pass compressive force through this joint and as a result have a more extensive facet for the meniscus (Lewis, 1969, 1971; Corruccini, 1978). An additional trait limiting ulnar deviation in the cercopithecoid carpus is a ridge delimiting the facet for the ulnar styloid on the distal articular surface of the pisiform which is lacking in *Proconsul* and extant hominoids (O'Connor, 1975; Beard, 1986; Rae, 1999).

Overall, *Proconsul* possesses an intermediate morphology, lacking the extensive weight-bearing articulation of the cercopithecoids (Lewis, 1971, 1972; Beard, 1986), but with greater contact than is seen in the derived hominoid condition (Napier and Davis, 1959; Morbeck, 1972, 1977a; Schon and Ziemer, 1973; O'Connor, 1976; Cartmill and Milton, 1977; Harrison, 1982; Robertson, 1984; Beard et al., 1986; Beard, 1986, 1993; Harrison, 1987; Sarmiento, 1988, 1995, 2002; Lewis, 1989; Rose, 1994; Youlatos, 1996; Daver and Nakatsukasa, 2015). Generally, the *Proconsul* carpus suggests palmigrade hand postures, most similar to arboreal quadrupeds with a higher degree of mobility than that seen in extant cercopithecoids, but not as mobile as the hominoid condition (Napier and Davis, 1959; Morbeck, 1972, 1975, 1977; Preuschoft, 1973; Schon and Ziemer, 1973; Corruccini et al., 1975; O'Connor, 1976; Harrison, 1982; McHenry and Corruccini, 1983; Robertson, 1984; Jouffroy et al., 1991; Ward, 1993; Rose, 1996; Zylstra, 1999; Richmond and Strait, 2000; Daver and Nakatsukasa, 2015).

In addition to the increased abduction/adduction abilities allowed by the presence of an intraarticular meniscus between the ulna and carpus, the radio-ulnar joint is also separated by an intraarticular meniscus in hominoids. This meniscus allows for a greater degree of rotation of the radius and hand around the ulna and is beneficial for both suspension and vertical climbing (Lewis, 1965, 1969; Sarmiento, 1987, 1988; Daver and Nakatsukasa, 2015). Osteologically this is reflected in a more extensive radio-ulnar articulation among hominoids. Previously

researchers (Harrison, 1987; Walker et al., 1993) inferred *Proconsul* lacked the extensive articulation seen among hominoids, but this conclusion was based primarily on sub-adult material. Daver and Nakatsukasa (2015) reevaluated this morphology with adult material from the Kaswanga Primate Site (KPS) and found *Proconsul* did in fact possess the intraarticular meniscus at the distal radio-ulnar joint characteristic of the hominoids. A final carpal character involves the spiral articulation between the hamate and triquetral. The *Proconsul* hamate possesses a 'spiralized' triquetral facet (Lewis, 1972, 1989; Almecija et al, 2014) that is oriented proximodistally (Beard, 1986; Rae, 1999; Begun, 2004; Kivell, 2007) as it is in the hominoids.

The *Proconsul* hand is characterized by strong grasping abilities—indicated by broad phalangeal shafts, large palmar tubercles on the proximal phalanges, short intermediate phalanges and markings for strong pollical flexors—similar to hominoids (Walker and Pickford, 1983; Begun et al., 1994; Kelley, 1997; Nakatsukasa et al., 1998, 2002, 2003). Palmigrade arboreal quadrupeds, including many platyrrhines and cercopithecoids (Walker and Pickford, 1983; Kelley, 1997; Nakatsukasa et al., 1998, 2002, 2003) and particularly those practicing slow climbing and bridging behaviors (more common among certain platyrrhines) (Cartmill and Milton, 1977; Rose, 1983, 1992, 1996, 1997; Ward et al., 1991; Nakatsukasa et al., 2003; Daver and Nakatsukasa, 2015), also exhibit strong grasping abilities. The first metacarpo-phalangeal joint has been described as saddle shaped and more mobile in hominoids and *Proconsul* (Lewis, 1977; Rae, 1999), though others have described the *Proconsul* joint as being a cylindrical hinge, more similar to the non-catarrhine condition (Napier, 1961, 1962; Day and Napier, 1963). Beard (1984) sees a saddle shaped morph as a common pattern across primates and therefore does not consider this characterization useful for inferring phylogeny, recognizing instead a similarity between *Proconsul,* hominoids and ceboids in the orientation of this joint as distinct from a more

derived cercopithecoid orientation. This is interpreted as an adaptation to compressive forces exerted during pad-to-pad gripping similar to the hominoids (Marzke, 1997; McHenry, 1983; Moyà-Solà, 1999). Begun et al. (1994) also suggested that long thumbs may be a synapomorphy linking *Proconsul* and crown hominoids.

Similar to the hand, the grasping abilities in the foot have been suggested to be synapomorphic for *Proconsul* and extant hominoids (Fleagle, 1983; Langdon, 1976; Preuschoft, 1973; Rose, 1983; Begun et al., 1994). The possession of a long, divergent hallux with powerful hallucal flexors, broad hallucal terminal phalanges and short intermediate phalanges in *Proconsul* all support this hypothesis. Begun et al. (1994) further identified morphology differentiating between manual and pedal phalanges, which foreshadows the differentiation in hominoid hand and foot postures during suspension and slow climbing (Begun et al., 1994). Torsion of the first and second metatarsal heads also is shared between *Proconsul* and the hominoids (Rose, 1993; Kelley, 1997; Ward, 1997). Morphology of the tarsus and particularly mid-tarsal joints have also been implicated as potential synapomorphies supporting this hypothesis (Sarmiento, 1983; Langdon, 1984; Szalay and Langdon, 1986; Rose, 1986; Ward, 1997); but, as this primarily indicates an affinity between *Proconsul* and the hominids it will be discussed under H3. While hominids may retain more of the primitive hominoid condition than hylobatids, synapomorphies linking *Proconsul* to hominids must be first evaluated as supporting the position of *Proconsul* among hominoids.

Proconsul possesses a relatively shallow acetabulum, a feature also present in hominoids that has been related to possessing a greater range of motion at the hip. In extant hominoids, a shallow acetabulum is accompanied by a lunate surface that may be expanded cranially and reduced dorsally, indicating increased cranial loading and reduced dorsal loading (Ward, 1991,

1993; MacLatchy and Bossert, 1996). *Proconsul* does not, however, share this configuration of the lunate surface (Ruff et al., 1989; Ward et al., 1992, 1993; Rose, 1993; MacLatchy and Bossert, 1996). While cercopithecoids are derived in generally having a deeper acetabulum, a shallow acetabulum is likely primitive for anthropoids as it is seen in both platyrrhines and hominoids (Ward et al., 1993). Configuration of the sacro-iliac joint is also similar between *Proconsul* and hominoids (Ward, 1991, 1993; Kelley, 1997). Non-hominoid anthropoids possess a sacro-iliac joint involving only two vertebrae, whereas three are involved in hominoids (Schultz, 1930, 1961, 1969; Ward, 1991). The height of the auricular surface and subsequent height of the sacro-iliac joint above the auricular surface differs between monkeys and hominoids, with *Proconsul* intermediate or hominoid-like (Ward, 1991).

1.2.2.1 H2 evolutionary implications

Proconsul is interpreted as possessing a wrist joint with an intermediate degree of abduction and adduction with a ulno-carpal articulation intermediate between the highly mobile hominoid condition and the more stable cercopithecoid morph (Lewis, 1972; Beard,1986; Daver and Nakatsukasa, 2015) and a hominoid-like ability to pronate-supinate its hand and radius around the ulna (Daver and Nakatsukasa, 2015). It possesses an elbow joint capable of full extension unlike cercopithecoids (Napier and Davis, 1959; Rose, 1983, Walker and Pickford, 1983, 1989; Andrews, 1985; Andrews and Martin, 1987; Gebo et al., 1988; Gebo, 1996, 2009; Kelley, 1997; Walker, 1997; Fleagle, 1998; Larson and Stern, 2006; Nakatsukasa and Kunimatsu, 2009), indicating a move towards incorporating more climbing behaviors resulting in preadaptation of the skeleton to the derived suspensory behaviors expressed in extant hominoids (Le Gros Clark, 1959; Schultz, 1961; Ashton and Oxnard, 1964; Oxnard, 1967, 1969; Groves, 1972; Corruccini, 1975; Ciochon and Corruccini, 1977; Cartmill and Milton, 1977; Larson,

1988; Gebo, 1996; Young, 2003, 2008). *Proconsul* is inferred to closely approximate the basal hominoid morphotype. However, this morphotype appears to be essentially unlike the crown hominoid morphotype (Rose, 1983, 1993; Ward, 1998; Nakatsukasa and Kunimatsu, 2009; Daver and Nakatsukasa, 2015), with many features related to orthograde and suspensory behaviors evolving later in the hominoid lineage (Young and MacLatchy, 2004; Ward, 2007).

1.2.3 H3: *Proconsul* is a basal hominid

This hypothesis has historically been established on many of the same characters used to support the position of *Proconsul* within Hominoidea. However, researchers have recognized that the similarity between *Proconsul* and hominids is due to the highly derived nature of hylobatids (Cartmill, 1985; Shea, 1986; Gebo, 1997; Young, 2003; Young and MacLatchy, 2004) as opposed to a closer relationship between *Proconsul* and the great apes. Under this framework it is assumed that the hominids are morphologically closer to the ancestral hominoid morphotype than hylobatids. As a result, H3 characters are often discussed primarily as synapomorphies supporting H2. A proponent of H3, however, would infer a more hylobatid-like hominoid ancestral morph and infer similarities between *Proconsul* and hominids indicate a closer evolutionary relationship (excluding hylobatids). This position is no longer prevalent in literature, though it remains a viable hypothesis. Recently, Rae (1993, 1998, 1999, 2004) has been the main proponent of this hypothesis and it relies heavily on cranio-facial characters.

Proconsul possesses a relatively deep, moderately prognathic face, with a well-developed maxillary jugum similar to the facial morphology of crown hominids (Andrews, 1985; Rae, 1993). This general characterization of similarity in facial morphology is compelling, though the diversity of facial morphs among fossil and extant catarrhines makes the inference of character polarities difficult to interpret. Inferring synapomorphic similarity between *Proconsul* and the

hominids is consistent with an ancestral catarrhine facial morphology characterized by the symplesiomorphic similarity of hylobatids and colobines, which both have short faces and lack the prognathism and maxillary morphology shared by *Proconsul* and the hominids (Vogel, 1966, 1968; Szalay and Delson, 1979; Harrison, 1987). However, as noted above, there is disagreement over the degree to which the hylobatid morphotype can be interpreted as primitive or derived for catarrhines and hominoids. Regarding the facial skeleton in particular, Benefit and McCrossin (1991) have suggested that the similarities between *Aegyptopithecus, Afropithecus* and *Victoriapithecus*, including a deep and prognathic face, are a better model for the primitive catarrhine condition, making the similarities between *Proconsul* and the great apes symplesiomorphic. Expanding on this, others have suggested that facial depth, prognathism and maxillary jugum development may be linked to allometric effects (Vogel 1968; Shea, 1983, 1984, 1985; Harrison, 1987).

Proconsul is similar to the hominids in having a broad anterior palate (Rae, 1999). While a narrower palate is symplesiomorphic for catarrhines (Andrews, 1985) others have interpreted the broad anterior palate as primitive for hominoids (Andrews, 1985; Zalmout, 2010) and not specific to the great apes. Another character that has received little attention in the literature is the height of the naso-alveolar (subnasal) clivus. Andrews (1985) identified a low clivus as primitive for catarrhines. Rae (1999) demonstrated that while hylobatids and cercopithecoids express a primitively short clivus, *Proconsul* and the hominids possess a taller clivus.

The lack of ischial callosities in *Proconsul* and the hominids may be synapomorphic (Walker and Teaford, 1989), though this character may also be interpreted as symplesiomorphically shared between *Proconsul* and stem catarrhines (Harrison and Sanders, 1999). The only other postcranial features that may support a close relationship between

Proconsul and the hominids are drawn from the hand and foot. The presence of a dorsal tubercle on the proximolateral margin of the trapezium-MC1 facet is present in both *Proconsul* and the hominids (Lewis, 1977; Beard, 1986; Rae, 1999). Beard (1986) argues, however, that the gracile, palmarly oriented tubercle in *Proconsul* differs significantly from the robust, laterally oriented morphology seen among hominids. *Proconsul* also possesses a metacarpo-capitate facet that is proximally directed and dorso-palmarly elongated similar to hominids (Rose, 1997; Moyà-Solà, 1999). *Proconsul* has a flexible, grasping foot with a mobile ankle and generally appears similar in its foot and ankle morphology to the primitive anthropoid pattern. However, the shallow navicular and slightly sellar naviculo-cuneiform facet is similar to that seen in the great apes (Sarmiento, 1983; Langdon, 1984; Szalay and Langdon, 1986; Rose, 1986; Ward, 1997). The talus of *Proconsul* also exhibits similarities to the hominid condition, with a deep, sharply defined trochlea and overall similarity in shape and degree of curvature (Langdon, 1984). The talo-calcaneal facets are large and antero-medially expanded in *Proconsul* and the great apes (Langdon, 1984). However, a similar suite of features can be seen in many Miocene catarrhines and Oligocene anthropoids, suggesting that this morphology may be a plesiomorphic adaptation among anthropoids associated with arboreal quadrupedalism (Gebo, 1989; Ward, 1993; Rose, 1994; Seiffert et al., 2001; Dunsworth, 2006). This morphology is distinct primarily when compared to the close-packed articulations of cercopithecoids (Harrison, 1982, 1989; Strasser, 1988; Gebo, 1993; Seiffert et al., 2001). Whether the *Proconsul* foot conforms to the primitive arboreal quadrupedal anthropoid pattern or shares greater mobility at the mid-tarsus with extant hominids rests on the degree to which researchers choose to interpret intermediate variation for which cercopithecoids and hominoids represent the extreme ends.

1.2.3.1 H3 evolutionary implications

Inferences concerning the stem catarrhine morphotype for this hypothesis do not differ from H2. The basal hominoid morphotype is again inferred to be similar to *Proconsul*. Hylobatids may approximate the basal hominoid condition or have acquired their unique adaptations to suspension and brachiation independently of the other hominoids (Gebo, 1997; Young and MacLatchy, 2004). *Proconsul* most closely approximates the ancestral hominid morphotype, possessing cranial synapomorphies (see above) linking it with extant hominids (Rae, 1993, 1999). Certain postcranial similarities including loss of the ischial callosities and adaptations related to mobility in the ankle and foot are synapomorphic for a clade including *Proconsul* and crown hominids.

1.3 PHYLOGENETIC ANALYSES

This dissertation approaches the problem of how to distinguish between stem catarrhines and stem hominoids by testing alternative hypotheses concerning the phylogenetic position of *Proconsul.* Perceived by most authorities as an archetypal stem hominoid, the phylogenetic position of *Proconsul* is often assumed rather than tested. It most often appears in phylogenetic analyses as a de facto outgroup in analyses of hominoids (Moyà-Solà et al., 1995; Begun and Kordos, 1997; Cameron, 1997; Begun, 2002; Finarelli and Clyde, 2004). Few analyses (Rae, 1993, 1999; Rossie, 2008; Zalmout et al., 2010) have been conducted that address all three prevailing phylogenetic hypotheses tested in this dissertation: H1- *Proconsul* is a stem catarrhine, H2- *Proconsul* is a stem hominoid, and H3- *Proconsul* is a stem hominid. Here I review phylogenetic analyses that have included *Proconsul* as an ingroup taxon.

Begun and colleagues (1997) conducted a phylogenetic analysis including *Proconsul* and extant and Miocene hominoids. This analysis set the bar for Miocene hominoid systematics, with other researchers adding to this data set as new material was analyzed (Young and MacLatchy, 2004). The analysis included 240 characters drawn from across the skeleton. Begun et al. (1997) defined their outgroup by deducing primitive character states from observation of *Propliopithecus, Aegyptopitheucs, Epipliopithecus* and modern platyrrhines and cercopithecoids. *Proconsul* was inferred to be the sister taxon of all other extant and fossil taxa included in the analysis: *Pan, Gorilla, Pongo, Hylobates, Australopithecus, Dryopithecus, Sivapithecus, Lufengpithecus, Oreopithecus, Afropithecus* and *Kenyapithecus*. Begun et al. (1997) concluded that the results supported the position of *Proconsul* as a stem hominoid. However, by not including cercopithecoids in the ingroup, this analysis was not able to distinguish between stem hominoids and stem catarrhines. In this case, the phylogenetic position of *Proconsul* is consistent with it being either a stem hominoid or a stem catarrhine.

Begun et al. (1997) did not discuss the significance of individual characters, but broadly argued that *Proconsul* shares with crown hominoids characters related to increased mobility of the limbs and greater manual and pedal grasping abilities. It has been well established that orthogrady and forelimb suspension, as exemplified by the extant hominoids, require a greater range of joint mobility in the limbs. This includes the ability to raise the forelimb above the head, increased extension possible at both shoulder and hip, a greater ability to abduct both hind and forelimb in the medio-lateral plane and a greater degree of rotation at the elbow and abduction and adduction at the wrist (Gomberg, 1981; Rose, 1987, 1994; Lewis, 1989; Ward et al., 1993). This mobility is accompanied by specializations of the hand for powerful grasping of

arboreal supports (Rose, 1983, 1988; Walker and Pickford, 1983; Begun et al., 1994; Kelley, 1997; Nakatsukasa et al., 1998, 2002, 2003).

Young and MacLatchy (2004) extended the Begun et al. (1997) analysis by adding 13 postcranial characters and two fossil catarrhines: *Morotopithecus,* an early Miocene catarrhine from Uganda, and *Rudapithecus*, a late Miocene hominid from Hungary. They also ran phylogenetic analyses using the data sets of Moyà-Solà and Kohler (1995) and Cameron (1997), but these analyses did not include *Proconsul* in the ingroup so will not be discussed here. Young and MacLatchy's results placed *Proconsul* in a clade with *Afropithecus* and *Kenyapithecus* as a stem hominoid. Once again without inclusion of cercopithecoids these results cannot be used to distinguish between whether *Proconsul* is a stem hominoid or a more basal stem catarrhine. Additionally, disagreement concerning the phylogenetic position of *Afropithecus*—with some researchers placing it within Hominoidea (Gebo et al., 1997; MacLatchy, 2004) and others among stem catarrhines (Harrison, 2010)—means this result could be used to support H1. Each of the additional characters added to the Begun et al. (1997) data set either grouped *Proconsul* with cercopithecoids or linked *Proconsul* and hylobatids to the exclusion of other fossil and other extant apes.

More recently, Zalmout et al. (2010) included *Proconsul* in a phylogenetic analysis of the Oligocene catarrhine *Saadanius*. They included a sample of 36 cranial and postcranial characters for 19 taxa of Oligocene and Miocene stem catarrhines and hominoids, as well as one stem cercopithecoid, *Victoriapithecus* and two extant hominoids, *Pan* and *Hylobates*. *Aegyptopithecus* was used as the outgroup. Their final results placed Proconsulidae (including *Afropithecus, Heliopithecus, Morotopithecus, Turkanapithecus, Nyanzapithecus, Rangwapithecus, Nacholapithecus, Equatorius, P. heseloni* and *P. nyanzae*) as the sister group to extant

hominoids. They constrained this set of taxa as monophyletic despite their unconstrained analysis identifying Proconsulidae as paraphyletic. Eight synapomorphies were identified linking proconsulids to crown hominoids: increase in body size, broad anterior palate, pronounced alveolar prognathism, tail loss, a deep and narrow zona conoidea, deep olecranon fossa, absence of entepicondylar foramen and epitrochlear fossa. A surprising result from their unconstrained analysis placed *Victoriapithecus* closer to the base of the catarrhine tree than *Epipliopithecus*. This indicates their analysis was unable to parse out derived cercopithecoid and crown catarrhine characters. The inclusion of crown cercopithecoids may have helped resolve this issue by linking *Victoriapithecus* to the more derived morphology of extant cercopithecoids and thereby also better rooting the crown catarrhine morphotype.

It is useful to discuss each synapomorphy identified by Zalmout et al. (2010) in order to fully consider the implications of their results, as many of these characters are difficult to interpret. Even considering only extant taxa, there is a wide range of body sizes among extant apes. If one only considers the great apes, they can be clearly distinguished from the mostly small to medium sized cercopithecoids. However, the larger bodied papionins as well as *Nasalis* challenge this dichotomous characterization. *Proconsul* exhibits a range of body sizes, with the large bodied *P. major* estimated at 60-90 kg (Rafferty et al., 1995; Ruff, 2003), comparable in size to a female gorilla, while the smaller species, *P. heseloni* and *P. africanus,* are similar in body mass to siamangs with an estimate of 9-15 kg (Rafferty et al., 1995; Ruff, 2003). Many extant hylobatids are even smaller. Among Zalmout's constrained proconsulid clade, *Nyanzapithecus, Turkanapithecus*, *Rangwapithecus, Nacholapithecus and Equatorius* all may be considered medium-sized catarrhines (Harrison, 2010). Zalmout et al. (2010) infer a large bodied

most recent common ancestor for proconsulids and hominoids, but if this is the case then it must accommodate many character reversals.

Among cranial characters, pronounced alveolar prognathism and a broad anterior palate were identified as proconsulid + hominoid synapomorphies. As discussed above, the wide diversity of facial morphs present among fossil catarrhines, with ambiguous or contradictory signals relative to extant clades, makes inferring character polarities for these features problematic. Some even suggest that in its degree of prognathism and facial orientation *Proconsul* is more similar to cercopithecines (Moyà-Solà, 2009).

Perhaps the most notable diagnostic character distinguishing extant hominoids and cercopithecoids is the absence of a tail (Ward and Walker, 1991; Ward, 1993; McCrossin, 1994; Harrison, 1998; Nakatsukasa et al., 2003, 2004; Larson and Stern, 2006). All extant New World monkeys and most Old World monkeys possess tails, suggesting the ancestral anthropoids and catarrhines also possessed tails. Caudal vertebrae have not been found for *Proconsul*, despite the wealth of fossil remains that have been recovered for this taxon, leading most researchers to infer that *Proconsul* did not have a tail (Ward and Walker, 1991; Ward, 1993; McCrossin, 1994; Nakatsukasa et al., 2003, 2004; Larson and stern, 2006). Harrison (1998) suggested that vertebrae recovered from Kaswanga Primate Site on Rusinga Island, Kenya were caudal vertebrae providing evidence of a tail. Ward and Walker (1991; Ward et al., 1999), however, suggested that these vertebrae were actually last sacral vertebrae whose morphology indicated that *Proconsul* did not have a tail. Further evidence for presence of a tail may be indicated by the size of the ischial spine (McCrossin and Benefit, 1992; McCrossin, 1994; Benefit and McCrossin, 1995). The ischial spine serves as the origin for tail abductor and depressor muscles. In apes these muscles are reorganized to support the pelvic viscera and the ischial spine is moved

more superiorly on the ischium. In *Proconsul*, the position of the ischial spine is more similar to that seen in primates with mobile tails than in the tail-less apes (McCrossin and Benefit, 1992; McCrossin, 1994; Benefit and McCrossin, 1995). Russo (2016) used sacral morphology to create a predictive framework for inferring tail morphology among fossils and inferred *Proconsul* was tail-less based on the degree of tapering of the last sacral vertebrae (following Ward et al., 1991), medio-lateral breadth of the transverse process and caudal articular surface shape. Other evidence from the fossil record comes not from *Proconsul,* but from *Nacholapithecus*, a contemporaneous Miocene catarrhine that Harrison (2010) places within the afropithecine proconsulids. This taxon has been definitively demonstrated to lack a tail through the presence of a coccyx and has led researchers to infer other members of the clade are also likely to have been tail-less (Nakatsukasa et al., 2003). Given this body of evidence (or lack of), it is likely *Proconsul* also lacked a tail, though there is evidence of multiple cases of tail loss among catarrhines questioning the significance of this character. Pig tailed macaques have undergone tail reduction—though not complete tail-loss--(Wilson, 1972; Larson and Stern, 2006) and while there have been various proposed adaptive explanations, none would explain the convergence between macaques and Miocene catarrhines.

Zalmout et al. (2010) identified two characters from the elbow—possession of a deep narrow zona conoidea and deep olecranon fossa—that form a subset of the suite of characters used by researchers to describe the hominoid-like affinities of the *Proconsul* elbow discussed in detail in the previous section. The final two characters –lack of an entepicondylar foramen and dorsal epitrochlear fossa—are commonly used to distinguish crown catarrhines from stem catarrhines (Harrison, 2013). The entepicondylar foramen is a primitive placental mammal character shared by many strepsirrhines, fossil anthropoids and ceboids, but is lost in crown

catarrhines (Fleagle et al., 1982). The dorsal epitrochlear fossa is also present among many stem catarrhines and platyrrhines, but is absent in both cercopithecoids and hominoids (Conroy, 1976; Fleagle and Kay, 1987; Harrison, 1987, 2013).

Rossie (2008) investigated the comparative morphology of the paranasal sinuses and tested the phylogenetic hypotheses of Harrison (1987), Begun et al., (1997) and Cameron (1997). Rossie (2008) assessed which was the most parsimonious scenario using the distribution of paranasal sinus anatomy in anthropoids. Based on the results, Rossie could not distinguish between the hypotheses, with each representing equally parsimonious possibilities.

Paranasal sinuses have been central in arguments linking *Proconsul* and other Miocene hominoids with extant lineages. The presence of a frontal sinus in particular has been used to argue that *Proconsul* is linked to extant great apes (Clark and Leakey, 1951; Walker and Pickford, 1983; Walker and Teaford, 1989; Andrews, 1992; Walker, 1997; Rae and Koppe, 2004). Enlargement of the paranasal and particularly the maxillary sinuses have been discussed as a hominoid trait (Andrews and Martin, 1987). Others contend that paranasal sinuses and particularly the frontal sinus are symplesiomorphic for anthropoids, given that they are present in many platyrrhines (Hershkovitz, 1977; Rae, 1999b, 2000; Rossie et al., 20002, 2005; Rae and Koppe, 2004). As researchers explored the complex morphology of the paranasal sinuses the evolutionary significance became even less clear. Maxillary sinuses are common across mammals and highly variable (Rossie, 2008). Among catarrhines, maxillary sinus morphology is variable, with loss of the maxillary sinus in most cercopithecoids (Rae, 1993; Rae et al., 2002; Rossie, 2008) and a range of variation in Miocene and extant hominoids (Andrews, 1978; Ward and Pilbeam, 1983; Teaford et al., 1988). The frontal sinus has been shown to be an expansion of the ethmoid sinuses in African apes and humans and appears to be a shared derived feature of

the clade. In hominines and *Proconsul* the ethmoid and frontal sinuses expand to form an ethmoid labyrinth (Rossie, 2005, 2008). Rossie et al. (2002) demonstrated that *Aegyptopithecus zeuxis*, a stem catarrhine, also possesses an ethmoidal labyrinth suggesting this morphology is probably primitive for catarrhines. Interpretation is further complicated, however, by the lack of an ethmoidal labyrinth in all platyrrhines, cercopithecoids and the Asian apes (Rossie, 2008). The frontal sinus is also difficult to interpret as it is widely distributed across anthropoids and its morphology is highly variable. Rossie (2005) argued that given that its taxonomic distribution it cannot be used as a hominine synapomorphy or to link Miocene taxa to crown lineages. Without a confident assessment of homology it cannot be evaluated for its phylogenetic signal (Rossie, 2008).

Rossie and MacLatchy (2006) performed one of the most comprehensive phylogenetic analyses of catarrhines to date. They included 191 craniodental and postcranial characters focused on resolving the phylogenetic position of *Lomorupithecus*. *Proconsul* was included in the ingroup and the platyrrhine taxa *Ateles, Saimiri and Cebus* comprised the outgroup clade. Cercopithecoids were included in the analysis. Their results placed *Lomorupithecus* with the pliopithecoids, but was unable to resolve the phylogenetic position of *Proconsul*. *Proconsul* was placed in a clade including all catarrhine taxa except the pliopithecoids, *Aegyptopithecus* and *Catopithecus*. Extant cercopithecoids formed a clade, as did extant hominoids and nyanzapithecines, but the relationships between these clades, *Proconsul* and other catarrhines included in the analysis were unresolved.

Rae (1993, 1999) conducted a phylogenetic analysis focused on the position of *Proconsul*, which included both extant cercopithecoids and hominoids in the ingroup and platyrrhines as a chimeric outgroup. The analysis considered facial morphology independently

from the rest of the skeleton and, based on 12 facial characters, including four hominid synapomorphies, inferred that *Proconsul* was a hominid (Rae, 1993). A subsequent analysis (Rae, 1999) incorporated 79 additional postcranial characters, testing whether postcranial and facial characters exhibited differing phylogenetic signals. His results identified 13 hominoid + *Proconsul* synapomorphies in the postcranium, this time inferring *Proconsul* to be a stem hominoid (Rae, 1999). Rae (1999, 2004) concluded that hylobatids represent a derived lineage perhaps undergoing character reversals to the primitive condition, while hominids are a better model for the ancestral hominoid morphotype. This explains the seemingly contradictory results from facial and postcranial skeletons. Rae (1999, 2004) further argued that the incongruity between these data sets suggests that the changes in the hominoid facial skeleton preceded the locomotor adaptations considered characteristic of hominoids.

The four facial synapomorphies linking *Proconsul* with hominoids are: configuration of the premaxillo-nasal suture, nasals flat and non-projecting across the bridge of the nose, a wide anterior palate, a tall naso-alveolar clivus (see discussion from previous section). The thirteen postcranial synapomorphies include two characters describing beveling of the radial head as it relates to depth of the zona conoidea and stability across the radio-humeral joint. A majority of characters were drawn from the carpus, including: morphology of the trapezial tubercle, pisiform-ulnar articulation, pisiform-trapezium articular ridge and facet form and triquetral-ulnar articulation. The final characters were taken from vertebral morphology: caudal orientation of the neural spine, small anapophyses, six lumbar vertebrae and a narrow sacral canal. Loss or reduction of the anapophyses is likely related to a dorsally positioned transverse process (Ward, 1993; Nakatsukasa, 2007). Position of the transverse process reflects a reduction in the size of intrinsic muscles of the back as this position leaves less space for large back muscles (Ward,

1993; Nakatsukasa, 2007). Both features are present in hominoids, who do not have intrinsic back muscles as large as in the quadrupedal cercopithecoids or platyrrhines. During quadrupedal locomotion in non-hominoid anthropoids, flexion and extension of the spine, particularly in the lumbar region accompanies limb movements, increasing stride length (Jenkins, 1974; Preuschoft et al., 1979; Jungers, 1984; Shapiro, 1993; Ward, 1993; Sanders and Bodenbender, 1994; Johnson and Shapiro, 1998). During suspensory, bridging and vertical climbing behaviors, however, flexion and extension of the spine is limited to reduce the risk of buckling and to stabilize the spine (Cartmill and Milton, 1977; Jungers, 1984). A caudally oriented neural spine has also been linked to reduced lumbar mobility. This inference proceeds from convergence with non-primate climbing and suspensory mammals that possess more caudally oriented neural spines than their quadrupedal relatives (Lemellin, 1999; Argot, 2003; Nakatsukasa, 2007). Rae (1999) interprets *Proconsul* as falling on a linear trajectory of reduction in the number of lumbar vertebrae, identifying monkeys as having seven lumbar vertebrae, hylobatids and *Proconsul* having six and hominids having four to five. This is a simplification of the range of variation in lumbar vertebrae found among these groups (Ward, 1993; Williams and Russo, 2015). Considering the full range of variation, Ward (1993) argued that *Proconsul* is more similar to monkeys for this trait, though it is plausible that the intermediate morphology expressed by *Proconsul* may be indicative of an evolutionary trajectory leadings towards shortening of the lumbar region. Finally, sacral canal size and shape is linked to tail length (Ankel, 1972; Ward, 1991; Nakatsukasa, 2004; Russo, 2016) and a narrow V-shaped canal may be indicative of tail loss or reduction.

1.4 OVERVIEW

The Miocene fossil record is inconsistent with a linear progression of catarrhine evolution in which extant hominoids–with their skeletal adaptations to suspensory behaviors and orthograde body postures—become more derived over time relative to the quadrupedal cercopithecoids which more closely approximate the primitive catarrhine condition. Researchers have struggled with how best to resolve the position of fossil forms that may bear little resemblance to either the cercopithecoids or hominoids. This difficulty is further complicated by the great temporal and morphological divide between catarrhines and their closest living outgroup, the platyrrhines. The traditional view has historically been to place nearly all fossil non-cercopithecoid catarrhines within the hominoid clade. Reevaluation has led certain taxa to be removed, however, where there is little confidence or consensus many taxa remain referred to Hominoidea simply due to taxonomic convention with recognition that this placement results in a para- or polyphyletic hominoid clade.

Researchers have been unable to confidently resolve the phylogenetic relationships of basal catarrhine taxa falling near the divergence of the hominoid and cercopithecoid clades. The results of prior analyses highlight the need for a comprehensive analysis to address the phylogenetic position of *Proconsul.* Appropriate taxonomic sampling is imperative to address the range of possible hypotheses and previous analyses have limited the evolutionary scenarios they evaluated due to the difficulties of extensive taxonomic sampling (Begun et al., 1997; Young and MacLatchy, 2004; Zalmout, 2010). In morphology, more problematic than taxonomic sampling is character sampling. Recent advances in systematics have emphasized the importance of extensive characters lists as the prime driver of confident phylogenetic inference (Huelsenbeck, 1991; Wheeler, 1992; Wiens, 1998, 2003a, 2005; Wiens and Moen, 2008;

Prevosti and Cheminquy, 2010; Wiens and Tiu, 2012). Previous analyses prioritized carefully curated character lists over extensive sampling and the shift in our understanding of these methods has not yet been fully addressed in the current literature.

This dissertation strives to apply current morphological systematic methods to critically assessing the phylogenetic position of *Proconsul* by collecting an extensive character list from a broad sample of living and fossil anthropoids. It will be the first application of Bayesian systematics and of recent advances in parsimony methods to address the phylogenetic relationships of *Proconsul*. I will test the three alternative hypotheses described above and will explore the evolutionary trajectories and ancestral morphotypes inherent in each evolutionary scenario. Results from this dissertation provide evidence regarding the timing and morphological affinities of basal crown catarrhine nodes and the position of *Proconsul* relative to the dichotomy between cercopithecoids and hominoids. It is the goal of this dissertation to provide greater confidence in the assessment of the phylogenetic position of *Proconsul* in order to allow the study of catarrhine and hominoid evolution to rest on a confidently resolved foundation.

CHAPTER 2: MATERIALS

2.1 TAXONOMIC SAMPLING

Catarrhine, platyrrhine and anthropoid ancestral morphotypes are not well established and yet all analyses conducted in this thesis are necessarily built on a framework defined by the morphology at these basal nodes. Character polarities in phylogenetic analyses are dependent on the relationships between ingroup taxa and a definitional primitive taxon: the outgroup (Hennig, 1966; Hillis, 1996, 1998; Graybeal, 1998; Scotland et al., 2003). It is essential to carefully select one's outgroup based on the evolutionary questions one wishes to ask. An outgroup must be as indicative of primitive morphology for your ingroup as possible. It also will ideally be closely related to your ingroup in order to best approximate a primitive morphotype and limit the amount of time for character evolution between the outgroup and the most basal ingroup taxon. There also must not be any ambiguity concerning how the outgroup and ingroup are related as all analyses begin by asserting, as opposed to testing, the ingroup/outgroup relationship. Selection of an outgroup for analyses of crown catarrhine relationships is, as a result of these considerations, challenging and fulfilling all of these requirements is not always possible. As discussed in the previous chapter, many analyses have been hampered by inappropriate outgroup selection leading to potentially misleading results. By using cercopithecoids as an outgroup in an analysis of hominoid relationships, a researcher defines cercopithecoid morphology as primitive and uses it as the starting point from which all other morphological changes among hominoids proceed. In order to be confident in the ingroup/outgroup relationship extant taxa should be preferred. A platyrrhine is the nearest extant primate that may serve as an outgroup to catarrhines; however, there is not consensus as to which platyrrhine best approximates the

primitive platyrrhine morphotype and certainly they are all derived relative to the primitive condition. To best confront this issue, a wide sampling of extant platyrrhines are used as an outgroup clade. Given that extant platyrrhines are a distant outgroup, the confidently inferred (see discussion below) basal catarrhines *Epipliopithecus* and *Aegyptopithecus* are used as successive outgroups.

Taxonomic sampling within the ingroup can also bias results before analysis begins. Sampling must reflect the hypotheses being addressed. As was discussed in the introduction, a phylogenetic analysis inferring *Proconsul* forms a clade with extant hominoids to the exclusion of basal catarrhines where cercopithecoids are not included in the analysis, can only infer *Proconsul* is more closely related to crown catarrhines than basal catarrhines. One can only infer *Proconsul* is a hominoid if it is shown to diverge from the hominoid lineage after the origination of the cercopithecoids. Where cercopithecoids are left out of the ingroup there is no way to identify topographically the distinction between crown catarrhines and hominoids. The problem of incomplete taxonomic sampling leading to potentially misleading conclusions has hampered phylogenetic analyses of *Proconsul* in the past (see discussion above). By including a broad sampling of platyrrhine taxa as an outgroup clade, sampling widely within cercopithecoids and hominoids and including stem catarrhines as a successive outgroup, I am better positioned to evaluate the phylogenetic position of *Proconsul* relative to each of these groups.

Inferring character polarities is particularly difficult in cases where there is little resolution in the evolutionary relationships near the root of the tree and when long branches separate major clades. Sampling stem taxa and fossils may help break up these long branches and provide valuable information concerning character polarities (Hillis and Wiens, 2000). Adding more taxa, however, also adds more variation, which has the potential to increase

ambiguity in the directionality of character changes (Kim, 1996; Graybeal, 1998; Poe, 1998; Rosenberg and Kumar, 2001; Hillis et al., 2003; Scotland et al., 2003). The difficulties of this increased ambiguity, however, do not outweigh the benefits from broad taxonomic sampling (Hillis and Wiens, 2000). Additionally, taxonomic sampling is essential to including the full spectrum of variation within clades. The case of *Proconsul* is particularly illustrative of this issue, as many characters previously thought synapomorphic for a clade including *Proconsul* within Hominoidea were questioned when the same variation was identified outside of Hominoidea (see chapter 1). As such, I have included representative taxa from each major extant catarrhine clade and fossils have been selected as stem representatives of major clades. Fossil taxa were selected as those with the best representation across the skeleton. The decision to limit sampling of fossil taxa to only those most complete specimens was made not only to ensure adequate sampling across the skeleton, but also to allow for direct focus on the taxon of interest: *Proconsul.* Limiting included fossil taxa to those with no disagreement in the literature regarding their phylogenetic inclusion within major clades was deemed essential to most confidently constraining extant clades and helping root character polarities. This meant some well sampled fossils such as *Nacholapithecus* and *Turkanapithecus* were not included. The wide range of morphological variation present among Miocene forms (Harrison, 1993, 2010; Begun, 2002) makes for a difficult phylogenetic problem. While other analyses have sampled more broadly and this is recognized as a valuable and often desirable sampling strategy, this dissertation chose another priority—to focus explicitly on *Proconsul* and eliminate the potential confounding effects of a wider range of variation (Kim, 1996, 1998; Rosenberg and Kumar, 2003; DeBry, 2005). Additionally, in order to accommodate the long branch separation between the platyrrhine outgroup and crown catarrhines, inclusion of a basal catarrhine was deemed

valuable. Unfortunately no individual taxon included all sampled characters making it necessary to include multiple fossil taxa, compromising one of the methodological choices of this dissertation to limit inclusion of fossil taxa that may hinder the success of phylogenetic analyses by introducing additional uncertainty into character polarity determination. *Aegyptopithecus* and *Epipliopithecus* were deemed the most appropriate basal catarrhines to include in this successive outgroup as previous studies have placed them with reasonable confidence as successive sister taxa to all crown catarrhines and between them they cover the majority of sampled characters (Simons, 1987; Andrews et al., 1996; van der Made, 1999; Harrison, 2005; Seiffert, 2006; Zalmout et al., 2010).

Table 1. Taxonomy of extant and fossil species included in this study † Designates an extinct species

Order **Primates** Linnaeus, 1758
- Semiorder **Haplorhini** Pocock, 1918
  - Suborder **Anthropoidea** Mivart, 1864
    - Infraorder **Platyrrhini** É. Geoffroy, 1812
      - Superfamily **Ceboidea** Simpson, 1931
        - Family **Pitheciidae** Mivart, 1865
          - Subfamily **Pitheciinae** Mivart, 1865
            - ***Pithecia monachus*** (Geoffroy Saint-Hilaire, 1812)
        - Family **Cebidae** Bonaparte, 1831
          - Subfamily **Cebinae** Bonaparte, 1831
            - ***Cebus apella*** **(**Linnaeus, 1758)
          - Subfamily **Callitrichinae** Gray, 1821
            - ***Saguinus oedipus*** (Linnaeus, 1758)
          - Subfamily **Saimiriinae** Miller, 1812
            - ***Saimiri oerstedii*** (Reinhardt, 1872)
        - Family **Atelidae** Gray, 1825
          - Subfamily **Atelinae** Gray, 1825
            - Tribe **Atelini** Gray, 1825
              - ***Ateles geoffroyi*** Kuhl, 1820
            - Tribe **Alouattini** Trouessart, 1897
              - ***Alouatta palliata*** (Gray, 1848)
        - Family **Aotidae** Poche, 1908
          - ***Aotus azarae*** (Humboldt, 1811)
    - Infraorder **Catarrhini** É. Geoffroy, 1812
      - Superfamily **Propliopithecoidea** Straus, 1961
        - Family **Propliopithecidae** Straus, 1961

Aegyptopithecus zeuxis Simons, 1965†
Superfamily **Pliopithecoidea** Zapfe, 1960
Family **Pliopithecidae** Zapfe, 1960
Epipliopithecus vindobonensis Zapfe & Hürzeler, 1957†
Superfamily **Proconsuloidea** Leakey, 1963
Family **Proconsulidae** Leakey, 1963
Subfamily **Proconsulinae** Leakey, 1963
Proconsul africanus Hopwood, 1933†
Proconsul nyanzae Le Gros Clark & Leakey, 1950†
Proconsul heseloni Walker et al., 1993†
Proconsul major Le Gros Clark & Leakey, 1950†
Superfamily **Cercopithecoidea** Gray, 1821
Family **Cercopithecidae** Gray, 1821
Subfamily **Victoriapithecinae** von Koenigswald, 1969
Victoriapithecus macinnesi von Koenigswald, 1969†
Subfamily **Cercopithecinae** Gray, 1821
Tribe **Cercopithecini** Gray, 1821
Cercopithecus mitis Wolf, 1822
Erythrocebus patas (Schreber, 1775)
Tribe **Papionini** Burnett, 1828
Macaca nemestrina (Linnaeus, 1766)
Papio cynocephalus (Linnaeus, 1766)
Subfamily **Colobinae** Jerdon, 1867
Tribe **Colobini** Jerdon, 1867
Colobus guereza Rüppell, 1835
Tribe **Presbytini** Gray, 1825
Nasalis larvatus (Wurmb, 1787)
Presbytis rubicundus (Müller, 1838)
Superfamily **Hominoidea** Gray, 1825
Family **Hylobatidae** Gray, 1870
Hylobates lar **(**Linnaeus, 1771)
Symphalangus syndactylus (Raffles, 1821)
Family **Hominidae** Gray, 1825
Subfamily **Oreopithecinae** Schwalbe, 1915
Oreopithecus bambolii Gervais, 1872†
Subfamily **Ponginae** Elliot, 1913
Pongo pygmaeus **(**Hoppius, 1760)
Subfamily **Homininae** Gray, 1825
Tribe **Dryopithecini** Gregory & Hellman, 1939
Pierolapithecus catalaunicus Moyà-Solà et al., 2004†
Tribe **Gorillini** Frechkop, 1943
Gorilla gorilla **(**Savage &Wyman, 1847)
Tribe **Hominini** Gray, 1825
Subtribe **Panina** Delson, 1977
Pan troglodytes **(**Blumenbach, 1775)

2.1.1 Samples of Extant Anthropoids

This study sampled seven platyrrhine taxa (table 1): *Pithecia, Saimiri, Cebus, Alouatta, Ateles, Saguinus* and *Aotus*. Within the ingroup, seven extant cercopithecoids (*Cercopithecus, Erythrocebus, Colobus, Papio, Presbytis, Nasalis and Macaca*) and five extant hominoids (*Hylobates, Symphalangus, Pongo, Gorilla* and *Pan*) were sampled. This broad taxonomic sampling, representing each of the major clades within Anthropoidea (i.e., Pitheciidae, Cebidae, Atelidae, Cercopithecinae, Colobinae, Hylobatidae, Hominidae), is necessary to represent morphological diversity within the suborder. The target sample size for extant species was 20 individuals, with 10 males and 10 females each.

While many of these taxa are derived and will significantly expand the range of variation encompassed within the extant sample, it is necessary to sample comprehensively across crown taxa in order not to make a priori decisions about what variation to include. This reasoning differs from that used to select fossil taxa as phylogenetic position is unambiguous for most extant taxa based on molecular studies (Purvis, 1995; Page and Goodman, 2001; Perelman et al., 2011).

Table 2. Fossil samples used in this study

"% complete" refers to the percent of characters sampled for each taxon. All other numbers in the table are the absolute number of specimens for each region. Abbrevitions: MC- metacarpals, MT- metatarsals

Genus	% complete	N	Cranial	Mandible	Pelvis	Radius	Ulna	Humerus	MC	Carpals	MT	Tarsals
All Proconsul	100.00	177	10	14	2	5	7	6	14	37	25	57
P. africanus	20.20	18	3	0	0	0	1	0	1	8	1	4
P. heseloni	89.60	109	6	2	1	4	4	3	13	24	19	33
P. nyanzae	42.29	37	1	8	1	0	1	2	0	5	4	15
P. major	17.87	13	0	4	0	1	1	1	0	0	1	5
Epipliopithecus	70.62	39	2	3	2	2	3	2	6	7	7	5
Aegyptopithecus	35.25	40	13	16	0	0	1	6	0	0	1	3
Victoriapithecus	67.68	117	4	7	2	0	11	13	5	27	2	46
Oreopithecus	47.86	54	2	1	0	1	2	3	4	6	15	20
Pierolapithecus	9.06	14	1	0	0	0	0	0	2	7	1	3

2.1.2 Samples of fossil catarrhines

Fossil taxa (Table 2) were chosen based on their representation in the fossil record. Particular emphasis was placed on choosing fossils that sampled across the skeleton, from each of the morphological regions included in this analysis. By including stem members of Hominoidea and Cercopithecoidea I am including additional data from other Miocene taxa, potentially breaking up branches separating *Proconsul* from extant catarrhines. This helps root character polarities at the base of the crown catarrhine lineage.

Two fossil catarrhines were included in this analysis that are widely considered to represent basal clades: Pliopithecidae and Propliopithecidae (Simons, 1987; Andrews et al., 1996; van der Made, 1999; Harrison, 2005; Seiffert, 2006; Zalmout et al., 2010). Their inclusion incorporates basal catarrhine outgroups—in addition to the platyrrhine outgroup—in order to break up the long branches separating platyrrhines from crown catarrhines. It will help establish the inferred ancestral character states for the anthropoid and catarrhine morphotypes. The lack of consensus concerning stem catarrhine relationships is a key component of the difficulty in inferring the phylogenetic position of *Proconsul* that will be partially confronted by their addition.

2.1.2.1 *Aegyptopithecus zeuxis*

Aegyptopithecus is an Oligocene catarrhine known from the Fayum from 30-29 Ma (Seiffert, 2006). It belongs to Propliopithecoidea, a stem catarrhine group and the earlier of the two basal groups sampled in this analysis. *Aegyptopithecus* was selected as a well-represented fossil propliopithecid, known from numerous cranial and postcranial specimens. This taxon possesses a number of features (see below) that place it with reasonable confidence as a stem

catarrhine, falling within the catarrhine clade, but lacking the derived morphology of either crown catarrhine clade.

Phenetic similarities in facial morphology shared with *Victoriapithecus* and *Afropithecus* (Leakey & Leakey, 1986; Simons, 1987; Leakey et al.. 1988, 1991; Benefit & McCrossin, 1991, 1993)—including a relatively long snout, wide inter-orbital region and moderate face length—have been argued to be indicative of the primitive catarrhine morphology (Benefit and McCrossin, 1993). Additionally, *Aegyptopithecus* possesses a suite of primitive catarrhine features lost in the crown catarrhines including a distal humerus that primitively retains an entepicondylar foramen and dorsal epitrochlear fossa, an annular ectotympanic, broad ascending wing of the premaxilla and an atrioturbinal in the nasal cavity (Seiffert et al., 2010; Harrison, 2013). *Aegyptopithecus* has served as a baseline for defining the ancestral catarrhine morphotype in both cladistic and phenetic discussions of later catarrhine morphology (Rose, 1983; Leakey et al., 1991; Rossie et al., 2002; Zalmout et al., 2010; Perez et al., 2012).

Data on *Aegyptopithecus* were collected from the Duke Primate Center (DPC) and included 40 specimens, with 10 partial crania, 16 partial mandibles, six distal humeri, one ulna, three tali and one 4th metatarsal (table 2). Data were also collected on casts of three partial crania of which the originals are housed at the Cairo Geological Museum: CGM40237, CGM42842, CGM85785. All specimens were from Localities I and M in the Jebel Qatrani Formation, Fayum Province, Egypt (Simons, 1965, 1967). Across all specimens of this genus, 35.25% of total number of characters evaluated in this study were sampled.

2.1.2.2 *Epipliopithecus vindobonensis*

Epipliopithecus vindobonensis is a pliopithecoid from the middle Miocene of Central Europe, dated to ~15 Ma (Zapfe & Hürzeler, 1957; Zapfe, 1958, 1960; Ginsburg, 1986; Andrews

et al., 1996; Harrison and Gu, 1999; Begun, 2002; Alba et al., 2010). The pliopithecoids were the first catarrhine lineage to disperse out of Africa into Eurasia (Andrews et al., 1996; Rögl, 1999; van der Made, 1999; Harrison, 2005). The postcranial skeleton of *Epipliopithecus* is indicative of a generalized, above-branch quadruped (Zapfe 1960; Fleagle 1983; Rose 1983, 1993; Harrison, 2013). Mobile limb joints suggest climbing, bridging and suspensory behaviors were part of its locomotor repertoire (Zapfe, 1960; Scherf, 2007; Ward, 2007; Rein et al., 2011; Harrison, 2013). *Epipliopithecus* possesses an entepicondylar foramen in its distal humerus, similar to that of *Aegyptopithecu*s, but is more derived in possessing a short, partially enclosed ectotympanic tube differing from the platyrrhine annular morphology also exhibited by *Aegyptopithecus* and potentially approaching the derived extant catarrhine tube-like ectotympanic (Zapfe, 1960; Delson & Andrews, 1975; Szalay & Delson, 1979; Harrison, 1987; Begun, 2002; Harrison, 2005; Alba et al., 2010). *Epipliopithecus* has a relatively short snout and broad face, unlike *Aegyptopithecus*. The presence of both a long and short facial morph among these early catarrhine fossils makes inference of the primitive condition uncertain. Together, these features place this taxon along with *Aegyptopithecus* as basal to crown catarrhines. The differences in cranial and particularly facial morphology between *Aegyptopithecus* and *Epipliopithecus* have led to disagreements in the literature over the primitive catarrhine morphotype (Leakey & Leakey, 1986; Simons, 1987; Leakey et al., 1988, 1991; Benefit & McCrossin, 1991, 1993). The facial morphology of the stem catarrhine *Saadanius* appears most similar to the *Aegyptopithecus* facial morphology (Zalmout et al., 2010) suggesting the long facial morph was common among stem catarrhines, though it does not resolve the difficulty to inferring character polarity caused by having both morphs represented in the stem catarrhine sample. While it is unreasonable to assume these two taxa represent the range of variation

present among the earliest catarrhines, they are the best representatives currently available and, by including both, incorporate some of the diversity present early in catarrhine evolution.

Data on *Epipliopithecus vindobonensis* were collected at the Naturhistorisches Museums in Vienna and Basel. Specimens included four individuals and sampled multiple anatomical elements across all regions. *Epipliopithecus* sampled 70.62% of characters (table 2).

2.1.2.3 *Victoriapithecus*

Victoriapithecus is the only stem cercopithecoid included in this analysis, as the best represented Miocene Old World monkey. *Victoriapithecus* is found in eastern Africa from 19.5-12.5 mya (Gundling & Hill, 2000; Benefit and McCrossin, 2002; Miller et al., 2009; Gilbert et. al, 2010). It possesses derived features in its craniodental anatomy linking it with extant cercopithecoids, particularly their diagnostic bilophodont molars. *Victoriapithecus* lacks, however, the specialization in molar morphology that distinguishes extant colobines and cercopithecines and possesses a number of primitive features in its dentition not shared with extant cercopithecoids including: variable presence of the crista obliqua on the upper molars and small hypoconulids on the lower molars (Benefit, 1993, 1999; Miller et al., 2009). These features are shared by non-cercopithecoid primates and suggest this taxon is best positioned at the base of the cercopithecoid lineage. Additionally, it retains a number of primitive catarrhine features in the facial skeleton, appearing similar to *Aegyptopithecus*. These include: a long snout, wide palate, tall orbits, supra-orbital costae with a frontal trigone and deep malar region of the zygomatic (Szalay & Delson, 1979; Benefit and McCrossin, 1991, 1993, 1997, 2002; Benefit, 1999; Jablonski & Frost, 2010). When compared to extant cercopithecoids, *Victoriapithecus* generally exhibits more similarities with cercopithecines than with colobines due to postcranial features indicating at least semi-terrestriality and morphology of the snout and cranial vault

(Szalay & Delson, 1979; Harrison, 1989; Benefit, 1999; Benefit and McCrossin, 2002; Jablonski and Frost, 2010). Postcranially, the narrow distal humerus, stout phalanges and limited flexibility at the elbow, hip and ankle all suggest a degree of terrestrially similar to modern vervet monkeys (Von Koenigswald, 1969; Delson, 1975; Senut, 1986; Harrison, 1989; McCrossin & Benefit, 1992; Benefit and McCrossin, 1995, 2002; McCrossin et al., 1998)

Data were collected from 117 specimens representing each region except the radius, for which no specimens were available. All data were collected at the National Museum of Kenya in Nairobi. For *Victoriapithecus* 67.68% of characters were sampled (table 2).

2.1.3 Fossil hominoids

Two fossil hominoids were sampled in order to help root the stem hominoid node. *Oreopithecus* and *Pierolapithecus* were chosen as they each include partial skeletons and thus sample features across the skeleton. *Hispanopithecus* was not included as the available material included more than 80% missing data and did not include the characters utilized in controlling for allometric effects, meaning cranial and post-cranial elements could not have been included. The included taxa sample all regions in this analysis with the exception of the pelvis, as the preservation of the *Oreopithecus* pelvis did not allow for the pelvic characters included to be reliably collected (table 2). It was particularly important in selecting hominoid taxa that there is no disagreement in the literature regarding their inclusion within Hominoidea. This meant other well sampled fossils such as *Equatorius, Nacholapithecus* and *Turkanapithecus* were not included (Harrison, 2010). Fossil taxa falling further up the hominoid tree (e.g. *Dryopithecus, Sivapithecus*) were also not included as only those taxa deemed necessary to root major crown clades were included (See discussion above).

2.1.3.1 *Oreopithecus*

Oreopithecus bambolii is a late Miocene ape from Italy. It has been one of the more contentious fossils since it was first described (Gervais, 1872). This taxon has been suggested to be a cercopithecoid (Gervais, 1872; Gregory, 1922; Simons, 1972; Szalay and Delson, 1979; Riesenfeld, 1975; Rosenberger and Delson, 1985), stem hominid (Forsyth Major, 1880; Schwalbe, 1915; Harrison et al., 1991; Harrison, 1986; Sarmiento, 1987; Andrews et al., 1996; Cameron, 1997; Harrison & Rook, 1997; Begun, 2007) and basal hominin (Hürzeler, 1954, 1960; Strauss, 1963). It has been suggested to be similar to *Nyanzapithecus* (Harrison, 1986; Kunimatsu, 1992, 1997; McCrossin, 1992), which could also push it into the stem catarrhines (Gamarra et al., 2016). Despite a long history of contentious debate, consesnsus now rests on inclusion of *Oreopithecus* within Hominoidea (Harrison & Rook, 1997; Begun, 2002, 2007; Susman, 2005; Gamarra et al., 2016).

Oreopithecus possesses a long forelimb and short hind limb with a mobile hip and grasping foot well adapted to climbing and suspensory behaviors (Jungers, 1988, 1990; Sussman, 2005; Begun, 2007). Given that these postcranial similarities linking *Oreopithecus* to extant hominoids, recent researchers concur that this taxon should be included within Hominoidea (Stern and Jungers, 1985; Susman, 1985, 2005; Harrison, 1986, 1987, 1991; Harrison & Rook, 1997; Sarmiento, 1987, 1988; Rose, 1988, 1993; Fleagle, 1988; Senut, 1989; Martin, 1990; Begun, 2002, 2007). Craniodental morphology is more difficult to interpret with highly autapomorphic cranial features related to powerful chewing combined with cranial morphology including a small neurocranium that may be either primitive or autapomorphic (Harrison & Rook, 1997; Begun, 2007).

The *Oreopithecus* data were collected at the Naturhistorisches Museum in Basel and included 54 specimens from 26 individuals (table 2). All regions except the pelvis were

represented. The pelvis was excluded as its preservation did not allow for accurate collection of the characters included in this analysis. The final sample includes 52.14% missing data.

2.1.3.2 *Pierolapithecus*

Pierolapithecus catalaunicus is a middle Miocene ape from Spain. It possesses many features in its thorax and forelimb indicating it practiced suspensory behaviors and orthograde postures (Moyà-Solà et al., 2004; Almecija et al., 2009). Aspects of its facial anatomy align it with the hominids, suggesting it may either be a basal member of the Hominidae or fall closer to the root of the hominoid clade (Moyà-Solà et al., 2004; Perez de los Rios et al., 2012). Others point to cranio-dental characters that more closely align it with hominines (Begun et al., 1997; Begun and Ward, 2005; Begun et al., 2012). A mix of primitive hominoid and derived hominid characters across the skeleton make it a likely early member of the Hominidae (Moyà-Solà et al., 2004, 2009; Casanovas-Vilar et al., 2008, 2011).

Pierolapithecus material was studied at the Institut Catalá de Paleontologia. All material belonged to a single partial skeleton (IPS-21350). The sample comprised 14 specimens including: 1 partial cranium, 2 metacarpals, 7 carpals, 1 metatarsal and 3 tarsals (table 2). It included 90.94% missing data.

2.1.3.4 *Proconsul*

Proconsul includes as many as seven species: *P. africanus, P. heseloni, P. nyanzae, P. major, P. meswae, P. legetetensis* and *P. gitongai* (Pickford et al., 2009; McNulty et al., 2015; Harrison, 2010). However, some researchers prefer to allocate the latter four species to *Ugandapithecus* (Senut, 2000; Pickford et al., 2009), while others do not recognize *P. legetetensis* and propose *P. africanus* should also be included among these species, retaining *Proconsul* for this group and placing *P. heseloni* and *P. nyanzae* in the new genus *Ekembo*

(McNulty et al., 2015). This analysis will include *P. africanus*, *P. heseloni, P. nyanzae and P. major* from the early Miocene of Kenya and Uganda, because these are the best-represented taxa and allow inclusion of the most morphological characters. *P. africanus* is poorly sampled, but is included as the type species with 79.80% missing data.

Proconsul species are medium to large bodied catarrhines from the early and middle Miocene of Kenya and Uganda. *P. africanus*, the type species for the genus, was first described by Hopwood in 1933. This species, known from the early Miocene of western Kenya, is comparable in age to *P. major* at 19-20 Ma (Pickford, 1981). It is medium sized, ~9-15kg (Rafferty et al., 1995; Ruff, 2003), making it smaller than its contemporary *P. major* –the largest bodied *Proconsul* species, estimated at approximately 60-90kg (Harrison, 1982; Rafferty et al., 1995; Ruff, 2003). *P. major* is found at localities in eastern Uganda and western Kenya. The large body size and configuration of the proximal femur of *P. major* led researchers to suggest it may be different enough to be placed within its own genus (Senut et al., 2000; Pickford et al., 2009; McNulty et al., 2015). Further exploration of the *Proconsul* hypodigm identified dental synapomorphies shared by *P. major* with *P. gitongai, P. meswae* and *P. legetetensis*, leading some to suggest these taxa should be given that their own genus: *Ugandapithecus* (Senut et al., 2000; Pickford et al., 2009).

P. heseloni is well known, with multiple partial skeletons. This species may be younger than *P. africanus* and *P. major*, dating to 17.0-20 Ma (Peppe et al., 2009; McCollum et al., 2013; McNulty et al., 2015). It is similar in body size to *P. africanus* and smaller than the contemporaneous *P. nyanzae* (~20-50kg) (Rafferty et al., 1995; Ruff, 2003). Both *P. heseloni* and *P. nyanzae* are known from Rusinga and Mfwangano islands in Kenya (Drake et al., 1988). McNulty et al. (2015) combine these two taxa into the new genus *Ekembo* based on a suite of

dentognathic characters (Harrison, 2010) including: lacking the derived blade-like canine morphology present in other *Proconsul* taxa, molars that are more bunodont with inflated occlusal crests that contribute to the cusps themselves, reduced heteromorphy of the premolars and vertical inclination of the planum alveolare. Many of these characters were used by Senut and colleagues (2000) to distinguish between *Proconsul* and *Ugandapithecus*—though differing in the taxonomic designation of *P. africanus.*

Material was studied at the Kenya National Museum in Nairobi, with additional *P. major* material studied at the Uganda National Museum in Kampala and type specimen data collected from the British Natural History Museum in London. Data were collected from a total of 65 specimens and 177 individual elements (table 2). As only characters for which *Proconsul* data were present were included in the final data set, 100% of characters were sampled across all *Proconsul* species. *P. heseloni* is the best represented, with only 10.40% of characters missing.

Table 3. Summary of character sampling
Percentages refer to percent of the total sample. AlloOrdered characters are those characters that were influenced by allometric affect and were recoded into metric characters using the general allometric method

	Total	total%	Continuous	Cont%	AlloOrdered	AlloOrd%	Ordered	Ord%
Cranium	99	12.13	6	6.06	36	36.36	57	57.58
Mandible	38	4.66	4	10.53	26	68.42	8	21.05
Forelimb	164	20.10	126	76.83	6	3.66	32	19.51
Manus	216	26.47	164	75.93	25	11.57	27	12.50
Pelvis	45	5.51	24	53.33	10	22.22	11	24.44
Pes	254	31.13	159	62.60	80	31.50	15	5.91
total	**816**	**100.00**	**483**	**59.00**	**183**	**22.00**	**150**	**18.00**

2.2 MORPHOLOGICAL DATA

Comprehensive, objective and unbiased character sampling must be a central tennet of a rigorous phylogenetic analysis. “Comprehensive” becomes a difficult value here and in any morphological analysis given how time intensive morphological sampling is. No analysis may

ever be able to be completely comprehensive in describing all morphological variation, leaving researchers to make choices in how they prioritize sampling. Sampling superficially across the entire skeleton is one manner of being comprehensive. This is the most applied mehod within paleoanthropology, though it requires prioritizing some characters over others within morphologic regions. Instead of choosing to limit sampling by some means of character selection within regions, this dissertation limits sampling by region only, striving to collect as much variation as possible within included regions as an alternate means of attempting to limit character selection bias. While both of these methods are ultimately vulnerable to character selection bias it is for different reasons. The method of character selection presented here is novel and suffers from different biases, but by approaching the problem of selection bias in a different manner it confronts the question of the phylogenetic position of *Proconsul* with an entirely unique data set. This method does limit the regions of the skeleton that may be sampled and results must be considered in terms of what regions were the focus of analysis.

Four morphological regions were sampled in this analysis: the skull, forelimb, pelvis and foot. While sampling across the full skeleton would be ideal, given that the level of morphological detail and the broad sampling of taxa needed to generate statistically robust results, it was necessary for practical purposes to limit the regions sampled. Particular attention was paid to anatomical regions represented in *Proconsul*, with fewer characters included from other regions. These morphological regions were chosen as they have previously been found to be phylogenetically informative among catarrhine primates (Napier and Davis, 1959; Lewis, 1972; Szalay and Delson, 1979; Rose, 1983, 1992; Andrews, 1985; Beard, 1986; Szalay and Langdon, 1986; Ward, 1992, 1997, 2007; Dunsworth, 2006; Almecija et al., 2009) and because they are functionally disparate, representing four distinct structural-functional complexes (Table

3). The cranium and mandible are essential to include as this suite of morphology that plays a central role in species definitions, catarrhines exhibit a range of variation in their crania that is conducive to species designation (Begun, 1997; Young and MacLatchy, 2004; Rae, 1999, 2004; Zalmout, 2010). The forelimb has been central to debate concerning the phylogenetic position of *Proconsul,* with particular focus given that to the elbow (Napier and Davis, 1959; Andrews, 1985; Rose, 1988; Benefit and McCrossin, 1995; Rae, 1999; Gebo, 2009) and wrist (Lewis, 1972, 1989; O'Connor, 1975; Beard, 1986; Rose, 1992; Móya-Solá, 1999; Richmond, 2006). While the hindlimb is not as well represented for *Proconsul* as other anatomical regions, there are a number of specimens from the pes. The pelvis has also played an important role in the *Proconsul* debate, particularly concerning the evolution of ischial callosities (Ward, 1993; Harrison and Sanders, 1999) and is a region that may be easily added with few elements making data collection manageable. Certainly, there are other regions (notably the vertebral column) that have been implicated as being central to debate concerning the phylogenetic position of *Proconsul* (especially loss of the tail) (Ward 1993; Sanders & Bodenbender, 1994), however incorporating additional anatomical regions would be impractical given the priority of comprehensive sampling within included regions. The vertebral column in particular could not be included along with the carpus and tarsus for this project to be completed in a timely fashion. Incorporating vertebral morphology in the future would be a priority. Dentition was excluded from the analysis for similar reasons related to time constraints and the priority not to cherry pick characters. Again, if it were possible to collect data from every morphological region, that would be preferable. The justification for excluding the dentition is additionally due to the recognition that hominoid dentition is symplesiomorphically similar to stem catarrhines in many ways (Gregory, 1922; Von Koenigswald, 1968, 1969) and as a result the dentition may not be as

informative as other regions (e.g. the forelimb, carpus, pelvis) concerning the three hypotheses being tested in this analysis. While lack of inclusion of dental characters may complicate placement of the fossil cercopithecoid *Victoriapithecus* in phylogenetic analyses any confounding effects may be avoided simply by constraining this taxon to fall within Cercopithecoidea based on the previous work that has been done incorporating the dentition (Szalay and Delson, 1979; Benefit, 1993, 1999; Miller et al., 2009). Cherry picking individual characters from other regions not included in the analysis simply because they have been inferred in the past to be phylogenetically informative conflicts with the methodological perspective taken in this dissertation.

If analyses reevaluate the same hypotheses without significantly changing character lists and recapitulate previous results, the question remains is it simply the same data telling the same story? For difficult phylogenetic questions, with low confidence in results, rerunning the same data sets may not be sufficient to improving on previous analyses. Particularly given a taxon such as *Proconsul* with a long history of debate concerning its phylogenetic position, the exercise of rerunning analyses must be sure that it is not simply inputting the same data into updated algorithms. There can be no surprise in such cases if results are consistent. In order for this dissertation to add to the literature, it is important to strive to consider the data in a different way. Analyzing only or a majority of characters that have previously been the focus of similar studies would not be as valuable. The character list considered here differs significantly from the characters more commonly used to address these questions. If analyses infer the same results, then it introduces new characters and greater confidence. If results differ it encourages further exploration of these hypotheses and provides insight as to the possible morphology driving conflicting results.

2.2.1 Measurement techniques

Two types of data were collected: metric and non-metric. Metric data were collected as linear measurements using sliding calipers. Measurements describing length along a curved surface were collected using waxed string and then measured flat. For non-metric characters, a range of character states was defined based on observed variation.

2.2.2 Character selection

Characters were selected for inclusion based on comparisons of extant anthropoid taxa. Characters for which differences were observed between taxa and which could be consistently measured were included in the analysis. Many metric characters recorded the same morphology (e.g., measurements from articulating facets). It is clear that many of these characters are non-independent. However, at this stage, there was an attempt to minimize decision-making based on presumed integration. The character list was constructed recognizing there would be non-independent characters that would need to be evaluated at a later stage (see chapter 5).

Both metric and non-metric characters are included in the character list, though where possible morphology was described using metric characters as they are subject to less individual decision making than non-metric characters. Non-metric characters were used when there was not a reliable way to capture the morphology with linear measurements. Non-metric data were collected systematically, and there was no attempt to limit the number of non-metric characters that could not be collected as metric.

The final character list (table 3) included 816 characters distributed as follows: 150 (18%) non-metric, 666 (82%) metric, 137 (16.79%) cranio-mandibular, 164 (20.1%) forelimb (without manus), 216 (26.47%) manus, 45 (5.15%) pelvis, 254 (31.13%) pes [See appendix A for descriptions of all characters].

Due to unequal sampling between regions, particularly driven by the large number of individual bony elements in the hand and the foot, making up 57.6% of the total character list, it is essential that regions be evaluated separately. The great number of characters drawn from these regions is a result of the complex morphology particularly of the carpus and tarsus, with many bones and articulating facets. Combined analyses must be evaluated for whether individual regions are driving results and, if results from regions differ, further evaluation may be necessary.

The unconventionality of this data set should be seen as a benefit to expanding the body of evidence commenting on the hypotheses addressed in this dissertation. No matter what morphological region is being considered it is unlikely to lack variation supporting or at least congruent with the evolutionary history of the species. There is not reason to expect a phylogenetic analysis of the hand to be less informative than analyses of the cranium or dentition. Each region shares the evolutionary history of the species and will reflect this in one way or another. It is not the intention of this dissertation to suggest morphological regions not included in this analysis will return the same result. Analyses presented here must be interpreted in the context of previous analyses and certainly a discussion of the morphological regions not present here will be essential to making any convincing argument supporting an optimal hypothesis.

2.2.3 Metric character handling

When dealing with metric data there are two main issues that must be overcome: (1) comparing the morphology of specimens that are not the same size; and (2) converting continuous metric data into discrete categorical data.

2.2.3.1 Allometry

The first issue is relatively easy to solve in complete data sets, where the geometric mean of all measures is the preferred method for accounting for size differences (Jungers et al., 1995). This is, however, rarely possible when dealing with the fossil record. In order to accommodate missing data (and therefore fossil taxa) and retain as many characters per taxon as possible, all metric characters (for both extant and fossil taxa) were divided into cranial and postcranial data sets. Species means for the cranial data set were divided by the species mean of orbit height, which has been shown to be strongly correlated with body size (Spocter and Manger, 2007). The postcranial data set species means were divided by the species mean for transverse width of the trochlea on the talus (Tsubamoto, 2014; Yapuncich et al., 2014, 2015). Dividing by these body size proxies standardizes the data set, but does not account for allometric effect. In order to remove allometric affect as much as possible metric characters must be further evaluated for correlation with a body size proxy. In order for this to be most effective, the chosen body size proxy should be the best available among extant taxa that does not reflect locomotor mode (Ruff, 2003) and ideally will be from a region not included in the analysis in order to limit removing characters that may be correlated with the character for reasons other than allometric affect. This test of allometric affect was only performed using extant taxa due to the difficulties of missing data among fossil taxa. Ruff (2003) demonstrated that the medio-lateral breadth of the tibial plateau is a good predictor of body mass regardless of locomotor adaptations, making it a suitable proxy for body size. Body size is known to have a phylogenetic signal, resulting in the possibility that characters may appear to be correlated with a body size proxy simply due to phylogenetic inertia (Clutton-Brock and Harvey, 1979; Garland and Huey, 1987; Pagel and Harvey, 1988, 1989; Harvey and Pagel, 1991; Ackerly & Donoghue 1998; Garland & Ives,

2000). This makes a simple correlation analysis problematic as it is unable to distinguish between allometric affect and body size as a phylogenetically informative character. To overcome this difficulty, it is necessary to incorporate phylogeny as a model into correlation analyses. Phylogenetic independent contrasts do just that. Instead of simply considering the correlation between body size and a continuous character, the difference between character states of sister taxa ("contrasts") are used, weighting differences between taxa by relatedness. These contrasts then reflect variation, but remove inherent non-independence due to phylogeny. Contrasts then may be used for statistical analyses, in this case determining correlation between characters and body size (Felstenstein, 1985; Harvey & Pagel, 1991; Garland et al., 1992).

Results from the phylogenetic independent contrasts analysis identified 183 characters that were strongly and significantly correlated with the body size proxy (medio-lateral breadth of the tibial plateau) (table 3). These size corrected characters were then recoded into discrete character states following the general allometric coding method (Gilbert et al., 2009). This method removes allometric effect by regressing each size standardized character against a measure of body size and then coding them as binary, falling either above (1) or below (0) a best fit line. This indicates whether the character is large or small relative to average body size for the species, therefore removing any residual allometric effect. Breadth of the tibial plateau was used for consistency with the previous PIC analysis as an initial step and was compared with regression against body size estimates taken from the literature (Rowe and Fleagle, 2013) for inclusion of fossil taxa lacking proximal tibia. Coding did not differ between body size measures.

2.2.3.2 Discretization and Continuous Characters

Discretizing metric data in a non-arbitrary way is problematic. Many methods have been proposed to discretize data (Mickevich and Johnson, 1976; Simon, 1983; Archie, 1985; Thiele,

1993), but all suffer from the problem that the categories produced may not be biologically meaningful. Particularly problematic is that these methods have a tendency to arbitrarily over-weight character state changes based on the spread of variation across a group of taxa (Farris, 1990). Goloboff et al. (2006) implemented a method for treating continuous characters as additive and ordered, following Farris' (1970) original algorithm and avoiding many of these difficulties. Treating characters as additive and ordered (a reasonable assumption for continuous characters) simply assumes a character state measuring a length of 3, also encompasses that of 2 and 1, equaling the sum of these lesser character states. Farris' algorithm (1970) was designed to treat characters in intervals—the difference between values. Following with the example above, if taxon A has a character state of 3 and taxon B has a character state of 1, the algorithm would calculate an interval of 2 separating these taxa. Given only these data, a parsimony model of minimum evolution would infer a character state of 2 for the ancestral node, with an increase in length 1 along the branch leading to taxon A and a decrease in length 1 on the branch leading to taxon B (Farris, 1970; Goloboff, 2006). In this way, continuous traits are never divided into discrete character states and morphological evolution is modeled not in terms of 'is taxon A morphologically the same as B,' but instead considers the degree of difference between A and B (whether that's 5mm or 0.01mm), optimizing phylogenies that infer sister group relationships between taxa appearing the most similar to eachother. The only barrier to direct application of this method to continuous data sets was implementation, a problem solved with TNT: Tree analysis using new technology (Goloboff et al., 2003; Goloboff, 2006). This provides, arguably, the best method for dealing with continuous data as it avoids the problems of discretization, but may only be implemented applying the parsimony optimality criterion. Due to this limitation, continuous characters were also discretized using gap weighting for inclusion in the Bayesian

phylogenetic analysis (Thiele, 1993). All gap weighted characters were treated as ordered and divided into three character states as this is the modal number of character states for other ordered characters in the data set. This dual approach will allow for data to be analyzed using both Bayesian and parsimony optimality criteria. As it is still ideal to treat continuous characters as such (Goloboff, 2006), the parsimony analysis will apply this method, but will also run an analysis on the gap weighted data in order to evaluate whether discretization significantly alters results.

2.2.3.3 Missing data

Any analysis including fossils must take into account that data sets will not be complete. Missing data can have a serious impact on phenetic analyses, particularly principal component analyses, which rely on having complete data sets in order to summarize variation across all variables. Unlike phenetic analyses, phylogenetic analyses consider variation on a character by character basis. Missing data will mean that a taxon or specimen is silent regarding the missing character change and will adopt the optimal character state given its sister taxa. This may affect the degree of resolution, support and number of shortest trees (Gauthier, 1986; Nixon and Davis, 1991; Platnick et al., 1991; Nixon and Wheeler, 1992; Maddison, 1993; Wilkinson and Benton, 1995; Gao and Norell, 1998), but will not negatively affect results (Novacek, 1992; Wiens, 1998, 2003a,b, 2005, 2006; Wiens and Moen, 2008; Prevosti and Cheminquy, 2010). The exception is in cases where there are few characters to begin with. The effects of missing data are not related to how many missing data there are, but instead to how many characters there are in the analysis overall (Prevosti and Checmisquy, 2010). Extensive character sampling is therefore essential to any phylogenetic analysis incorporating fossil taxa with large amounts of missing data. Sampling as many morphological characters as can practically be collected should be the goal of

any morphological analysis aimed at inferring phylogenies, but sampling at this level is rarely if ever possible. Researchers must make decisions about what morphology to include and what must be left out. While some researchers carefully select characters and test their data sets in order to identify which characters may be best suited to their phylogenetic questions, winnowing character lists to a curated few (Pilbeam, 1996; Poe and Wiens, 2000; Zalmout et al., 2010; Worthington, 2012; Dembo et al., 2015), this analysis takes the opposite approach. Careful character selection has proven more of a hindrance than a help to inferring well-supported, fully resolved phylogenies (Novacek, 1992; Wiens, 1998, 2003a, 2006; Wiens and Moen, 2008; Prevosti and Cheminquy, 2010; Wiens and Tiu, 2012). This analysis takes those results as a driving principle and includes many characters from a limited number of regions in order to minimize the effects of missing data and avoid cherry-picking characters. While this reasoning could allow for broader taxonomic sampling as well, this analysis prioritizes focus on *Proconsul,* limiting the possibility of confounding variation from stem catarrhine taxa and only including Miocene crown taxa whose membership within Hominoidea or Cercopithecoidea is uncontested.

2.3 MOLECULAR DATA

Molecular data are included in this analysis in order to more confidently infer the phylogenetic relationships of extant taxa, infer divergence dates and incorporate as much available data as possible to more confidently address evolutionary questions. All molecular data were taken from Perelman et al. (2011). This data set includes 34,927 base pairs from 54 genes. Their alignment of the molecular data was used for the analysis (Perelman et al., 2011). Including molecular data in analyses focused on fossil specimens integrates both types of evidence in a data driven manner without applying a priori constraints.

Morphological data from fossils, often with substantial missing data, may be incorporated into analyses of morphological and molecular data from extant taxa, thereby integrating information from the fossil record into a substantial character list that will likely avoid the pitfalls of significant amounts of missing data (see discussion above). It is now commonplace for morphological phylogenetic analyses focused on fossil taxa to incorporate results from molecular phylogenies (Eernisse and Kluge, 1993; Shaffer, 1997; Kluge, 1998; Egge et al., 2009; Magallon et al., 2010; Wiens, 2010; Lopardo et al., 2011; Pyron et al., 2011; Ronquist et al., 2012; Wood et al., 2013; Arcila et al., 2015; Zhang et al., 2015), but true total evidence analyses remain uncommon in the primate literature. Including morphological data into molecular analyses, however, has been shown to potentially improve results, particularly in reconstructing crown groups with many extinct taxa. While the outcome of analyses incorporating a molecular backbone may not differ from results in which morphological and molecular data are analyzed in a single character matrix (Page, 1996: Rieppel, 2009), conducting the analysis including both character types allows for the possibility that morphological data may affect the molecular result and therefore considers a wider range of possible phylogenies. Given these potential benefits (Kluge, 1989; Kluge and Wolf, 1993; Eernisse and Kluge, 1993; Barrett el al., 1991; Shaffer, 1997) and the straight forward application of this more rigorous methodology, total evidence was deemed desirable to any other method for combining data types.

CHAPTER 3: PHENETIC ANALYSIS

As an initial step, this chapter will address the question: Where does *Proconsul* fall relative to other catarrhines using phenetic morphological similarity? While phenetic methods cannot explicitly test any of the phylogenetic hypotheses in this dissertation, the resulting visualizations of variation provide an initial exploration of the data set that will help with interpretation of the phylogenetic analyses. This will be accomplished through a series of principal component analyses.

3.1 METHODS

Principal component analyses summarize patterns of covariation in multivariate data sets by rotating and flattening data in order to reduce dimensionality (Sokal and Rohlf, 2012). As this dissertation is focused on the position of *Proconsul* among crown catarrhines, only extant crown catarrhine taxa were used to define axes of variation; fossils were projected into this space using the eigenvector matrix derived from extant taxa. As principal component analyses are unable to handle missing data, only those fossils with the least missing data were included: *Epipliopithecus*, *Victoriapithecus and P. heseloni*. Missing values cannot be included in principal component analyses, so where missing data were minimal enough to still include the taxon in the analysis (25% or less) values were taken from closely related taxa. As *Aegyptopithecus* and *Epipliopithecus* are included in analyses as indicative of basal catarrhine morphology, where there were missing data in *Aegyptopithecus* the *Epipliopithecus* value was substituted in order to complete the data set; therefore, the position of this taxon should be judged as reflecting basal catarrhine morphology. The same logic was applied for missing

characters in *Victoriapithecus.* As *Victoriapithecus* is being included in order to root basal catarrhine morphology and not to evaluate the morphological affinities of this taxon missing values were replaced with the average across all cercopithecoids. Missing values in *P. heseloni* were taken from other *Proconsul* taxa. Only characters that were present in at least one *Proconsul* species were included in PCAs. Species means of size corrected data (see previous chapter) were used for all continuous characters and modes were used for discrete characters. Where males and females were not evenly sampled, mean values were calculated for each sex and then male and female means were averaged together for the final species mean. While species means may not reflect biological reality, there has been inadequate consideration of this issue across the phylognetetics literature. Researchers are only beginning to address this problematic and often ignored complication, with perhaps the best attempt at resolving this issue presented in Gilbert et al. (2009; Gilbert, 2013), where males and females were assigned separate characters that were then concatenated into a single character matrix. The high degree of sexual dimorphism in their sample made it an ideal test for this novel methodology and the systematics community should expand on it to become applicable to data sets (such as this) where sex determination of fossils is less straightforward. Certainly this is an issue that needs more careful consideration. It is likely that some data sets are more sensitive to issues of sex-averaging than others (Bjarnason et al., 2011). Therefore, as an initial approach to this complicated issue, cluster dendrograms were conducted using Euclidean distance analyses and a PCA was run across all characters using separate male and female means for each species. If results from this first analysis indicate males and females within a species are expressing morphology more similar to each other than to other taxonomic units, it will be deemed appropriate to apply the more conventionally supported methodology within the literature to use species means (Wiens, 2001;

Bjarnason et al., 2011); otherwise, additional steps must be taken to address sexual dimorphism in subsequent analyses.

All platyrrhines and fossil catarrhines were projected into the morphospace defined by extant crown catarrhines. Platyrrhines were excluded from this stage of analysis in order to ordinate a morphospace that was defined by differences between cercopithecoids and hominoids. Including platyrrhines in the initial analyses would ordinate axes around differences between platyrrhines and catarrhines, which would not address the questions that are the focus of this thesis. Appropriate taxonomic selection is just as important in PCAs as in phylogenetic analyses and must target the specific hypotheses being addressed (Reyment, 1991; Sokal and Rohlf, 2012). Fossil taxa were excluded for similar reasons. PCAs ordinate around the axes with the most variation (Sokal and Rohlf, 2012). Unique fossil taxa may end up driving all results as opposed to focusing on variation separating cercopithecoids and hominoids. Analyses were conducted using the correlation matrix to allow for inclusion of continuous and discrete characters and were run across the entire data set and by morphological complex: cranium, mandible, forelimb, manus, pelvis and pes. Euclidean distance matrices were calculated using the APE (Paradis et al., 2004) R package, indicating the proximity of all taxa to each other across all axes. Neighbor joining was applied on these distance matrices to visualize overall similarity using dendrograms. PCA projections were constructed in R using ggplot2 (Whickam, 2009). Regression analyses were run on the first three PCs to test for residual (allometric) correlations with body size. Medio-lateral breadth of the tibial plateau was used as a body size proxy. As only extant catarrhines were used to ordinate axes and because these taxa do not have issues with missing data, only extant catarrhines were used to test for correlation with body size.

3.2 RESULTS

3.2.1 All characters: sex separate

Principal component 1 through 3 account for 59.44% of variation (Fig. 4). PC1 alone accounts for 27.8% of variation. This PC was not significantly correlated with body size. Loadings for PCs are presented in appendix B and are comparable to results from the sex-averaged analysis and will be discussed in that section. PC2 accounted for 20.5% of variation. This axis is significantly correlated with body size with an R^2 of 0.87 ($p<0.05$). PC3 accounts for 11.2% of variation and is not significantly correlated with body size.

Figure 1. PCA sex separate- PC1 & PC2

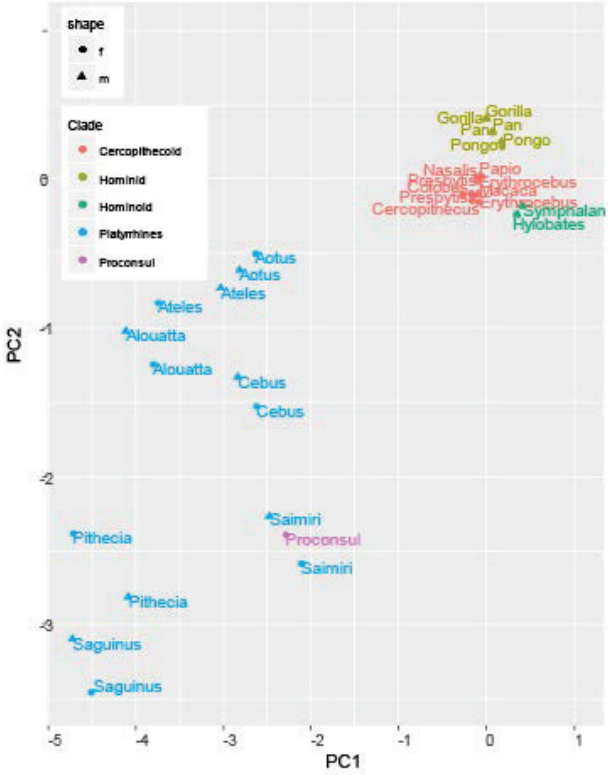

Figure 2. PCA sex separate- PC2 & PC3

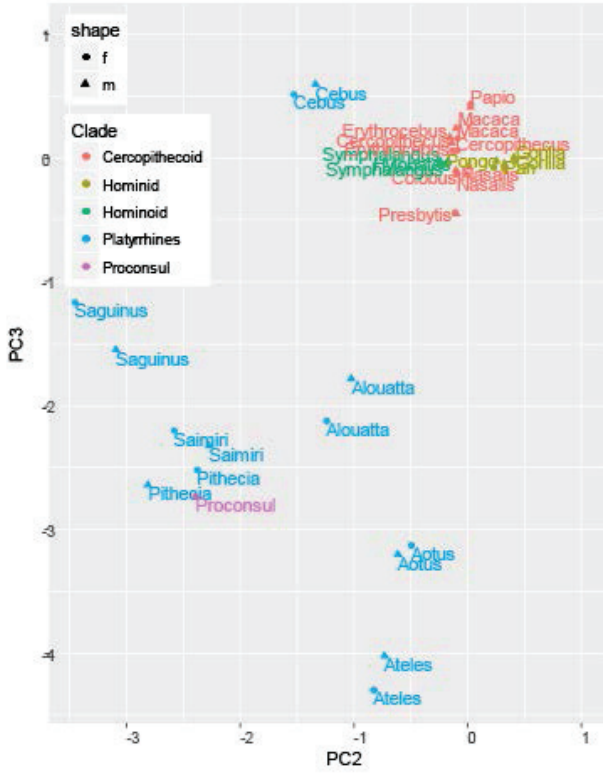

The distance matrix (Fig. 3, appendix C) indicates males and females within the same species are morphologically nearest to each other across all characters than they are to any other

species of either sex. This is taken as support to justify sex-averaging as a defensible methodology for application in subsequent analyses presented in this dissertation.

Figure 3. Cluster diagram for all data, constructed as NJ tree run on Euclidean distance matrix

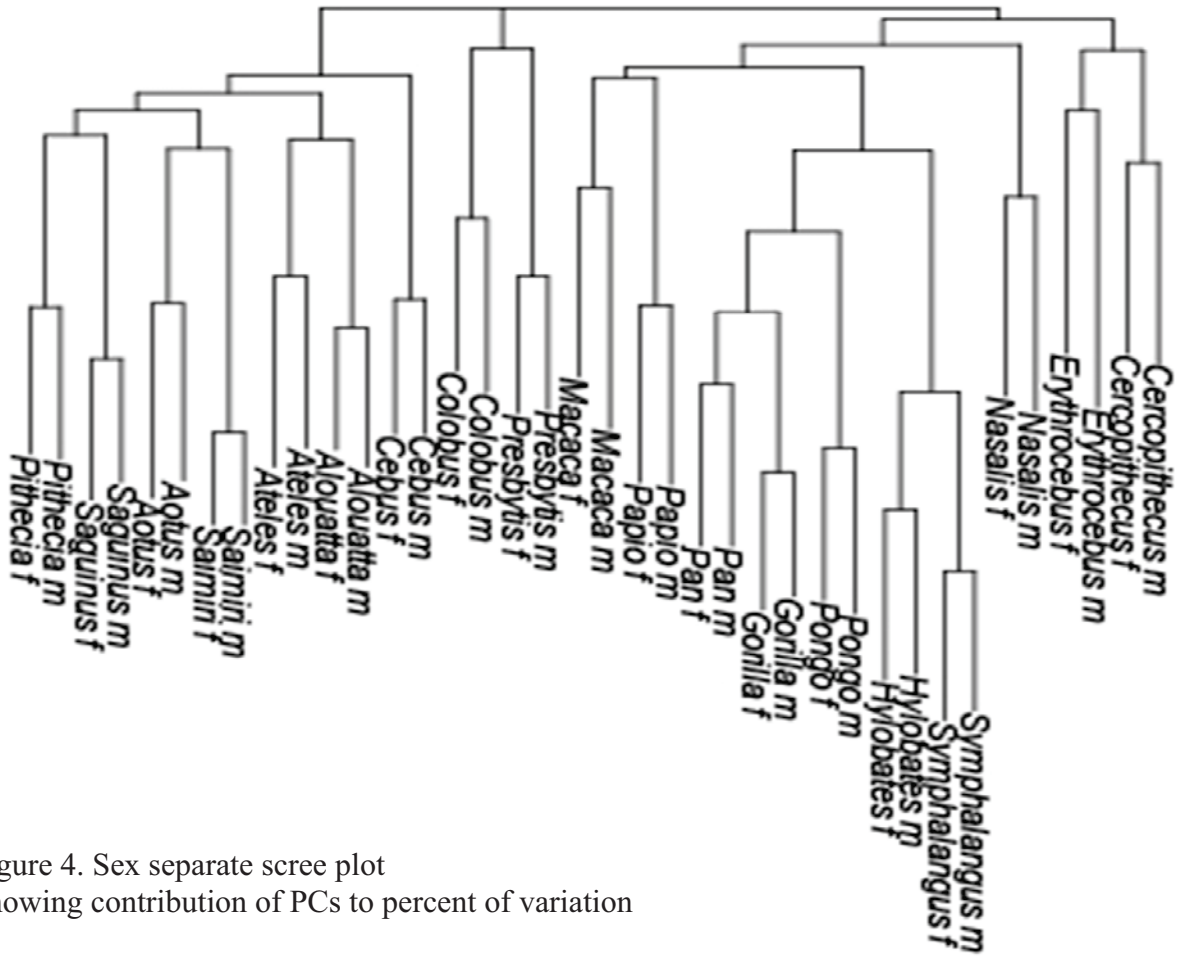

Figure 4. Sex separate scree plot
Showing contribution of PCs to percent of variation

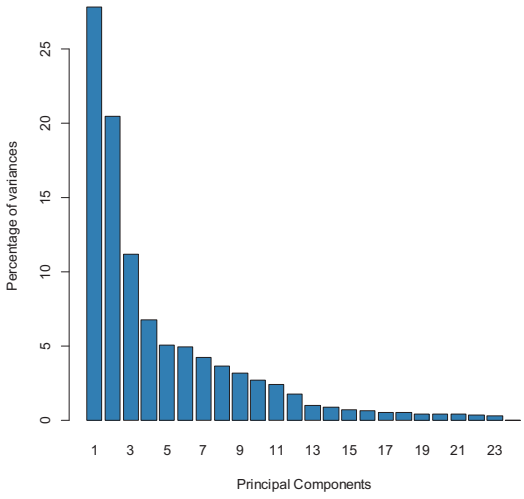

3.2.2 All characters: sex averaged

Principal component 1 through 3 account for 61.2% of variation (Fig. 8). PC1 alone accounts for 29.4% of variation. This PC was not significantly correlated with body size. Loadings for PCs are presented in appendix B. Length of the

radius was a prime driver of variation along PC1 (see appendix B for loadings). The ulna contributed a disproportionately large number of characters to the prime drivers of this axis. Morphology of the malar region also contributed substantially to this axis. PC1 primarily separates hylobatids from other catarrhines, with cercopithecoids falling closer to the platyrrhine distribution. The hominids fall intermediate between the hylobatids and cercopithecoids. *Proconsul* falls at the extreme end of the hominoid distribution.

Figure 5. PCA all characters- PC1 & PC2

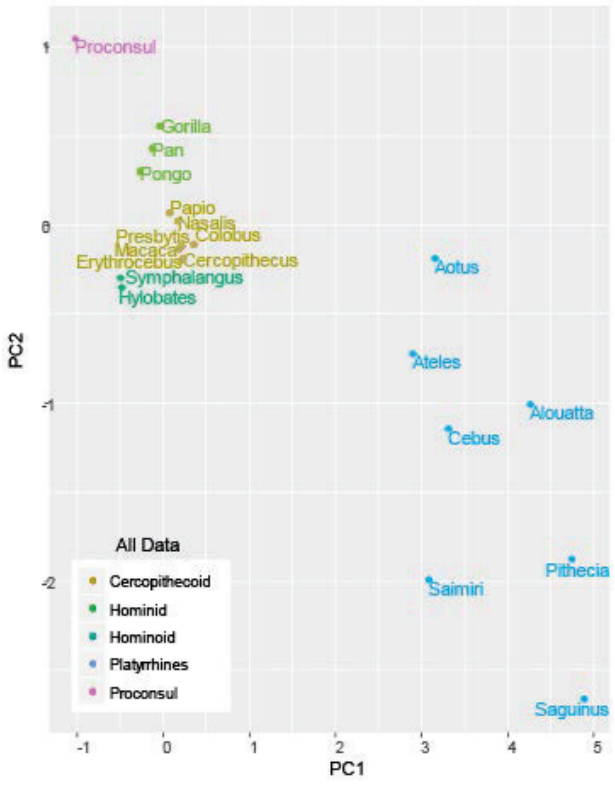

Figure 6. PCA all characters- PC2 & PC3

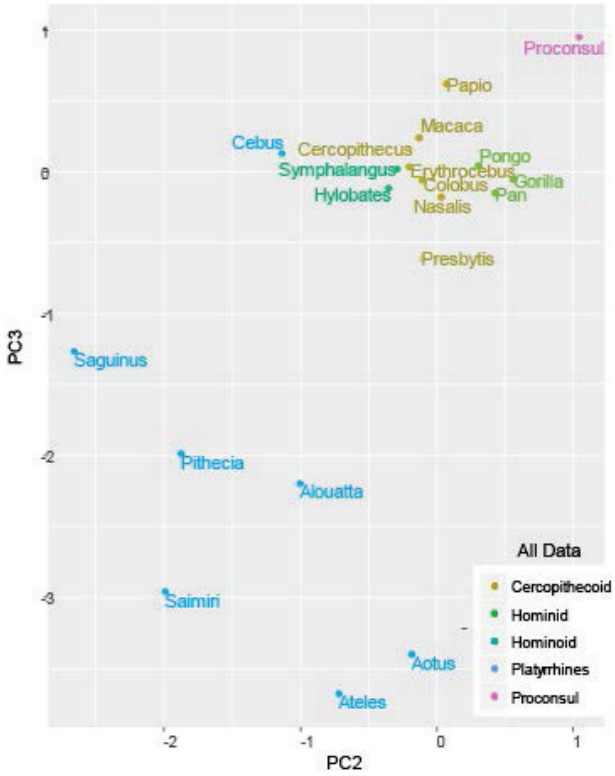

PC2 accounts for 20.3% of variation. This axis is significantly correlated with body size with an R^2 of 0.89 ($p<0.05$). Length of the radius is again a prime driver of this axis, along with orientation of the navicular facet on the lateral cuneiform. Despite the steps taken to remove body size and allometric effects, the distribution of taxa corresponds closely to the distribution for body size with few exceptions (including *Aotus, Proconsul* and *Symphalangus*). PC2

separates catarrhines from platyrrhines, with *Aotus* falling among the catarrhines. The hylobatids fall closest to the platyrrhine distribution, with cercopithecoids intermediate between hylobatids and hominids. *Proconsul* falls at the upper limit of this axis above the hominids.

PC3 accounts for 11.4% of variation and is not significantly correlated with body size. The cranium accounts for most characters primarily driving variation along this axis, including characters from the face, temporal and occipital regions. PC3 separates platyrrhines from catarrhines, with the exception of *Cebus*, which falls among the catarrhines. *Proconsul* appears quite distinctive, defining the upper end of the axis, nearest *Papio*.

Figure 7. Cluster diagram for all data, constructed as NJ tree run on Euclidean distance matrix

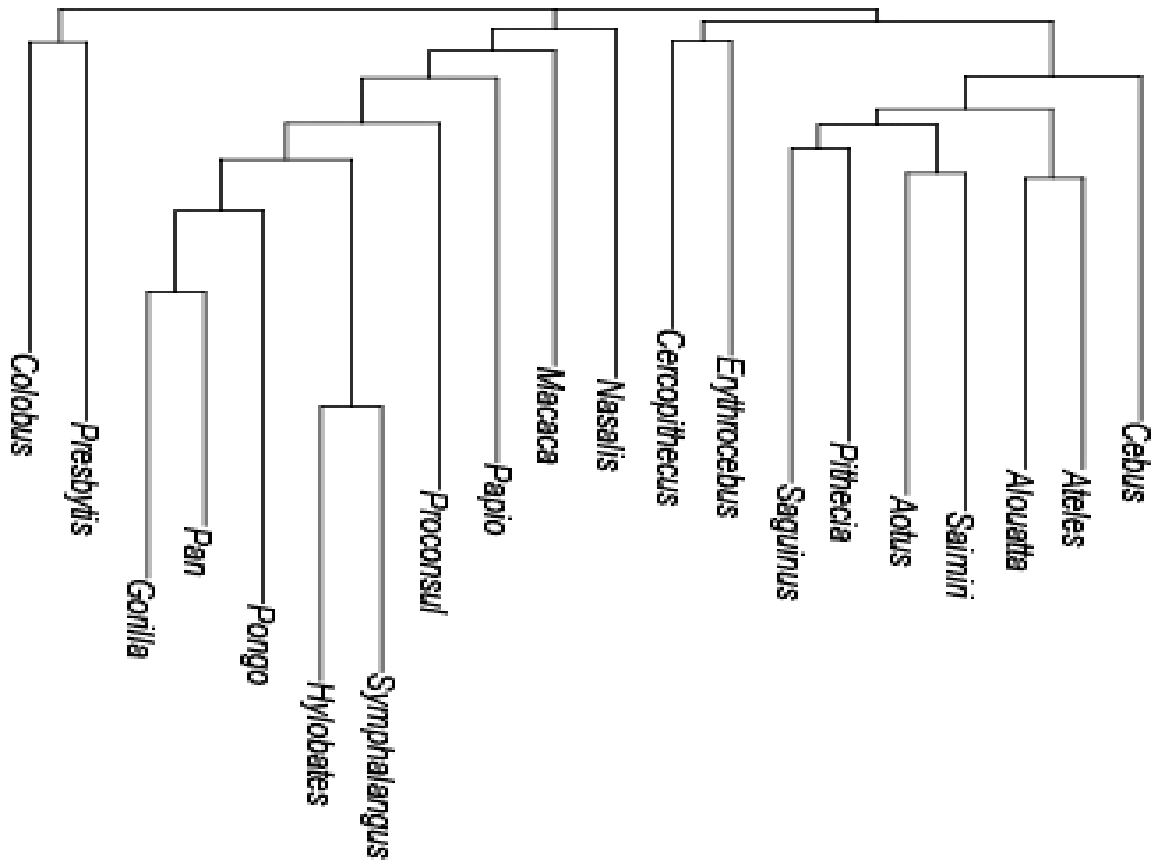

The distance matrix (Fig. 7, appendix C) accurately reconstructs hominoid relationships and places *Proconsul* as the sister to the hominoid cluster. Platyrrhines also cluster together, though the cercopithecoids are distributed across the dendrogram. Only *Cercopithecus* and *Erythrocebus* cluster together near the platyrrhines and *Colobus* and *Presbytis* also form a cluster. *Macaca, Papio and Nasalis* all group closer to the hominoids.

Figure 8. All data scree plot
Showing contribution of PCs to percent of variation

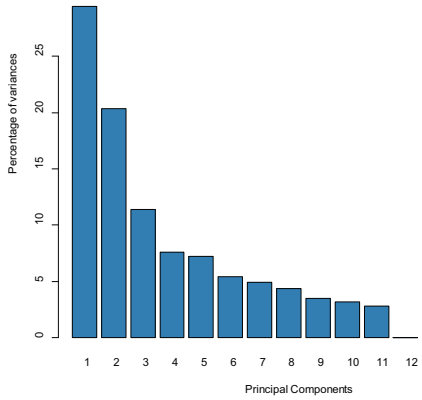

Figure 9. Cranium scree plot

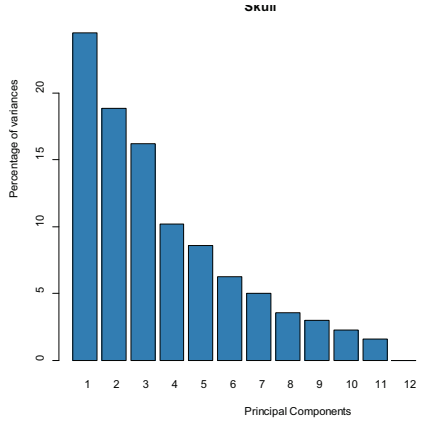

3.2.3 Cranium

The first three principal components account for 59.5% of variation. PC 1 accounts for 24.5% of variation (Fig. 9). Influential characters are concentrated in the face. PC 1 identifies *Proconsul* as highly distinctive and separates hominoids and cercopithecoids. Platyrrhines are distributed across the extant hominoid and cercopithecoid range. *Victoriapithecus* falls at the high end of the axis on the cercopithecoid side of the distribution. *Aegyptopithecus* falls in the middle of the cercopithecoid distribution.

PC2 accounts for 18.8% of variation and is not significantly correlated with body size. Morphology of the malar region is again a prime driver of variation along this axis. It clearly distinguishes platyrrhines and catarrhines, with *Victoriapithecus* defining an upper limit to the catarrhine distribution and overlapping the platyrrhines. Hominids and colobines fall

Figure 10. PCA cranial characters- PC1 & PC2

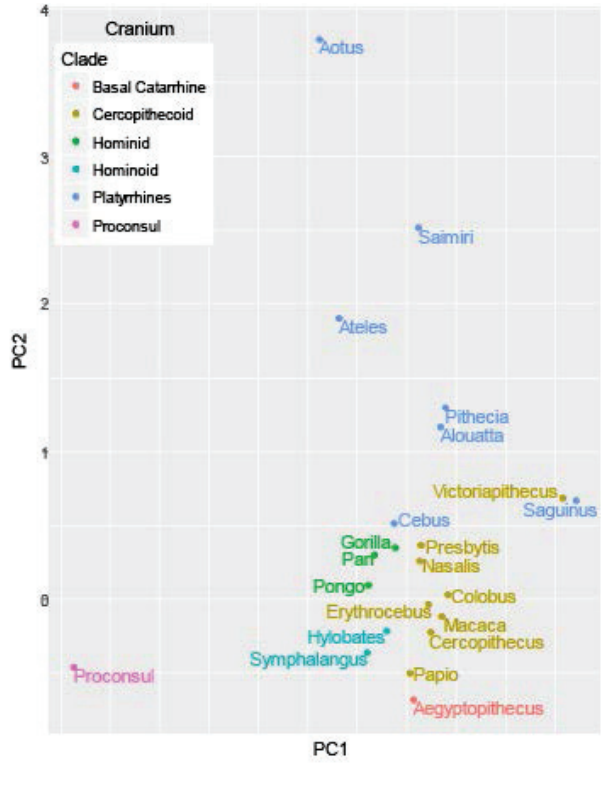

Figure 11. PCA cranial characters- PC2 & PC3

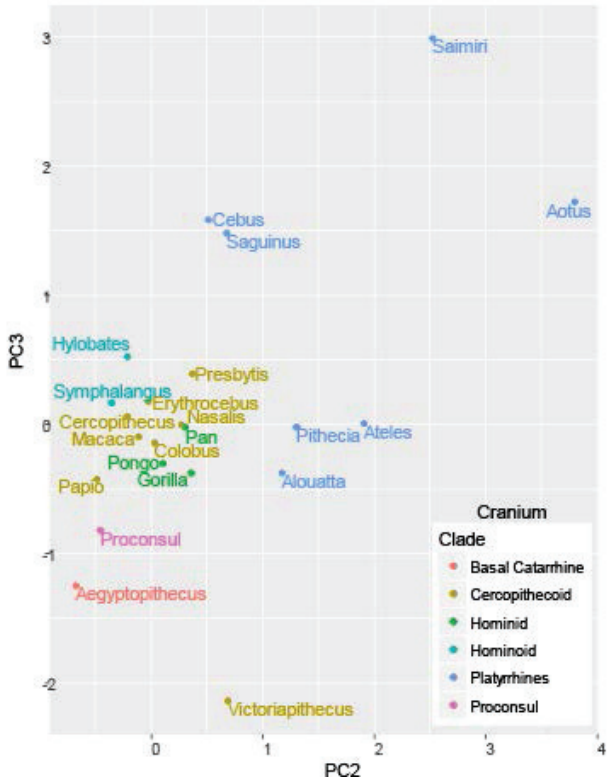

towards this upper extent as well, with cercopithecines, hylobatids, *Proconsul* and *Aegyptopithecus* falling at the low end of the axis.

PC 3 accounts for 16.2% of variation and is weakly but significantly correlated with body size, with an R^2 of 0.40 ($p<0.05$). It is driven by the morphology of the temporal lines and occipital protuberance. All fossil taxa (*Proconsul, Victoriapithecus, Aegyptopithecus)* are distinguished from extant taxa, defining the low end of the axis. The correlation of body size with this axis predicts taxa at the low end of the axis should have the largest body size, which is not the case for the fossil sample.

The distance matrix (Fig. 12) groups *Proconsul* with the hylobatids among the hominoids. *Aegyptopithecus* and *Victoriapithecus* fall closest to each other among a cluster including all cercopithecoids except *Presbytis. Presbytis* falls within the platyrrhine cluster.

Figure 12. Cluster dendrogram cranial data, constructed as NJ tree run on distance matrix

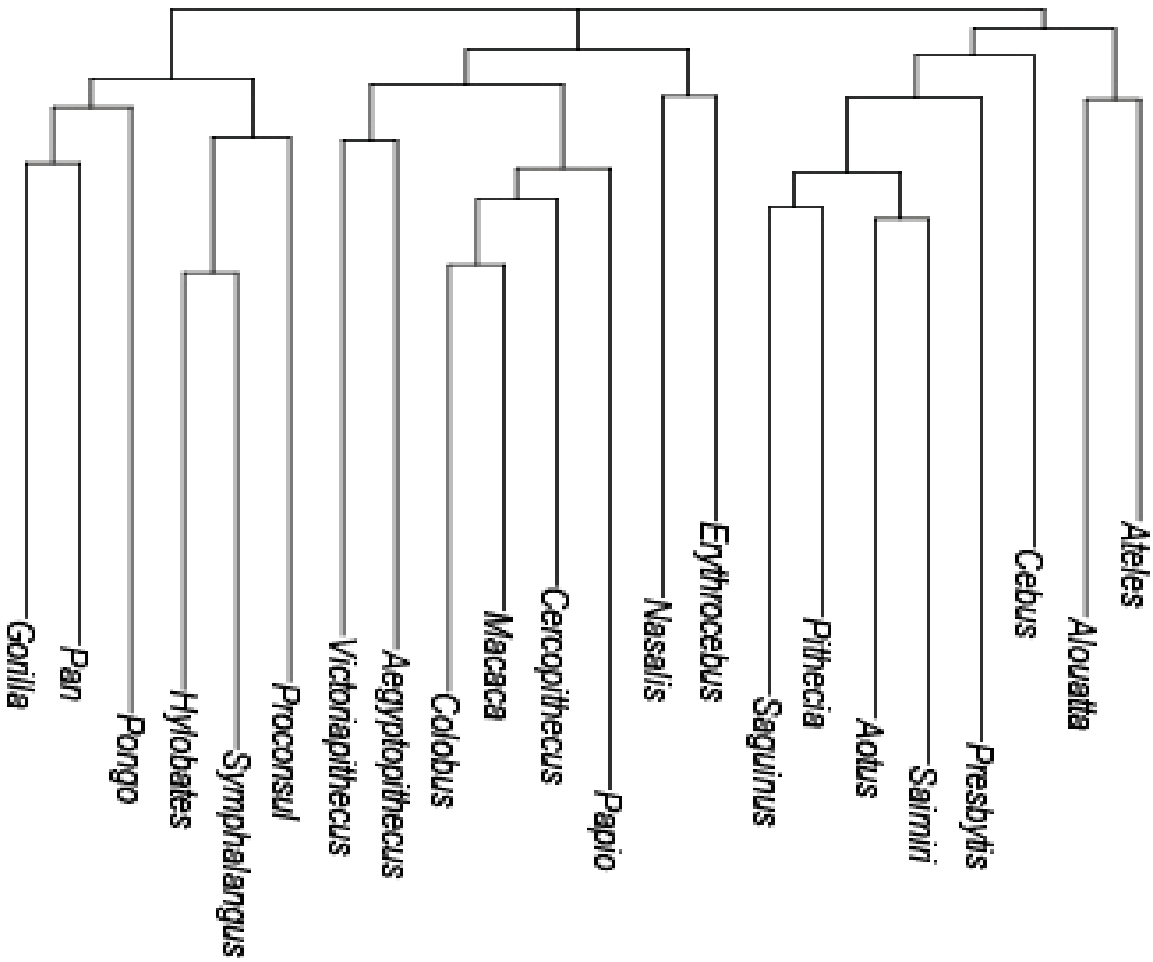

3.2.4 Mandible

The first three principal components account for 74.3% of variation. PC 1 accounts for 40.1% of variation (Fig. 16) and is significantly correlated with body size with an R^2 of 0.40 ($p<0.05$). This axis is driven by morphology of the mandibular condyle and height and width of the corpus. Extant catarrhines cluster towards the middle of the plot, with platyrrhines distributed across the axis. Hominids are located at the lower end of the extant catarrhine distribution. *Epipliopithecus* is distinctive, falling at the extreme low end of the axis.

Aegyptopithecus and *Proconsul* fall above the upper limit of the extant catarrhine distribution at the opposite end of the axis from *Epipliopithecus*.

PC 2 accounts for 21.3% of variation and is not significantly correlated with body size. It is driven by variation in the mandibular condyle, coronoid process and mental foramen. Hominids form a distinct cluster, but otherwise clades are dispersed across the axis. *Epipliopithecus* and *Aegyptopithecus* again fall on opposite ends of the axis.

Figure 13. PCA mandible - PC1 & PC2

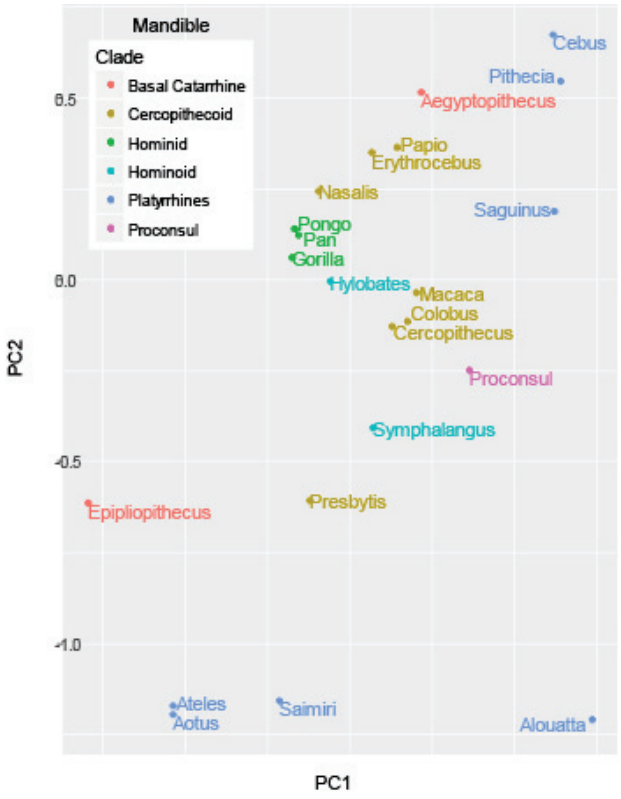

Figure 14. PCA mandible- PC2 & PC3

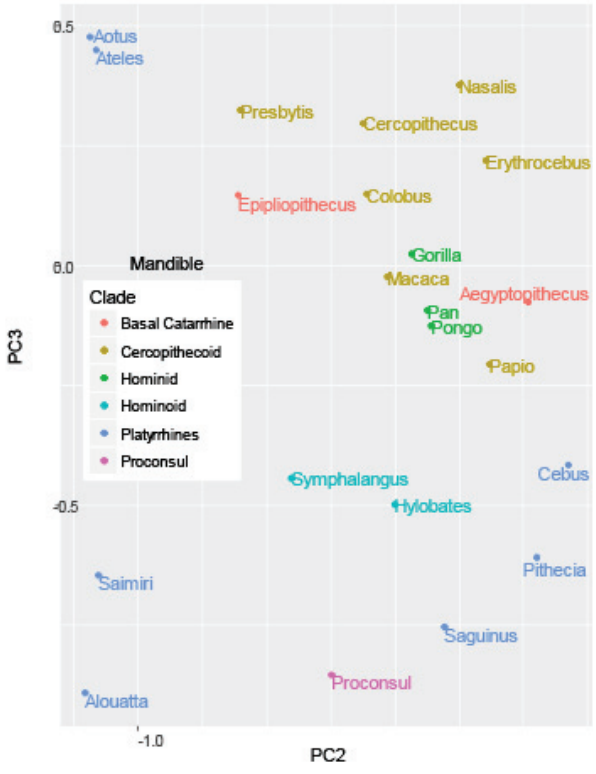

PC 3 accounts for 12.9% of variation and is not correlated with body size. This axis is driven by width across the mandible and mandibular corpus height. Extant catarrhines cluster together with the exception of the hylobatids. Platyrrhines are distributed across the axis, with all taxa falling at the low end of the axis excepting *Aotus* and *Ateles,* which define its upper limit.

Epipliopithecus and *Aegyptopithecus* both fall within the extant catarrhine distribution, though *Proconsul* falls at the extreme low end of the axis, nearest *Alouatta* and *Saguinus.*

The dendrogram also disperses clades. *Proconsul* groups with *Alouatta* and *Symphalangus*, while the hominids group with *Nasalis*. *Aegyptopithecus* and *Epipliopithecus* both group with sets of platyrrhines.

Figure 15. Cluster dendrogram for mandibular data, constructed as NJ tree run on distance matrix

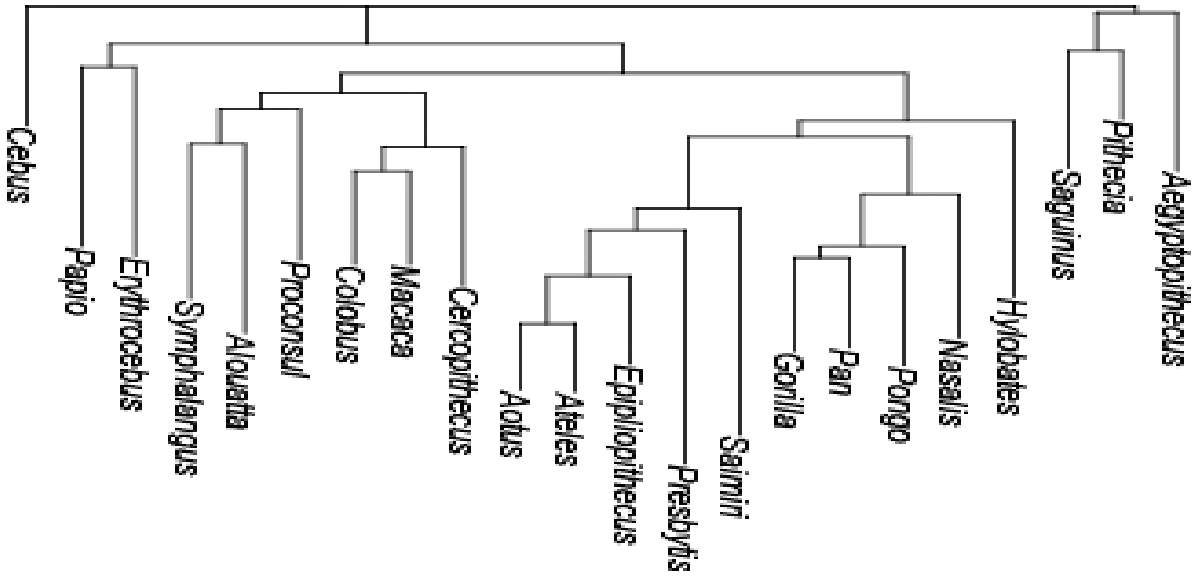

Figure 16. Mandible scree plot showing contribution of PCs to percent of variation

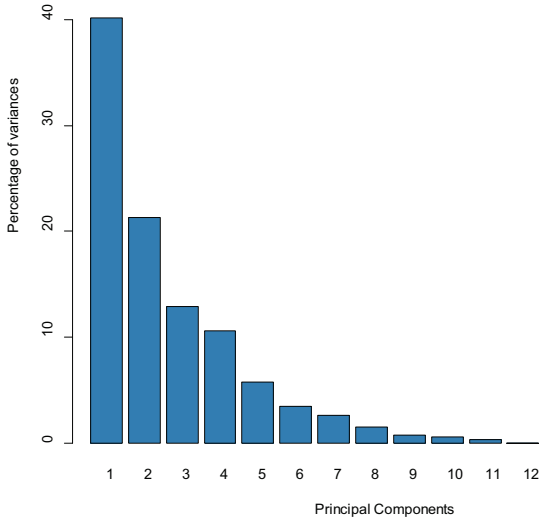

Figure 17. Forelimb scree plot

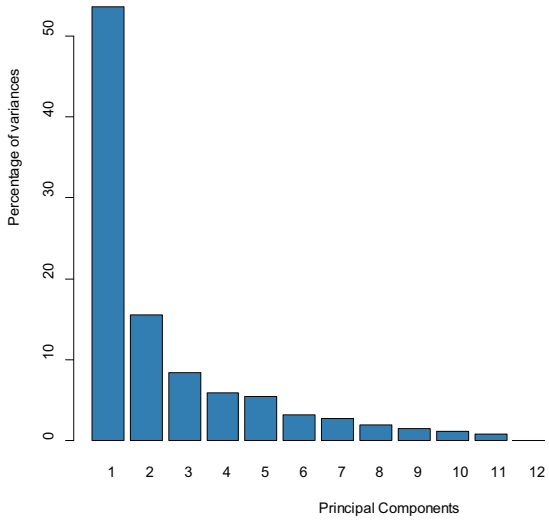

3.2.5 Forelimb

The first three principal components account for 77.6% of variation (Fig. 17). PC 1 account for 53.6% of variation and is not correlated with body size. This PC is primarily driven by length of the radius. It clearly distinguished between extant catarrhines and platyrrhines. The fossil catarrhines (*Epipliopithecus, Victoriapithecus* and *Proconsul*) fall intermediate between extant catarrhines and the platyrrhines. The hylobatids define the upper extent of the axis, with platyrrhines at the lower end.

Figure 18. PCA forelimb - PC1 & PC2

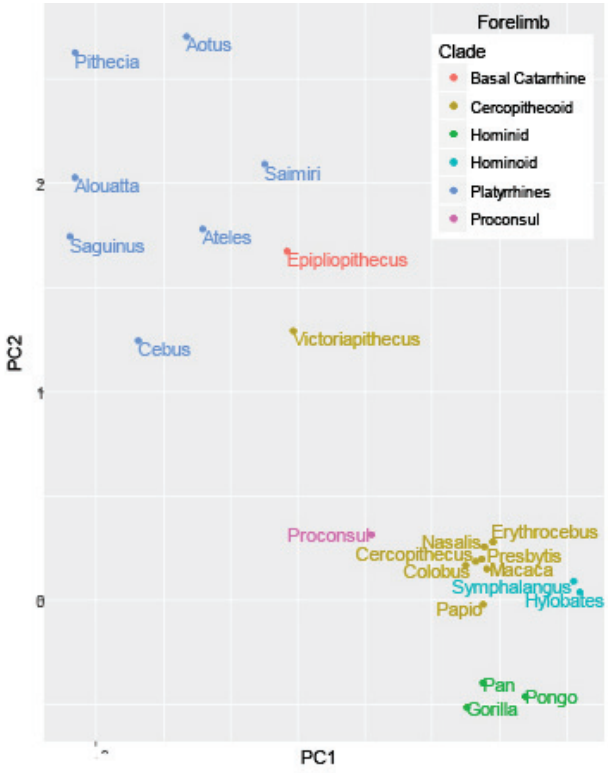

Figure 19. PCA forelimb - PC2 & PC3

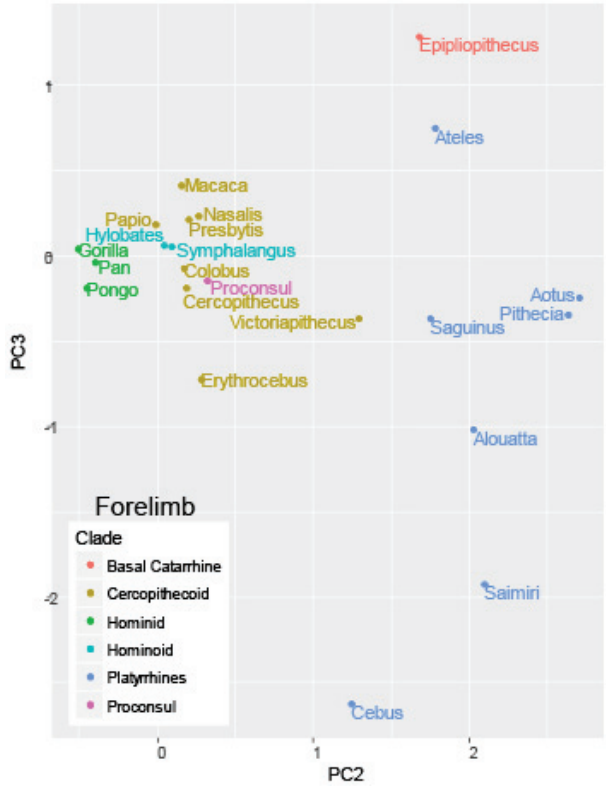

PC 2 accounts for 15.5% of variation and is strongly correlated with body size ($p<0.05$, $R^2=0.85$). Radial length again is a prime driver of this axis, along with depth of the coronoid and radial fossae on the humerus, morphology of the trochlear notch and distal ulna. Platyrrhines and catarrhines are separated on this axis in a manner not explained by body size alone.

Epipliopithecus and *Victoriapithecus* fall within the platyrrhine distribution in the high end of the axis, while *Proconsul* falls at the high end of the extant catarrhine distribution, with the cercopithecoids. Hominids define the low end of the axis, with hylobatids falling nearest the cercopithecoids.

Figure 20. Cluster dendrogram for forelimb data, constructed as NJ tree run on distance matrix

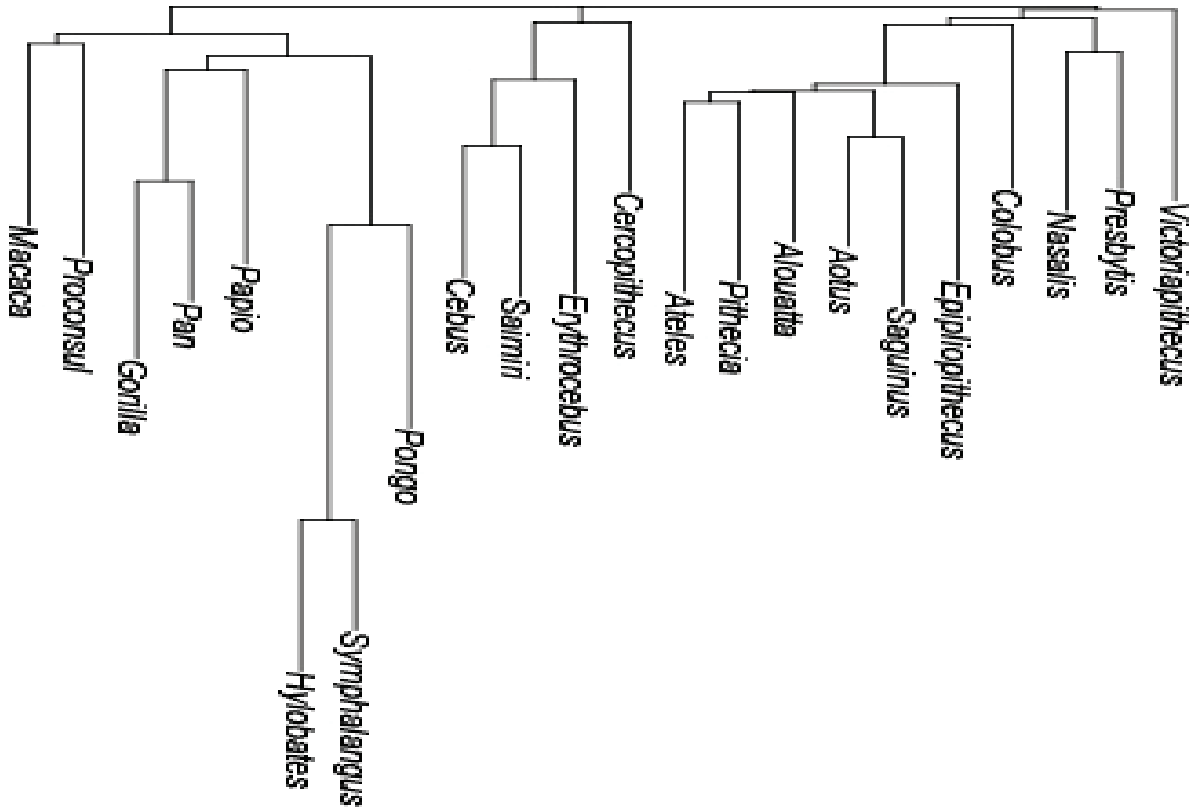

PC 3 accounts for 8.4% of variation and is not correlated with body size. This axis is strongly driven by depth of the coronoid and radial fossae of the humerus and the morphology of the supra-condylar ridge. Platyrrhines are spread across the axis, encompassing all variation among extant catarrhines. Only *Epipliopithecus* falls outside the platyrrhine distribution, defining the upper limit of the axis. The cercopithecoid distribution encompasses the hominoid

distribution, with *Proconsul* falling in the middle of both. The distance matrix (appendix C, fig. 20) places *Proconsul* nearest *Macaca*, in a cluster including the other hominoids and *Papio*. *Epipliopithecus* groups with the platyrrhines excluding *Cebus* and *Saimiri* who group with *Cercopithecus* and *Erythrocebus*. *Victoriapithecus* falls in the group including *Epipliopithecus*, the other platyrrhines and the colobines.

3.2.6 Manus

The first three principal components account for 73.6% of variation (Fig. 24). PC 1 accounts for 48% of variation and is not significantly correlated with body size. It is driven by shape of the hamate/triquetral facet and topography of the hamate and capitate metacarpal facets. It separates platyrrhines from extant catarrhines, with *Epipliopithecus* and *Victoriapithecus* grouping with the platyrrhines. It also separates hominoids from cercopithecoids, with cercopithecoids falling between hominoids and platyrrhines. *Proconsul* is intermediate between the cercopithecoid and hominoid distributions.

Figure 21. PCA manus - PC1 & PC2

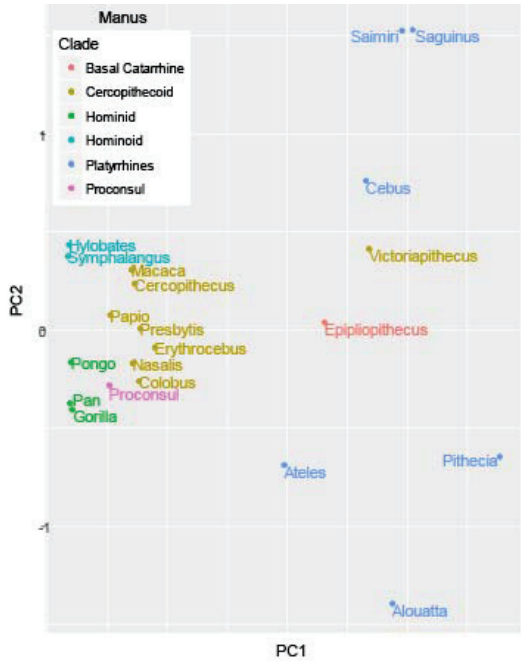

Figure 22. PCA manus - PC2 & PC3

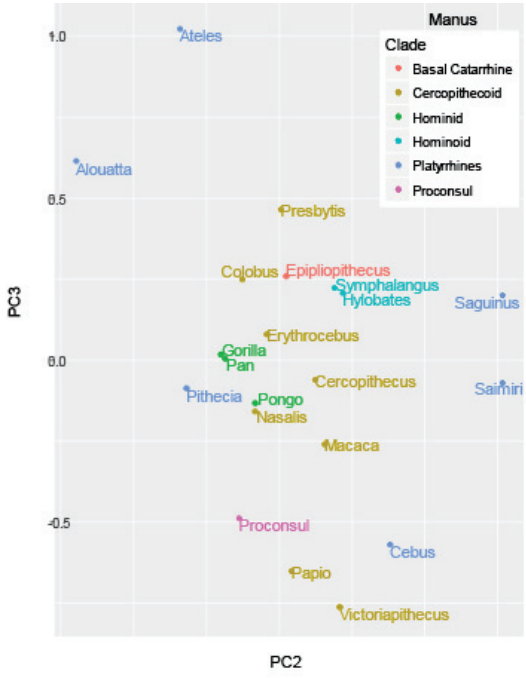

PC 2 accounts for 14.4% of variation and is significantly correlated with body size (R^2=0.47, p=0.02). It is driven by topography of the pisiform/triquetral facet and length of MC2. Variation among platyrrhines encompasses all other taxa. All catarrhines fall towards the center of the axis. Hominids and hylobatids fall on either end of the catarrhine distribution, with the cercopithecoids in between. *Epipliopithecus* falls in the middle of the cercopithecoid distribution, with *Victoriapithecus* falling nearer the hylobatids at the lower end of the cercopithecoid distribution. *Proconsul* falls with the hominids.

Figure 23. Cluster dendrogram of manus data, constructed as NJ tree run on distance matrix

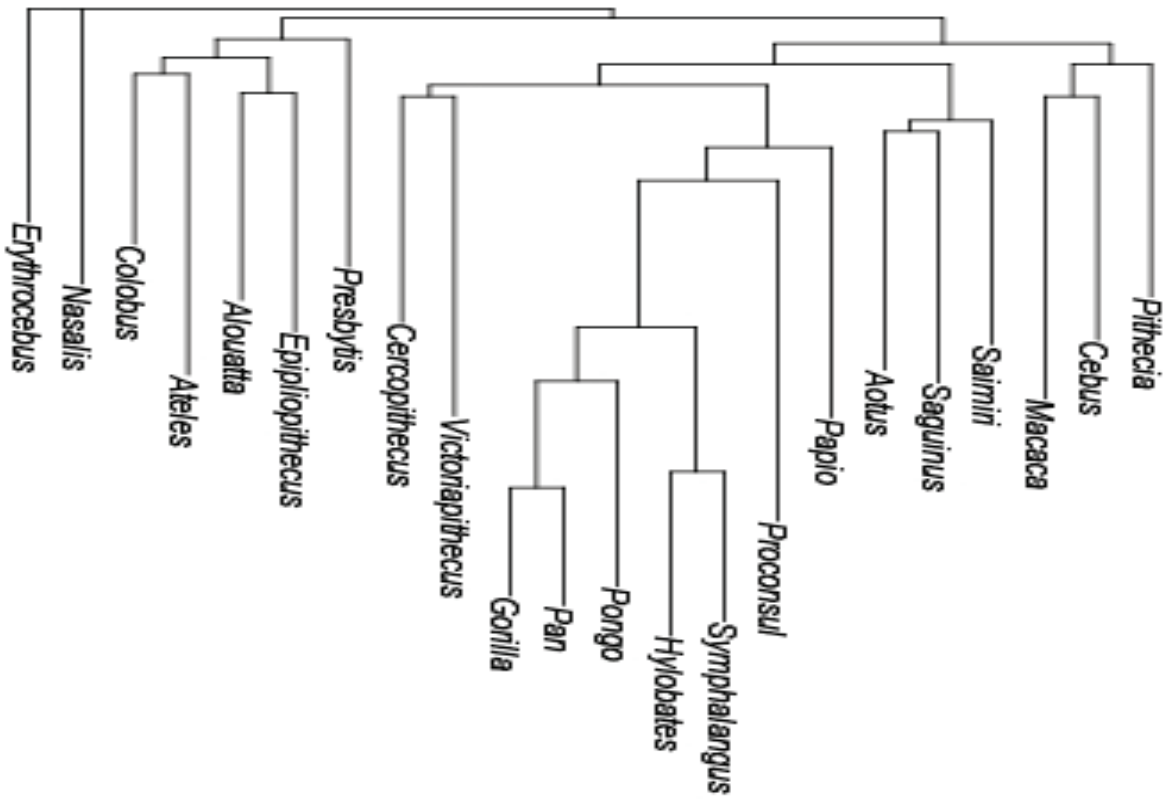

PC 3 accounts for 11.2% of variation and is not correlated with body size. Variation along this axis is driven by topography of the hamate/MC facet, morphology of the MC2/MC3

facet and breadth of the triquetral/pisiform facet. Variation among platyrrhines covers nearly all of the axis, with only *Victoriapithecus* and *Papio* falling outside of the platyrrhine distribution. Cercopithecoids are also widely distributed, with hominoids occupying a more limited range towards the center of the plot. *Proconsul* falls towards the lower end of the axis, near *Cebus, Papio* and *Victoriapithecus. Epipliopithecus* falls near *Colobus* and the hylobatids.

The distance matrix (appendix C, Fig. 23) accurately reconstructs the hominoid phylogeny and groups *Proconsul* as the sister to hominoids. *Victoriapithecus, Cercopithecus* and *Papio* also fall close to the hominoid cluster. *Epipliopithecus* falls nearest *Alouatta* and otherwise cercopithecoids and platyrrhines are dispersed across the dendrogram.

Figure 24. Manus scree plot showing contribution of PCs to percent of variation

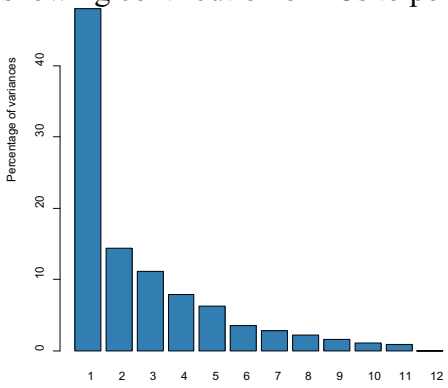

Figure 25. Pelvis scree plot

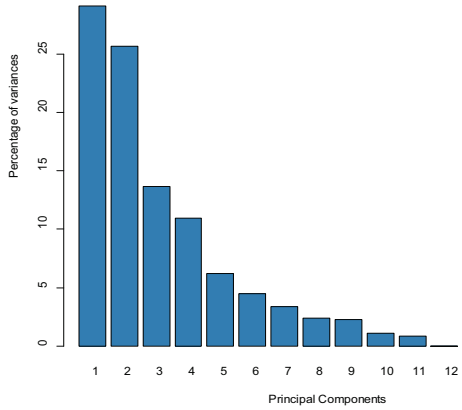

3.2.7 Pelvis

The first three principal components account for 68.4% of the variation (Fig. 25). PC 1 accounts for 29.1% of variation and is not correlated with body size. It is driven primarily by prominence of the obturator crest. Platyrrhines fall on the upper half of the axis, while catarrhines fall on the lower half. There is substantial overlap in their distributions. The hylobatids, African apes and *Proconsul* all fall towards the center of the axis along with *Alouatta, Ateles, Cebus, Presbytis* and *Cercopithecus.*

PC 2 accounts for 25.7% of variation and is significantly correlated with body size (R^2=0.41, p=0.04). This axis is driven by the shape of the obturator foramen, height of the ischial spine, prominence of the sciatic notch and presence of a tubercle on the superior pubis. This axis distinguishes between platyrrhines, cercopithecoids and hominoids. Platyrrhines fall on the lower end of the axis with the exception of *Saguinus*. Hominoids fall at the upper extent along with *Saguinus* and cercopithecoids are intermediate. *Proconsul* falls within the platyrrhine distribution.

PC 3 accounts for 13.6% of variation and is not correlated with body size. It is driven by length and height of the iliac blade, prominence of the lunate surface and prominence of the ischial spine. There is significant overlap among platyrrhines, cercopithecoids and hominoids. *Proconsul* falls towards the middle of the distribution nearest *Presbytis, Cebus* and *Gorilla.*

Figure 26. PCA pelvis- PC1 & PC2

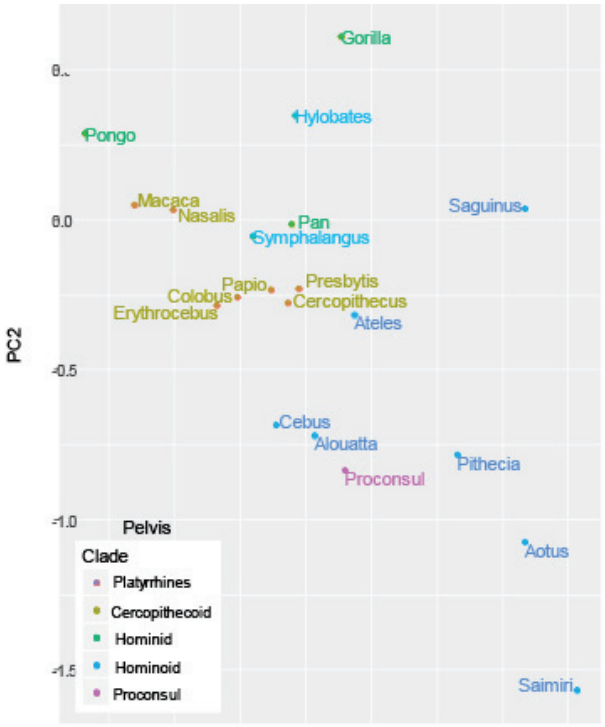

Figure 27. PCA pelvis- PC2 & PC3

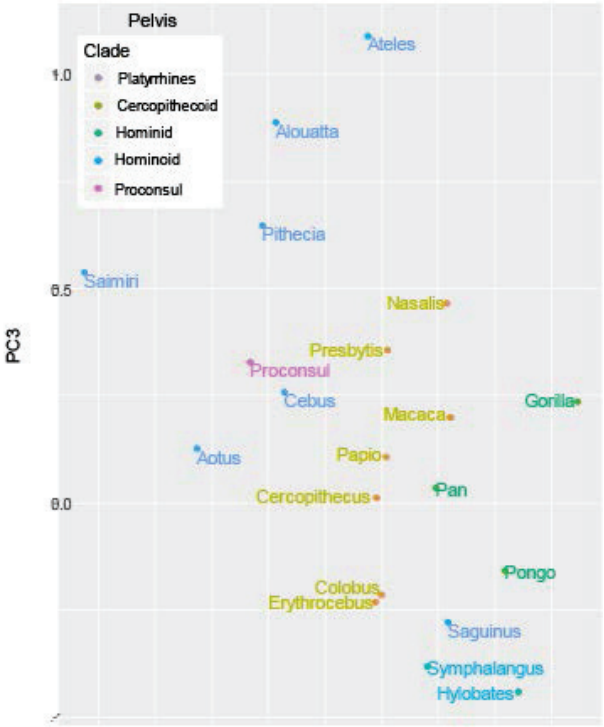

Figure 28. Cluster dendrogram pelvis data, constructed as NJ tree run on distance matrix

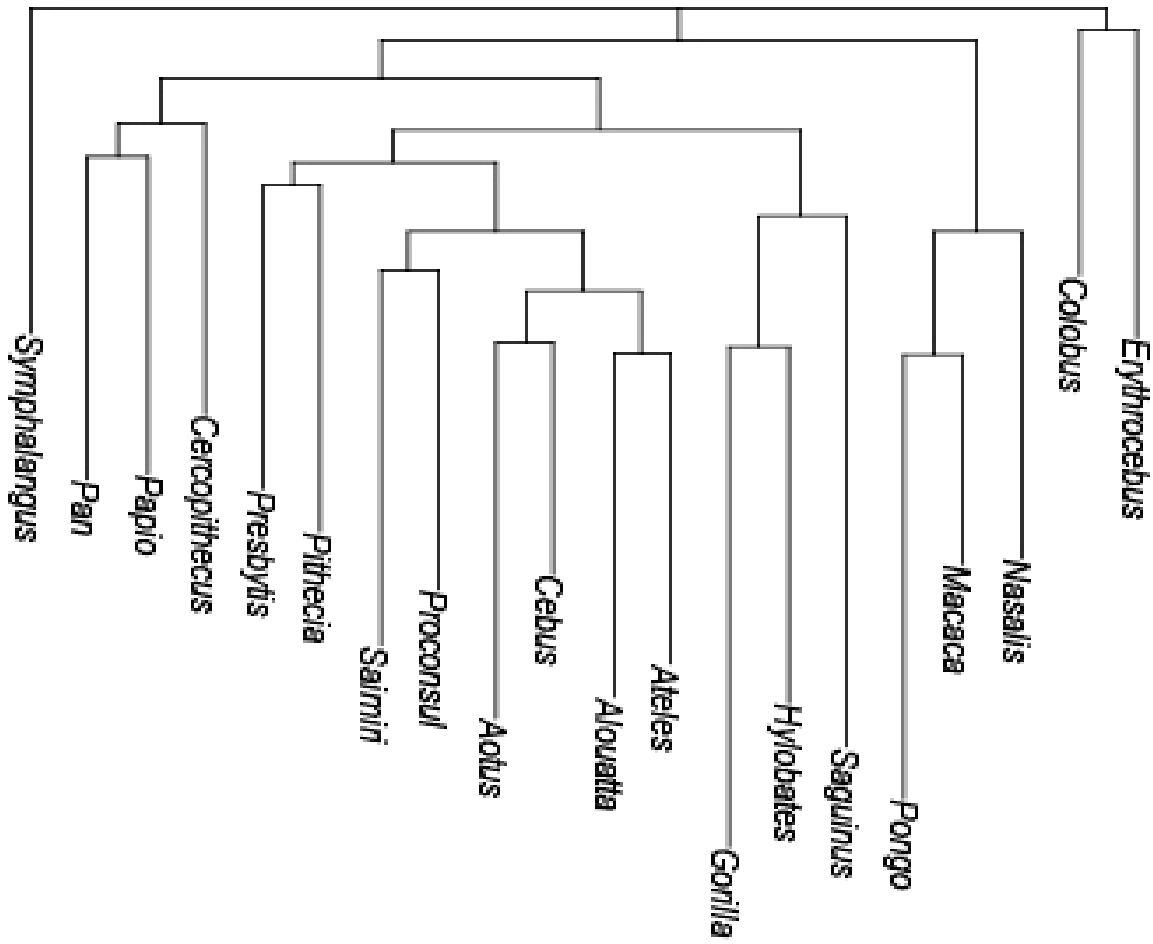

The distance matrix (appendix C, fig. 32) places *Proconsul* with the platyrrhines, nearest *Saimiri*. All platyrrhines group together. *Presbytis, Hylobates* and *Gorilla* also group with the platyrrhines. The other hominoids are distributed among the remaining cercopithecoids.

3.2.8 Pes

The first three principal components account for 63.0% of variation (Fig. 31). PC 1 accounts for 32.9% of variation and is strongly correlated with body size (R^2=0.75, p<0.00).

Variation is strongly driven by the orientation of the navicular/lateral cuneiform facet. This axis separates platyrrhines from extant catarrhines and cercopithecoids from hominids. Hylobatids fall with cercopithecoids and *Proconsul* falls within the hominid distribution. *Epipliopithecus* and *Oreopithecus* group with platyrrhines.

PC 2 accounts for 18.6% of variation and is not correlated with body size. No individual variable or set of variables primarily drive variation along this axis. This axis primarily indicates the distinctiveness of *Epipliopithecus* and *Proconsul*. *Oreopithecus* falls with the hylobatids. All three genera fall nearest the other fossil taxa.

PC 3 accounts for 11.5% of variation and is not correlated with body size. No individual or set of variables are responsible for driving variation along this axis. All extant catarrhines fall towards the center of the axis, with platyrrhines distributed across the entire axis. *Epipliopithecus*

Figure 29. PCA pes characters- PC1 & PC2

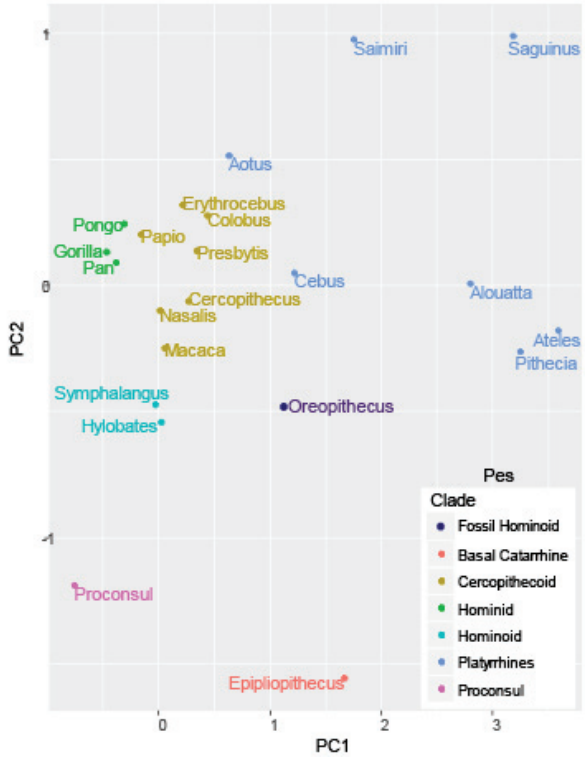

Figure 30. PCA pes characters- PC2 & PC3

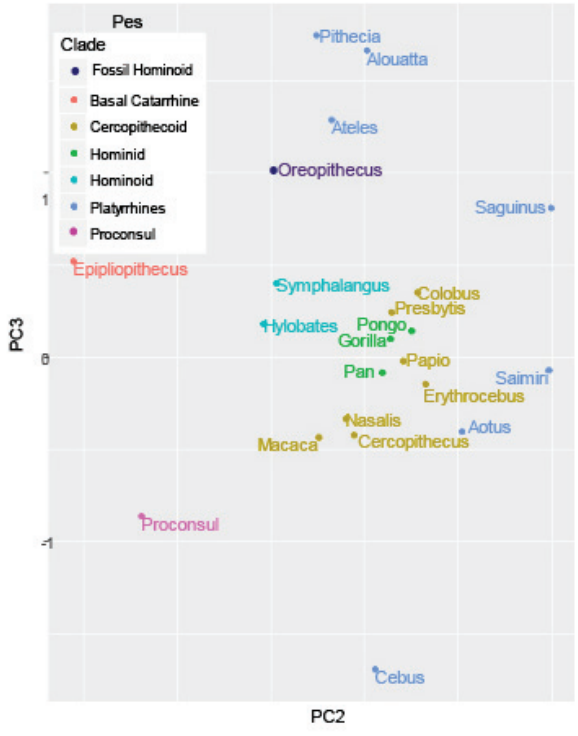

defines the upper limit of the catarrhine distribution. *Oreopithecus* falls at the upper end of the axis with the platyrrhines. *Proconsul* falls at the lower end, appearing distinctive relative to other catarrhines and similar to *Cebus*.

The distance matrix (appendix C, fig. 32) groups all platyrrhines together in a cluster that also includes *Epipliopithecus* and *Oreopithecus*. *Proconsul* groups with *Nasalis* and *Macaca.*

Figure 31. Pes scree plot

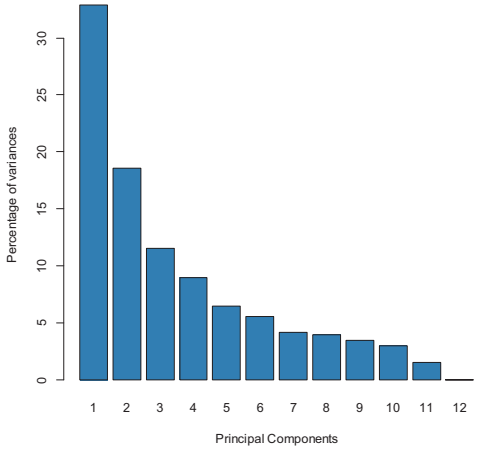

Figure 32. Cluster dendrogram pes data, constructed as NJ tree run on Euclidean distance matrix

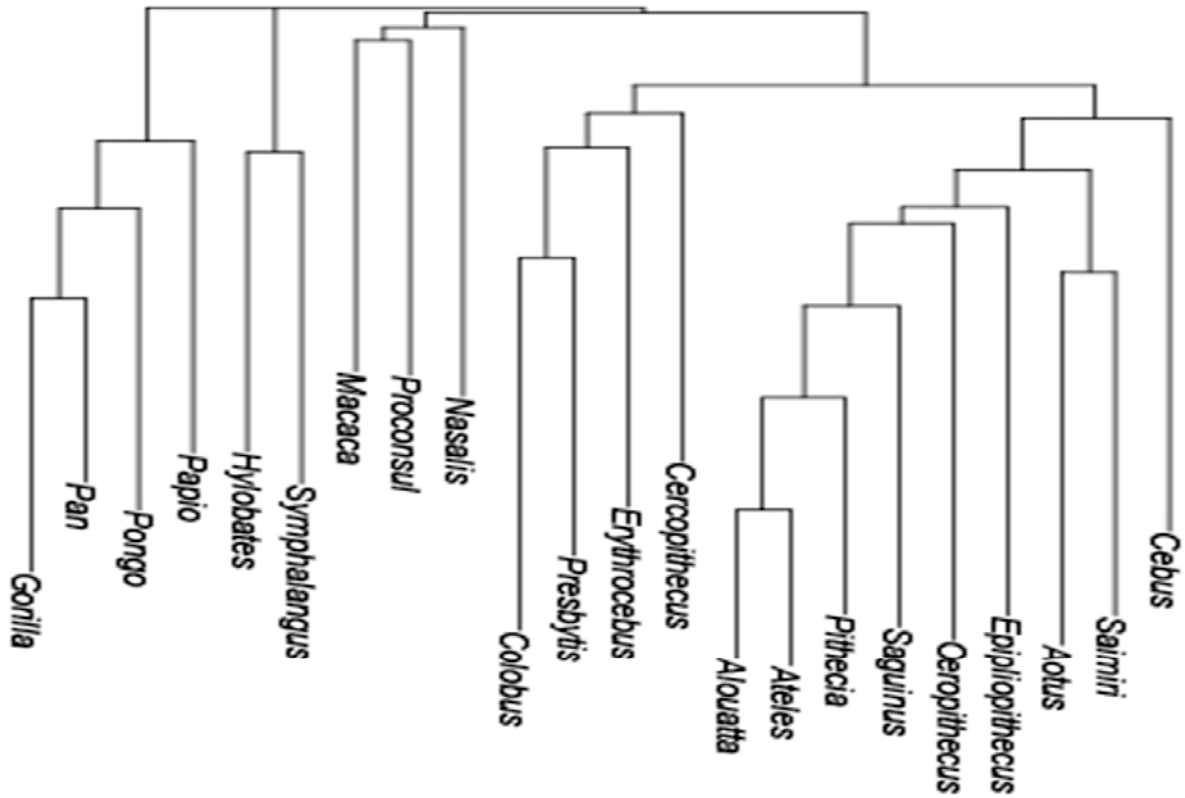

3.3 DISCUSSION

This chapter presented an analysis of the phenetic position of *Proconsul* relative to crown catarrhine taxa and evaluates whether use of a sex-averaged data set is defensible. The initial analysis observing the effects of sexual dimorphism within this data set indicated that males and females within a species were consistently more similar to each other than to males or females of any other species. This suggests that while sex-averaging may still not be ideal, given the focus of this dissertation and results of the sex-separate analysis it is deemed appropriate to conduct phylogenetic analyses with sex-averaged data. While this chapter did not address specific hypotheses concerning the phylogenetic position of *Proconsul*, it implemented an initial exploration of the data set that will be used to further test phylogenetic relationships among catarrhines. Its goal was to visualize morphological distance between taxa and groups. Results were often able to reconstruct crown clades and distance matrices were able to correctly reconstruct phylogenetic relationships, particularly within Hominoidea. This suggests this data set will be useful in inferring phylogenetic relationships. It also provided an initial exploration that identified certain characters as being particularly useful in separating groups.

3.3.1 Extant taxa

Across all data, platyrrhines were shown to be highly variable for the set of characters best describing variation among catarrhines. This does not comment on the overall phonetic variation within these groups as is discussed elsewhere in the literature (see Fleagle et al., 2010), but rather results from platyrrhines not being included in the ordination of axes. This only further emphasizes, however, the greater variability among platyrrhines for the set of characters that

ordinate cercopithecoid and hominoid variation. In many cases variation among platyrrhines encompassed all variation among catarrhines.

The hominids form a tight cluster with limited variation relative to the cercopithecoids (the pelvis data set is the only exception). Hylobatids always cluster together and expand this range of variation. The distance matrices for the pes, manus and cranial data sets are all able to reconstruct the known hominoid phylogeny. The cranial data set reconstructs distinct platyrrhine, hominoid, and cercopithecoid groups, with the exception of *Presbytis*, which groups with the platyrrhines. The entire data set again recreates the phylogenetic relationships of the hominoids and isolates a platyrrhine group as well. The pelvis and mandibular data sets—those with the fewest characters—perform worst at recreating known phylogenetic relationship.

3.3.2 Fossil taxa

Across all data, *Proconsul* groups with the hominoids. *Proconsul* also groups with the hominoids for the cranium, manus and forelimb data sets. The forelimb is complicated, however, as *Macaca* and *Papio* also fall within the hominoid group, with *Proconsul* actually falling nearest *Macaca*. In each of these cases (though less so in the forelimb data set) *Proconsul* is separated from the other hominoids by long branches. This explains why in the PCA plots, *Proconsul* only appears similar to the hominoids in the manus data set and most often appears quite distinctive. This distinctiveness may be an additional difficulty in resolving the phylogenetic position of *Proconsul.*

Epipliopithecus consistently groups with the platyrrhines in all analyses for which it is present. *Aegyptopithecus* also groups with the platyrrhines in the mandibular data set, but in the cranial data set falls nears *Victoriapithecus* within the cercopithecoid cluster. *Victoriapithecus* falls nearest the colobines in the forelimb data set, but nearest *Cercopithecus* in the manus data

set. The manus data set also places *Victoriapithecus* and *Cercopithecus* within the cluster including hominoids and *Proconsul*. *Oreopithecus* is only present in the pes data set, but groups with the platyrrhines and *Epipliopithecus,* nearest *Epipliopithecus* and *Saguinus*.

3.4 CONCLUSIONS

The most important findings from this chapter can be summarized as follows: 1) *Proconsul* is distinctive relative to extant and fossil taxa, 2) *Proconsul* consistently appears phenetically most similar to the hominoids, 3) there is a wider range of variation among platyrrhines than catarrhines, 4) fossil taxa extend the range of variation for crown clades. The results do raise the question whether phylogenetic analyses will be able to extract enough synapomorphies to overcome this pattern of variation. Phenetically *Proconsul* most often falls nearest the hominoids, but it is also quite distinctive relative all other taxa. Long branches are often problematic for phylogenetic analyses, but will be particularly difficult when assessing a potential stem taxon relative to derived clades (i.e., the cercopithecoids and hominoids). This may be a particularly significant issue given the more limited range of variation they express relative to the outgroup clade. Properly rooted character polarities are essential to any phylogenetic analysis and rely on the outgroup to define morphology at the root of the tree. This analysis may struggle with confidently rooting character polarities due to the wide range of variation in the outgroup. Inclusion of the successive basal catarrhine outrgroup is meant to address this issue, but is complicated by the fact that *Aegyptopithecus* and *Epipliopithecus* also express a range of variation and may suffer from the same issue.

CHAPTER 4: Phylogenetic Analyses

This chapter presents the results from total evidence phylogenetic analyses run using parsimony and Bayesian methods. Bayesian methods have only recently been applied to morphological data sets and provide a new toolkit for addressing questions of morphological evolution (Nylander et al., 2004; Ronquist, 2004; Dembo et al., 2015). The analyses described below include the largest character set yet assembled concerning the inferred phylogenetic position of *Proconsul.* Chapter 5 will deal with exploration of the results.

4.1 PARSIMONY

4.1.1 Methods

Parsimony analyses were run in TNT (Goloboff et al., 2003) treating continuous characters as such in one analysis (Goloboff, 2006) and discretizing data using gap coding in another (Thiele, 1993; Wiens, 2001) (see chapter 2 for full discretion of the benefits of these coding methods). Molecular data taken from Perelman et al. (2011) were included in order to root phylogenetic relationships of extant taxa. All analyses constrained cercopithecoid and hominoid clades (including *Victoriapithecus* among the cercopithecoids and *Pierolapithecus* and *Oreopithecus* among the hominoids), with platyrrhines, *Aegyptopithecus* and *Epipliopithecus* constrained as stem catarrhines, outside a clade including all other catarrhine taxa. Despite these constraints where there was no support for constrained ingroup clades, results collapse relationships indicating this lack of support (see figs. 37, 38, 41, 45). Only *Proconsul* was unconstrained, allowed to fall at any position within the catarrhine ingroup. A series of phylogenetic analyses was conducted in order to explore the relationships of crown and fossil

taxa and test the alternative hypotheses about the phylogenetic status of *Proconsul*. All analyses applied TNT's new technologies search (Goloboff et al., 2003) using 10 initial replications, with 27 rounds of drifting and 7 rounds of fusing. Bootstrap support values were calculated for all clades (1000 replicates) and homoplasy scores were recorded for all characters on both constrained and unconstrained trees.

Analysis 1: Continuous. This analysis included undiscretized morphological data and molecular data.

Analysis 2: Discretized. This analysis included morphological data that were gap weighted (Thiele, 1993) with 3 character states. Molecular data were included in this analysis.

Analysis 3: Morphological regions. This series of analyses ran each morphological region separately, inferring the phylogenetic signal of each. No molecular data were included. The data set was broken into six regions: cranium, mandible, forelimb without manus, manus, pelvis, and pes.

Analysis 4: H1- stem catarrhine. This analysis employed undiscretized morphological data in order to observe the phylogenetic signal of morphology alone, without the influence of molecular data. These hypothesis specific analyses do not test the phylogenetic position of *Proconsul* as this is constrained, but instead are used to infer specific morphological synapomorphies for each hypothesis. As such, molecular data is not necessary to inferring synapomorphies on these constrained trees and therefore no molecular data were included. All phylogenetic relationships were constrained according to the H1 phylogeny (fig. 33), inferring *Proconsul* to be a stem catarrhine.

Figure 33. H1 constraint tree

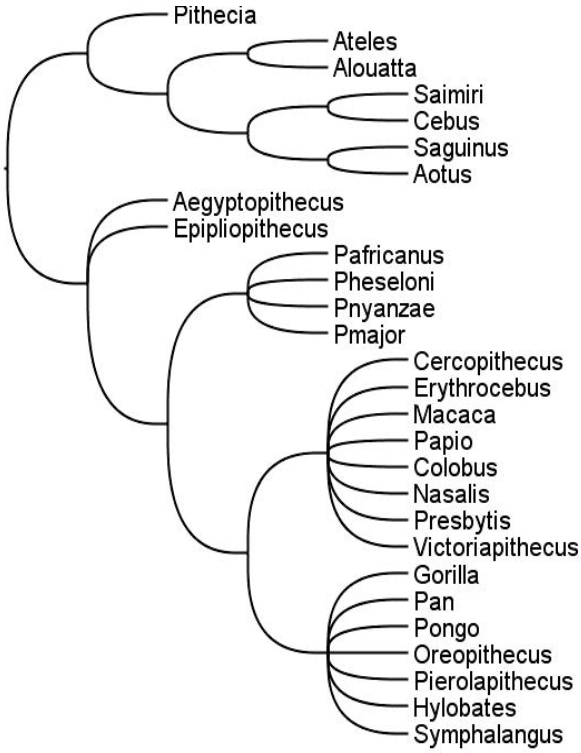

Figure 34. H2 constraint tree

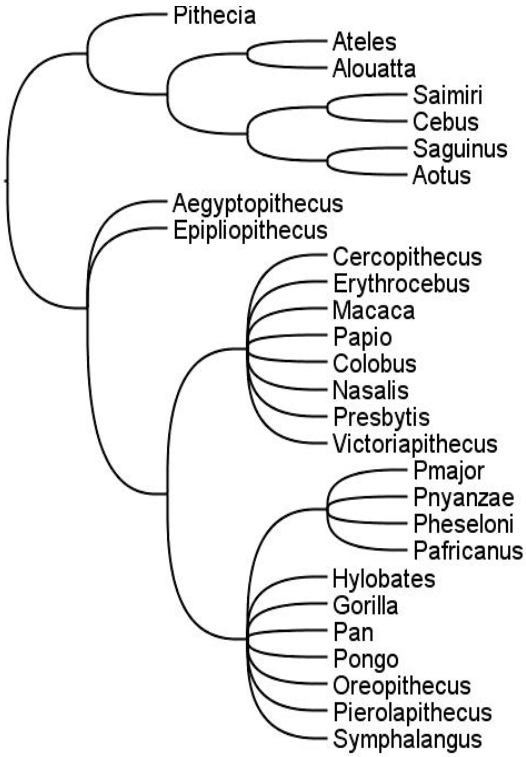

Figure 35. H3 constraint tree

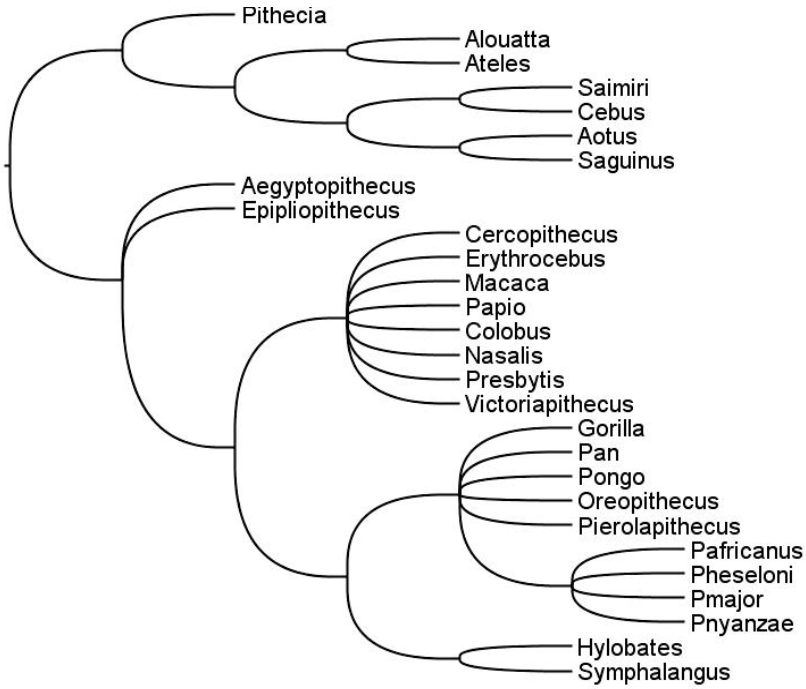

Analysis 5: H2- hominoid. This analysis employed undiscretized morphological data. No molecular data were included. All phylogenetic relationships were constrained according to H2 (Fig. 34)—*Proconsul* is inferred to be a hominoid.

Analysis 6: H3-hominid. This analysis employed undiscretized morphological data. No molecular data were included. All phylogenetic relationships were constrained according to the H3 phylogeny (fig. 35), inferring *Proconsul* to be a hominid.

Analysis 7: Unconstrained. A final analysis removed all catarrhine constraints, only constraining platyrrhines as the outgroup. Continuous morphological data were used along with no molecular data.

4.1.2 Results

4.1.2.1 Analysis 1: Continuous.

Two most parsimonious trees were found after examining 180,491 rearrangements (fig. 36). They differ in the position of *Pierolapithecus*, falling either as a basal hominoid or basal hominid. This analysis supported H2: *Proconsul* is a stem hominoid. *Proconsul* is inferred to be sister to a clade comprising extant and fossil hominoids. Bootstrap support for the *Proconsul* + hominoid clade is 84. The analysis identified 125 synapomorphies supporting the inclusion of *Proconsul* within Hominoidea. The forelimb, manus and pes contributed the most synapomorphies (96 characters), which is predictable given the overwhelming number of characters are drawn from these regions. Only the forelimb, mandible and pelvis contributed more synapomorphies than expected if synapomorphies were evenly sampled across the data set. The manus and pes contributed fewer synapomorphies than expected (4% and 2% less respectively); while the forelimb contributes 6% more synapomorphies than expected and the pelvis and mandible each contribute 3% more than expected. The cranium and manus each

contributed the least given the distribution of characters, each contributing 4% fewer synapomorphies than expected. This distribution of synapomorphies clearly indicates that unequal sampling within character list is resulting in the forelimb, manus and pes driving results of these analyses. This makes evaluation of each morphological region separately particularly important to evaluating the signicance of results from the combined analysis.

Figure 36. Strict consensus of two most parsimonious trees from analysis of all characters treated as continuous. Numbers refer to bootstrap support for unconstrained clades.

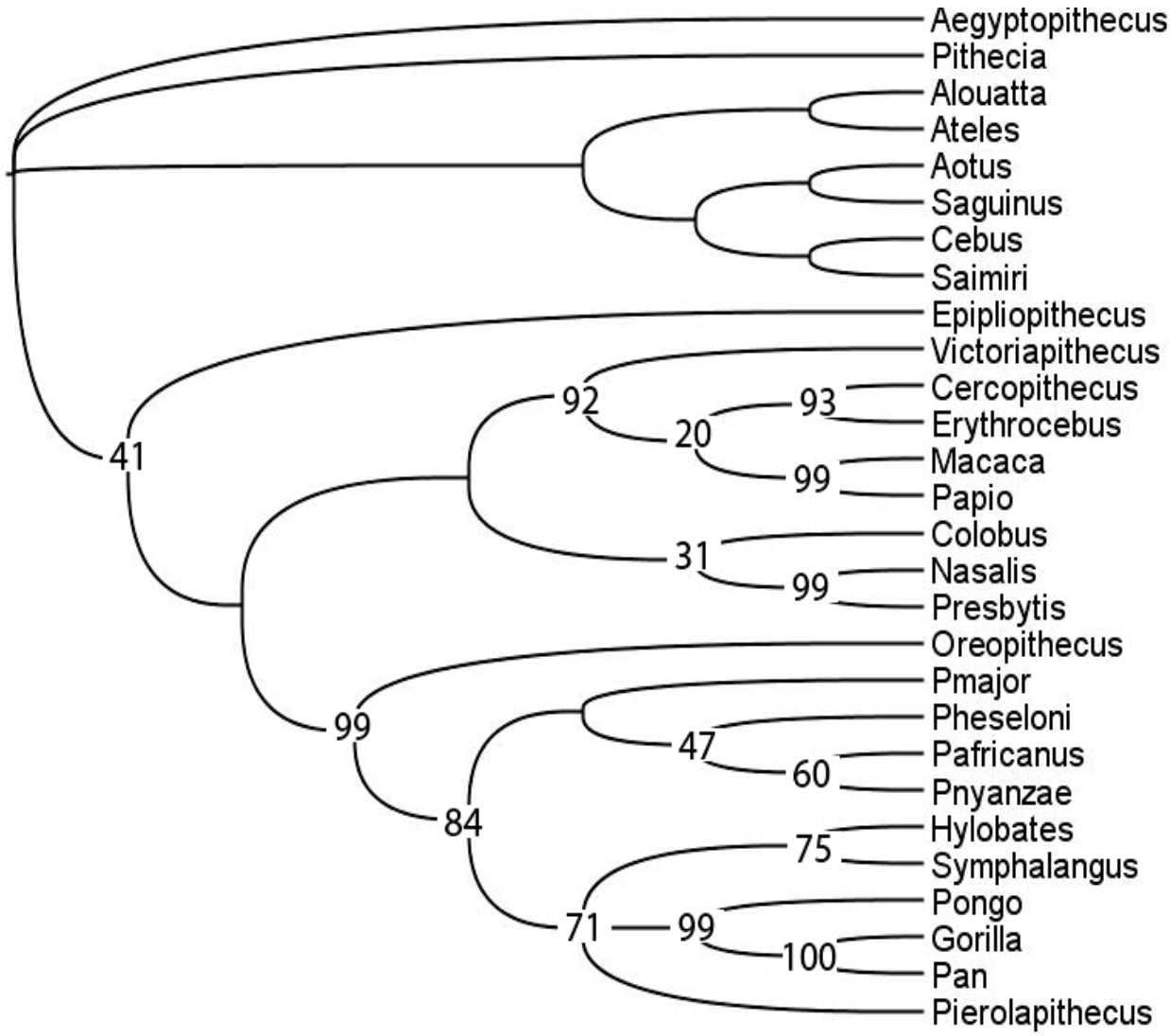

Average homoplasy across the tree was 2.32, with homoplasy across synapomorphies being 1.94. The manus and pes synapomorphies were overall the most reliable, with the lowest homoplasy (0.71 and 0.75 respectively). Cranial synapomorphies had the highest homoplasy (4), while the forelimb and pelvis had homoplasy scores of 1.56 and 1.44 respectively. These homplasy scores could be effected by unequal sampling and perhaps more significantly, by the relative numbers of discrete and continuous characters. Homoplasy for continuous characters were lower than that of discrete characters, with the highest homoplasy found among characters coded via the general allometric method. The cranium possessed the most characters coded in this manner, suggesting discretization may be the prime driver of this difference in homoplasy scores.

4.1.2.2 Analysis 2: Discretized.

Three most parsimonious trees were identified and a strict consensus tree was calculated (fig. 37). Results were unable to resolve whether *Aegyptopithecus* or *Epipliopithecus* were more basal within the catarrhine clade and also could not distinguish between placing *Proconsul* as sister taxon to the hylobatids or more basally within Hominoidea. All optimal trees support H2, placing *Proconsul* within the hominoid clade, with a bootstrap support of 66. They differ in the phylogenetic position of *Victoriapithecus*. The continuous data set infers *Victoriapithecus* falls as sister to the cercopithecine clade, while the discretized analysis places *Victoriapithecus* as sister to the papionins. The discretized analysis resolved the position of *Pierolapithecus* within the hominid clade, whereas the continuous analysis found it equally parsimonious to fall sister to all extant hominoids. The discretized analysis inferred only 48 synapomorphies, fewer than half as many as the continuous data set.

Figure 37. Strict consensus of the three most parsimonious trees inferred from discretized data. Node values indicate bootstrap support for unconstrained clades.

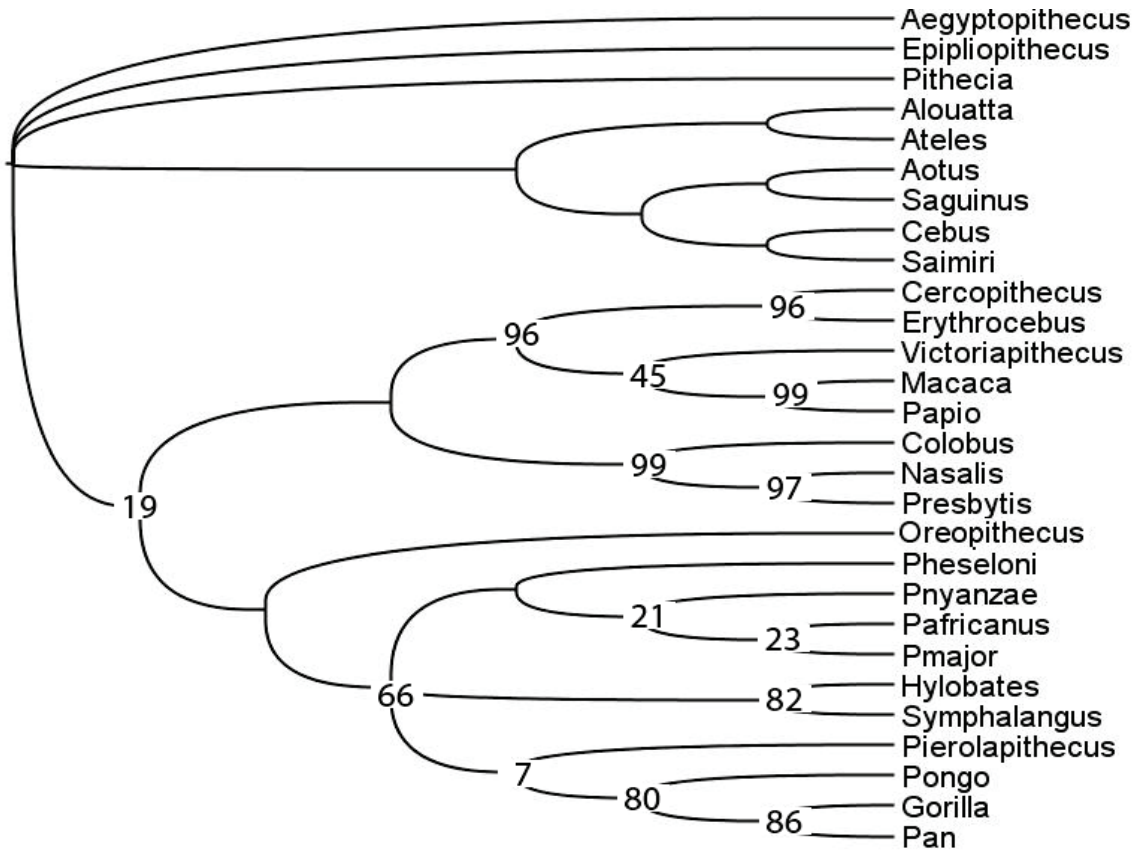

4.1.2.3 Analysis 3: Morphological regions

Three of the six regions (forelimb, manus, pelvis) supported the findings of the previous analyses, inferring *Proconsul* to be a hominoid. The cranium, mandible and pes data sets, however, place *Proconsul* within Cercopithecoidea. None of the morphological regions support either H1—*Proconsul* is a stem catarrhine, or H2—*Proconsul* is a hominid.

Two most parsimonious trees were inferred for the cranial data set (fig. 38). Both optimal trees placed *Proconsul* with the cercopithecoids, sister taxon to a clade including all other fossil and extant cercopithecoids. Bootstrap support for the clade including *Proconsul* and cercopithecoids was only 4. Five synapomorphies support this phylogenetic position: facial

Figure 38. Strict consensus of two optimal trees inferred from cranial data with bootstrap support

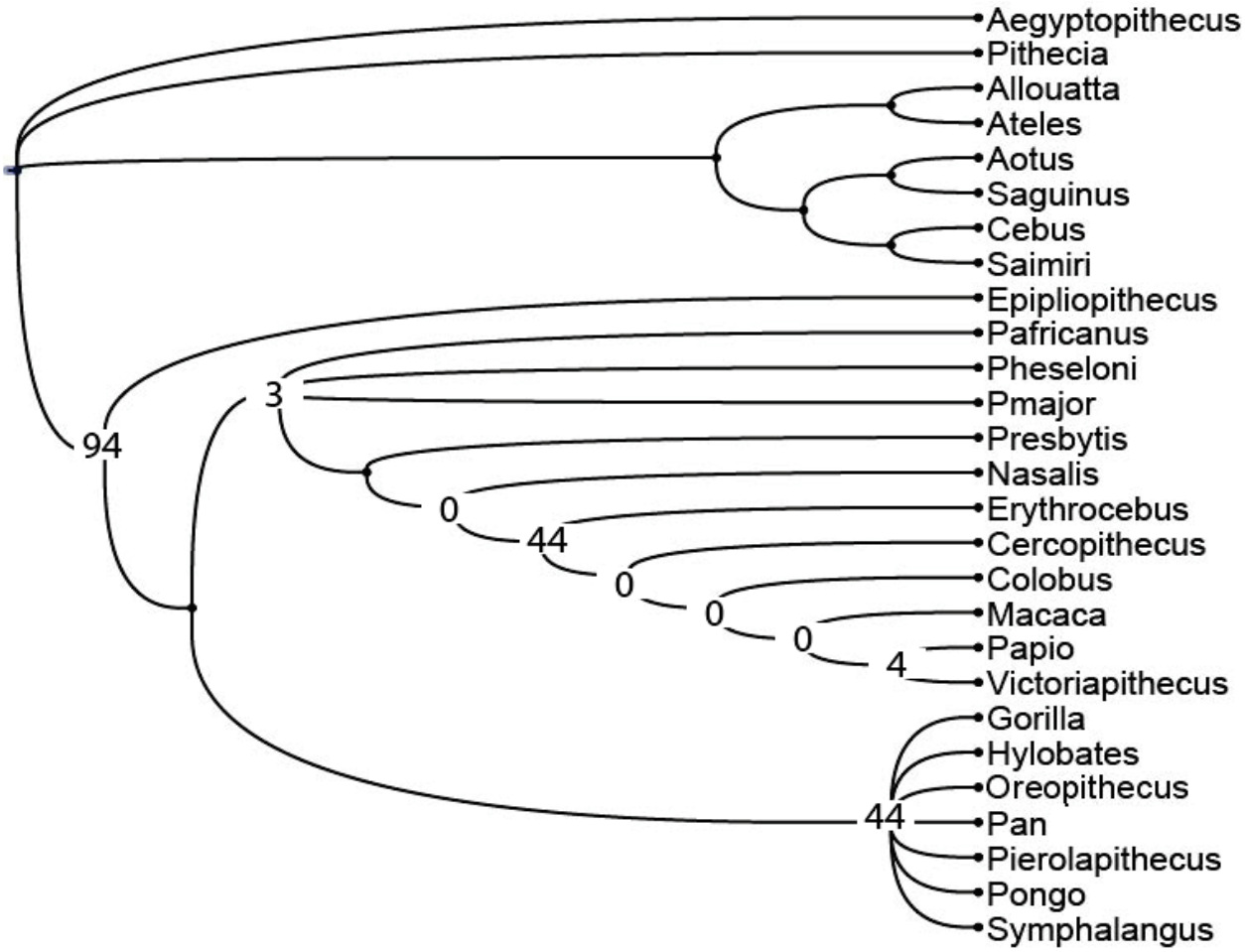

height, palate topography, infraorbital foramen shape, width behind orbits, and width of the ectotympanic tube.

A single most parsimonious tree was inferred for the mandible data set (fig. 39). *Proconsul* was again placed within Cercopithecoidea, with a bootstrap support of 23. Only one synapomorphy supports this position: degree of flare at the gonial angle. Inclusion of dental characters in this or the cranial data set would certainly move *Proconsul* out of the cercopithecoid clade given the distinctive derived morphology of that clade (Gregory, 1922; Von Koenigswald, 1968, 1969; Szalay and Delson, 1979).

Figure 39. Single most parsimonious tree for mandibular data with bootstrap support

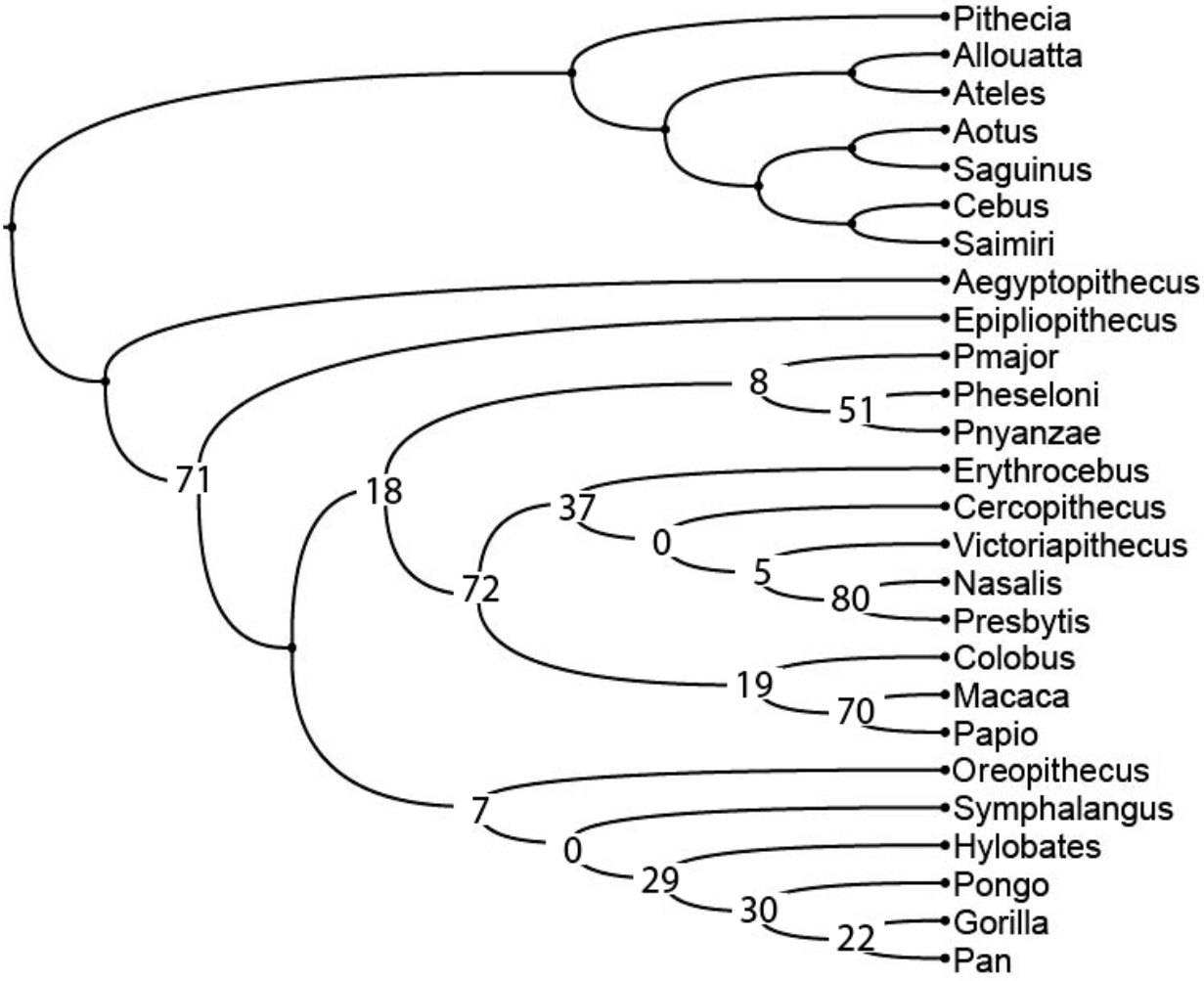

The forelimb analysis returned a single most parsimonious tree (fig. 40). *Proconsul* was placed within Hominoidea, sister to all other extant and fossil hominoids. Bootstrap support for inclusion within Hominoidea was 42 and was supported by 25 synapomorphies. *Oreopithecus* was inferred as sister to *Gorilla*.

The manus data set inferred two equally parsimonious trees (Fig 41). In both optimal trees *Proconsul* was placed as sister taxon to all other hominoids, with a bootstrap support of 60. *Oreopithecus* and *Pierolapithecus* are also inferred to be basal hominoids. Twelve synapomorphies support a clade including *Proconsul* and all other hominoids.

Figure 40. Single most parsimonious tree for forelimb data with bootstrap support

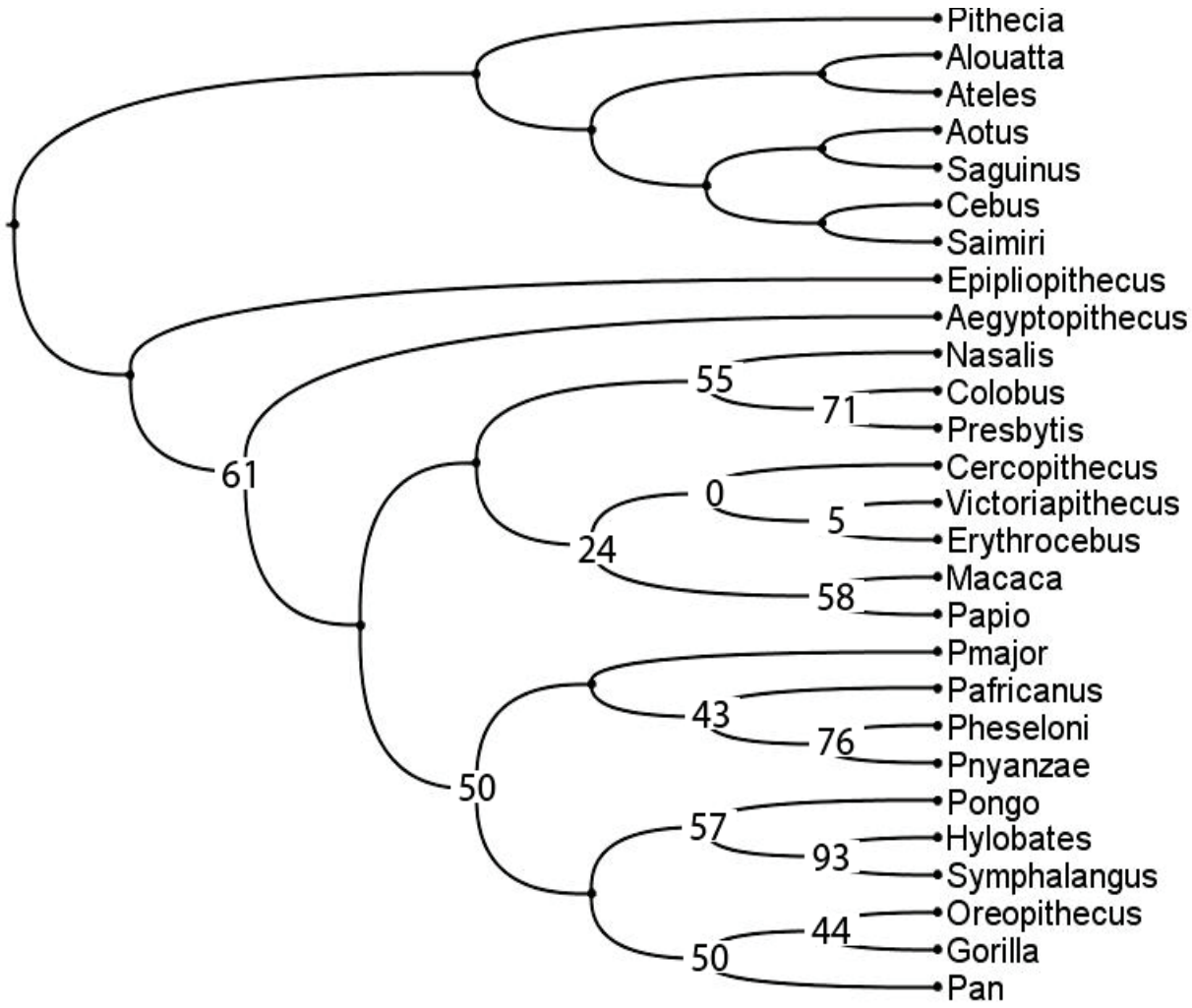

The pelvis analysis produced a single most parsimonious tree (Fig. 42). *Proconsul* was inferred to be a basal member of the hominoid clade with a bootstrap support of 67. The position was inferred from seven synapomorphies. The pes data set inferred a single most parsimonious tree (fig. 43). *Proconsul* was placed within Cercopithecoidea with a bootstrap support of 43 and inferred with 48 synapomorphies.

Figure 41. Strict consensus of two optimal tree for manus data with bootstrap support.

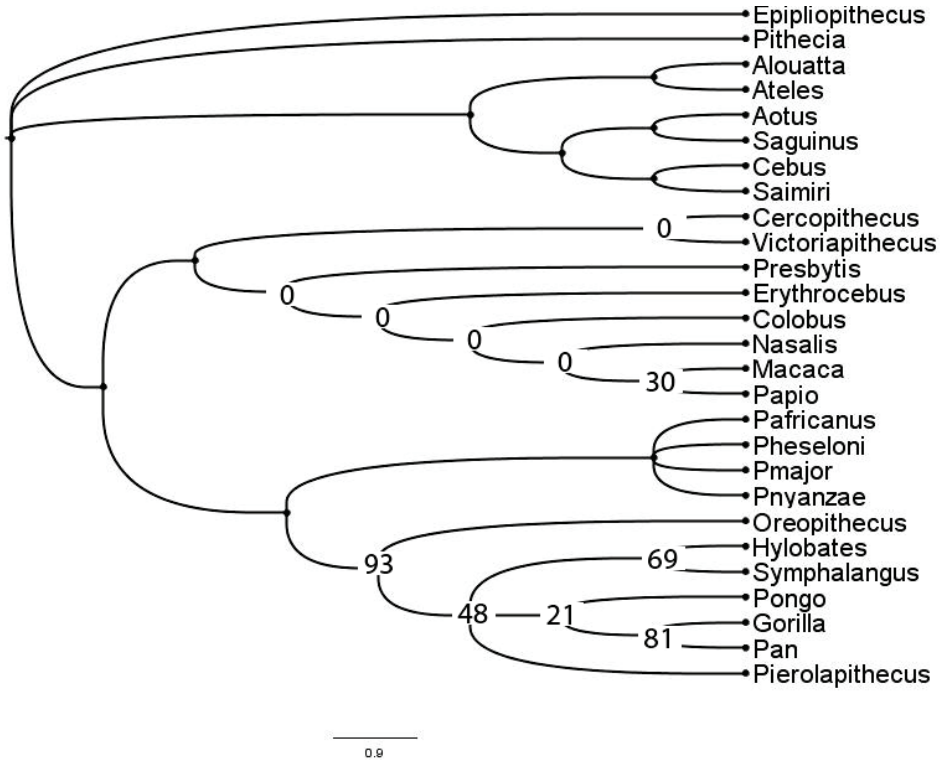

Figure 42. Single most parsimonious tree for pelvis data with bootstrap support.

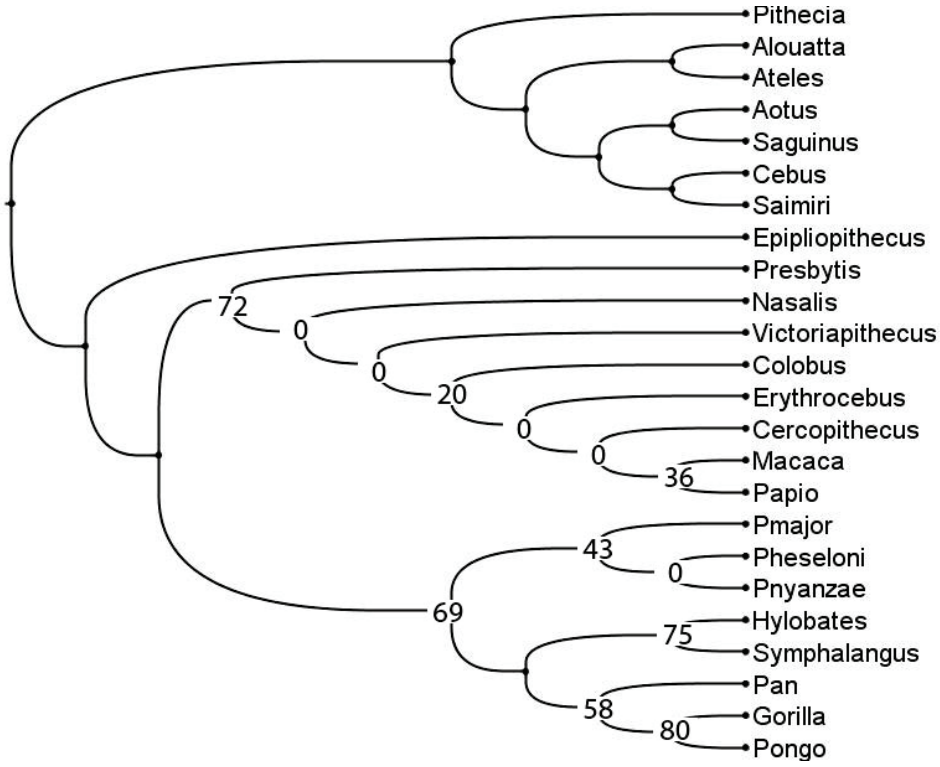

Figure 43. Single most parsimonious tree for pes data with bootstrap support.

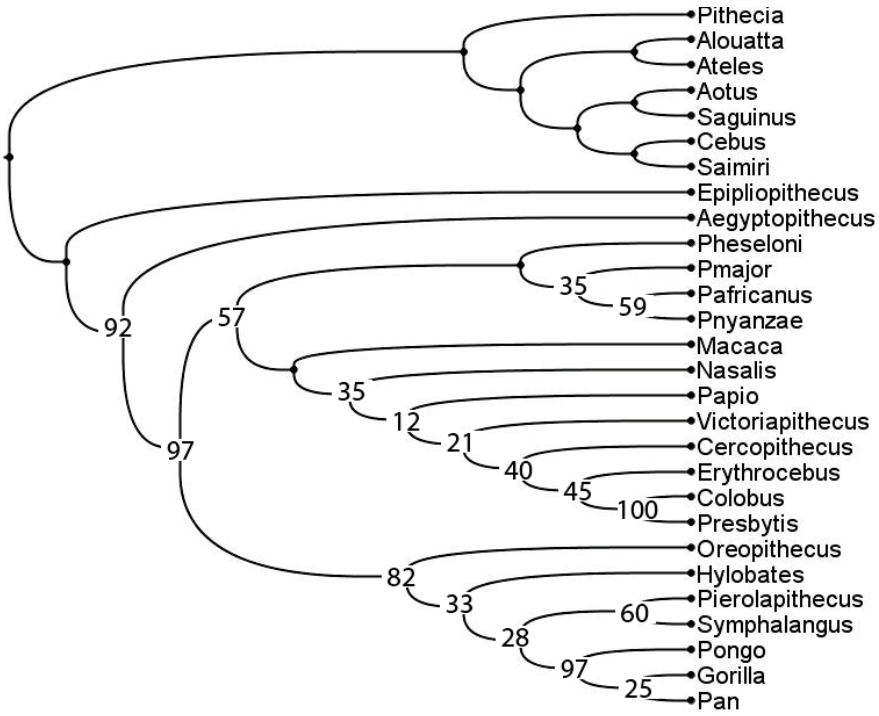

Figure 44. Most parsimonious H1 tree with bootstrap support

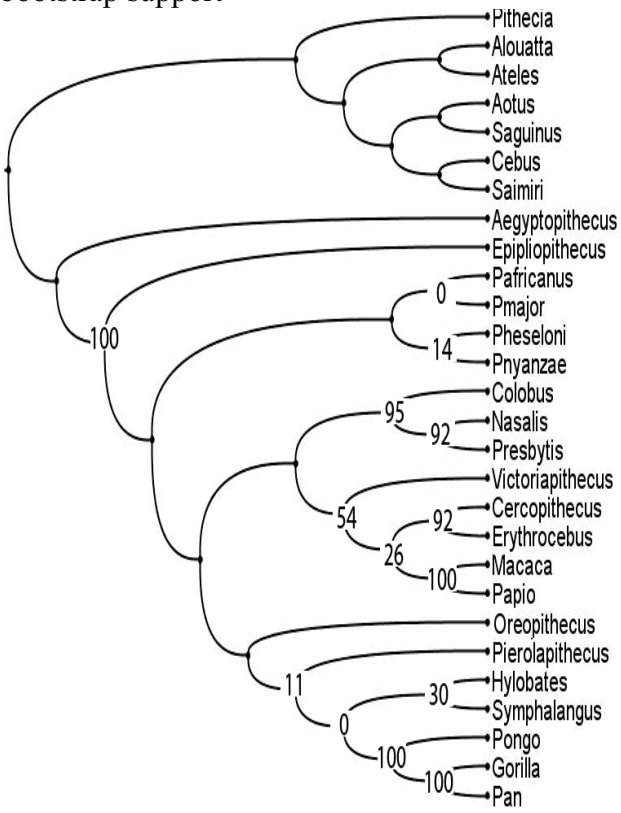

4.1.2.4 Analysis 4: H1- stem catarrhine

This analysis identified 37 synapomorphies supporting the hypothesis that *Proconsul* is a stem catarrhine (fig. 44). The tree cost was 11081.814. Synapomorphies are drawn from each region except the mandible, with a majority of characters in the forelimb (10 synapomorphies) and pes (11 synapomorphies). Only the forelimb and pelvis included more synapomorphies than expected if they were sampled was equally

Figure 45. Most parsimonious H2 tree

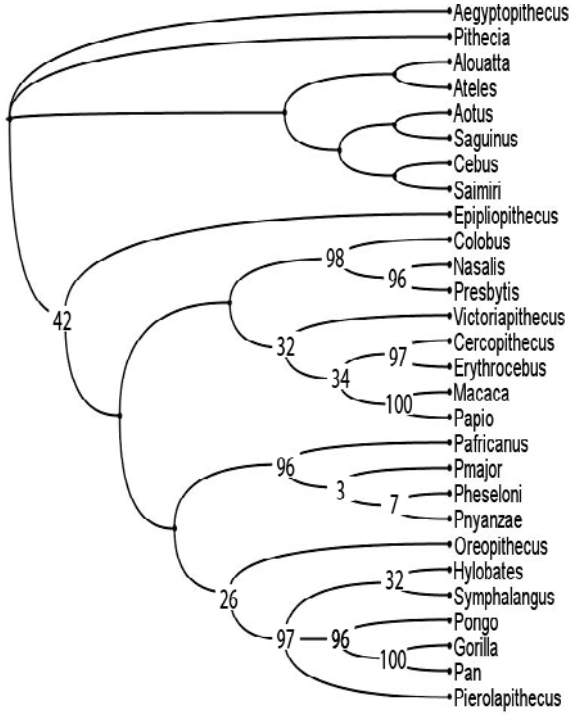

Figure 46. Most parsimonious H3 tree

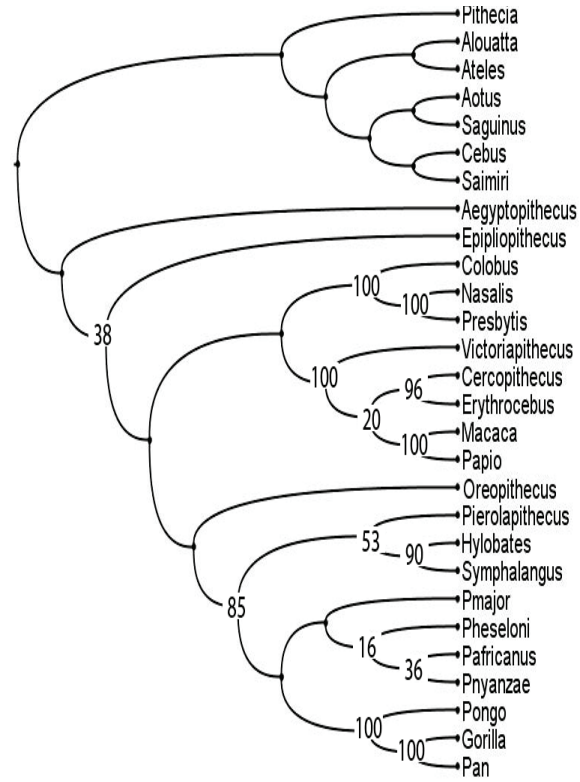

across characters. The average homoplasy score for these synapomorphies was 1.41.

4.1.2.5 Analysis 5: H2- stem hominoid.

These results are the same as the optimal tree from analysis 1 (fig.36, fig. 44). One-hundred and twenty-five synapomorphies were identified supporting a *Proconsul* + hominoid clade. This analysis had the lowest tree cost of the final three analyses, 11069.863 and the most synapomorphies. Synapomorphies range across all regions except the pelvis, with most synapomorphies drawn from the forelimb (32 synapomorphies), manus (28 synapomorphies) and pes (36 synapomorphies). The forelimb, pelvis and mandible each exhibited more synapomorphies than expected. The average homoplasy score for these synapomorphies was 1.94, with the manus exhibiting the least homoplasy and the cranium the most.

4.1.2.6 Analysis 6: H3- stem hominid.

The final analysis identified 37 synapomorphies supporting a *Proconsul* +

hominid clade (fig. 46). The optimal tree cost 11093.992, making it the least supported of the three hypotheses. The majority of synapomorphies were from the forelimb (15 synapomorphies). Only the forelimb had more synapomorphies than expected. The average homoplasy score across all synapomorphies was 2.2.

Figure 47. Most parsimonious unconstrained tree with bootstrap support

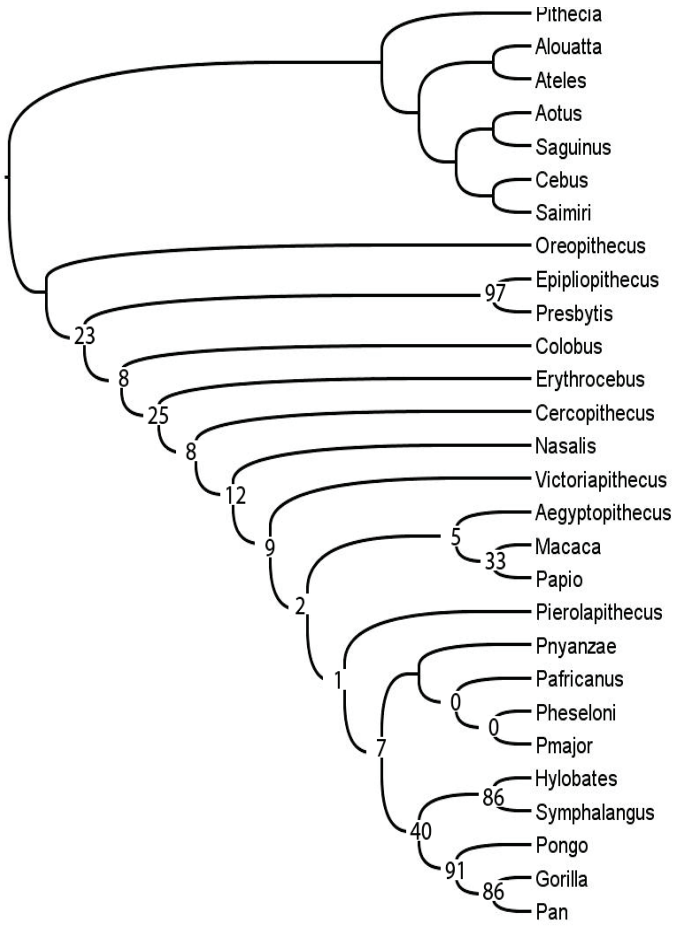

4.1.2.7 Analysis 7: Unconstrained.

The unconstrained analysis inferred a single most parsimonious tree (fig. 47). *Proconsul* was again inferred to be a hominoid, sister to a clade including extant hominoids and *Pierolapithecus*. Bootstrap support for this position is only 1. *Oreopithecus* is inferred to be the most basal catarrhine taxon, with a clade including *Presbytis* and *Epipliopithecus* inferred as sister to the remaining catarrhine taxa. *Aegyptopithecus* groups with *Papio* and *Macaca,* sister taxon to the hominoids, with *Victoriapithecus* diverging prior to this clade. Clearly this result is demonstrative of the regions sampled in this analysis, with dental characters conspicuously absent and likely able to infer the cercopithecoid clade, resolving many of the incongrueties between this and established phylogenies. It does, however, support the stance taken by this dissertation that dental characters are not necessary to infer the phylogenetic

position of *Proconsul* as falling among the hominoid clade and not within the Hominidae or more basally among the stem catarrhines.

4.1.3 Discussion

These analyses place *Proconsul* within Hominoidea, sister to a clade including all fossil and extant hominoids included in the analysis. Results from the unconstrained analysis emphasize the distinctiveness of hominoids relative to cercopithecoids in this data set. *Oreopithecus* is a notable exception to this pattern—While the unconstrained analysis was unable to identify synapomorphies supporting a monophyletic cercopithecoid clade, it did infer a monophyletic extant hominoid clade. *Aegyptopithecus, Victoriapithecus, Macaca* and *Papio* are inferred to fall nearer the hominoid clade than other cercopithecoids, and *Oreopithecus* is pushed to the base of the catarrhine clade—perhaps unsurprising given the problematic nature of this taxon (Gervais, 1872; Schwalbe, 1915; Gregory, 1922; Hürzeler, 1954, 1960; Strauss, 1963; Simons, 1972; Szalay and Delson, 1979; Riesenfeld, 1975; Forsyth Major, 1880; Rosenberger and Delson, 1985; Harrison, 1986; Sarmiento, 1987; Harrison et al., 1991; Andrews et al., 1996; Cameron, 1997; Harrison & Rook, 1997; Begun, 2007).

The full analysis of all characters supports H2—*Proconsul* is a stem hominoid—but the distribution of synapomorphies, driven primarily by the forelimb, manus and pes, indicated that sampling bias was driving results. Consideration of each morphological region in isolation is then necessary to address the applicability of this inference. Each morphological region, however, confirmed the result from the full character list either supporting H2 or placing *Proconsul* among the cercopithecoids (as in the pes, madible and cranium) and thus supporting none of the three proposed hypotheses. These mandible and cranium suffered from the lack of dental characters, which would have easily distinguished between the *Proconsul* and the

cercopithecoid morphology. As placing *Proconsul* within Cercopithecoidea is not a viable hypothesis given a wealth of contraio- dental characters that were not included in this analysis, it is likely these characters are reflecting symplesiomorphic similarity between *Proconsul* and the cercopithecoids in regions for which hominoids are more derived.

The overall congruence between regions in supporting H2 suggests that unequal sampling across the skeleton in this data set (with the notable exception of excluding dental characters) is not impacting the inferred phylogenetic position of *Proconsul*. The breakdown of synapomorphies by region supporting H2 indicates the forelimb and pelvis are primary regions driving similarity between *Proconsul* and crown hominoids, though each hypothesis identifies the forelimb as a region with many potential synapomorphies. Across all hypotheses the cranium, the mandible and the pes were the most problematic, identifying more similarities between *Proconsul* and cercopithecoids than either between *Proconsul* and hominoids or among crown catarrhines. The mandible, however, still inferred 9 synapomorphies supporting H2 (3% more than expected given equal sampling).

Across all regions, homoplasy is likely reflecting the proportion of discretized characters as TNT calculates homoplasy for continuous characters in terms of intervals (see discussion above) that can be as small as 0.001, while descritized homoplasy is calculate only in full steps (Goloboff, 2000). Regions that possess large numbers of discretized characters (such as the cranium) possess the highest homoplasy score. The number of discretized characters is also reflected in the degree of resolution, with the cranial data set unable to resolve relationships among hominoids. The forelimb, manus and pes contributed the most synapomorphies across all regions, with the forelimb, pelvis and mandible contributing more synapomorphies than expected given equal sampling. The manus and pelvis were able to accurately infer the phylogenetic

relationships of all extant taxa. The mandible and pes both struggled with inferring a hylobatid clade, though were able to infer accurate relationships among the great apes. *Oreopithecus* was inferred to fall at the base of the hominoid clade and was even inferred to be more basal than *Proconsul* for the manus data set (a result that was also present in the analysis of all characters). This result is surprising given the derived suspensory adaptations possessed by this taxon (Harrison, 1991), and—given the consensus in the literature that it is likely a basal hominid (Sarmiento, 1987; Harrison, 1991; Begun et al., 1997; Harrison and Rook, 1997; Begun, 2001) or even hominan (Hürzeler, 1958; Straus, 1963; Williams, 2008)—could be indicative of primitive features shared with the pliopithecoids and dendropithecoids; taxa which express a greater degree of suspensory abilities than the cercopithecoids (Leakey and Leakey, 1987; Rose, 1983. 1993; Harrison, 2010, 2013). Only the forelimb data set places this taxon within the Hominidae, as sister to *Gorilla*—a similarity discussed early in its study by Gervais (1872). These results further complicate interpretation of this fossil, suggesting its inclusion within the Hominidae should be reconsidered. *Pierolapithecus* could only be included in the pes data set, which was unable to distinguish between placing this taxon within Hominidae or as a stem hominoid. The pelvis, forelimb and the mandible all support a clade including *P. heseloni* and *P. nyanze*, potentially adding further support for *Ekembo* (McNulty et al., 2015), with no region supporting *Ugandapithecus* (*P. africanus* + *P. major*) as a valid clade (Senut, 2000; Pickford et al., 2009).

4.2 BAYESIAN

4.2.1 Methods

Bayesian MCMC (multi-chain Monte-Carlo) methods can be applied to morphological data by using Lewis' (2001) mk (Markov) model. Bayesian analyses were run using Beast2

(Bouckaert et al., 2014), which allows for the inclusion of missing data. Characters were discretized into three character states using gap weighting (Thiele, 1993). Maximum sum of clade credibilities trees were used across all analyses, as opposed to clade Bayes. While clade Bayes optimizes posterior probabilities for individual clades and builds trees by assembling optimal clades, it may support sub-optimal trees across the entire typology (Wheeler and Pickett, 2008). Maximum sum of clade credibilities trees do not suffer from this problem as the method only considers the sum of posterior probabilities across the entire tree typology and not within isolated clades. Three runs of each analysis were performed in order to assess convergence on the same solution. RWTY (Warren et al., 2016) was used to test for convergence in order to ensure enough tree space was explored. This is an essential step in any Bayesian analysis as optimal solutions may be found before analyses reach stationarity, the point at which the optimal solution is consistently supported, no longer fluctuating between multiple optimal solutions. Testing for convergence requires running analyses multiple times (here all analyses were run three times) and comparing results from the separate runs. Topological autorrelation plots (Penny and Hendy, 1985; Nylander et al., 2008, Warren et al., 2016) were used to assess convergence between runs. This summarizes the average distance between trees across runs. If a trend is apparent throughout the plot it indicates that trees that are close to each other in the chain are more similar than those in other chains or at different points within the chain, indicating insufficient mixing. Where plots are flat adequate mixing has been achieved.

I incorporate mode and tempo of evolutionary changes by integrating a dating analysis following Ronquist et al. (2012) tip dating method into all analyses. Morphological evolution is calibrated to molecular evolutionary rates allowing inferences concerning divergence dates between fossil lineages that lack molecular information. Instead of simply inferring tree

topology, analyses simultaneously infer timing of cladogenic events based on dated fossils, molecular clocks and morphological evolution. This allows alternative hypotheses to be tested concerning the timing of evolutionary events and rates of morphological change (Magallon et al., 2010; Pyron et al., 2011; Ronquist et al., 2012; Wood et al., 2013). With these methods, incorporating dating results into phylogenetic analyses is becoming commonplace (Pyron et al., 2011; Ronquist et al., 2012; Wood et al., 2013; Gavruyshkina et al., 2014; Arcila et al., 2015; Zhang et al., 2015). A further advantage of these methods is avoiding using arbitrary and often overlapping calibration priors in order to estimate earliest appearance dates for each fossil separately (Heath et al. 2014). Calibration priors place all dating inferences on the framework of an arbitrary prior that does not take into account information from the fossil record. The fossilized birth-death model (FBD) applied here uses a single model with only four parameters to calibrate phylogenies: speciation rate, extinction rate, fossilization rate and proportion of sampled extant species (Heath et al., 2014). By using a single model across the phylogeny and not using separate priors for calibration nodes and full tree calibration, the FBD model assumes fossils and extant taxa are all evolving as a result of the same macroevolutionary processes. These methods have been shown to accurately infer ancestral ages with simulated data (Heath et al., 2014) and real data sets (Gavryushkina et al., 2014; Arcila et al., 2015; Grimm et al., 2015; Zhang et al., 2015).

Analysis 1: Combined total evidence analysis This analysis combined both morphological and molecular data. All data were linked to infer a single tree. Each morphological and molecular site was allowed to evolve on separate site models. Morphological sites in this case are defined by one of six morphological regions (i.e., cranium, mandible, forelimb, manus, pelvis and pes) and further divided by the number of character states, with characters within the same

region and having the same number of characters states treated as a single site. All morphological data employed a Lewis MK model of character evolution, estimating substitution rate and shape parameters. Rate variation was modeled using the gamma distribution with 4 rate categories. Molecular data were handled following the methods presented in the Perelman (2011) analysis: GTR+I+G with four rate categories. FBD models were employed in order to infer node ages using tip dating (see above). Fossil ages were included as tip dates and all data were linked under a single relaxed clock model. Cercopithecoids were constrained as monophyletic, with basal catarrhines (*Aegyptopithecus* and *Epipliopithecus*) and platyrrhines constrained as successive outgroups. *Proconsul* species were constrained as monophyletic. Three separate MCMC analyses were run for 75,000,000 iterations sampling every 1000 generations.

Analysis 2: Morphological regions. While systematic methods require large amounts of data sampling across morphological regions (Huelsenbeck, 1991; Wheeler, 1992; Wiens, 1998, 2003a, 2005; Wiens and Moen, 2008; Prevosti and Cheminquy, 2010; Wiens and Tiu, 2012), individual anatomical regions are often discussed in isolation. This is useful for interpreting evolutionary change in specific regions, but it is often simply a necessity when dealing with incomplete fossils. Researchers should not assume that an individual structural-functional complex will provide robust support for phylogenies, but observing the phylogenetic signal of individual complexes can portray a more detailed picture of the evolving skeleton and provide additional information when it comes to interpreting results.

This analysis did not include molecular data in order to observe the phylogenetic relationships inferred from morphology alone. Morphological regions were consistent with the previous analyses described in previous chapters: the cranium, mandible, forelimb, manus, pelvis

and pes. A Lewis MK model of character evolution was applied to all data, estimating substitution rate and shape parameters. Rate variation was modeled using the gamma distribution with a category count of 4. Separate regions evolved under their own unlinked model. Fossilized birth-death models were employed in order to infer node ages using tip dating. Fossil ages were included as tip dates and each region evolved under its own unlinked relaxed clock model. Cercopithecoids were constrained as monophyletic, with platyrrhines and stem catarrhines (*Aegyptopithecus* and *Epipliopithecus*) constrained as successive outgroups. *Proconsul* species were constrained as monophyletic. An MCMC analysis was run for 75,000,000 iterations sampling every 1000 generations. Three runs were performed for each region.

Analysis 3: Unconstrained. A final analysis removed all constraints, only constraining platyrrhines as the outgroup and run with only morphological data. Otherwise, the methods were the same as in Analysis 1.

4.2.2 Results

4.2.2.1 Analysis 1: Combined total evidence

The sum of clade credibilities tree (fig. 48) places *Proconsul* within Hominoidea, as sister to all other hominoid taxa. The hominoid node including *Proconsul* is strongly supported with a posterior probability of 0.90. This posterior is significantly higher than the alternate hypotheses. A clade including crown catarrhines and excluding *Proconsul* (fig. 49) has a posterior probability of 0.01, while the posterior probability of a hominid + *Proconsul* clade is 0.00. The inferred most recent common ancestor (MRCA) age is also inconsistent with the hominid hypothesis as the hominoid MRCA is inferred to be younger than the *Proconsul* + hominid MRCA age. The optimal tree (supporting H2) infers *Proconsul* would be morphologically similar to the ancestral

Figure 48. Analysis 1: Optimal bayes tree

Node values denote posterior probability of clades. Color indicates evolutionary rate, with yellow indicating rapid evolution and blue indicating slow evolution.

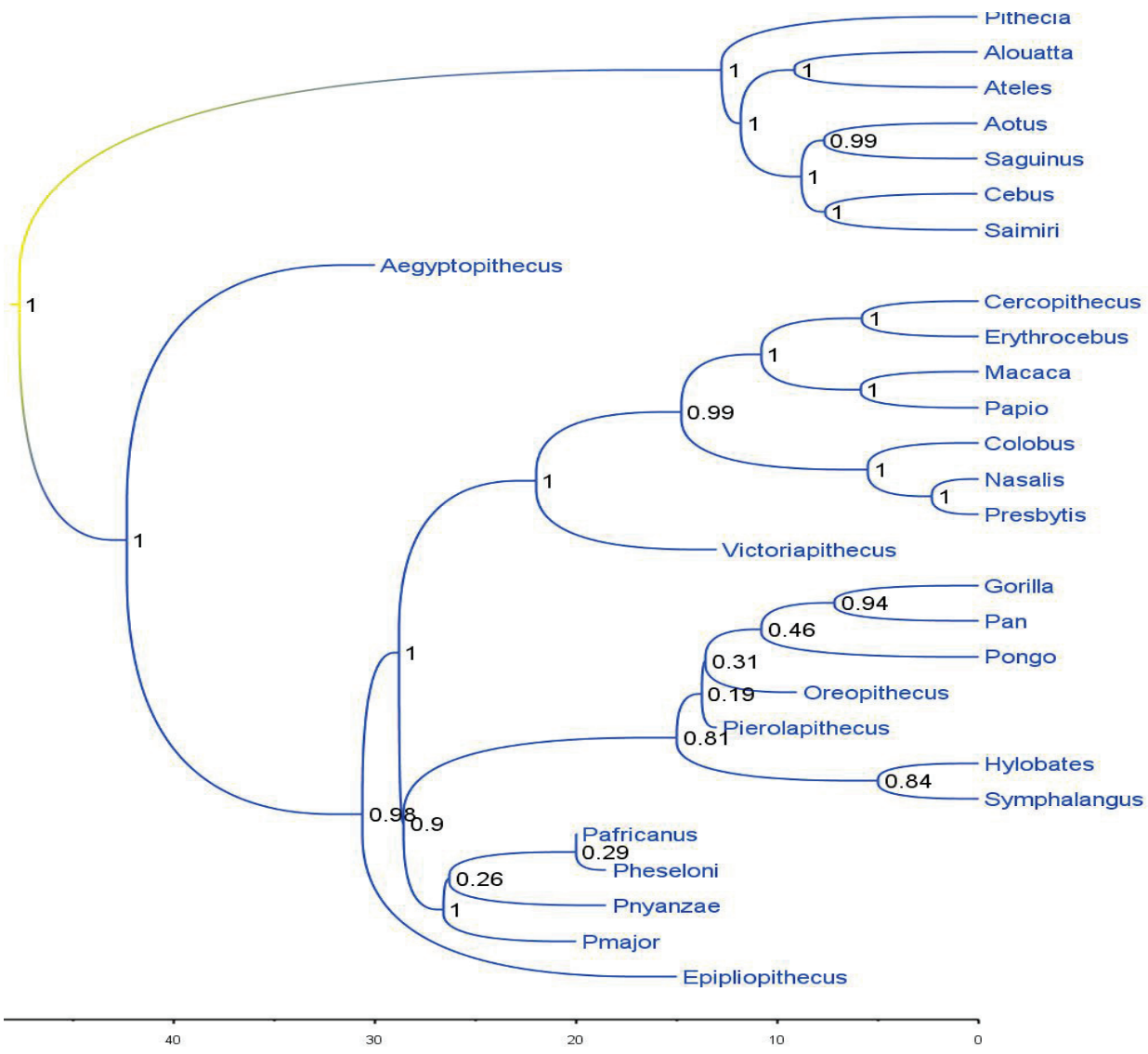

crown catarrhine morphotype, with the origination of the *Proconsul* lineage occurring nearly simultaneously with the divergence of the hominoid and cercopithecoid lineages. *Proconsul* is separated from the other hominoids by a long branch, along which much of the morphology associated with extant hominoids evolved. A crown hominoid clade excluding *Proconsul* is strongly supported, with a posterior probability of 0.81. The hylobatids are inferred to diverge

from the other hominoids early in the evolution of crown hominoids and separated from them by a long branch. The hylobatids are inferred to be the sister taxon to a clade including *Oreopithecus, Pierolapithecus* and the extant hominids, though this clade is only weakly supported (pp=0.19).

A long branch separates *Aegyptopithecus* from *Epipliopithecus*, whose divergence occurs near the diversification of crown catarrhines. *Victoriapithecus* is inferred to be a basal cercopithecoid, sister taxon to all extant cercopithecoids, supported with a posterior probability of 0.99. Evolutionary rates do not differ between analyses, with rapid evolution occurring at the root of the anthropoid tree.

Figure 49. Analysis 1: H1- stem catarrhine tree

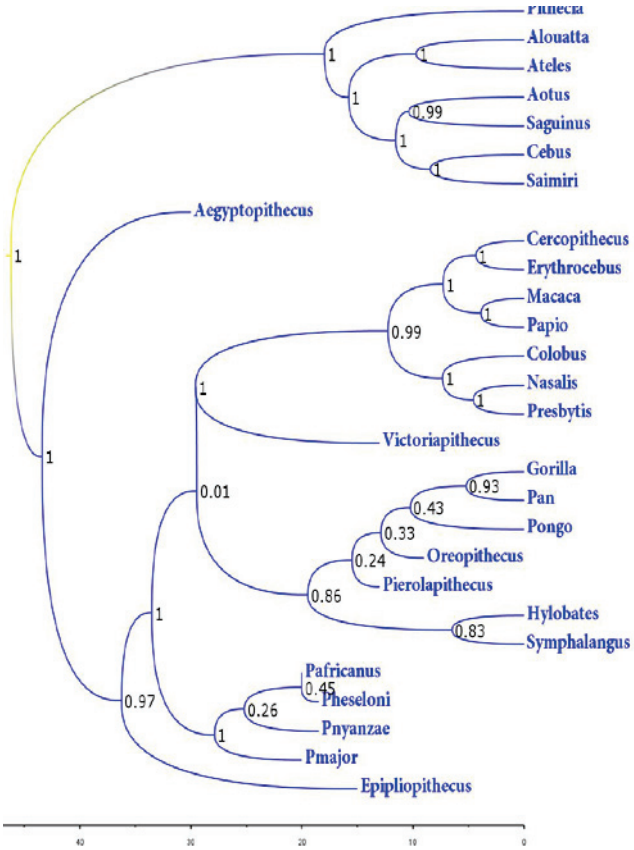

Figure 50. Analysis 1: H3- stem hominid tree

Node values denote posterior probability of clades. Color indicates evolutionary rate, with yellow indicating rapid evolution and blue indicating slow evolution.

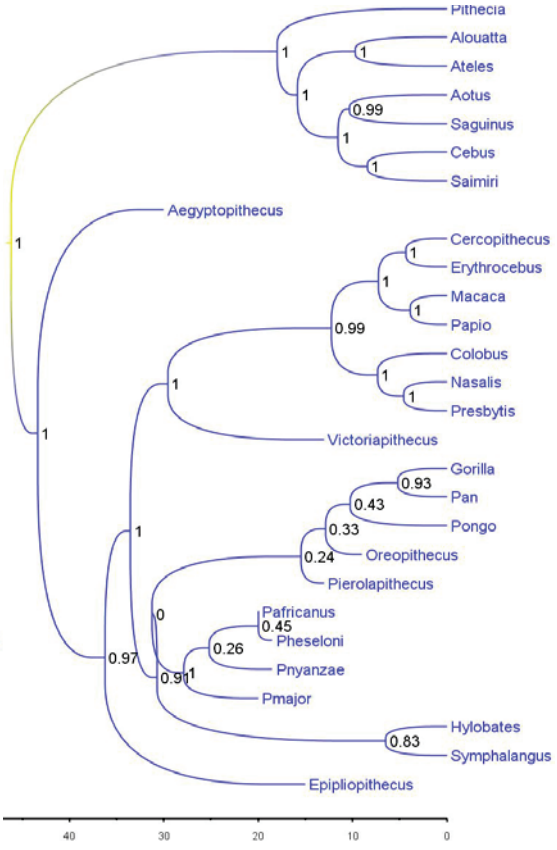

Table 4. MRCA age estimates by hypothesis and molecular dates from Perelman et al., (2011)
Values in parentheses are 95% HPD intervals

	Perelman	H1- stem	H2- hominoid	H3- hominid
Hominidae	16.52 (13.45-19.68)	15.56	13.75	31.22
Hominoidea	20.32 (16.59-24.22)	19.52	28.54	31.22
Cercopithecoidea	17.57 (13.88-21.52)	12.23	14.77	12.74
Crown catarrhines	31.56 (25.66-37.88)	29.56	28.8	34.02
Catarrhini	31.56 (25.66-37.88)	43.47	42.34	43.89

Node age estimates are similar between H1, H2, with the exception of the hominoid date. Under H2 the hominoid date is older and falls outside the 95% HPD (highest posterior density) range from Perelman (2011), though agrees with the updated age estimate from the fossil record of Stevens (2013). This updated estimate incorporates fossil material from the newly described taxon *Rukwapithecus*, which possesses potential dental synapomorphies with the hominoids and appears similar to the nyanzapithecine *Rangwapithecus* (Stevens et al., 2013). Under H3, hominid and hominoid ancestral age estimates are significantly older than expected in order to accommodate placing *Proconsul* within Hominidae. The inferred origin of the catarrhine MRCA is comparable across analyses and is consistently older than Perelman's estimate. Other inferred ages fall in 95% HPD from Perelman (2011).

Figure. 51. RWTY: Autocorrelation plot
Summarizes the average distance between trees across runs indicating convergence if no clear trend is apparent. Colors indicate separate runs.

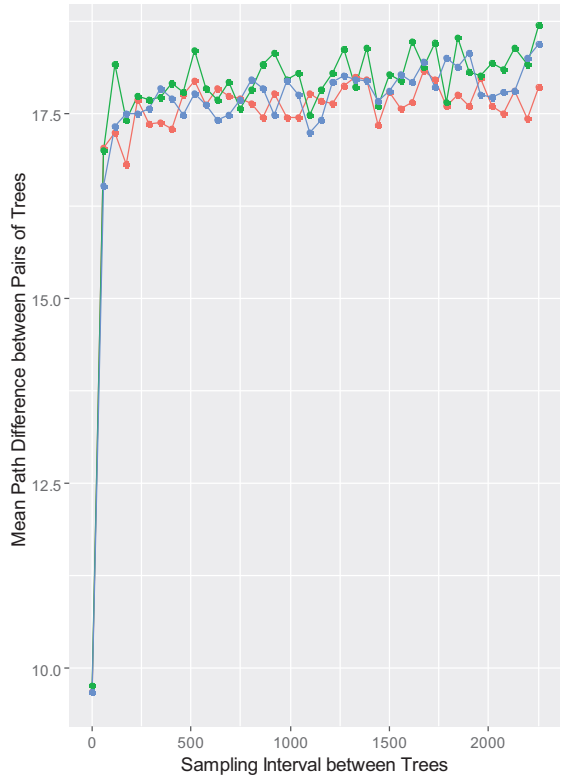

Convergence analyses (figs. 51) demonstrate convergence was reached, with no apparent trend over the runs, demonstrating adequate mixing among chains, indicating chains are sampling the same treespace.

4.2.2.2 Analysis 2: Morphological regions

Each region except the mandible supports H2, placing *Proconsul* at the base of the hominoid tree (figs.52-58). The mandible supports H1, inferring *Proconsul* is sister taxon to crown catarrhines. The crown catarrhine node without *Proconsul* is weakly supported with a posterior probability of 0.35. The pes data set most strongly supports placing *Proconsul* within Hominoidea, with a posterior probability approaching 1. This is surprising given that results from the parsimony analysis of pes data place *Proconsul* as sister to the cercopithecoids. However, evolutionary rates for the pes are slow across the catarrhine tree, suggesting there may be little support for either hypothesis as differences between crown and stem taxa may be limited. Alternately it could result from differences between the discretized and continuous data sets. If discretization method is the source of the discrepancy, the continuous result would be preferred as it is least likely to be biased through additional manipulation (Felsenstein, 1988, 2002; Goloboff, 2006; Worthington, 2012). The forelimb data set also strongly supports a *Proconsul* + hominoid clade (pp=0.80). The manus and pelvis weakly support this placement with posterior probabilities of 0.49 and 0.48 respectively. The pelvis data set infers rapid evolutionary changes across the anthropoid tree. The cranium provides moderate support with a posterior probability of a hominoid + *Proconsul* clade of 0.63.

Figure 52. Cranium optimal Bayes tree
Node values denote posterior probability of clades.

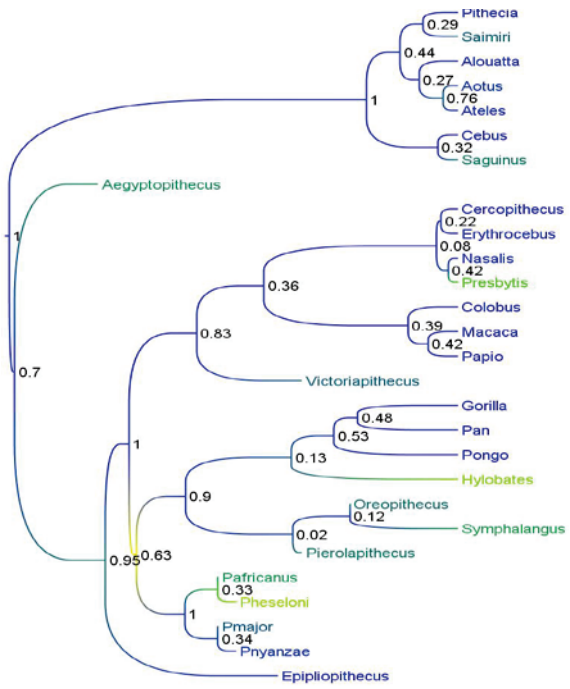

Figure 53. Manidble optimal Bayes tree
Color indicates evolutionary rate, with yellow indicating rapid evolution and blue indicating slow evolution.

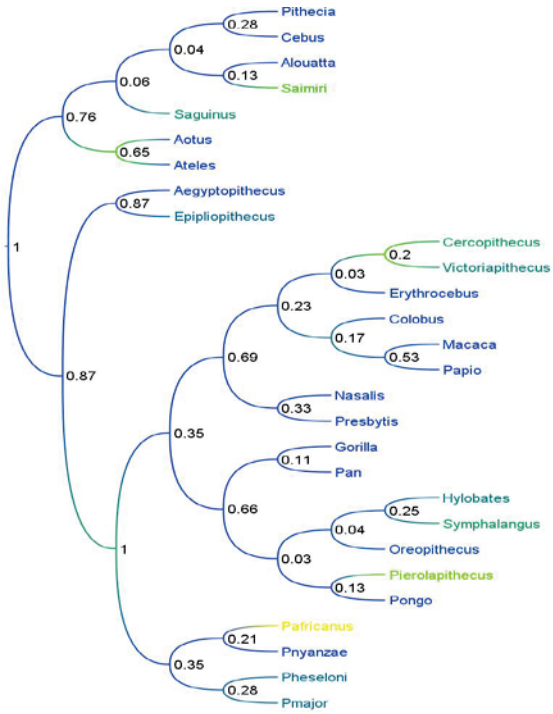

Figure 54. Forelimb optimal Bayes tree
Node values denote posterior probability of clades.

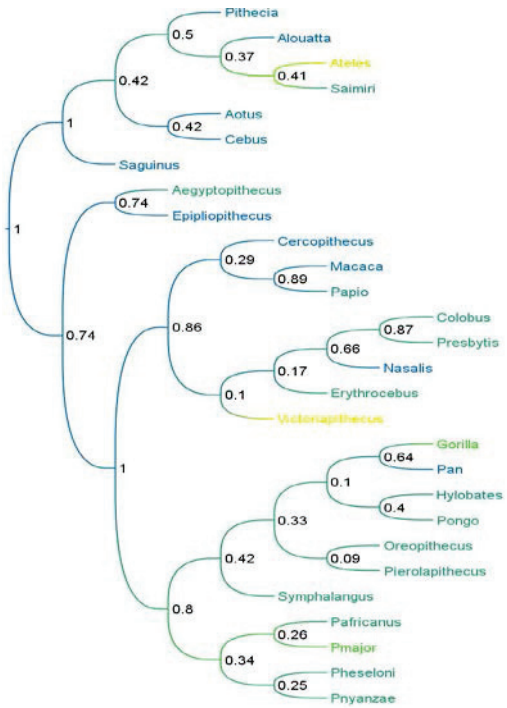

Figure 55. Manus optimal Bayes tree
Color indicates evolutionary rate, with yellow indicating rapid evolution and blue indicating slow evolution.

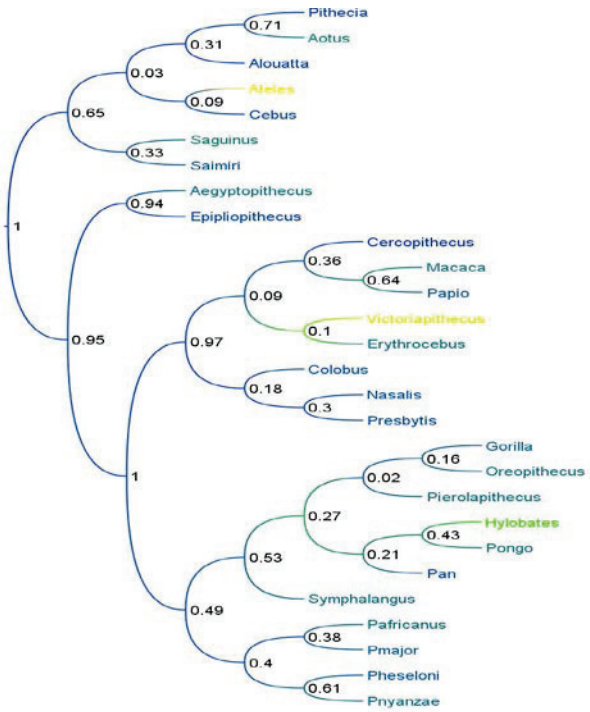

Figure 56. Pelvis optimal Bayes tree

Node values denote posterior probability of clades.

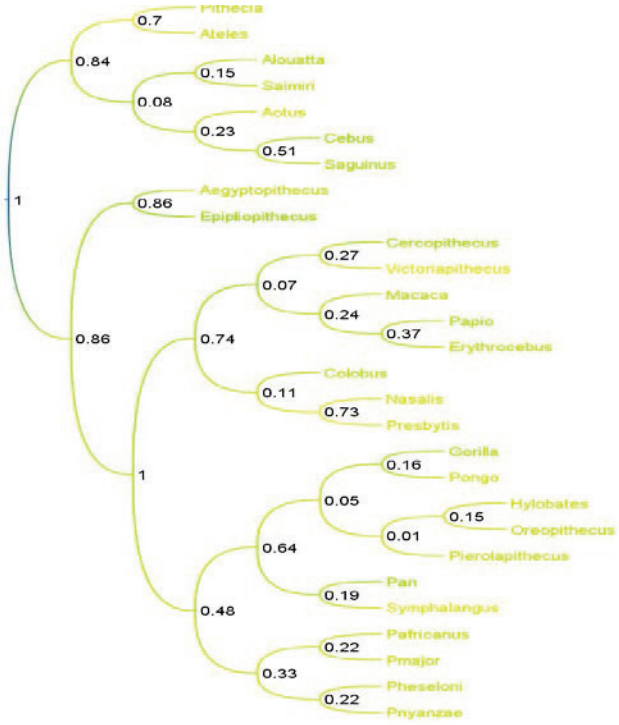

Figure 57. Pes optimal Bayes tree

Color indicates evolutionary rate, with yellow indicating rapid evolution and blue indicating slow evolution.

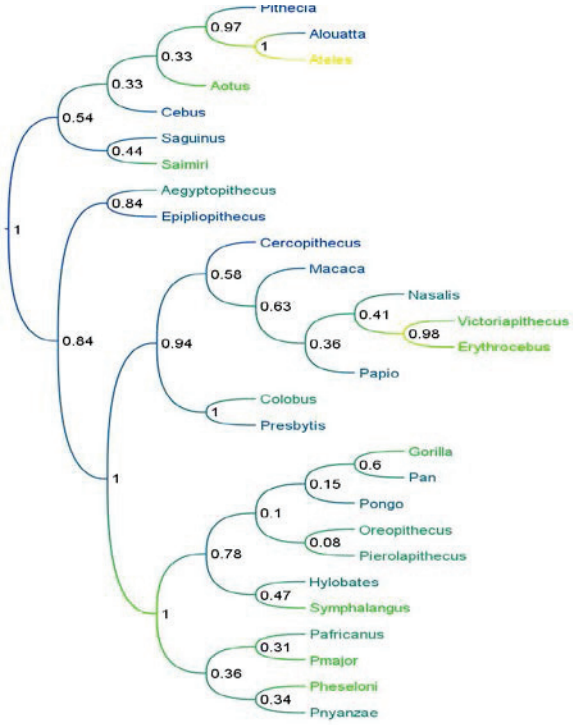

Figure. 58. RWTY: Autocorrelation plot

Summarizes the average distance between trees across runs indicating convergence if no clear trend is apparent. Colors indicate separate regions and runs

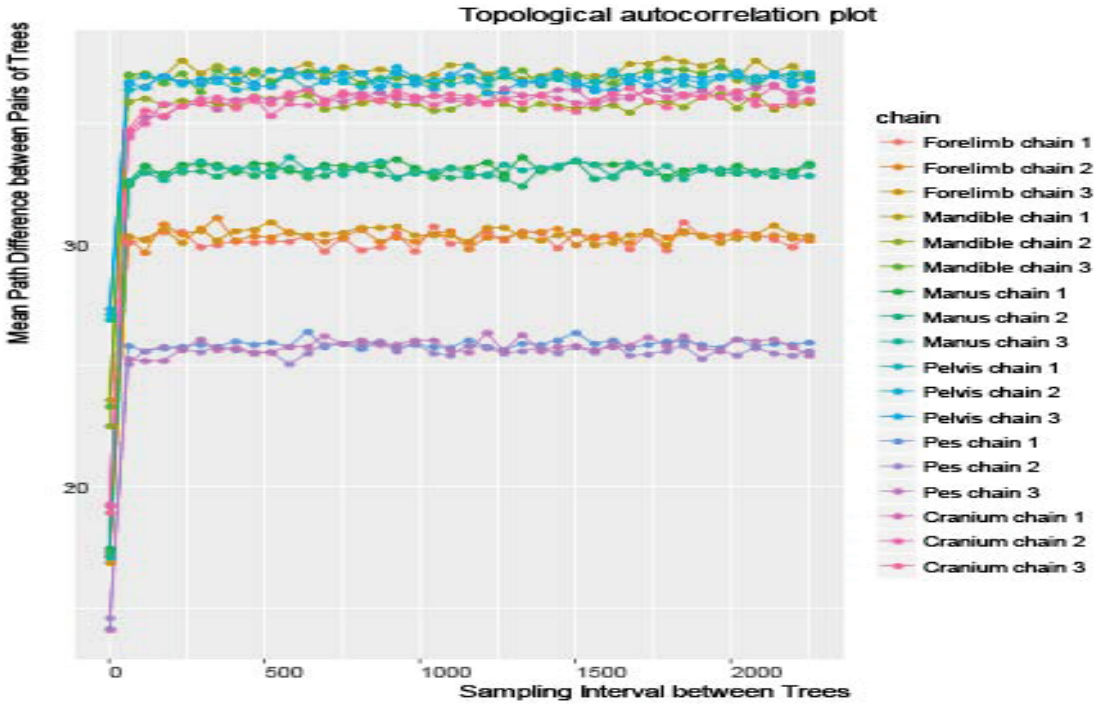

4.2.2.3 Analysis 3: Unconstrained.

The unconstrained analysis did not reach convergence after 75 million generations, but is nevertheless interesting to discuss in terms of the distribution of taxa in the optimal typology. *Proconsul* is pushed to the base of the catarrhine tree, forming a clade with *Aegyptopithecus* that is sister to all other catarrhines. Extant hominids are inferred to be monophyletic, though *Victoriapithecus* is inferred to fall within the hominoid clade, likely clustering with hominoids due to shared primitive characteristics that other cercopithecoids lack. *Macaca* and *Papio* are also pulled out of the cercopithecoid clade and placed with the hominoids, perhaps due to similarities with *Victoriapithecus*. *Epipliopithecus* falls as sister to a colobine clade.

Figure 59. Unconstrained Bayes tree
Node values denote posterior probability of clades. Color indicates evolutionary rate, with yellow indicating rapid evolution and blue indicating slow evolution.

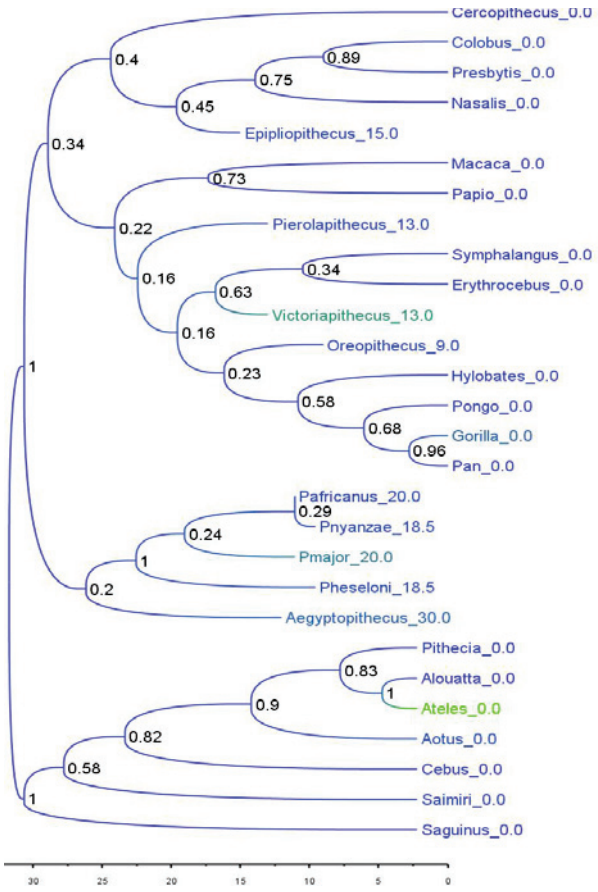

As in the unconstrained parsimony analysis, the inability of these data to infer a cercopithecoid clade is due to the absence of dental characters.

4.2.3 Discussion

Similar to results from the parsimony analyses, *Proconsul* is inferred to fall within Hominoidea and thus H2 is supported. Confidence in this result is high, with a high posterior probability (0.90) supporting a hominoid + *Proconsul* clade and very low posterior probabilities supporting key clades for both H1 (0.01) and H3 (pp<0.01).

Ancestral age estimates are broadly consistent with estimates from molecular analyses with the exception of the inferred age of the catarrhine MRCA and hominid and hominoid ages under H3 (Poux and Douzery, 2004; Matsui et al., 2009; Perelman et al., 2011). This provides an additional piece of evidence suggesting H3 is unlikely to be the optimal hypothesis. Further, age estimates for the hominoid MRCA on the optimal tree push into the Oligocene, supporting findings by Stevens (2013) that the potential hominoid *Rukwapithecus* dated to 25.2 mya could indicate the hominoids radiation originated before the Miocene.

The unconstrained analysis differs from the parsimony result in inferring *Proconsul* is a stem catarrhine. The two analyses are similar, however, in the position of *Victoriapithecus* within Hominoidea, likely indicating a symplesiomorphic similarity to the basal catarrhine morphotype that has been lost in extant cercopithecoids.

Figure 60. RWTY: Autocorrelation plot for unconstrained analysis
Summarizes the average distance between trees across runs indicating convergence if no clear trend is apparent. Colors indicate separate runs.

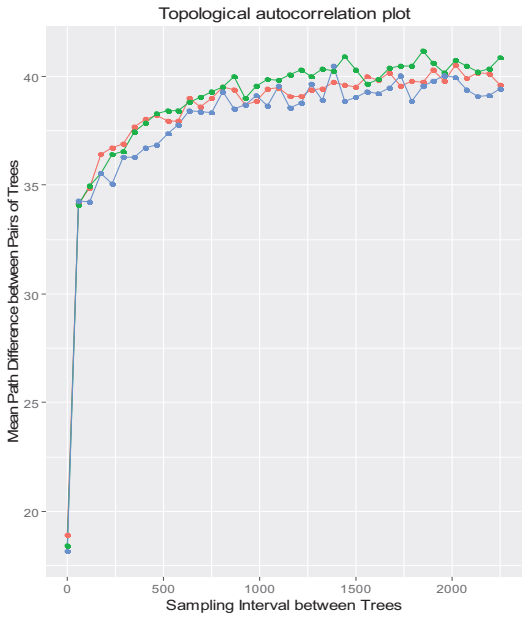

4.3 CONCLUSION

Both parsimony and Bayesian analyses strongly support H2—*Proconsul* is a hominoid. This result—employing a robust data set, rigorous phylogenetic methods and validation by multiple methods—provides robust support for acceptance of a hominoid clade including *Proconsul*. *Proconsul* is identified as falling near the divergence of cercopithecoid and hominoid lineages and is morphologically closer to the ancestral crown catarrhine morphotype than the extant hominoid

ancestral morph. This elucidates the difficulty researchers have had in resolving the phylogenetic position of this taxon. However, enough synapomorphies were identified to justify inclusion of *Proconsul* within Hominoidea. Synapomorphies were drawn from across the skeleton, but a majority were identified in the forelimb. The cranium, manus and pes contributed fewer synapomorphies than expected given character sampling in this analysis, while the forelimb, pelvis and mandible contributed more.

These results corroborate results from the previous chapter in which *Proconsul* consistently appeared phenetically most similar to the hominoids. *Proconsul* is also identified as being morphologically distinct relative to extant taxa, separated from other taxa and ancestral nodes by long branches. Other fossil taxa were also shown to extend the range of variation exhibited by extant taxa. *Oreopithecus* in particular was identified as being problematic and often pushed to the base of clades. *Victoriapithecus* was demonstrated within the unconstrained analyses to be symplesiomorphically similar to the hominoids.

In order to better understand morphologically what is happening at the base of the catarrhine and hominoid clades the next chapter will use the synapomorphies identified here to infer ancestral morphotypes and explore morphological evolution among catarrhines. Further analysis, outside of a strict cladistic framework, is necessary to develop a comprehensive model of catarrhine morphological evolution.

CHAPTER 5: CHARACTER EVOLUTION

The phylogenetic analyses in this thesis have confidently rejected H1 and H3, supporting H2—*Proconsul* is a hominoid—as the optimal hypothesis. This chapter further explores the broader assumptions concerning catarrhine evolution associated with this result. Synapomorphies are taken from the previous analyses and further evaluated for which hypothesis they optimally support. Those that optimally support H2 are discussed in detail and compared to character lists from the literature as outlined in chapter 1. Finally, ancestral morphotypes are inferred for the full list of H2 synapomorphies and projected into a morphospace defined by these synapomorphies. This visualizes the evolutionary trajectories—moving from ancestral morphotypes to fossil taxa to extant taxa—associated with placing *Proconsul* within Hominoidea.

Simply inferring that *Proconsul* falls within Hominoidea does not elucidate the trajectory of catarrhine morphological evolution. Further exploration is needed in order to infer how the earliest crown catarrhines are different from basal catarrhines and to determine the affinities between the earliest cercopithecoids and hominoids both to each other and to the stem catarrhine morphotype. Results from phylogenetic analyses alone cannot be used to address the morphology of the earliest catarrhines, crown catarrhines or even the degree of similarity between *Proconsul* and the first hominoids.

As discussed in chapter 1, paleoanthropologists often rely on lists of carefully selected and tested characters which they deem most significant for inferring the phylogenetic relationships of a tax on (e.g. Rae, 1993, 1999; Begun et al., 1997; Young and MacLatchy, 2004; Rossie and MacLatchy, 2006; Rossie, 2008; Zalmout, 2010). They use these selected character

lists to infer phylogenies. This analysis adopted a different approach, using as much morphological data as could be reasonably collected within the confines of this project in order to limit character selection bias. While this meant certain traditionally favored characters were excluded from the analysis, it also allowed for the possibility of identifying new characters in neglected regions and not simply relying on established lists, which may simply recreate prior results (Bjarnason et al., 2011). This resulted in a data set including the most comprehensive character list for addressing the question of where *Proconsul* falls on the catarrhine tree. While this methodology is ideal for applying cladistic methods, it is unable to evaluate key characters to the same extent as studies prioritizing character selection. In this final analysis I combine the two methodologies by using the list of H2 synapomorphies to phenetically explore evolution of this key set of characters. In this way I achieve the aim of compiling a more limited character list that allows for discussion of specific morphological changes across the catarrhine tree.

This analysis includes three stages: compiling synapomorphies, inferring ancestral morphotypes at relevant nodes, and visualizing results in cluster dendrograms and PCAs. Finally, a detailed discussion of the significance of these synapomorphies (supporting H2) follows. By inferring ancestral morphotypes for the synapomorphies one can infer the evolutionary trajectories leading to each lineage and explore the implications of these trajectories to our understanding of catarrhine evolution.

5.1 METHODS

The 125 synapomorphies (appendix D) supporting H2 inferred using TNT (treating continuous character as such) in the previous chapter comprise the character list for this analysis. Phylogenetic analyses are able to deal with the problem of significant amounts of missing data,

but it introduces unnecessary error when inferring ancestral morphotypes and particularly in plotting PCAs. It is necessary, therefore, to limit missing data for these analyses and any characters or taxa with extensive missing data were removed.

5.1.1 Bayesian-Ancestral Morphotype Reconstruction

Bayesian analysis was used to infer ancestral character states for platyrrhines, catarrhines, crown catarrhines, hominoids and hominids using all characters inferred as synapomorphic even where they did not optimally support H2 (appendix D). Any remaining missing data were also inferred in these analyses. BayesTraits (Pagel and Meade, 2011) was used to conduct MCMC analyses on character lists. Metric characters were treated as continuous, using a non-directional, random walk model (Pagel, 1997, 1999). This allows characters to vary along phylogenetic trees where branch lengths are used to inform transition rates for characters. The tree with branch lengths was taken from the combined total evidence Bayes analysis (see chapter 4). Separate analyses were run for each region. A single analysis across all regions was not possible given that current limitations of the program, which cannot handle large numbers of characters. Analyses were run in two stages, first running an MCMC analysis to create a model of character evolution and then a second run applying that model to infer ancestral morphotypes. Each analysis ran for 75,000,000 iterations.

5.1.2 Phylo-morphospace analysis

Phylo-morphospace analyses combine results from phonetic and phylogenetic analyses into a single visualization. Often these visualizations are simply PCAs with phylogenetic trees linking taxa across the phonetic distribution. This analysis does not include phylogenetic results into phenetic analyses by superimposing phylogenetic trees, but instead maps results from the

ancestral morphotype reconstructions onto PCAs ordinated using extant catarrhine morphology. This allows for visualization of evolutionary trajectories of key synapomorphies. Euclidean distances between taxa were calculated across all key synapomorphies and visualized in cluster dendrograms using the neighbor joining method. This directly visualizes the phenetic morphological disparity between taxa for each data set.

As the position of *Proconsul* and ancestral morphotypes relative to catarrhine clades is the focus of this analysis, principal component analyses (PCAs) were constructed using only extant cercopithecoids and hominoids to define PCs. Platyrrhines, fossil taxa and ancestral morphotypes inferred under each of the hypotheses were then mapped onto current PCs. These data did not define axes of variation. In this way *Proconsul,* ancestral morphotypes and platyrrhine morphology are observed relative to a morphospace defined by the differences between cercopithecoids and hominoids. PCAs were constructed for each region, with a final PCA including all synapomorphies.

5.2 RESULTS

5.2.1 Synapomorphies

One-hundred and twenty-five synapomorphies were identified supporting a clade including *Proconsul* and extant and fossil hominoids. Of all 125 synapomorphies, only 20 optimally supported H2 and a *Proconsul* + hominoid clade (table 5). Ten synapomorphies were equally parsimonious for H1 and H3 and the remaining were equally parsimonious across each hypothesis. Only the 20 key synapomorphies for which H2 is optimal (possessing the lowest homoplasy score) will be discussed here, though the full 125 are used in the subsequent phylo-morphospace analysis.

Table 5. Key synapomorphies

code	Char	Hypothesis	*Proconsul*	Basal platyrrhine	Basal Catarrhine	Basal Cercopithecoid	Extant cercopithecoid	Hylobatids	Hominids	Hominans
hum13	Humerus	medio-lateral width of trochlear keel at disto-anterior surface	widest	narrow	narrow	intermediate	intermediate	wide	wide	wide
hum20	Humerus	medio-lateral width capitulum at midline of trochlea	wide	narrow	narrowest	intermediate	intermediate	widest	wide	wide
hum38	Humerus	proximo-distal height lateral trochlear keel on posterior aspect	long	short	short	intermediate	intermediate	long	lomg	intermediate
hum46	Humerus	projection of median trochlear keel distal to margin of medial epicondyle	intermediate	short	short	intermediate	short-intermediate	tall	tall	tall
hum47	Humerus	wdiest point of coronoid fossa	wide	intermediate	narrow	intermediate	narrow-intermediate	wide	wide	wide
PVM10	Pelvis	cranio-caudal diameter of the acetabulum	intermediate	short	short	intermediate	short-intermediate	tall	tall	tall
MC5M25	MC5	medio-lateral width shaft at midpoint	widest	narrow	wide	widest	intermediate	intermediate	wide	wide
HM4	Hamate	palmo-dorsal width hamulus at midpoint	wide	intermediate	intermediate	intermediate	narrow-intermediate	wide	wide	wide
PM1	Pisiform	length of articular facet on triquetral surface	intermediate	intermediate	intermediate	intermediate	intermediate-long	short	short	short
TZDM2	Trapezoid	medio-lateral width MC facet	widest	narrow	widest	intermediate	narrow-wide	wide	intermediate	intermediate
TZMM5	Trapezium	dorso-palmar length MC2 facet	long	short	intermediate	short	intermediate	long	long	short-intermediate
CCM25	Calcaneus	planto-dorsal height sustentaculum	intermediate	short	intermediate	tallest	intermediate	short	short	tallest
NM7	Navicular	proximo-distal length of tubercle	short	intermediate-long	intermediate-long	intermediate	intermediate-long	long	short	short
NM13	Navicular	dorso-plantar height cuboid facet	intermediate	short	intermediate	tall	short-tall	intermediate	intermediate	intermediate
NM17	Navicular	dorso plantar height at lateral cuneiform facet	intermediate	short	intermediate	tall	tall	intermediate	intermediate	short-intermediate
NM21	Navicular	dorso plantar height astragular facet in midline	tall	short-tall	intermediate	tall	short-tall	tall	intermediate	short-intermediate

All regions except the cranium are represented among the key synapomorphies (table 5). Six characters are drawn from the elbow and another seven from the wrist and hand. Five key synapomorphies are present in the ankle and there is a single pelvic and single mandibular character. This distribution of key synapomorphies again reflects the sampling strategy taken by this dissertation, emphasizing the forelimb, manus and pes. This novel sampling provides additional support to results from more conventional data sets and emphasizes the utility of these regions to addressing phylogenetic questions of catarrhine evolution. The mandibular character is breadth across the incisors. Broad incisors are present among hominoids reflecting a reliance on foods (particularly fruit) which require incisal processing (Ungar, 1996; Teaford and Ungar, 2007). *Epipliopithecus* and the platyrrhines (with the exception of *Alouatta)* have narrower incisal breadth, while *Pan* and *Pongo* have the broadest incisors. The narrow incisors of *Aegyptopithecus* and *Dendropithecus* (Simons, 1987; Simons and Seiffert, 2007; Pickford et al., 2010; Harrison, 2013) further suggest that narrow incisors are primitive for catarrhines. *Proconsul* falls between *Symphalangus* and *Gorilla*, well within the hominoid range, but not approaching the derived condition seen in *Pongo* and *Pan*, which rely more heavily on a more frugivorous diet (Kay and Highlander, 1978; Ungar, 1995; Goodall, 1996; Teaford and Ungar, 2007). This result is consistent with previous studies of *Proconsul* dentition and incisal morphology suggesting it may have had a frugivorous diet similar to *Pan* (Kay, 1977; Kelley, 1986; Kay and Ungar, 1997; Deane, 2009).

All six of the key synapomorphies drawn from the elbow are located on the distal humerus. Three characters describe the width of the distal humeral articular surface. This analysis infers that a wide distal humerus—particularly a wide capitulum—is derived for hominoids and *Proconsul.* Cercopithecoids and platyrrhines have narrower distal humeri.

Hominoids and *Proconsul* also have a pronounced median trochlear keel. *Epipliopithecus* and the platyrrhines have narrower keels, while *Proconsul* and the hominoids have broad keels. *Victoriapithecus* and other cercopithecoids are intermediate. This distribution of variation suggests the earliest catarrhines had narrow median keels with all crown catarrhines evolving slightly broader keels that broaden further with the earliest hominoids including *Proconsul*.

Two of the remaining humeral synapomorphies involve the size of the medial and lateral trochlear keels. Hominoids including *Proconsul* also have large, projecting, medial and lateral trochlear keels. While there is extensive overlap between groups for these features (particularly in medial trochlear keel projection), this analysis recognized a trend towards larger more projecting keels in hominoids and *Proconsul* as the most parsimonious scenario. All crown catarrhines have taller keels than platyrrhines, with *Proconsul* and the Asian apes possessing the tallest lateral trochlear keels. The hominines are not as pronounced in this feature, suggesting a character reversal. *Victoriapithecus* and the cercopithecines approach the condition seen in the Asian apes, with the colobines having smaller keels more similar to the platyrrhines. Length of the medial trochlear keel more clearly separates the extant hominoids as having the largest keels, however the platyrrhines and cercopithecoids occupy the same range and *Proconsul* is intermediate. *Proconsul,* along with the cercopithecines, approaches the hominoid condition, however this analysis does suggest the similarity between *Proconsul* and the other hominoids is synapomorphic. The weak keels of the dendropithecoids further support this character polarity (Harrison, 2010, 2013).

The final key synapomorphy from the elbow is the width of the coronoid fossa. Cercopithecoids have a narrow or intermediate coronoid fossa, while *Proconsul* and the hominoids have a wide coronoid fossa. *Epipliopithecus* has a narrow fossa and platyrrhines are

intermediate. Variation in the morphology and development of the coronoid fossa has been widely discussed as a trait seen among Miocene catarrhines, possibly distinguishing early and late Miocene forms (Ward et al., 1999; Nakatsukasa et al., 2007; McNulty et al., 2015), but is not well understood functionally. Here a wide coronoid fossa is inferred to be synapomorphic for hominoids.

Six key synapomorphies are drawn from the wrist: one each from the radius, ulna, trapezoid, trapezium, pisiform and hamate. The radial character involves breadth of the radio-carpal articular facet. Hominoids, particularly hominids, have a broad radio-carpal articulation. *Epipliopithecus*, the colobines, and certain platyrrhines (*Alouatta, Ateles and Aotus*) all have a narrow radio-carpal articulation. Cercopithecines and the remainder of the platyrrhines are intermediate. *Proconsul* has a wide radio-carpal articulation similar to *Pan*, with only *Pongo* expressing a wider morph. The basal catarrhine morphotype is inferred to be narrow, with all crown catarrhines derived in having slightly wider radio-carpal articulations. The earliest hominoids + *Proconsul* have an even broader articulation. Functionally, there is a relationship between a broad radio-carpal articulation allowing for a greater range of motion during suspension and vertical climbing (Sarmiento, 1988; Daver and Nakatsukasa, 2015).

Hominoids and *Proconsul* also have a large distal radio-ulnar articular facet, suggesting a broader hand than dendropithecoids (Leakey and Leakey 1987; Rose et al. 1992; Rose 1993; Harrison, 2010). Hominoids are unique among primates in possessing an intra-articular meniscus between the radius and ulna, allowing a greater degree of rotation of the radius and hand around the ulna and resulting in a more extensive articular facet (Lewis, 1965, 1969; Harrison, 1987; Sarmiento, 1988; Dave and Nakatsukasa, 2015). The catarrhine MRCA radio-ulnar articulation is inferred to be small to moderate, an inference supported by the narrow hand

of *Simiolus* (Leakey and Leakey 1987; Rose et al. 1992; Rose 1993; Harrison, 2010). This articulation is inferred to increase in size in the earliest hominoids + *Proconsul* and decrease in size with the earliest cercopithecoids. A second increase in size occurs with the last common ancestor of extant hominoids.

The trapezoid is broad medio-laterally, possessing a broad MCII facet. This character is difficult to interpret as there is extensive overlap among hominoid, cercopithecoid and platyrrhine ranges. H2 is only 0.01 fewer steps than the alternate hypotheses (appendix D). Platyrrhines tend to have narrower trapezoids, with *Saimiri* and *Ateles* having the narrowest of all sampled taxa. Hominoids fall on the upper end of the spectrum and cercopithecoids cover the full range of variation. *Proconsul* has a wide trapezoid, along with *Papio* and *Macaca.* Hylobatids also have a wide trapezoid. This analysis infers the earliest catarrhines had a wide trapezoid, which was then reduced with the earliest hominoids and cercopithecoids.

The Asian apes and *Proconsul* possess a trapezium that is dorso-palmarly deep with a long MCII facet. The platyrrhines are variable, but most often have a shallow trapezium and this is inferred to be the primitive platyrrhine morphotype. *Victoriapithecus* has a shallow trapezium, but extant cercopithecoids are variable, overlapping the platyrrhine range, and approaching the Asian apes. The basal catarrhine morphotype is inferred to be intermediate, with a decrease inferred for the earliest cercopithecoids and an increase in depth with the earliest hominoids. Hominines are inferred to reverse this trend as *Pan* and *Gorilla* have an intermediate and shallow trapezium respectively.

One character from the pisiform is synapomorphic: length of the triquetral facet. The hominoids and *Ateles* possess a smaller pisiform-triquetral facet. The colobines, *Saimiri, Saguinus,* and *Proconsul* are intermediate in this feature. The catarrhine MRCA morphotype is

also inferred to be intermediate. While the intermediate morph present in *Proconsul* makes interpretation difficult, this analysis leads to the inference that *Proconsul* synapomorphically approaches the derived hominoid morphotype. Pisiform morphology has been central to discussion concerning the phylogenetic position of *Proconsul* related to ulnar deviation of the wrist related to vertical climbing and suspension (Lewis, 1965, 1972, 1989; Conroy and Fleagle, 1972; O'Connor, 1975; Youlatos, 1996; Daver and Nakatsukasa, 2015).

Width of the hamulus on the hamate is inferred to be a key synapomorphy, with *Proconsul* and the hominoids possessing a wide hamulus. *Epipliopithecus* possesses a narrow hamulus and the cercopithecoids are intermediate. The platyrrhines exhibit the full range of variation, with *Aotus* and *Saimiri* falling within the hominoid range. *Gorilla* possesses the widest hamulus, while *Proconsul* falls within the narrower end of the hominoid range near *Pongo* and *Symphalangus*. This feature may be related to powerful flexion during full extension of the wrist as the flexor carpi ulnaris acts on the hamulus via the piso-hamate ligament (O'Connor, 1975; Lewis, 1977; Sarmiento, 1988; Almecija et al., 2014).

The only key synapomorphy identified from the hand, not part of the carpus, is the width of the fifth metacarpal shaft. All the hominoids, including *Proconsul,* have a robust fifth metacarpal. The hylobatids fall at the bottom of this range, while *Proconsul* and *Pongo* possess the widest MC5. *Epipliopithecus* and the platyrrhines all possess a gracile MC5 and cercopithecoids are intermediate. Enlargement of the MC5 shaft has been associated with increased importance of the power grip, which is used to grasp vertical supports (Napier, 1960, 1964; Marzke et al., 1992) and could also be reflecting a general increase in breadth of the hand.

A single pelvic synapomorphy places *Proconsul* within Hominoidea: cranio-caudal diameter of the acetabulum. This may reflect cranial expansion of the lunate surface that has

been related to cranial loading of the hip joint in vertical body postures (Latimer, 1987; Ward, 1991, 1993; MacLatchy and Bossert, 1996). There is not a good separation between extant clades for this character, though hominoids consistently have a tall acetabulum. *Papio* and *Colobus* also possess a tall acetabulum, while *Presbytis* and *Ateles* have the shortest acetabula. *Proconsul* appears most similar to *Macaca* for this feature and is intermediate. Basal catarrhines and platyrrhines are inferred to have short acetabula, with the earliest crown catarrhines having taller acetabula, with the earliest hominids having the tallest acetabula. While *Proconsul* falls within both the hominoid and cercopithecoid ranges and is similar to the inferred crown catarrhine MRCA for this feature. This analysis leads to the placement of *Proconsul* within Hominoidea and requires the least homoplasy (though only by 0.01 steps).

Five key synapomorphies are present in the ankle. All except one are from the navicular: planto-dorsal depth of the sustentaculum on the calcaneus. The Asian apes (along with most platyrrhines) have a shallow sustentaculum, while the hominines have a robust sustentaculum. *Victoriapithecus, Aotus,* and *Cebus* also have a robust sustentaculum, though not as robust as in *Pan* and *Gorilla.* Extant cercopithecoids are intermediate. *Epipliopithecus* has a shallow sustentaculum and *Proconsul* is intermediate, approaching the hominine range. This analysis leads to an inference that a shallow sustentaculum is primitive for anthropoids, catarrhines and hominoids. The earliest cercopithecoids are inferred to evolve a more robust sustentaculum that is paralleled in the hominines. This synapomorphy is only 0.007 steps shorter for H2 than either of the other two hypotheses.

The final four key synapomorphies include length of the navicular tubercle and three characters describing dorso-plantar height of the navicular. Hominids and *Proconsul* exhibit a short navicular tubercle. It is less straight forward distinguishing among clades of other taxa.

Platyrrhines and cercopithecoids exhibit a range of variation from intermediate to long. Hylobatids possess long navicular tubercles. *Victoriapithecus* is intermediate for this character. The primitive catarrhine and hominoid ancestral morphs are inferred to be intermediate, with hominids evolving shorter tubercles and cercopithecoids evolving longer tubercles. Dorso-plantar navicular height is similarly difficult to interpret as variation within clades is broadly distributed. *Victoriapithecus* has the deepest navicular, f ollowed by *Presbytis* and *Pongo.* *Saguinus* and *Ateles* have the shallowest navicular. *Proconsul* is intermediate, most similar to *Symphalangus* and *Cebus.* The basal platyrrhine morph is inferred to be shallow, while the basal catarrhine morph is inferred to be tall. The basal cercopithecoid morph is inferred to be tall and the hominoid morph is inferred to be intermediate.

Figure 61. All synapomorphies scree plot

5.2.2 Phylo-morphospace analyses

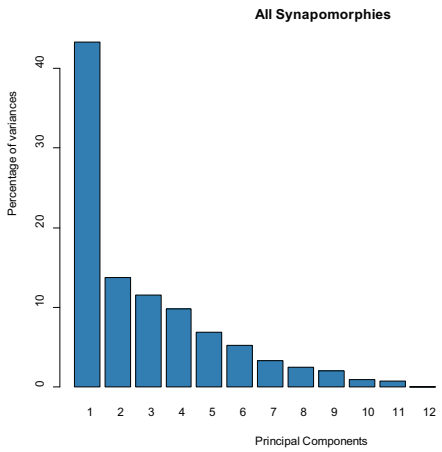

5.2.2.1 All key synapomorphies

PC1 accounts for 43.3% of variation (fig. 61) and is not significantly correlated with body size. This axis is primarily driven by the distinctiveness of hominids relative to other catarrhines. *Ateles, Aotus, Alouatta* and *Saimiri* all fall towards the hominid end of the axis, with *Aotus* and *Ateles* appearing distinctive and widely separated from all other taxa. Platyrrhines cover the full range of variation across this axis, with *Cebus* and *Saguinus* falling nearest *Victoriapithecus* at the high end of the cercopithecoid distribution. The hylobatids are intermediate between cercopithecoids and hominids. The hominids form a tight cluster towards the center of the axis, with *Epipliopithecus* falling between the hominids and *Aotus* on the lower

half of the axis. All other taxa are distributed across the upper half of the axis with *Proconsul* falling near *Cebus* and *Victoriapithecus*. All ancestral morphotypes are also inferred to fall in the upper half of the axis, with the exception of the hominid MRCA, which falls in the lower half between *Aotus* and *Ateles.* The cercopithecoid MRCA falls at the opposite end of the spectrum, defining the upper limit of the axis. Both the hominoid and catarrhine MRCA morphs fall near *Proconsul.* Cranio-mandibular characters drive variation along this axis (appendix E).

PC2 accounts for 13.7% of variation and is not significantly correlated with body size. This axis also emphasizes the distinctiveness of *Aotus* and *Ateles*, but also *Epipliopithecus.* *Epipliopithecus* defines the lower bound of the range of variation (falling nearest *Aotus*) and *Proconsul* defines the upper bound. All other taxa fall between these two divergent fossils.

Figure 62. PCA of all H2 synapomorphies with inferred ancestral morphotypes

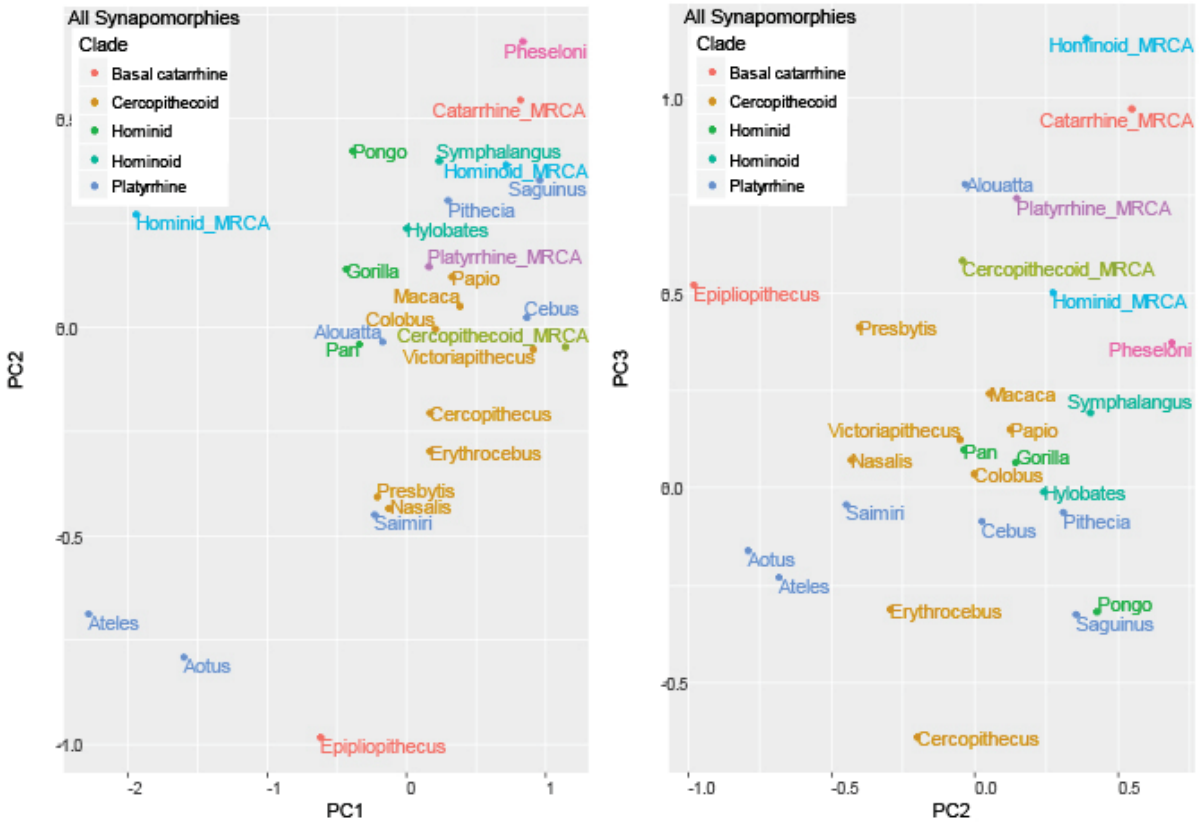

Cercopithecoids cluster towards the middle of the axis and hominoids towards *Proconsul* and the upper half of the axis. There is extensive overlap between their distributions, with the hominines falling within the cercopithecoid range. Despite *Epipliopithecus* falling at the bottom of the axis, the catarrhine MRCA is inferred to fall near *Proconsul* and the hominoids. The cercopithecoid MRCA falls towards the center of the axis near *Victoriapithecus.* This axis is again driven by cranio-mandibular characters, particularly those relating to facial height and breadth.

PC3 accounts for 11.6% of variation and is not correlated with body size. *Epipliopithecus, Proconsul* and the ancetral morphotypes occupy the upper half of the axis, along with *Alouatta* and *Presbytis*, with all other taxa falling on the lower half of the axis. Platyrrhines occupy a limited range of the axis—with the exception of *Alouatta*—while cercopithecoids and hominoids are distributed across the lower half. This axis is primarily driven by prominence of the temporal lines and further by pelvic and cranio-mandibular characters (appendix E).

The distance matrix (appendix F, fig. 63) places *Proconsul* in a cluster with the catarrhine and hominoid MRCA morphs, nearest *Pithecia* in a cluster with the platyrrhines—except *Aotus* and *Ateles.* These taxa fall near the hominids, which form their own cluster with the inferred hominid MRCA. *Nasalis, Presbytis* and *Epipliopithecus* also fall in a cluster with the hominids, the hylobatids join the cluster more distantly. The remaining cercopithecoids form two distinct clusters, one falling near the platyrrhines (*Victoriapithecus, Macaca, Papio*) and the other forming its own cluster (*Cercopithecus, Erythrocebus, Colobus*).

Figure 63. Dendrogram of all H2 synapomorphies with inferred ancestral morphotypes constructed as NJ tree run on Euclidean distance matrix

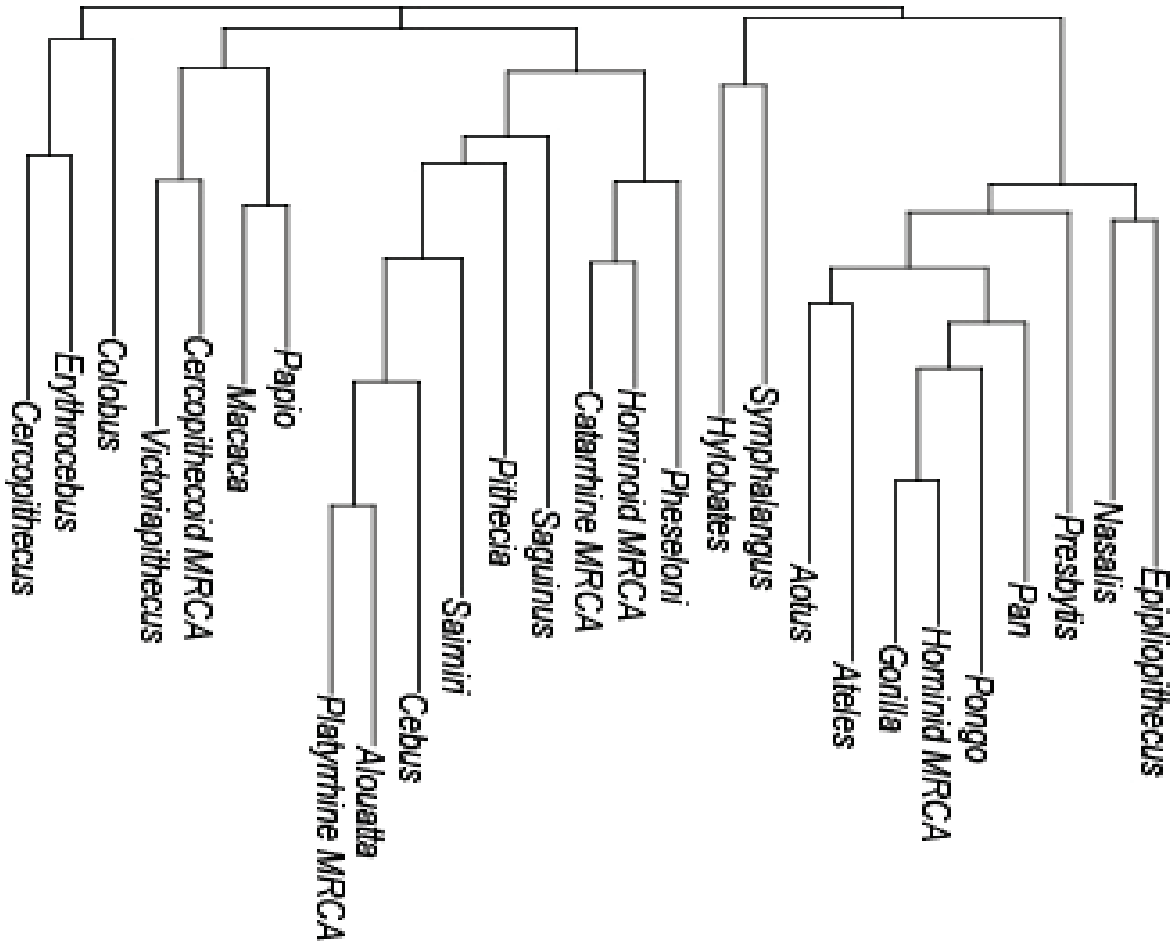

Figure 64. Cranial synapomorphies scree plot

5.2.2.2 Cranial synapomorphies

PC1 accounts for 51.2% of variation (figs. 64-65) and is not correlated with body size. Given that cranial characters were prime drivers of variation in the PCA including all key synapomorphies, it is unsurprising that this PC

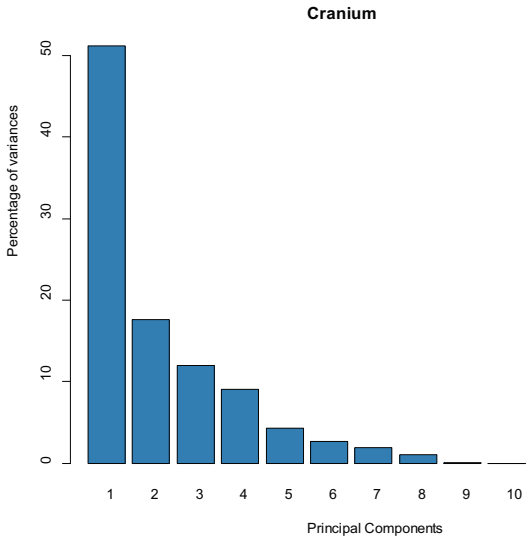

(fig. 65) is similar to PC1 from that analysis (fig. 61). *Ateles* and *Aotus* appear quite distinctive and define the upper end of the axis. The hominids and *Epipliopithecus* cluster towards the center of the axis and all other taxa (with the exception of *Alouatta*) fall on the lower half of the axis. *Victoriapithecus* defines the lower limit of the axis of variation. *Proconsul* falls nearest *Pithecia, Saimiri* and *Hylobates*. The hominid MRCA again falls far from extant hominids, and nearer to *Aotus* and *Ateles*. This axis is driven by palate length and width across the incisors (appendix E).

Figure 65. PCA of cranial H2 synapomorphies with inferred ancestral morphotypes

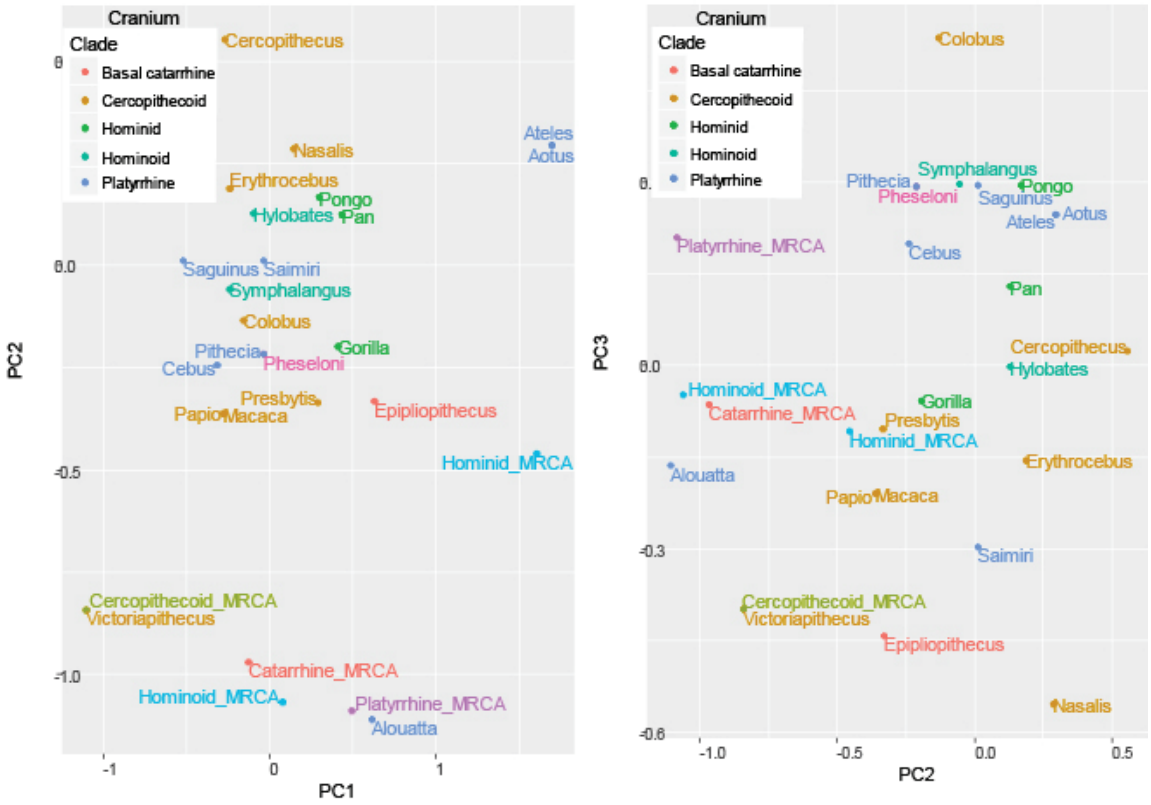

PC2 accounts for 17.6% of variation (figs. 64-65) and is not correlated with body size. Again there are similarities between this PC (fig. 65) and PC2 from the PCA including all key synapomorphies. The ancestral morphs occupy the lower half of the plot along with *Alouatta*

and *Victoriapithecus*. *Epipliopithecus* falls towards the middle of the axis along with *Presbytis, Papio* and *Macaca*. The hominoids occupy a limited range within the upper half of the axis, while extant cercopithecoids are distributed across this half of the axis. *Proconsul* falls just below the hominoids distribution, nearest *Pithecia, Cebus* and *Gorilla.* This axis is driven almost entirely by prominence of the temporal lines and to a lesser extent by palate width (appendix E).

PC3 accounts for 12.0% of variation (figs. 64-65) and is not driven by body size. The hominoids cluster on the upper half of the axis, while cercopithecoids (with the exception of *Colobus)* fall in the lower half of the axis. Their ranges overlap, particularly given that *Colobus* defines the upper limit of the axis. All platyrrhines—with the exception of *Alouatta* and *Saimiri*—form a tight cluster between *Pongo* and *Pan* on the upper half of the axis. *Proconsul* falls among the hominoids and platyrrhines, nearest *Pithecia, Saguinus, Symphalangus and Pongo.* The catarrhine, hominoid and hominid MRCA morphs are inferred to fall towards the middle of the axis, where the cercopithecoid and hominoid ranges overlap. The cercopithecoid MRCA falls with *Victoriapithecus* on the lower half of the axis, near *Epipliopithecus*. This axis is driven by facial height and supra-orbital morphology (appendix E).

The distance matrix (appendix F, fig.66) again emphasizes the similarity between *Pithecia* and *Proconsul*, with both taxa clustering with the hominoid and catarrhine MRCAs. *Aotus* and *Ateles* again cluster with the hominids. *Epipliopithecus* falls nearest the hominids, followed by *Presbytis* and *Nasalis*. The hylobatids do not cluster with the hominoids and fall far from the hominoid MRCA. The cercopithecoid MRCA falls far from the catarrhine MRCA, clustering with *Victoriapithecus, Macaca* and *Papio.*

Figure 66. Dendrogram of cranial H2 synapomorphies with inferred ancestral morphotypes constructed as NJ tree run on Euclidean distance matrix

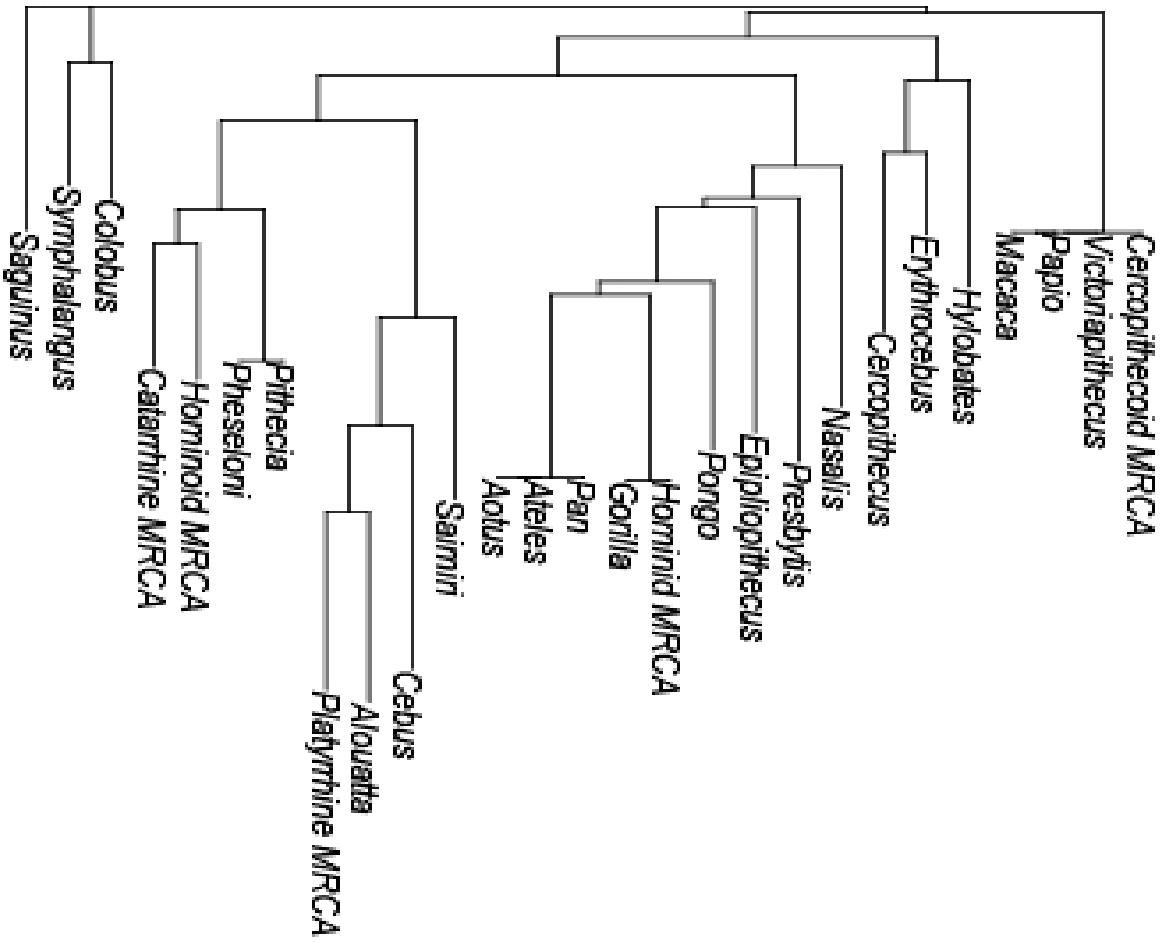

Figure 67. Mandibular synapomorphies scree plot

5.2.2.3 Mandible synapomorphies

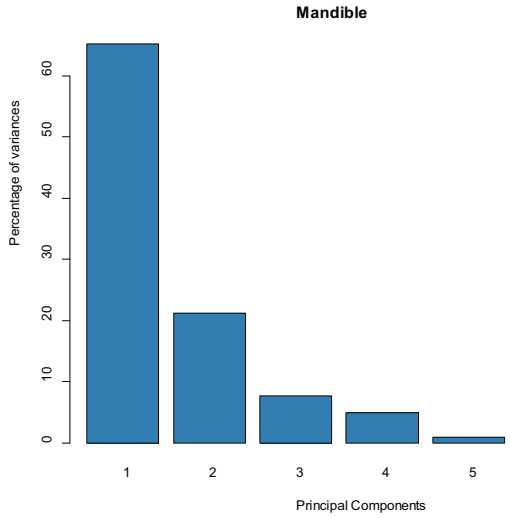

PC1 accounts for 65.2% of variation and is not correlated with body size (figs. 67-68). The platyrrhine, catarrhine and hominoid MRCAs—along with *Proconsul*—all fall at the upper end of the axis, while the hominid ancestral morph and *Epipliopithecus*—along with *Aotus* and *Ateles*—fall at

the lower end of the axis. All other platyrrhines cluster near the platyrrhine MRCA, except *Saimiri,* which falls nearer *Aotus* and *Ateles.* All other taxa are distributed between these two extremes. The hominids, particularly the hominines (joined by *Nasalis* and *Presbytis*), approach the hominid MRCA, while the hylobatids fall more towards the middle of the plot with the other cercopithecoids. This axis is driven by corpus width and height and width across the mandible (appendix E).

PC2 accounts for 21.2% of variation (figs. 67-68) and is not significantly correlated with body size. This PC is primarily driven by anterior mandibular corpus height (appendix E). Most taxa cluster towards the center of the axis, with *Saimiri* defining the lower bound and *Colobus, Cercopithecus* and *Erythrocebus* defining the upper bound. *Hylobates* and *Pongo* appear distinctive, falling near *Saimiri. Victoriapithecus* approaches the upper limit and all other taxa are intermediate.

Figure 68. PCA of mandibular H2 synapomorphies with inferred ancestral morphotypes

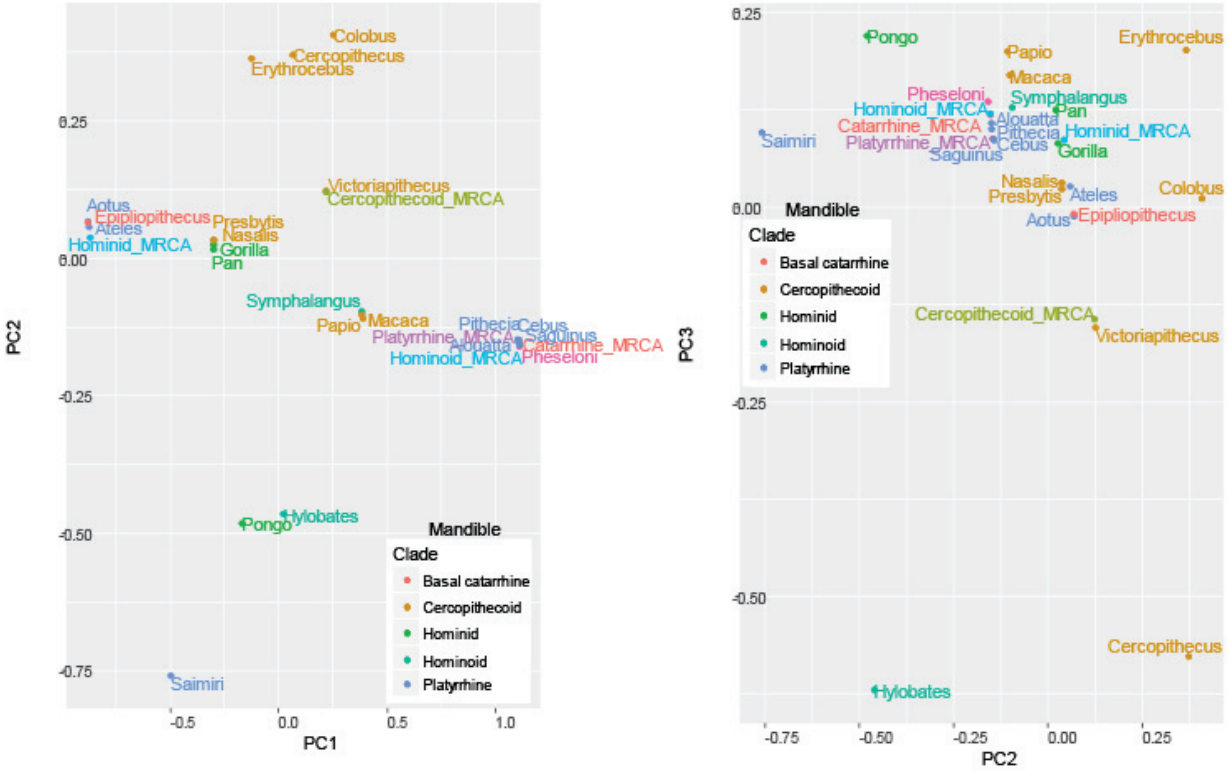

PC3 accounts for 7.7% of variation (figs. 67-68) and is not significantly correlated with body size. This axis primarily separates *Victoriapithecus, Cercopithecus* and *Hylobates* from all other taxa. *Hylobates* falls near *Cercopithecus* and both define the lower limit of the axis. *Proconsul* falls nearest *Symphalangus,* towards the upper extent of the axis. *Epipliopithecus* falls near *Aotus*, both at the lower range of the distribution of all taxa except the three distinctive forms. The cercopithecoid MRCA falls with *Victoriapithecus*. All other MRCA morphs cluster towards the center of the distribution of all other taxa at the upper end of the axis. This axis is driven by width across the mandible and corpus width (appendix E).

Figure 69. Dendrogram of mandibular H2 synapomorphies with inferred ancestral morphotypes constructed as NJ tree run on Euclidean distance matrix

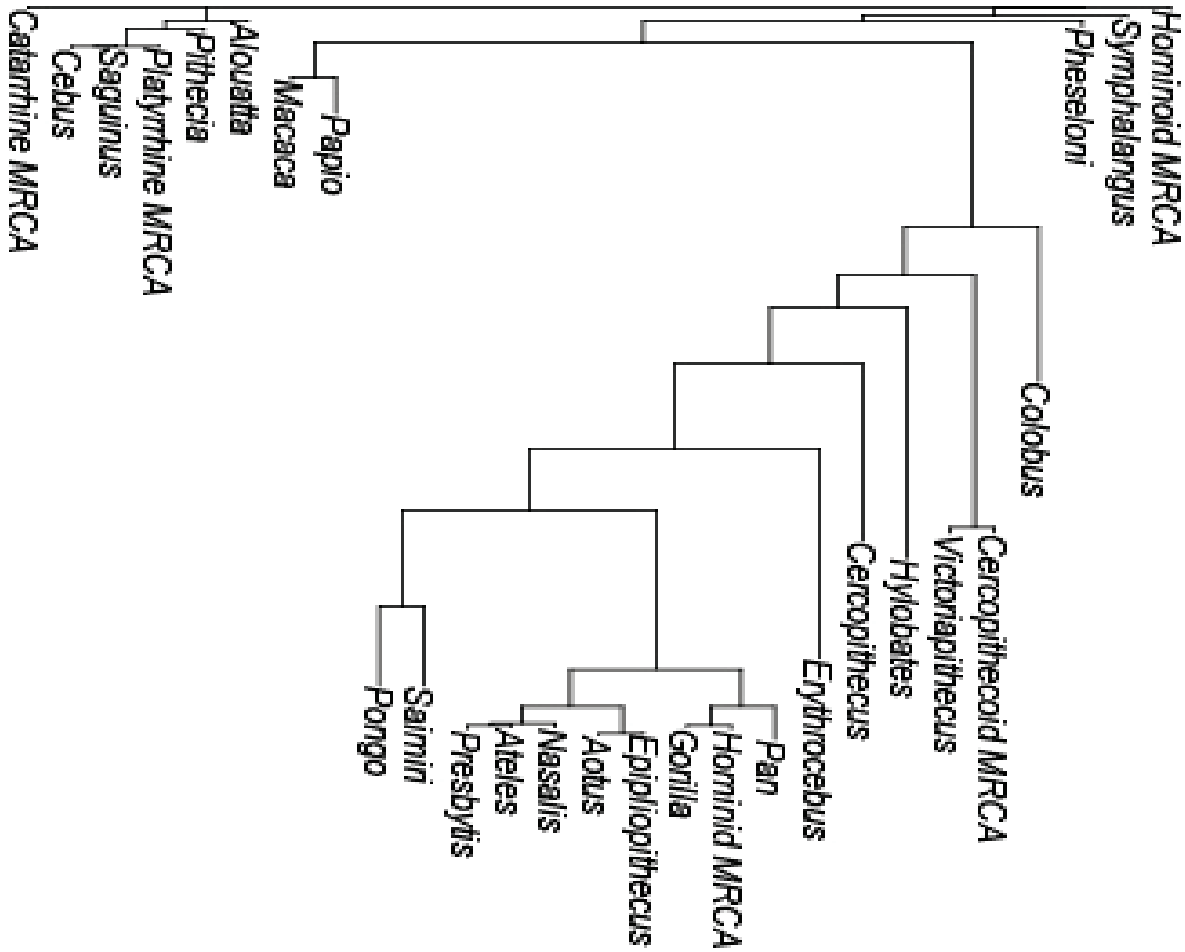

The distance matrix (appendix F, fig 69) separates a single cluster from all other taxa. The presence of the platyrrhine, catarrhine and hominoid MRCA morphs falling outside this cluster, along with a majority of platyrrhines, *Proconsul* and *Symphalangus,* suggests this distinctive cluster exhibits traits associated with primitive catarrhine morphology. The presence of platyrrhines (*Saimiri, Ateles, Aotus*) within this cluster emphasizes the finding from chapter 3: platyrrhines encompass the range of variation exhibitted by catarrhines. *Epipliopithecus* also falls within the catarrhine cluster, nearest *Aotus*, in a cluster incluging *Ateles, Nasalis, Presbytis*, the hominines and the hominid MRCA.

5.2.2.4 Forelimb key synapomorphies

PC1 accounts for 59.8% of variation (figs. 70-71) and is not significantly correlated with body size. The hominoids and *Proconsul* fall on the lower half of the axis, while *Epipliopithecus* and the platyrrhines cluster at the upper end of the axis. Cercopithecoids are intermediate, though there is extensive overlap between the cercopithecoid and platyrrhine ranges. The catarrhine and hominoid MRCA morphs fall near each other at the middle of the axis between the cercopithecoid and hominoid ranges. The hominid MRCA morph defines the lower bound of the axis. This axis is driven by ulnar morphology, particularly the morphology of the olecranon process and trochlear notch (appendix E).

Figure 70. Forelimb synapomorphies scree plot

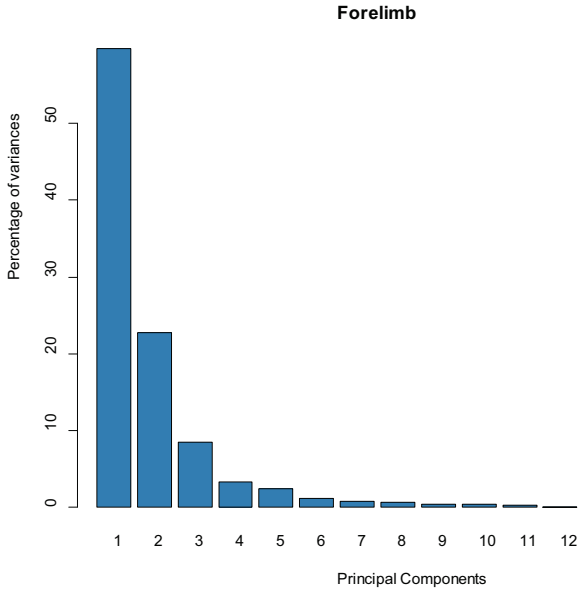

PC2 accounts for 22.8% of variation (figs. 70-71) and is not significantly correlated with body size. *Ateles* appears quite distinctive and defines the upper limit of the axis (fig. 32). *Proconsul* and the hylobatids, along with *Macaca* and *Saguinus* fall at the lower limit of the axis. *Epipliopithecus* falls towards the middle of the axis, between the catarrhine and hominoid MRCA morphs. There is extensive overlap between hominoid, cercopithecoid and platyrrhine ranges of variation. This axis is again driven by the morphology of the trochlear notch and additionally by articular morphology of the distal ulna and width of the distal humerus (appendix E).

Figure 71. PCA of forelimb H2 synapomorphies with inferred ancestral morphotypes

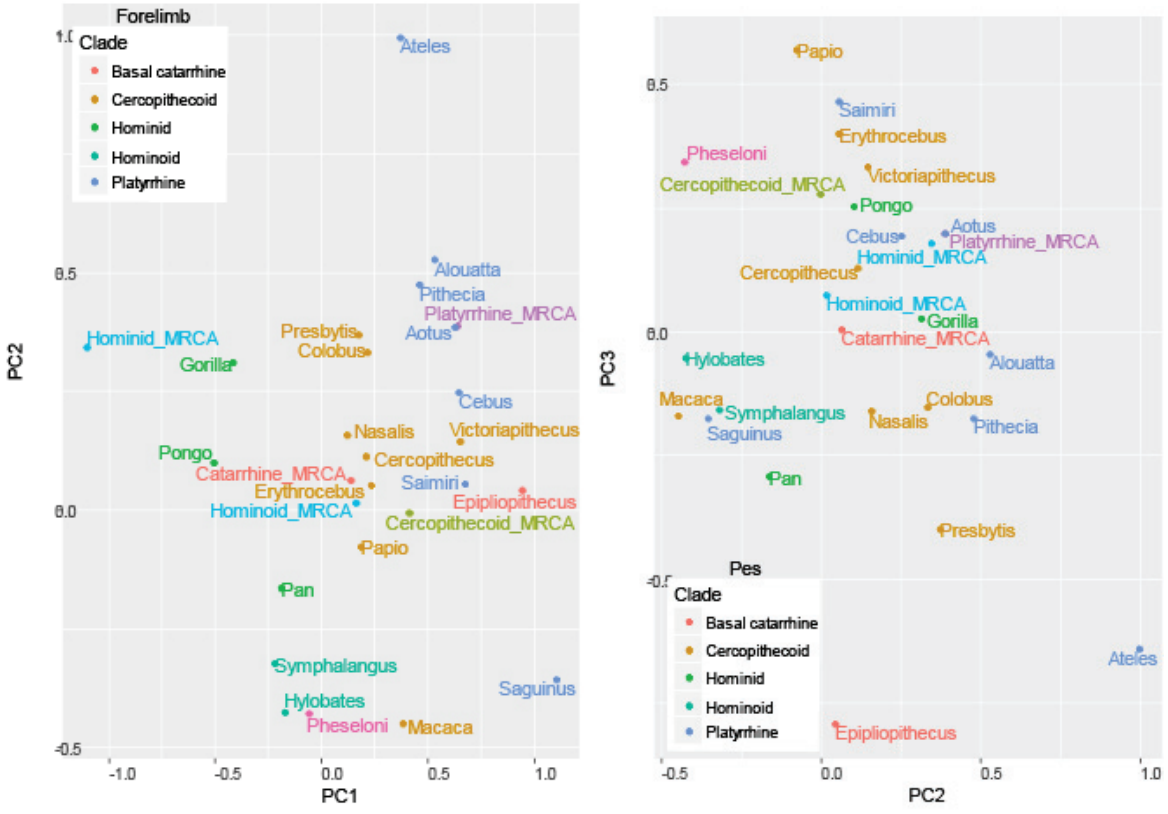

PC3 accounts for 8% of variation (figs. 70-71) and is not significantly correlated with body size. *Epipliopithecus* is distinctive along this axis and defines the lower bound. *Ateles* falls

nearest *Epipliopithecus* along this axis, with *Presbytis* also falling low on the axis. The remaining taxa are distributed across the upper half of the axis. *Papio* defines the upper bound. *Proconsul* also falls towards the upper limit, near *Victoriapithecus* and *Erythrocebus*. The hominoids are broadly distributed across the middle of the axis. There is extensive overlap between platyrrhine, cercopithecoid and hominoid ranges. This axis is also driven by morphology of the ulnar trochlear notch (appendix E).

Figure 72. Dendrogram of forelimb H2 synapomorphies with inferred ancestral morphotypes constructed as NJ tree run on Euclidean distance matrix

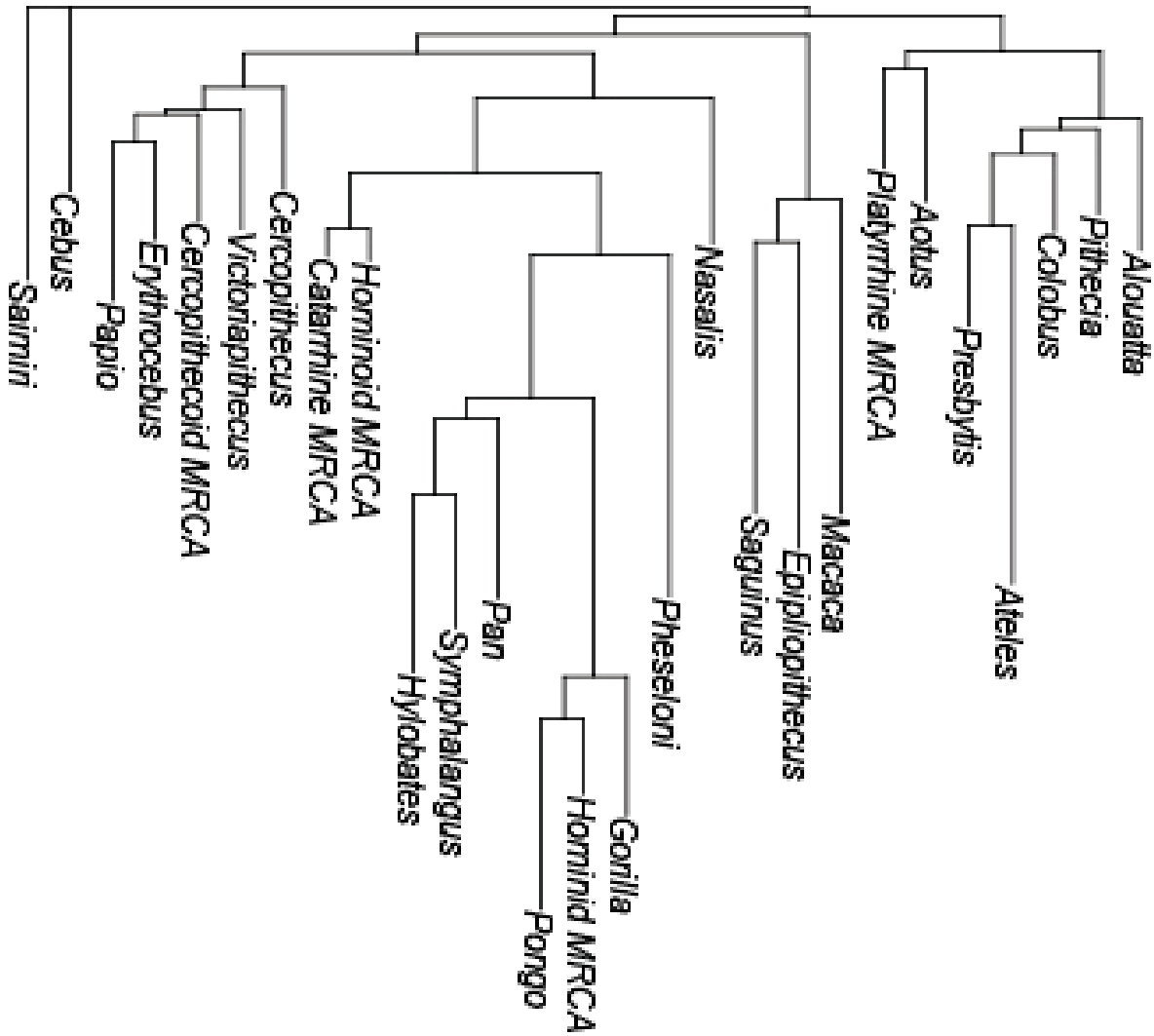

The distance matrix (appendix F, fig. 72) identifies a distinct hominoid cluster. *Proconsul* falls at the base of this cluster. Further out, the hominoid and catarrhine MRCA morphs also cluster with the hominoids, as does *Nasalis* (though overall, *Nasalis* is nearest *Pithecia,* followed by *Colobus* and *Cercopithecus*). *Epipliopithecus* falls nearest *Saguinus,* followed by *Macaca*. The cercopithecines (except *Macaca*) form a distinct cluster with *Victoriapithecus* and the cercopithecoid MRCA. Platyrrhines are variable, distributed across the dendrogram.

Figure 73. Manus synapomorphies scree plot

5.2.2.5 Manus synapomorphies

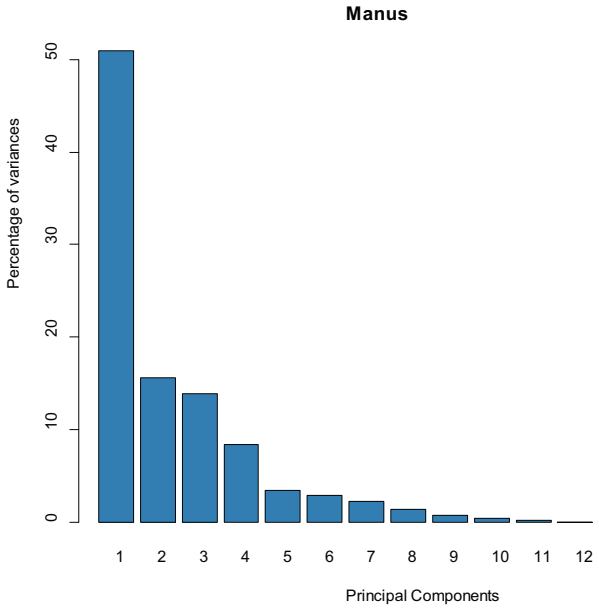

PC1 accounts for 50.9% of variation (figs. 73-74) and is not significantly correlated with body size. Hominoids occupy a distinct range on the low end of the axis, with hominids defining the lower bound and hylobatids more towards the center. *Ateles* approaches the hominoid range. The remainder of the platyrrhines occupy a limited range in the upper half of the axis. The cercopithecoids are more variable than the platyrrhines and also occupy the upper half of the axis. *Victoriapithecus* falls towards the middle of the cercopithecoid range. *Epipliopithecus* falls towards the middle of the axis at the low end of the platyrrhines and cercopithecoid ranges. *Proconsul* falls within the platyrrhine and cercopithecoid range, nearest *Alouatta, Pithecia* and *Victoriapithecus*. The hominid, hominoid and catarrhine MRCA morphs fall between the hominoid and cercopithecoid ranges. This axis is driven by morphology of the pisiform (appendix E).

PC2 accounts for 15.6% of variation and is not significantly correlated with body size. This axis primarily distinguishes *Pongo* from all other taxa. This axis is driven by pisiform length and morphology of the MC5 tubercle. The platyrrhines and other hominoids occupy the same range along this axis. The cercopithecoid range is larger and encompasses the hominine, hylobatid and platyrrhine ranges. All ancestral morphs fell on the lower half of the axis.

PC3 accounts for 13.9% of variation (figs. 73-74) and is not significantly correlated with body size. The platyrrhines are limited to the upper half of the axis. *Proconsul*, *Pan, Victoriapithecus, Macaca* and *Papio* all fall on the lower half of the axis. The remaining taxa are in the upper half. The catarrhine, cercopithecoid and hominoid MRCA morphs all fall at the middle of the axis. The hominid MRCA falls on the lower half near *Pan* and the hylobatids. This axis is driven by pisiform length and robusticity of the 2nd metacarpal (appendix E).

Figure 74. PCA of manus H2 key synapomorphies with inferred ancestral morphotypes

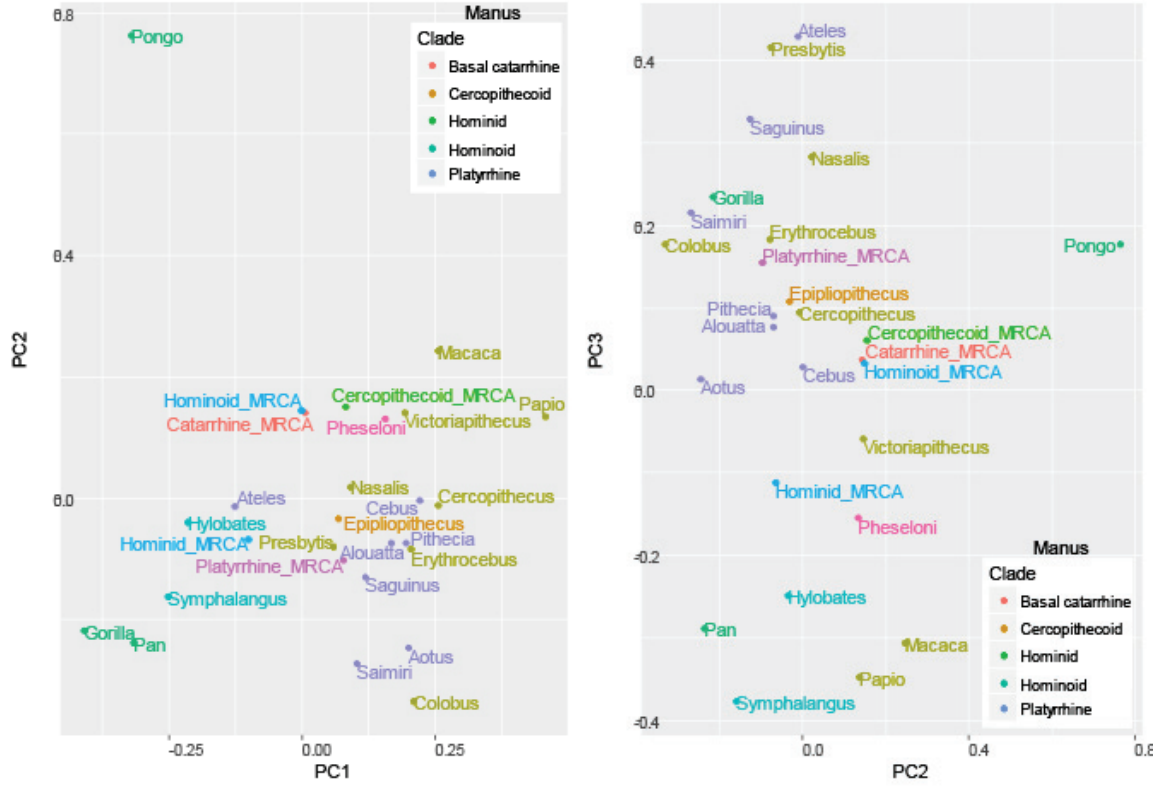

Figure 75. Dendrogram of manus H2 synapomorphies with inferred ancestral morphotypes constructed as NJ tree run on Euclidean distance matrix

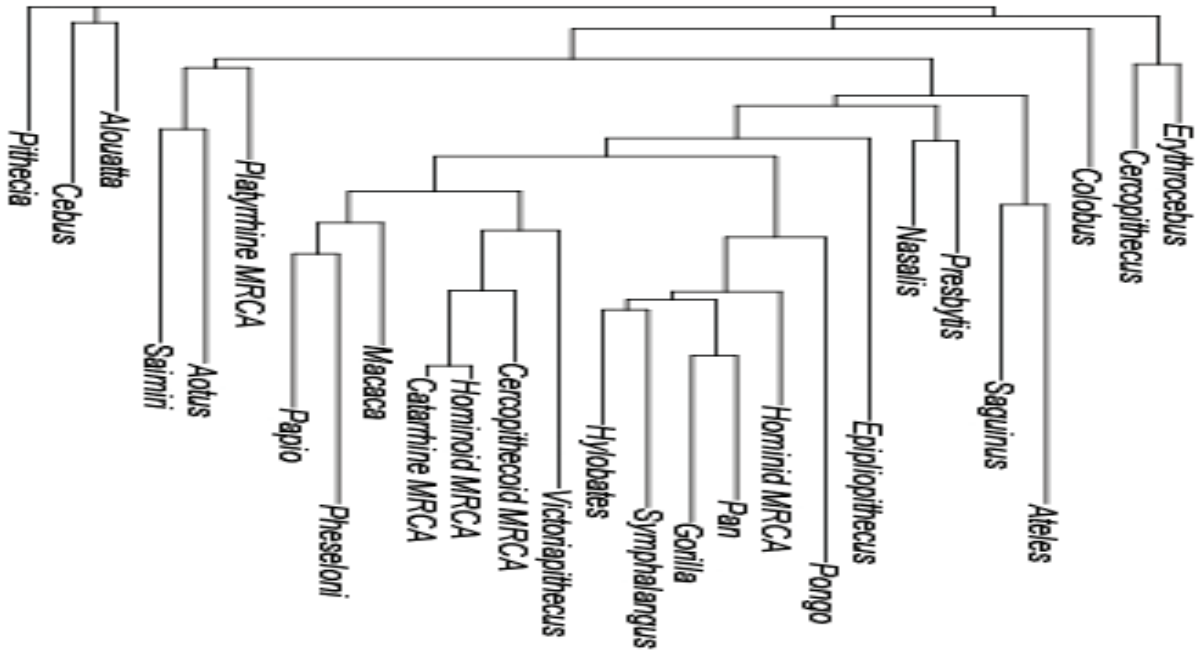

The distance matrix (appendix F, fig. 75) clusters all hominoids with the homind MRCA. *Proconsul* falls in a cluster with *Macaca, Papio, Victoriapithecus* and the catarrhine, hominoid and cercopithecoid MRCA morphs. Overall, *Proconsul* falls nearest *Papio*. One cluster includes all catarrhines except *Colobus, Cercopithecus* and *Erythrocebus*.

Figure 76. Pelvis synapomorphies scree plot

5.2.2.6 Pelvis synapomorphies

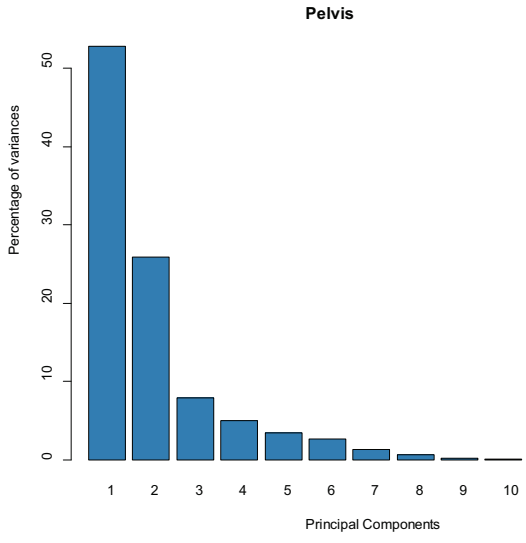

PC1 accounts for 52.8% of variation (figs. 76-77) and is not significantly correlated with body size. This axis separates platyrrhines from cercopithecoids. The hominids are intermediate and overlap the ranges of both. The hylobatids fall within the cercopithecoid range. *Proconsul* falls

nearest *Symphalangus* and *Nasalis*. *Epipliopithecus* falls within the hominoid and cercopithecoid ranges. *Victoriapithecus* falls with the platyrrhines, though many of these character states were estimated as there is little pelvic material for this taxon. This axis is driven by iliac blade height and morphology of the ischial tuberosity (appendix E).

Figure 77. PCA of pelvis H2 synapomorphies with inferred ancestral morphotypes

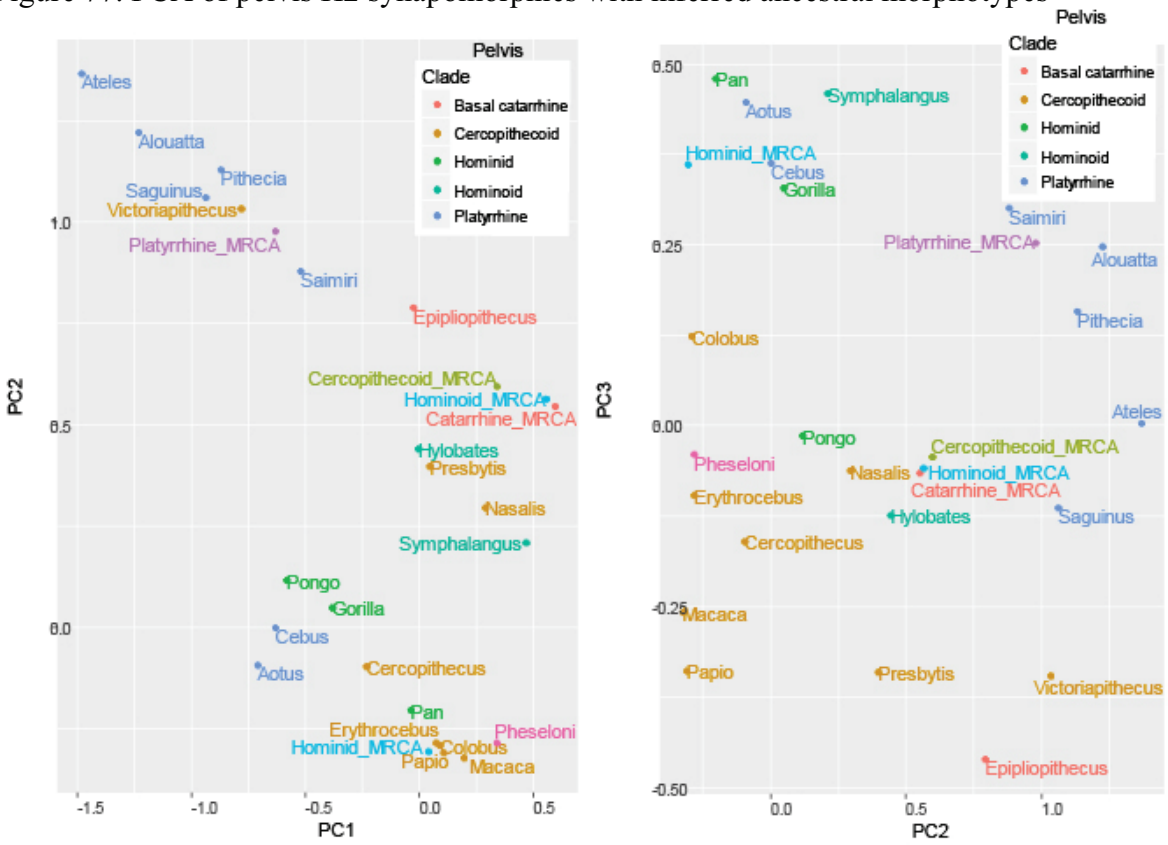

PC2 accounts for 25.9% of variation (figs. 76-77) and is not significantly correlated with body size. The hominoids occupy the lower half of the axis, with the hominids falling further towards the bottom than the hylobatids. *Presbytis* and *Nasalis* fall with the hylobatids, whereas the rest of the extant cercopithecoids fall at the bottom and define the lower bound of the range of variation. *Cebus* and *Aotus* fall with the hominids, while the other platyrrhines fall at the upper end of the axis. *Epipliopithecus* falls with the platyrrhines in the upper half of the axis. *Proconsul* falls towards the bottom of the axis nearest *Erythrocebus, Colobus and* the homind

MRCA. The catarrhine, cercopithecoid and hominoid MRCA morphs all fall towards the center of the axis between *Epipliopithecus* and *Hylobates*. This axis is driven by iliac height (appendix E).

Figure 78. Dendrogram of pelvis H2 synapomorphies with inferred ancestral morphotypes constructed as NJ tree run on Euclidean distance matrix

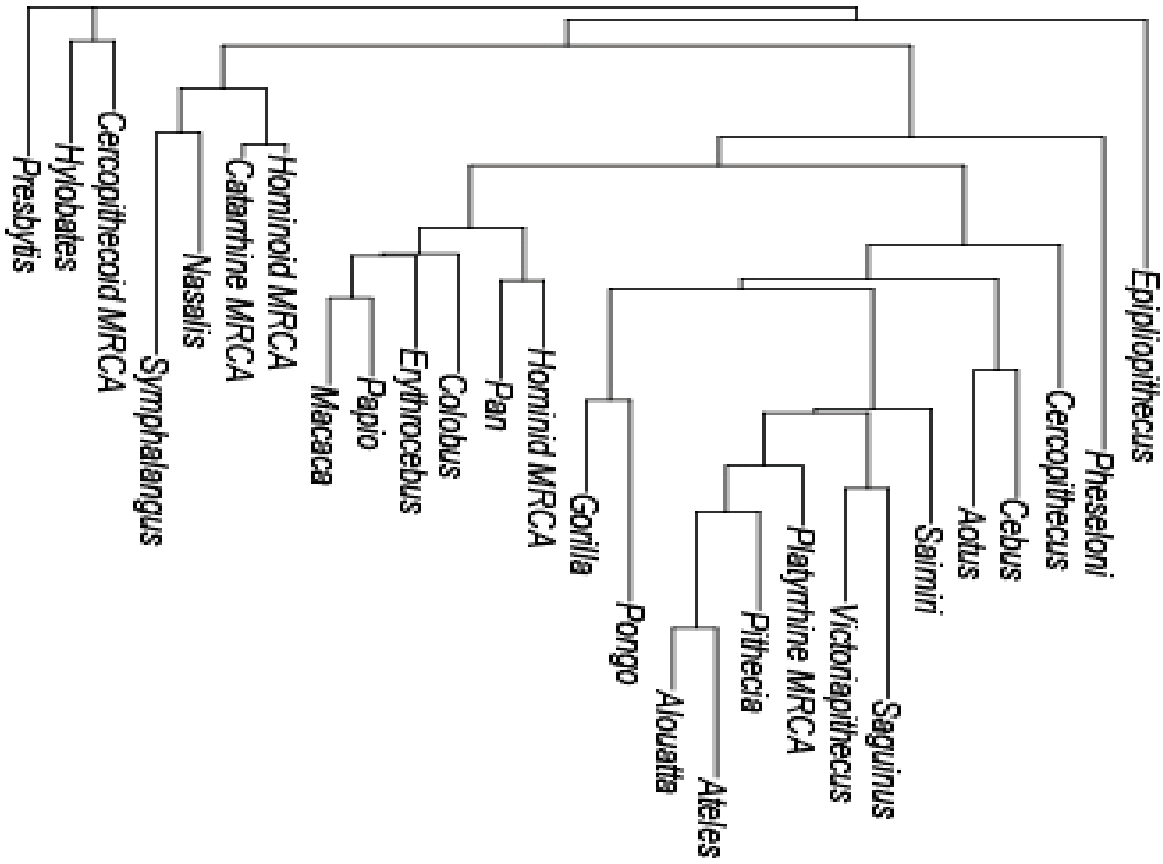

PC3 accounts for 7.9% of variation (figs. 76-77) and is not significantly correlated with body size. The cercopithecoids occupy the lower half the axis, while the platyrrhines and hominoids occupy the upper half. There is overlap between their ranges. *Proconsul* falls in the middle of the axis within both ranges, between *Pongo* and *Nasalis*. *Epipliopithecus* defines the lower bound of the axis, falling with the cercopithecoids, nearest *Victoriapithecus*. The

catarrhine, hominoid and cercopithecoid MRCA morphs all fall in the middle of the axis near *Proconsul*. This axis is driven by iliac blade height and width of the ischial tuberosity (appendix E).

The distance matrix (appendix F, fig. 78) indicates that *Proconsul* is distinctive, falling far from all other taxa, but nearest *Macaca*. The catarrhine and hominoid MRCA morphs fall nearest each other, in a cluster with *Nasalis* and *Symphalangus*. *Epipliopithecus* falls nearest *Hylobates*. These data do not recreate major clades in the cluster dendrogram.

5.2.2.7 Pes key synapomorphies

PC1 accounts for 86.5% of variation (figs. 79-80) and is not significantly correlated with body size. The platyrrhines fall at the upper end of the axis, with the hominoids falling towards the lower end. Cercopithecoids are intermediate, however *Papio* falls with the hominids. *Proconsul, Epipliopithecus* and *Victoriapithecus* all fall at the upper end of the axis with the platyrrhines. The catarrhine, hominoid and cercopithecoid MRCA morphs all fall near each other, nearest to *Epipliopithecus*. This axis is driven by the angle of the navicular-lateral cuneiform facet (appendix E).

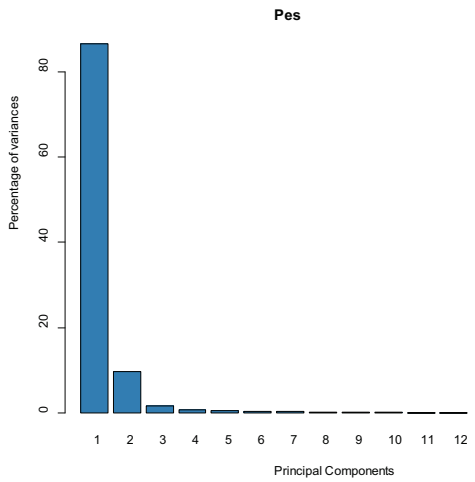

Figure 79. Pes synapomorphies scree plot

PC2 accounts for 9.6% of variation (figs. 79-80) and is not significantly correlated with body size. Taxa are divided into two clusters; one includes the hominines, hylobatids, *Proconsul, Epipliopithecus, Aotus, Saimiri, Papio and Macaca;* the other includes all other taxa. *Victoriapithecus* falls nearest *Ateles* and *Pithecia* and the platyrrhine and cercopithecoid MRCA morphs. This axis is driven by the size of the MT1 head (appendix E).

Figure 80. PCA of pes H2 synapomorphies with inferred ancestral morphotypes

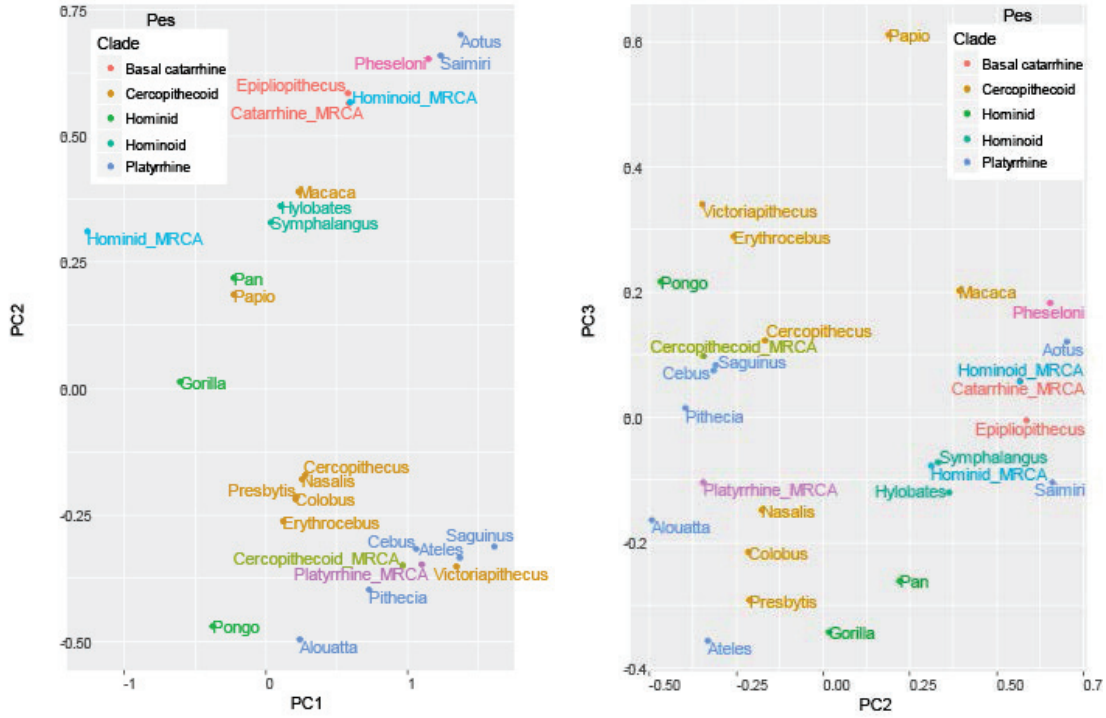

Figure 81. Dendrogram of pes H2 synapomorphies with inferred ancestral morphotypes constructed as NJ tree run on Euclidean distance matrix

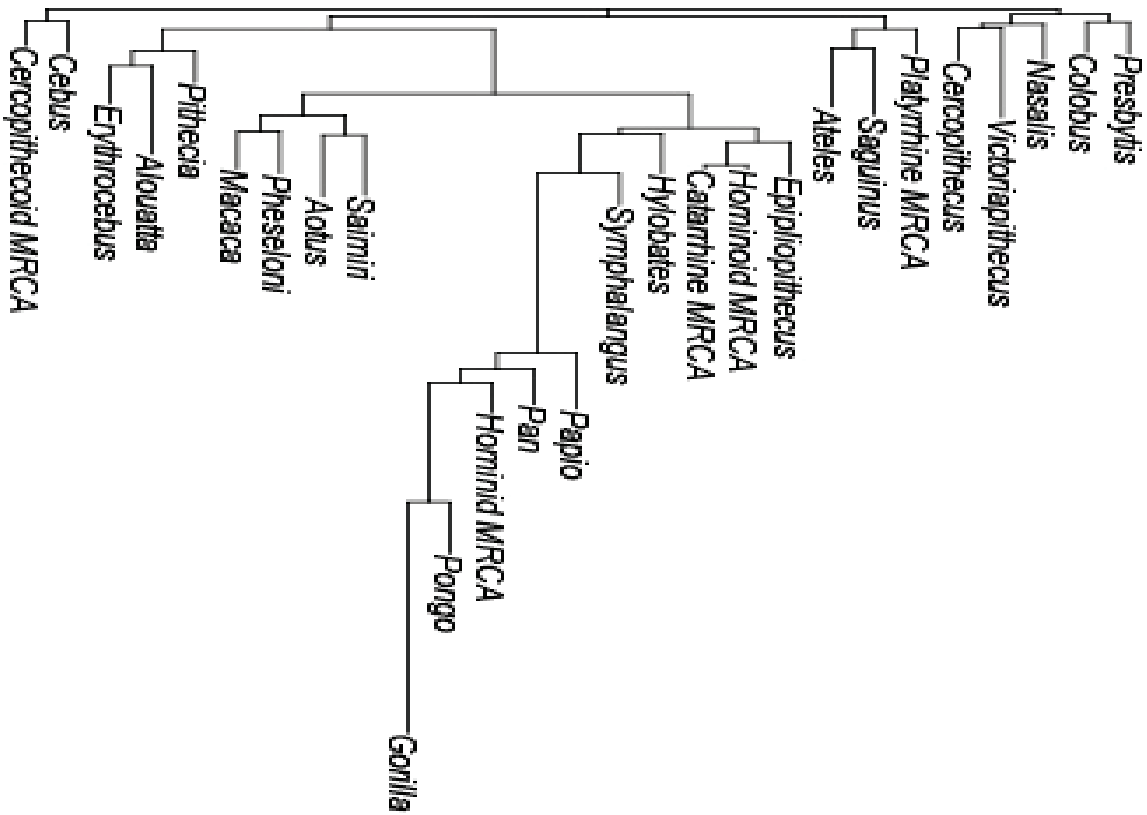

PC3 accounts for 1.6% of variation (figs.79-80) and is not significantly correlated with body size. The cercopithecines and *Victoriapithecus* fall on the upper half of the axis, all other taxa fall on the lower half. *Proconsul, Epipliopithecus* and all the catarrhine MRCA morphs fall towards the middle of the axis. This axis is driven by size of the 4th and 5th tarso-metatarsal facets and prominence of the astragular tubercles (appendix E).

The distance matrix (appendix F, fig. 81) again indicates *Proconsul* falls nearest *Macaca*. The hominoids cluster together, along with *Epipliopithecus, Papio* and the catarrhine and hominoid MRCA morphs. *Victoriapithecus* falls nearest *Cercopithecus,* in a cluster with the colobines.

5.3 DISCUSSION

A phenetic description of the spread of variation among anthropoids (see chapter 3) identified four main patterns of variation: 1) *Proconsul* is distinctive relative to extant and fossil taxa, 2) *Proconsul* consistently appears phenetically most similar to the hominoids, 3) there is a wider range of variation among platyrrhines than catarrhines for the set of characters distinguishing hominoids and cercopithecoids, 4) fossil taxa extend the range of variation for crown clades. Of these, all except the similarity of *Proconsul* to hominoids could have been problematic for phylogenetic analyses. Results from the previous chapter demonstrated that they did not, however, prevent inference of a well supported result. This chapter returned to phenetic depictions of variation—using only those characters inferred as synapomorphic in the previous chapter—in order to explore character evolution outside of a strictly phylogenetic framework. The spread of variation among taxa were used to infer ancestral morphotypes for extant clades allowing a more thorough investigation of catarrhine evolutionary history. *Victoriapithecus,*

Epipliopithecus and *Proconsul* were key to inferring these ancestral morphotypes. The great disparity in the morphology exhibited by these taxa illustrates the difficulty researchers have in inferring character polarities among fossil catarrhines. In particular, *Epipliopithecus* and *Proconsul*—the two more primitive taxa—often define opposite ends of axes of variation. If it were possible to include *Aegyptopithecus, Saadanius* or the dendropithecoids as well it is likely to further expand the area of morphospace covered by these primitive catarrhines. This corroborates the conclusion from chapter 3 that fossil taxa expand the range of variation exhibited by extant clades and furthers it by indicating that the range of variation among fossil catarrhines may encompass that of extant catarrhines.

Results from these analyses again emphasize the difficulty in inferring a simple evolutionary trajectory across catarrhine evolution and focusing on the origination of the hominoid and cercopithecoid clades. Among catarrhines, *Proconsul* appears phenetically most similar to the cercopithecoids (often the cercopithecines) across all regions except the mandible. While *Proconsul* is commonly used as a model for the earliest hominoids, among these PCAs it is never the nearest taxon to the inferred hominoid MRCA morph. For the analysis including all synapomorphies, however, *Proconsul* is the nearest taxon to the catarrhine MRCA. Despite not being the nearest taxon, *Proconsul* consistently falls near both the hominoid and catarrhine MRCA morphs.

Epipliopithecus consistently falls nearest the colobines and hylobatids across all regions and for the pes is the nearest taxon to the hominoid MRCA morph. This result suggests *Epipliopithecus* (among taxa included in this analysis) may be a better model for the morphology of the last common ancestor of extant hominoids than *Proconsul*. Adding the dendropithecoids to this analysis would be an interesting next step as it is likely they would also fall nearer

Epipliopithecus and the ancestral hominoid morph given the greater similarity of each of these taxa to the suspensory atelids than to *Proconsul* (Gebo, 1989, 2009; Rose et al., 1992; Rose, 1997; Harrison, 2010, 2013). The representation of these suspensory adaptations across the early catarrhine fossil record complicates interpretation of their phylogenetic significance and further problematizes inferring character polarities within Hominoidea given *Proconsul* is likely sister to all other hominoids and does not possess many of these features. This suggests that stem catarrhines exhibited morphology shared with extant hominoids and that cercopithecoids are derived away from this condition. This scenario, however, does not accommodate the greater similarity between *Proconsul* and the cercopithecoids. *Victoriapithecus* is an important taxon in testing this scenario.

Victoriapithecus most often falls nearest the cercopithecines; however, in its pelvic morphology it is nearest *Hylobates* and is nearest *Colobus* in its mandibular morphology. The fact that both *Victoriapithecus* and *Proconsul* often resemble cercopithecines among these characters, suggests that this morphology is primitive for crown catarrhines. The catarrhine ancestral morph is consistently inferred to be more similar to the hominoid ancestral morph than the cercopithecoid ancestral morph. In combination with *Proconsul* falling nearer the catarrhine MRCA than *Epipliopithecus* and the reduced similarity between *Aegyptopithecus* and the hominoids, this may suggest that *Epipliopithecus* functionally converges on the hominoid morphology. This is corroborated by a literature that notes the similarity in inferred locomotor repertoire between *Epipliopithecus,* the atelids and the hominoids ((Zapfe, 1960; Ward, 2007), a repertoire likely shared by the other potential stem catarrhines and hominoids such as the dendropipthecoids and nyanzapithecines (Rose, 1983, 1993; Harrison, 2013; Daver and Nakatsukasa, 2015). This further suggests that stem catarrhines and basal members of the

hominoid and cercopithecoid lineages were experimenting with a range of locomotor modes that did not resemble either the committed quadrupedalism of cercopithecines or the derived suspensory behaviors seen in extant hominoids.

CHAPTER 6: Discussion and Conclusions

6.1 DISCUSSION

This thesis set out to clarify the phylogenetic position of the Miocene African catarrhines belonging to the *Proconsul* hypodigm (including the newly proposed genera *Ugandapithecus* and *Ekembo*). While this taxon is well represented in the fossil record and has a long history of paleontological research, its phylogenetic position had not the focus of a comprehensive phylogenetic analysis. The consensus in the literature places *Proconsul* as the earliest hominoid and is often used to define the earliest hominoid morphotype (Andrews, 1985; Andrews and Martin, 1987; Begun, 1997). The *Proconsul* primitive, arboreal quadrupedal skeletal morphology differs significantly from the suite of features related to suspension and climbing that define extant hominoids (Le Gros Clark and Leakey, 1951; Napier and Davis, 1959; Cartmill and Milton, 1977; Andrews, 1978; Walker and Pickford, 1983; Andrews and Martin, 1987; Harrison, 1987; Rose, 1987, 1994, 1996; Ward et al., 1991, 1993; Nakatsukasa et al., 2003; Daver and Nakatsukasa, 2015), resembling instead the mix of quadrupedal adaptations with limited adaptations to susepnsion and climbing seen among stem catarrhines such as the pliopithecoids and dendropithecoids (Rose, 1983, 1993; Harrison, 2013). While this does not preclude *Proconsul* from inclusion within Hominoidea, its phylogenetic position does significantly alter inferences concerning hominoid character polarities. In order to interpret evolutionary events among hominoids, including within the hominin lineage, researchers must have confidence in the inferences on which these character polarities rest. The phylogenetic placement of *Proconsul* is central to defining these character polarities, particularly given that its current identification as one of the earliest hominoids.

Three possible phylogenetic hypotheses have been proposed in the literature: H1) *Proconsul* is a stem catarrhine, H2) *Proconsul* is a stem hominoid, H3) *Proconsul* is a stem hominid. The evidence used to support these hypotheses in previous analyses was reviewed. H2 is the hypothesis that is currently most widely supported in the literature, based on a suite of features primarily drawn from the postcranial skeleton that are shared by *Proconsul* and extant hominoids. Proponents of H3 rely more heavily on cranial characters shared by *Proconsul* and the hominids. H1 relies on the identification of synapomorphies supporting a clade including cercopithecoids and hominoids to the exclusion of *Proconsul.* The wide range of diversity within each of these clades along with each possessing an extensive suite of features separating them makes it unlikely there will be many crown catarrhine synapomorphies. Emphasis is placed on the similarities between the flexible quadrupedalism of *Proconsul*—including varying degrees of suspensory or climbing adaptiations—and that of stem catarrhines such as the pliopithecoids and dendropithecoids (Zapfe, 1960; Fleagle, 1983; Rose, 1983, 1993; Gebo, 1989, 2009; Ward, 2007; Harrison, 2010, 2013). H1 would also be supported however if there are no synapomorphies identified linking *Proconsul* to either hominoids or hominids, as H1 is the most conservative hypothesis.

This thesis improved on previous phylogenetic analyses of *Proconsul* by compiling the largest data set ever compiled for this purpose. This was achieved through extensive sampling of extant taxa and constructing a large character list sampling across a number of structural-functional complexes. A character list of 816 characters was compiled sampling from the cranium, forelimb, pelvis and foot for 17 ingroup taxa, in addition to the *Proconsul* material. These data were explored in three ways: 1) an initial phenetic exploration of the data set depicted patterns of variation among extant catarrhines, observing where fossil taxa and the outgroup

platyrrhines fall relative to this range of variation; 2) phylogenetic analyses inferred the phylogenetic position of *Proconsul* among catarrhines; 3) the spread of variation across synapomorphies were explored in a phylo-morphospace analysis.

The initial phenetic analysis employed principal component analyses and identified four main patterns of variation: 1) *Proconsul* is distinctive relative to extant and fossil taxa, 2) *Proconsul* consistently appears phenetically most similar to the hominoids, 3) there is a wider range of variation among platyrrhines than catarrhines for the set of characters that distinguish hominoids from cercopithecoids, 4) fossil taxa extend the range of variation for crown clades. Distance between taxa often reflected phylogenetic distance, clustering hominoids, cercopithecoids and platyrrhines separately. *Proconsul* consistently grouped with hominoids. This was the first line of evidence suggesting that *Proconsul* is a hominoid. This interpretation was complicated, however, by the fact that *Proconsul* was shown to be distinctive, falling far from all other taxa. The wide range of variation among platyrrhines relative to catarrhines also complicated interpretation as it was not possible in these analyses to distinguish between primitive and derived character states. It also suggested that phylogenetic analyses might struggle with rooting character polarities at the base of the anthropoid tree.

Where it was possible to include both basal catarrhine fossils (*Aegyptopithecus* and *Epipliopithecus*) in analyses, they exhibited divergent morphology. This again made assuming primitive versus derived ranges of variation impossible in phenetic analyses, where either taxon could more closely approximate the primitive condition. It also suggests the inference of the basal catarrhine morphology in phylogenetic analyses may be inaccurate.

The primary test of the phylogenetic position of *Proconsul* was conducted in a series of phylogenetic analyses applying both parsimony and Bayesian optimality criteria. Both methods

were able to identify H2—*Proconsul* is a hominoid—as the optimal hypothesis with a lower cost and greater support for a clade including *Proconsul* and extant and fossil hominoid taxa than in alternate hypotheses.

The phylo-morphospace analysis employed a novel combination of phylogenetic and phenetic methods to further explore morphological evolution across the catarrhine clade. This method is useful in exploring character evolution focused on stem taxa. This final set of analyses began by using results from phylogenetic analyses to identify the specific set of synapomorphies supporting the position of *Proconsul* within Hominoidea. While many of these synapomorphies have been discussed extensively in the literature, nine new characters were identified that have not previously been used to test the phylogenetic position of *Proconsul*: coronoid fossa width, radio-carpal facet width, robusticity of MC5, the hamulus of the hamate and the calcaneal sustentaculum and four characters describing dimensions of the navicular.

Synapomorphies were drawn from all regions except the cranium. In order to evaluate the evolution of these characters, all H2 synapomorphies (including those that were not optimal for this hypothesis) were then used to infer ancestral morphotypes. Principal component analyses depicted relationships between ancestral morphotypes and taxa in order to visualize patterns of morphological evolution. These results emphasized the importance of fossil taxa to inferring ancestral morphotypes and character polarities for crown catarrhine clades. Interestingly *Proconsul* may morphologically be more similar to the catarrhine MRCA than to the hominoid MRCA for these characters, while *Epipliopithecus* expresses a greater phenetic similarity to the hominoid MRCA.

A number of the characters reviewed in chapter 1 as possible synapomorphies were not identified as synapomorphic. Neither of the following characters exhibited synapomorphies

grouping *Proconsul* with hominoids: morphology of the premaxillary-nasal contact (Rae, 1999), projection of the inter-orbital region (Rae, 1999). Rae (1999) identified *Proconsul* and extant hominoids as having a premaxilla that contacts the nasals inferiorly, while in cercopithecoids the contact extends superiorly to the top of the nasals. He inferred the primitive catarrhine condition was intermediate, with the premaxilla contacting the nasals at their midpoint. This analysis found many platyrrhines also exhibit the more inferior premaxilla-nasal contact suggesting this is the primitive condition. Rae (1999) also suggested a non-projecting inter-orbital region is derived for *Proconsul* and Hominoids. This analysis found that while hominoids and *Proconsul* did consistently express a non-projecting inter-orbital region, it also identified more variation among cercopithecoids and platyrrhines. *Alouatta*, *Nasalis*, and *Erythrocebus* also variably expressed non-projecting inter-orbital regions and therefore this character was not identified as synapomorphic.

A number of characters were identified supporting previously proposed synapomorphies. These involved morphology of the distal humerus and ulnar trochlear notch (Napier and Davis, 1959; Fleagle, 1983; Andrews, 1985; Harrison, 1987; Rose, 1988; McCrossin, 1994; Benefit and McCrossin, 1995; Walker, 1997; Fleagle, 1998; Larson, 1998, 2006; Rae, 1999; Gebo, 2009), morphology of the hamate and pisiform (Lewis, 1972, 1989; Conroy and Fleagle, 1972; O'Connor, 1975; Daver and Nakatsukasa, 2015), cranial expansion of the acetabulum (Zykstra, 1999) and the sacro-iliac contact (Ward, 1991, 1993; Kelley, 1997) . *Proconsul* and extant hominoids share a broad trochlea with well-developed medial and lateral trochlear keels, a globular capitulum and an extensive trochlear notch. This analysis identified two further key synapomorphies from the forelimb: width of the radio-carpal facet and width of the coronoid

fossa. Additionally width across the incisors was also identified as a new synapomorphy along with morphology of the calcaneal sustentaculum and dimensions of the navicular.

Many of the characters drawn from the forelimb and manus reflect greater joint mobility across the forelimb, abduction/adduction at the wrist, radio-ulnar rotation, extension-flexion at the elbow, and greater robusticity of regions of the hand associated with gripping vertical supports. These characters distinguish *Proconsul* from committed quadrupeds (including crown cercopithecoids and some platyrrhines) and suggest vertical climbing, bridging and perhaps limited suspensory behaviors may have been incorporated into its locomotor repertoire (Napier and Davis, 1959; Rose, 1983, Walker and Pickford, 1983; 1989; Andrews, 1985; Andrews and Martin, 1987; Gebo et al., 1988; Andrews, 1985; Gebo, 1996; Kelley, 1997; Walker, 1997; Fleagle, 1998; Larson and Stern, 2006; Gebo, 2009; Nakatsukasa and Kunimatsu, 2009). Given results from these analyses, the presence of these synapomorphies in *Proconsul*—despite lacking the full suite of characters suggesting extant hominoid suspensory behaviors—likely indicates pre-adaptation to suspension and not symplesiomorphic similarity to stem catarrhines. It may further suggest that the dendropithecoids, expressing similar post-cranial adaptations (Fleagle, 1983; Rose, 1983, 1993; Gebo, 1989, 2009; Ward, 2007; Harrison, 2010, 2013) perhaps should also be placed within Hominoidea, though confident inference would require including them within a rigorous phylogenetic analysis. While many features in the forelimb and manus are synapomorphic for hominoids + *Proconsul,* there are also a number of other features drawn from the mandible, pelvis and pes that are less closely tied to the suite of suspensory and climbing behavior associated with the hominoids.

6.2 CONCLUSIONS

Results from this dissertation lead to the rejection of H1 (*Proconsul* is a stem catarrhine) and H3 (*Proconsul* is a hominid), identifying H2 (*Proconsul* is a hominoid) as the optimal hypothesis. A broader consideration of the distribution of morphology supporting this hypothesis elucidates the difficulty in inferring character polarities for the early stages of catarrhine and crown catarrhine evolution. A potential strength of this dissertation is the fact that while it recapitulated results from prior analyses, it did so with a novel character list that did not incorporate many of the characters and regions that have often held a central place in the discussion of catarrhine evolution and the phylogenetic position of *Proconsul*. This lends additional to support to the inference that *Proconsul* is a hominoid as this data set is clearly not simply rerunning the same data from previous analyses.

Proconsul primarily exhibits evidence for a pronograde arboreal quadrupedal locomotor style, expressing a greater range of motion across its forelimb than is seen in extant arboreal cercopithecoids and is more similar in this regard to platyrrhines (Szalay and Delson, 1979; Andrews, 1985; Andrews and Martin, 1987; Rose, 1987, 1994; Ward et al., 1993; Walker, 1997; Nakatsukasa, 2003, 2004, 2007, 2009; Dunsworth, 2006; Daver and Nakatsukasa, 2015). Results from the phylo-morphospace analysis show *Proconsul* falling nearest the platyrrhines (particularly *Pithecia*) across all anthropoids and to the cercopithecines among catarrhines. *Victoriapithecus* closely approximates the cercopithecoid MRCA morphotype and also is most similar to the cercopithecines among catarrhines, though often exhibiting greater morphological similarity to the platyrrhines. The Miocene basal catarrhine *Epipliopithecus* also exhibited forelimb morphology most similar to platyrrhines, a pattern also exhibited by the dendropithecoids (Gebo, 1989, 2009; Rose et al., 1992; Rose, 1997; Harrison, 2010, 2013). In

this analysis, *Epipliopithecus* expressed even more evidence for suspensory behaviors than *Proconsul*, appearing most similar to the atelids (Rose, 1994) and appearing closer morphologically to the hominoid MRCA than *Proconsul*. In this context, the committed quadrupedalism of cercopithecoids is likely more derived than the seemingly unique locomotion of the hominoids (Wood-Jones, 1929; Le Gros Clark, 1934; Von Koenigswald, 1968, 1969; Szalay and Delson, 1979; Fleagle, 1983; Harrison, 1987, 1993; Rose, 1988, 1994; Gebo, 1993; Benefit, 1999; Leakey et al., 2003; Elton, 2007; Jablonski and Frost, 2010), though this simplification is challenged by similarities between *Proconsul, Victoriapithecus* and the cercopithecines. Given this distribution of variation, *Proconsul* may be characterized as primarily monkey-like, possessing many crown catarrhine synapomorphies making it appear similar to *Victoriapithecus* and the cercopithecines, but also possessing hominoid synapomorphies for which it does not yet exhibit a fully derived morph, instead indicating pre-adaptations to the more derived morphology exhibited by more derived fossil and extant hominoids. Interestingly, *Proconsul* appears more primitive in its post-cranial adaptations than another middle Miocene ape *Kenyapithecus* (Pickford et al., 2006; Harrison, 2010). While this taxon also exhibits adaptations to quadrupedal locomotion, its elbow is more derived towards the hominoid condition (McCrossin and Benefit, 1994; Rose, 1997), suggesting a more complex scenario than *Proconsul* simply being the first and thus most primitive taxon. The potential that *Morotopithecus* and nyanzapithecines are also hominoids (Gebo, 1997; Kunimatsu 1997; MacLatchy et al. 2000; Young and MacLatchy 2004; Pickford and Kunimatsu, 2005) as opposed to stem catarrhines (Harrison, 2010, 2013) —a likely scenario given results from this dissertation, given the similarity between *Proconsul* and these taxa (Leakey and Leakey, 1986; Kunimatsu 1997; Pickford and Kunimatsu, 2005; Harrison, 2010)—could push the originiation

of the hominoid clade into the Oligocene (Gebo, 1997; Stevens et al., 2013). This result is confirmed by the dating analysis conducted here, which infers the MRCA of all hominoids, including *Proconsul*, to occur in the Oligocene, not long after the MRCA of all crown catarrhines.

Ultimately, the catarrhine, hominoid and cercopithecoid MRCA morphotypes are quite similar to each other morphologically for the set of synapomorphies placing *Proconsul* within Hominoidea. This result is confirmed in the literature by discussions of other basal catarrhine taxa, such as *Saadanius* and the dendropithecoids (Leakey and Leakey 1987; Gebo, 1989, 2009; Rose et al., 1992; Rose, 1997; Harrison, 2010, 2013; Zalmout et al., 2010), and demonstrates how little morphological variation there is distinguishing stem catarrhines from crown catarrhines. *Proconsul, Saadanius* and the dendropithecoids are the fossil taxa that fall nearest the divergence of crown catarrhines, with only *Saadanius* uncontested in the literature as falling before the divergence of cercopithecoids and hominoids (Zalmout et al., 2010). The range of variation expressed by these three taxa exemplifies the continued difficulty facing research into the early divergence of the hominoids.

Appendix A. Complete character list

Code	Region	Element	Metric/ Ordered	Description
o1	Cranium	Frontal	O	supraorbital notch morphology
				Absent (0) reduced (1) present (2) displaced laterally (3) foramen (4)
o2	Cranium	Orbit	O	location of highest point in orbital aperture
				Medial (0) middle (1) lateral (2)
o3	Cranium	Orbit	O	location of lowest point in orbital aperture
				Medial (0) middle (1) lateral (2)
o4	Cranium	Orbit	O	orbit width
				midline (0) diagonal (1) lateral (2) medial (3)
o5	Cranium	Orbit	O	orbits square or round
				square (0) or round (1)
o6	Cranium	Frontal	O	supra-orbital region undifferentiated from forehead
				No (0) yes (1)
o7	Cranium	Orbit	O	height of superior border of zygomatic at zygomatic root
				Below orbital margin (0) even with (1) above orbital margin (2)
o8	Cranium	Orbit	O	length of posterior lacrimal crest
				No (0) yes (1)
o9	Cranium	Orbit	O	presence of tubercle at termination of posterior lacrimal
				No (0) yes (1)
o10	Cranium	Orbit	O	prominence of lacrimal crest
				Rounded hangs over (0) flat (1) notched (2) nasals project into (3)
o11	Cranium	Lacrimal	O	lacrimal fossa position within orbit
				covered (1) uncovered (0)
o12	Cranium	Zygomatic	O	presence of zygomatico-facial foramina on frontal process of zygomatic
				Absent (0) single (1) more than one (2) at least one very large (3)
o13	Cranium	Zygomatic	O	presence of infero-lateral orbital notch.
				Absent (0) present (1)
o14	Cranium	Frontal	O	presence of supero-lateral orbital notch.
				Absent (0) present (1)
o15	Cranium	Facial	O	presence of foramina near fronto-zygomatic suture.

				Absent (0) notched/partial (1) one (2) at least one positioned far superior to suture on frontal (3) more than one (4)
o16	Cranium	Maxilla	O	infraorbital foramen shape
				Round (0) teardrop (1)
o17	Cranium	Maxilla	O	number of infraorbital foramina
				None (0) one (1) two (2) more than 2 (3)
o18	Cranium	Frontal	O	supra-orbital morphology continuous or divided
				Divided (0) continuous (1)
o19	Cranium	Facial	O	swelling at naso-frontal suture
				Depressed (0) none (1) minimal (2) moderate (3) pronounced (4)
o20	Cranium	Facial	O	tubercle present at inferior zygomatico-maxillary suture
				Absent (0) reduced (1) moderate (2) pronounced (3)
o21	Cranium	Facial	O	topography of inferior surface at zygomaxillary
				Sharp edge (0) grooved (1) broad rugose (2)
o22	Cranium	Facial	O	height of fronto-zygomatic suture in orbit
				Midline (0) above mid (1) just below sup orbit margin (2)
o23	Cranium	Maxilla	O	topography of malar region behind canines
				Not depressed (0) evenly depressed (1) groove (2) small circular (3) broad oval (4) deep circular (5) deep broad oval (6)
o24	Cranium	Maxilla	O	nasal aperture shape
				Tall oval (0) squat oval (1) heart shaped (2) pear shaped (3) upside down triangle/diamond (4)
o25	Cranium	Maxilla	O	inferior margin of nasal aperture flat or tapering
				Flat (0), tapering (1)
o26	Cranium	Maxilla	O	curvature of alveolar margin
				flat (0) moderately curved (1) curved (2)
o27	Cranium	Palate	O	topography of palate at m3
				flat (0) curved (1)
o28	Cranium	Maxilla	O	incisive foramen size
				small (0) medium (1) large (2)
o29	Cranium	Maxilla	O	incisive foramen shape
				Round (0), oval (1), triangle (2)
o30	Cranium	Maxilla	O	incisive foramen divided
				undivided (0), thin septum (1), thick septum (2)
o31	Cranium	Palatine	O	number of palatine foramina

				single (0), two (1), three (2), more than three (3)
o32	Cranium	Palatine	O	size of largest palatine foramina
				small (0) medium (1) large (2)
o33	Cranium	Palatine	O	prominence of palatine ridge
				Absent (0) slight protuberance (1) small clear ridge (2) large ridge (3)
o34	Cranium	Palate	O	topography of posterior palate
				flat (0) rounded (1)
o35	Cranium	Facial	O	naso-frontal suture flat or tapering
				flat (0) pointed (1)
o36	Cranium	Facial	O	naso-frontal suture extend superior to maxillary-frontal suture at lateral margins
				No (0) yes (1)
o37	Cranium	Maxilla	O	presence of premaxillary suture
				absent (0) present (1)
o38	Cranium	Nasals	O	nasals expand laterally into bulb at superior aspect
				No (0) yes (1)
o39	Cranium	Maxilla	O	premaxillary suture contacts nasal aperture or nasal bones
				Contacts aperture (0) contacts nasals (1) not visible (2)
o40	Cranium	Maxilla	O	outline of premaxillary suture on palate
				straight (0) v-shaped (1) w shaped (2)
o41	Cranium	Temporal	O	ectotympanic angle
				Postero lateral to antero medial (0) opposite (1) flat (2)
o42	Cranium	Temporal	O	ectotympanic tube presence
				ring (0) ectotympanic tube (1)
o43	Cranium	Temporal	O	angle of external auditory meatus
				flat (0) angled antero-medially 1) angled opposite (2)
o44	Cranium	Temporal	O	position of post glenoid tubercle
				middle (0) medial (1) lateral (2)
o45	Cranium	Temporal	O	number of stylomastoid foramina
				one (0), two (1)
o46	Cranium	Occipital	O	prominence of external occipital protuberance
				Broad flat center depressed (0) broad flat no edge (1) broad flat clear edge (2) broad flat sharp point (3) prominent crest (4) prominent sharp point (5)
o47	Cranium	Occipital	O	projection of median nuchal line

				Rounded (0) rounded prominent (1) small sharp (2) large sharp (3)
o48	Cranium	Parietals	O	convergence of temporal lines
				Not visible (0) not converging (1) approaches convergence (2) converge (3)
o49	Cranium	Neurocranium	O	prominence of temporal lines
				Not visible (0), not pronounced (1), prominent (2)
o50	Cranium	Parietals	O	degree of posterior sagittal keeling
				Absent (0) slight but not lines (1) true crest (2)
o51	Cranium	Neurocranium	O	prominence of horizontal occipital cresting at posterior aspect of neurocranium
				Absent (0) reduced rounded (1) pronounced rounded (2) small sharp (3) large sharp (4)
o52	Cranium	Neurocranium	O	height of squamosal suture
				inferior (0) superior (1)
o53	Cranium	Occipital	O	prominence of depression beneath external occipital protuberance
				none (0) moderate (1) pronounced (2)
o54	Cranium	Frontal	O	anterior position of temporal lines
				Medial (0) lateral (1)
o55	Cranium	Frontal	O	presence of frontal trigone
				Absent (0) present (1)
o56	Cranium	Temporal	O	presence of foramen at postero-medial corner of post-glenoid tubercle
				Absent (0) small (1) multiple small (2) medium (3) multiple medium (4)
o57	Cranium	Nasals	O	presence of midline crest on nasals
				absent (0) rounded (1) sharp (2)
m1	Cranium	Frontal	M	thickness of supra-orbital rim
m2	Cranium	Zygomatic	M	thickness of lateral orbital rim
m3	Cranium	Zygomatic	M	width from lateral orbital rim to zygomatic root
m4	Cranium	Facial	M	interorbital distance
m5	Cranium	Facial	M	orbit height
m6	Cranium	Facial	M	orbit width
m7	Cranium	Facial	M	width behind orbits
m8	Cranium	Facial	M	width between fronto-zygomatic sutures
m9	Cranium	Facial	M	width between superior zygomatic roots
m10	Cranium	Facial	M	width between inferior zygomaxillary
m11	Cranium	Maxilla	M	width between maxillary m2s
m12	Cranium	Maxilla	M	height of nasal aperture in midline
m13	Cranium	Maxilla	M	width of nasal aperture at top

m14	Cranium	Maxilla	M	width of nasal aperture at base
m15	Cranium	Maxilla	M	width of nasal aperture at midpoint
m16	Cranium	Maxilla	M	distance inferior nasal margin to interdentale
m17	Cranium	Facial	M	distance glabella to superior-most point of aperture in midline
m18	Cranium	Facial	M	interdentale in midline to glabella
m19	Cranium	Maxilla	M	palate depth (supero-inferior) at m3
m20	Cranium	Maxilla	M	palate length
m21	Cranium	Maxilla	M	palate width at first premolars
m22	Cranium	Maxilla	M	width across all incisors
m23	Cranium	Maxilla	M	width across canines
m24	Cranium	Temporal	M	height post-glenoid tubercle (from most posterior point to temporal line)
m25	Cranium	Temporal	M	height mandibular fossa (from most posterior point to temporal line)
m26	Cranium	Temporal	M	height articular tubercle (from most posterior point to temporal line)
m27	Cranium	Temporal	M	height narrowest point anterior to articular tubercle
m28	Cranium	Temporal	M	height at most posterior point of zygomatic root
m29	Cranium	Temporal	M	post-glenoid tubercle width at base
m30	Cranium	Temporal	M	length mandibular fossa of temporal
m31	Cranium	Temporal	M	width mandibular fossa of temporal
m32	Cranium	Occipital	M	occipital condyle length
m33	Cranium	Occipital	M	length posterior segment occipital condyle
m34	Cranium	Occipital	M	width posterior segment occipital condyle
m35	Cranium	Occipital	M	length anterior segment occipital condyle
m36	Cranium	Occipital	M	width anterior segment occipital condyle
m37	Cranium	Occipital	M	narrowest point in midline width of occipital condyle
m38	Cranium	Frontal	M	distance between temporal lines at highest degree of constriction
m39	Cranium	Temporal	M	breadth of external auditory meatus opening
m40	Cranium	Temporal	M	length ectotympanic ring/tube
m41	Cranium	Temporal	M	length ectotympanic ring/tube at posterior aspect
m42	Cranium	Temporal	M	width ectotympanic ring/tube
m43	Cranium	Temporal	M	distance from anterior most point of external auditory meatus opening to lateral margin of cranium
MO1	Mandible	Mandible	O	mandibular condyle curvature

				Flat (0), concave anteriorly (1), concave posteriorly (2)
MO2	Mandible	Mandible	O	gonion extends posterior to mandibular condyle
				no (0) yes (1)
MO3	Mandible	Mandible	O	prominence tubercle inferior to mandibular condyle
				none (0), small (1), large (2)
MO4	Mandible	Mandible	O	inward flare at gonial angle
				no (0), yes (1)
MO5	Mandible	Mandible	O	most anterior position of mental foramen
				canine (0) p3 (1) p4 (2) m1 (3)
MO6	Mandible	Mandible	O	number of mental foramina
				None (0), single (1), two (2), more than 2 (3)
MO7	Mandible	Mandible	O	height of mental foramen
				below mid (0) mid(1) above (2)
MO8	Mandible	Mandible	O	coronoid process turns backwards
				yes (1) no (0)
MM1	Mandible	Mandible	M	length of mandibular condyle
MM2	Mandible	Mandible	M	width mandibular condyle in midline of medial aspect
MM3	Mandible	Mandible	M	width mandibular condyle in midline of lateral aspect
MM4	Mandible	Mandible	M	width mandibular condyle in midline aspect
MM5	Mandible	Mandible	M	height from middle of mandibular condyle to gonial angle
MM6	Mandible	Mandible	M	height from coronoid process to base of mandible
MM7	Mandible	Mandible	M	length mandibular notch from anteriormost point of mandibular condyle to tip of coronoid process
MM8	Mandible	Mandible	M	thickness at gonial angle
MM12	Mandible	Mandible	M	antero-posterior width coronoid process at base
MM13	Mandible	Mandible	M	antero-posterior width coronoid process at tip
MM14	Mandible	Mandible	M	supero-inferior height from alveolar margin to inferior margin of corpus behind m3
MM15	Mandible	Mandible	M	supero-inferior height from alveolar margin to inferior margin of corpus between p3 and canine
MM16	Mandible	Mandible	M	width across incisors
MM17	Mandible	Mandible	M	width across canines
MM18	Mandible	Mandible	M	width at p3s

MM19	Mandible	Mandible	M	width across molars at m2
MM20	Mandible	Mandible	M	width across mandible (ramus) at last molar
MM21	Mandible	Mandible	M	antero-posterior width corpus at symphysis beneath digastric fossa
MM22	Mandible	Mandible	M	width corpus at symphysis above digastric fossa
MM23	Mandible	Mandible	M	height from inferior margin of mandible to digastric fossa
MM24	Mandible	Mandible	M	height from digastric fossa to alveolar margin
MM25	Mandible	Mandible	M	antero-posterior width ramus at alveolar margin
MM26	Mandible	Mandible	M	antero-posterior width ramus inferior to condyle
MM28	Mandible	Mandible	M	length toothrow
MM29	Mandible	Mandible	M	height corpus at m1
MM30	Mandible	Mandible	M	height corpus at symphysis
MM31	Mandible	Mandible	M	medio-lateral width mandible corpus at m1
MS1	Mandible	Mandible	M	length along curvature of mandibular notch
MS2	Mandible	Mandible	M	length along curvature midpoint medial aspect mandibular condyle
MS3	Mandible	Mandible	M	length along curvature midpoint lateral aspect mandibular condyle
UO1	Forelimb	Ulna	O	presence of midline ridge between medial and lateral segments of trochlear notch
				no (0) mild (1) clear (2)
UO2	Forelimb	Ulna	O	prominence of oblique line
				none (0) slight (1) sharp (2) broad rugose (3)
UO3	Forelimb	Ulna	O	presence of tubercle at termination of oblique line
				none (0) reduced (1) small (2) large (3)
UO4	Forelimb	Ulna	O	prominence of ridge running from posterior aspect of coronoid process down shaft
				none (0) slight (1) moderate (2) prominent (3)
UO5	Forelimb	Ulna	O	sharpness of anterior surface of proximal shaft
				flat (0) small crest (1) pronounced crest (2)
UO6	Forelimb	Ulna	O	groove prominence at level of tubercle on medial side of shaft
				convex (0) flat (1) moderate (2) deep (3)
UO7	Forelimb	Ulna	O	groove prominence at level of tubercle on lateral side of shaft
				convex (0) flat (1) slight (2) deep (3)
UO8	Forelimb	Ulna	O	shape distal carpal articulation
				crescent (0) flat bottom (1) circular (2) triangular (3)

UO9	Forelimb	Ulna	O	presence groove between styloid process and carpal articulation
				convex (0) flat (1) slight (2) deep (3)
UO10	Forelimb	Ulna	O	presence of tubercle at base of styloid
				absent-0 present-1 large-2
UO11	Forelimb	Ulna	O	orientation of lateral-most flange of radial facet
				laterally (0) anteriorly (1) superiorly (2)
UO12	Forelimb	Ulna	O	outline of lateral border of trochlea
				continuous line (0) notched (1) projects laterally (2)
UO13	Forelimb	Ulna	O	prominence of ridge for pronator quadratus
				none (0), reduced (1), prominent (2)
UO14	Forelimb	Ulna	O	radial facet single or divided
				single (0) notched (1) divided (2)
US9	Forelimb	Ulna	M	length along midline ridge of trochlear notch
US10	Forelimb	Ulna	M	length along curvature of medial edge of trochlear notch
US11	Forelimb	Ulna	M	length along curvature of lateral edge of trochlear notch
US12	Forelimb	Ulna	M	length along curvature of proximal border of trochlea
US13	Forelimb	Ulna	M	length along curvature of distal border of trochlea
US14	Forelimb	Ulna	M	length along curvature of anterior border distal carpal facet
UM1	Forelimb	Ulna	M	height olecranon process at medial border
UM2	Forelimb	Ulna	M	height olecranon process at midline
UM3	Forelimb	Ulna	M	height olecranon process at lateral border
UM4	Forelimb	Ulna	M	width olecranon process at anterior border
UM5	Forelimb	Ulna	M	width olecranon process at midline
UM6	Forelimb	Ulna	M	width olecranon process at posterior border
UM7	Forelimb	Ulna	M	length olecranon process to proximal border of trochlear notch at medial border
UM8	Forelimb	Ulna	M	length olecranon process to proximal border of trochlear notch in midline
UM9	Forelimb	Ulna	M	length olecranon process to proximal border of trochlear notch at lateral border
UM10	Forelimb	Ulna	M	width proximal to trochlear notch
UM11	Forelimb	Ulna	M	width proximal border trochlear notch
UM12	Forelimb	Ulna	M	width distal border trochlear notch
UM14	Forelimb	Ulna	M	length trochlear notch at medial border
UM15	Forelimb	Ulna	M	length trochlear notch in midline

UM16	Forelimb	Ulna	M	length trochlear notch at lateral border
UM17	Forelimb	Ulna	M	length of radial notch
UM18	Forelimb	Ulna	M	width of radial notch
UM19	Forelimb	Ulna	M	height articular facet on coronoid process
UM20	Forelimb	Ulna	M	width articular facet on coronoid process
UM21	Forelimb	Ulna	M	medio-lateral width from medial-most border of radial facet to medial-most point of coronoid process
UM22	Forelimb	Ulna	M	length medial border of coronoid process (for flexor digitorum)
UM23	Forelimb	Ulna	M	length oblique line
UM24	Forelimb	Ulna	M	length ridge extending from posterior aspect of coronoid process
UM25	Forelimb	Ulna	M	antero-posterior width shaft at termination of oblique line
UM26	Forelimb	Ulna	M	medio-lateral width at termination of oblique line
UM27	Forelimb	Ulna	M	medio-lateral width ulnar styloid at base
UM28	Forelimb	Ulna	M	medio-lateral width ulnar styloid at midline
UM29	Forelimb	Ulna	M	antero-posterior width ulnar styloid at base
UM30	Forelimb	Ulna	M	antero-posterior width ulnar styloid at midline
UM31	Forelimb	Ulna	M	medio-lateral width of distal carpal articulation
UM32	Forelimb	Ulna	M	antero-posterior width of distal carpal articulation in midline
UM34	Forelimb	Ulna	M	antero-posterior with distal radius
UM35	Forelimb	Ulna	M	proximo-distal length styloid process
UM36	Forelimb	Ulna	M	medio-lateral width shaft proximal to distal radial articulation
UM37	Forelimb	Ulna	M	antero-posterior width shaft proximal to distal radial articulation
UM38	Forelimb	Ulna	M	antero-posterior height from tip of coronoid process to bottom of shaft
UM39	Forelimb	Ulna	M	antero-posterior height from tip of olecranon process to bottom of shaft
UM40	Forelimb	Ulna	M	antero-posterior height from lowest point in trochlear notch to bottom of shaft
UM41	Forelimb	Ulna	M	medio-lateral width trochlea notch at narrowest point in midpoint
RO1	Forelimb	Radius	O	degree cresting of distal radial shaft
				none (0) slight (1) true crests (2)
RO2	Forelimb	Radius	O	presence rounded crest in midline of distal radius articular facet
				flat (0) crest (1) depressed (2)

RO3	Forelimb	Radius	O	prominence lateral ridge on dorsal aspect of distal radius for extensors
				absent (0) slight (1) pronounced (2)
RO4	Forelimb	Radius	O	prominence of middle ridge on dorsal aspect of distal radius for extensors
				absent (0) slight (1) pronounced (2)
RO5	Forelimb	Radius	O	prominence of medial ridge on dorsal aspect distal radius for extensors
				absent (0) slight (1) pronounced (2)
RO6	Forelimb	Radius	O	presence of facet on anterior aspect of styloid process
				Absent (0) present (1)
RO7	Forelimb	Radius	O	projection of anterior corner of ulnar facet
				no (0) yes (1)
RO8	Forelimb	Radius	O	degree curvature of shaft
				uncurved (0) slight (1) pronounced (2)
RM1	Forelimb	Radius	M	medio-lateral width radial head
RM2	Forelimb	Radius	M	antero-posterior width head
RM3	Forelimb	Radius	M	mediolateral width across depression at center of head
RM4	Forelimb	Radius	M	antero-posterior width across depression at center of head
RM5	Forelimb	Radius	M	proximo-distal height radial head at medial aspect
RM6	Forelimb	Radius	M	proximo-distal radial head height at lateral aspect
RM7	Forelimb	Radius	M	proximo-distal height radial head border on anterior aspect
RM8	Forelimb	Radius	M	proximo-distal height radial head border on posterior aspect
RM9	Forelimb	Radius	M	medio-lateral width across neck
RM10	Forelimb	Radius	M	antero-posterior width across neck
RM11	Forelimb	Radius	M	proximo-distal height tubercle
RM12	Forelimb	Radius	M	medio-lateral width tubercle
RM13	Forelimb	Radius	M	medio-lateral width across shaft at tubercle
RM14	Forelimb	Radius	M	antero-posterior width shaft at level of tubercle
RM15	Forelimb	Radius	M	medio-lateral width across shaft distal to tubercle
RM16	Forelimb	Radius	M	antero-posterior width across shaft distal to tubercle
RM17	Forelimb	Radius	M	medio-lateral width across distal radius in midline
RM18	Forelimb	Radius	M	antero-posterior breadth across distal radius in

				midline
RM19	Forelimb	Radius	M	breadth across distal radius at medial margin
RM20	Forelimb	Radius	M	breadth across distal radius at lateral margin
RM21	Forelimb	Radius	M	proximo-distal height styloid process
RM22	Forelimb	Radius	M	antero-posterior length facet for ulna
RM23	Forelimb	Radius	M	proximo-distal height facet for ulna in midline
RM24	Forelimb	Radius	M	medio-lateral width styloid process
RM25	Forelimb	Radius	M	antero-posterior width styloid process
RM26	Forelimb	Radius	M	proximo-distal length radius from midpoint of facets
RM27	Forelimb	Radius	M	medio-lateral length carpal facet through midline
RM28	Forelimb	Radius	M	medio-lateral length anterior border distal carpal facet
RM29	Forelimb	Radius	M	medio-lateral length posterior border distal carpal facet
RS1	Forelimb	Radius	M	medio-lateral length along curvature in midline of carpal facet
Rs2	Forelimb	Radius	M	antero-posterior length along curvature of medial border of carpal facet
huo1	Forelimb	Humerus	O	presence of entepicondylar foramen
				no (0), yes (1)
huo2	Forelimb	Humerus	O	presence of dorsal epitrochlear fossa
				no (0), yes (1)
huo3	Forelimb	Humerus	O	perforation of olecranon fossa
				no (0), yes (1)
huo4	Forelimb	Humerus	O	angle of medial epicondyle relative to trochlea
				unangled (0), angled (1)
huo5	Forelimb	Humerus	O	coronoid fossa depth
				indistinct (0), shallow (1) moderate (2) deep (3) deeper (4) perforated (5)
huo6	Forelimb	Humerus	O	radial fossa depth
				indistinct (0), shallow (1) moderate (2) deep indistinct borders (3) deep distinct (4) perforated (5)
huo7	Forelimb	Humerus	O	morphology of lateral supra-condylar ridge
				indistinct (0), shallow (1) moderate (2) deep indistinct borders (3) deep distinct (4) perforated (5)
huo8	Forelimb	Humerus	O	presence of globular capitulum
				no (0), yes (1)
huo9	Forelimb	Humerus	O	position of median keel termination

				posterior (0) midline (1)
huo10	Forelimb	Humerus	O	posterior border of capitulum completely isolated or continuous with posterior trochlea
				continuous (0), isolated (1)
hus5	Forelimb	Humerus	M	length along curvature between starting and ending point of trochlear at medial trochlear keel
hus9	Forelimb	Humerus	M	length along curvature between starting and ending point of trochlea medial to median trochlear keel
hus8	Forelimb	Humerus	M	length along curvature between starting and ending point of median trochlear keel
hus10	Forelimb	Humerus	M	length along curvature of medial border of capitulum between starting and ending point of trochlea lateral to median trochlear keel beginning from starting point of lateral trochlear keel
hus6	Forelimb	Humerus	M	length along curvature between starting and ending point of capitulum at point of greatest curvature in midline of capitulum
hus7	Forelimb	Humerus	M	length along curvature between starting and ending point of capitulum at lateral-most point of capitullum
hum1	Forelimb	Humerus	M	medio-lateral distance medial border trochlea to midline of median keel
hum2	Forelimb	Humerus	M	medio-lateral distance from lateral border of capitulum to midline of median keel
hum4	Forelimb	Humerus	M	medio-lateral projection of lateral epicondyle
hum5	Forelimb	Humerus	M	medio-lateral length from medial trochlear keel to narrowest point medial to keel at proximal border
hum7	Forelimb	Humerus	M	medio-lateral length trochlear keel at proximal border
hum8	Forelimb	Humerus	M	medio-lateral length capitulum at proximal border
hum9	Forelimb	Humerus	M	medio-lateral length across trochlea and capitulum at proximal border
hum10	Forelimb	Humerus	M	medio-lateral length of trochlea and capitulum at disto-anterior surface
hum11	Forelimb	Humerus	M	medio-lateral length from medial trochlear keel to narrowest point medial to keel at disto-anterior surface
hum13	Forelimb	Humerus	M	medio-lateral length trochlear keel at disto-anterior surface

hum14	Forelimb	Humerus	M	medio-lateral length capitulum at disto-anterior surface
hum15	Forelimb	Humerus	M	medio-lateral length trochlear and capitulum at distal border
hum16	Forelimb	Humerus	M	medio-lateral length trochlea at termination of capitulum
hum20	Forelimb	Humerus	M	medio-lateral length capitulum at midline of trochlea
hum22	Forelimb	Humerus	M	medio-lateral length proximal border of trochlea
hum23	Forelimb	Humerus	M	proximo-distal height of medial border trochlea
hum24	Forelimb	Humerus	M	proximo-distal height medial to median trochlear keel
hum25	Forelimb	Humerus	M	proximo-distal height at tallest point of median trochlear keel
hum26	Forelimb	Humerus	M	proximo-distal height lateral to median trochlear keel
hum27	Forelimb	Humerus	M	proximo-distal height at tallest point of capitulum
hum28	Forelimb	Humerus	M	proximo-distal height of lateral border capitulum
hum29	Forelimb	Humerus	M	antero-posterior depth of medial border trochlea
hum30	Forelimb	Humerus	M	antero-posterior depth medial to median trochlear keel
hum31	Forelimb	Humerus	M	antero-posterior depth at widest point of median trochlear keel
hum32	Forelimb	Humerus	M	antero-posterior depth lateral to median trochlear keel to termination of capitulum
hum33	Forelimb	Humerus	M	antero-posterior depth from most projecting point of capitulum
hum34	Forelimb	Humerus	M	antero-posterior depth of lateral border capitulum
hum35	Forelimb	Humerus	M	proximo-distal height medial trochlear keel
hum36	Forelimb	Humerus	M	proximo-distal height medial to median trochlear keel
hum37	Forelimb	Humerus	M	proximo-distal height at tallest point of median trochlear keel
hum38	Forelimb	Humerus	M	proximo-distal height lateral trochlear keel on posterior aspect
hum39	Forelimb	Humerus	M	width of olecranon fossa
hum40	Forelimb	Humerus	M	height of olecranon fossa
hum41	Forelimb	Humerus	M	length from proximal-most point of olecranon fossa to disto-medial corner of fossa

hum42	Forelimb	Humerus	M	length from proximal-most point of olecranon fossa to disto-lateral corner of fossa
hum43	Forelimb	Humerus	M	length medial epicondyle
hum44	Forelimb	Humerus	M	antero-posterior width of medial epicondyle
hum45	Forelimb	Humerus	M	proximo-distal height of medial epicondyle
hum46	Forelimb	Humerus	M	projection of median trochlear keel distal to margin of medial epicondyle
hum47	Forelimb	Humerus	M	widest point of coronoid fossa
hum48	Forelimb	Humerus	M	tallest point in midline of coronoid fossa
hum50	Forelimb	Humerus	M	widest point of radial fossa
hum51	Forelimb	Humerus	M	tallest point in midline of radial fossa
hum53	Forelimb	Humerus	M	proximo-distal height of lateral epicondyle
hum54	Forelimb	Humerus	M	medio-lateral length distal humerus
hum55	Forelimb	Humerus	M	medio-lateral width distal humerus immediately proximal to termination of epicondyles
hum56	Forelimb	Humerus	M	medio-lateral width of distal shaft
hum57	Forelimb	Humerus	M	antero-posterior width distal shaft
hum60	Forelimb	Humerus	M	antero-posterior depth distal humerus at medialmost point
hum62	Forelimb	Humerus	M	antero-posterior depth distal humerus at lateralmost point
PVM1	Pelvis	Pelvis	M	length superior pubic ramus
PVM2	Pelvis	Pelvis	M	length symphyseal surface
PVM3	Pelvis	Pelvis	M	height obturator foramen
PVM4	Pelvis	Pelvis	M	width obturator foramen
PVM5	Pelvis	Pelvis	M	medio-lateral width inferior pubic ramus at superior aspect
PVM6	Pelvis	Pelvis	M	medio-lateral width inferior pubic ramus at inferior aspect
PVM7	Pelvis	Pelvis	M	supero-inferior height superior pubic ramus at superior aspect
PVM8	Pelvis	Pelvis	M	supero-inferior height ramus of ischium at inferior aspect
PVM9	Pelvis	Pelvis	M	medio-lateral width ischium
PVM10	Pelvis	Pelvis	M	height of acetabulum
PVM11	Pelvis	Pelvis	M	width across acetabulum
PVM12	Pelvis	Pelvis	M	length ischial tuberosity
PVM13	Pelvis	Pelvis	M	width ischial tuberosity at widest point
PVM14	Pelvis	Pelvis	M	antero-posterior width ischium superior to tuberosity
PVM16	Pelvis	Pelvis	M	antero-posterior width ilium
PVM17	Pelvis	Pelvis	M	height of ilium

PVM18	Pelvis	Pelvis	M	height from ilio-ischial suture to iliac blade
PVM19	Pelvis	Pelvis	M	projection of posterior inferior iliac spine
PVM20	Pelvis	Pelvis	M	height posterior inferior iliac spine to level of ilio-ischial suture
PVM21	Pelvis	Pelvis	M	height from posterior inferior iliac spine to superior most point of posterior iliac blade border
PVM22	Pelvis	Pelvis	M	antero-posterior width across iliac blade at level of post. inf. iliac spine
PVM23	Pelvis	Pelvis	M	length top of iliac blade
PVM24	Pelvis	Pelvis	M	antero-posterior width auricular surface at midpoint
PVM25	Pelvis	Pelvis	M	height auricular surface at anterior aspect
PVM26	Pelvis	Pelvis	M	height auricular surface at posterior aspect
PVS5	Pelvis	Pelvis	M	circumference ilium at greater sciatic notch
PVS6	Pelvis	Pelvis	M	length along curvature of superior border of iliac blade
PVS9	Pelvis	Pelvis	M	height of lunate surface at infero-medial aspect
PVS10	Pelvis	Pelvis	M	height of lunate surface at superior aspect
PVS11	Pelvis	Pelvis	M	height of lunate surface at lateral aspect
PVS12	Pelvis	Pelvis	M	height of lunate surface at infero-lateral aspect
PVS13	Pelvis	Pelvis	M	width acetabulum not including lunate surface
PVS14	Pelvis	Pelvis	M	height acetabulum not including lunate surface
PVS15	Pelvis	Pelvis	M	length along curvature of ischial tuberosity
PVO1	Pelvis	Pelvis	O	prominence obturator crest
				absent (0), slight round (1), prominent round (2), small sharp (3), large sharp (4)
PVO2	Pelvis	Pelvis	O	shape obturator foramen. rounded-0 squared-1 triangular-2
				rounded (0), square (1), triangular (2)
PVO4	Pelvis	Pelvis	O	shape ischial tuberosity
				rectangular (0), triangular (1), rounded (2), wavy (3)
PVO5	Pelvis	Pelvis	O	height of position ischial spine
				low (0), below midpoint (1), midpoint of acetabulum (2), above midpoint (3), high (4)
PVO6	Pelvis	Pelvis	O	prominence of ischial spine
				absent (0), small (1), large (2)
PVO7	Pelvis	Pelvis	O	greatest degree of projection of iliac blade
				anterior (0), middle (1), posterior (2), flat (3) spike at anterior aspect (4)
PVO10	Pelvis	Pelvis	O	prominence of sciatic notch

				reduced (0), moderate (1), deep (2)
PVO14	Pelvis	Pelvis	O	main axis of arcuate line
				supero-inferior (0), antero-posterior (1)
PVO15	Pelvis	Pelvis	O	prominence of obturator groove
				absent (0), reduced (1), prominent (2)
PVO16	Pelvis	Pelvis	O	height of superior aspect of symphysis
				low (0), inferior margin acetabulum (1), midline of acetabulum (2), high (3)
PVO17	Pelvis	Pelvis	O	presence of tubercle on superior pubis
				no (0), yes (1)
MC1M1	Metacarpals	MC1	M	medio-lateral width proximal facet
MC1M2	Metacarpals	MC1	M	palmo-dorsal width proximal facet
MC1M3	Metacarpals	MC1	M	medio-lateral width palmar border head
MC1M4	Metacarpals	MC1	M	medio-lateral width dorsal border head
MC1M5	Metacarpals	MC1	M	medio-lateral width dorsal keeling beneath head
MC1M6	Metacarpals	MC1	M	palmo-dorsal width lateral border head
MC1M7	Metacarpals	MC1	M	palmo-dorsal width medial border head
MC1M8	Metacarpals	MC1	M	palmo-dorsal width midline head
MC1M9	Metacarpals	MC1	M	palmo-dorsal width midline head at keel
MC1M10	Metacarpals	MC1	M	height head at medial edge
MC1M11	Metacarpals	MC1	M	height head at lateral edge
MC1M12	Metacarpals	MC1	M	height head in midline
MC1M13	Metacarpals	MC1	M	proximo-distal length
MC1M14	Metacarpals	MC1	M	medio-lateral width shaft at midpoint
MC1M15	Metacarpals	MC1	M	palmo-dorsal width shaft at midpoint
MC1M16	Metacarpals	MC1	M	chord length on plantar surface from proximal border of head to proximal termination of shaft
MC1S1	Metacarpals	MC1	M	circumference proximal articular facet
MC1S2	Metacarpals	MC1	M	curvature of palmar surface from border of head in midline to proximal termination of shaft
MC1S3	Metacarpals	MC1	M	curvature along head in midline
MC2O1	Metacarpals	MC2	O	facet for MC3 divided or continuous
				Divided (0) continuous (1)
MC2M7	Metacarpals	MC2	M	width MC 3/capitate facet
MC2M8	Metacarpals	MC2	M	palmo-dorsal width palmar aspect MC 3/capitate facet at trapezoid facet
MC2M9	Metacarpals	MC2	M	width dorsal aspect MC 3/capitate facet at trapezoid facet
MC2M10	Metacarpals	MC2	M	proximo-distal height palmar aspect MC 3/capitate facet

MC2M11	Metacarpals	MC2	M	height dorsal aspect MC 3/capitate facet
MC2M12	Metacarpals	MC2	M	height MC 3/capitate facet in midline
MC2M13	Metacarpals	MC2	M	medio-lateral width palmar border head
MC2M14	Metacarpals	MC2	M	medio-lateral width dorsal border head
MC2M15	Metacarpals	MC2	M	medio-lateral width dorsal keeling beneath facet head
MC2M16	Metacarpals	MC2	M	palmo-dorsal width lateral border head
MC2M17	Metacarpals	MC2	M	palmo-dorsal width medial border head
MC2M18	Metacarpals	MC2	M	palmo-dorsal width midline head at head
MC2M19	Metacarpals	MC2	M	palmo-dorsal width midline head at keel
MC2M20	Metacarpals	MC2	M	height head at medial edge
MC2M21	Metacarpals	MC2	M	height head at lateral edge
MC2M22	Metacarpals	MC2	M	height head in midline
MC2M23	Metacarpals	MC2	M	proximo-distal length
MC2M24	Metacarpals	MC2	M	medio-lateral width shaft at midpoint
MC2M25	Metacarpals	MC2	M	palmo-dorsal width shaft at midpoint
MC2M26	Metacarpals	MC2	M	chord length on plantar surface from proximal border of head to proximal termination of shaft
MC2S2	Metacarpals	MC2	M	curvature of palmar surface from border of head in midline to proximal termination of shaft
MC2S3	Metacarpals	MC2	M	curvature along head in midline
MC3O2	Metacarpals	MC3	O	facet for MC4 divided or continuous
				Divided (0) continuous (1)
MC3O3	Metacarpals	MC3	O	topography of palmar capitate facet
				convex (0), flat (1), concave (2)
MC3M16	Metacarpals	MC3	M	width MC 4 facet
MC3M17	Metacarpals	MC3	M	dorso-palmar width palmar aspect MC 4 facet
MC3M18	Metacarpals	MC3	M	width dorsal aspect MC 4 facet
MC3M19	Metacarpals	MC3	M	height palmar aspect MC 4 facet
MC3M20	Metacarpals	MC3	M	height dorsal aspect MC 4 facet
MC3M21	Metacarpals	MC3	M	height MC 4 facet in midline
MC3M32	Metacarpals	MC3	M	proximo-distal length
MC3M33	Metacarpals	MC3	M	medio-lateral width shaft at midpoint
MC3M34	Metacarpals	MC3	M	palmo-dorsal width shaft at midpoint
MC4O2	Metacarpals	MC4	O	facet for MC5 divided or continuous
				Divided (0) continuous (1)
MC4O3	Metacarpals	MC4	O	topography of hamate facet
				convex (0), flat (1), concave (2)
MC4M16	Metacarpals	MC4	M	width MC 5 facet
MC4M17	Metacarpals	MC4	M	width palmar aspect MC 5 facet

MC4M18	Metacarpals	MC4	M	width dorsal aspect MC 5 facet
MC4M19	Metacarpals	MC4	M	height palmar aspect MC 5 facet
MC4M20	Metacarpals	MC4	M	height dorsal aspect MC 5 facet
MC4M21	Metacarpals	MC4	M	height MC 5 facet in midline
MC4M32	Metacarpals	MC4	M	proximo-distal length
MC4M33	Metacarpals	MC4	M	medio-lateral width shaft at midpoint
MC4M34	Metacarpals	MC4	M	palmo-dorsal width shaft at midpoint
MC5O1	Metacarpals	MC5	O	topography of hamate facet
				convex (0), flat (1), concave (2)
MC5M12	Metacarpals	MC5	M	width tubercle on medial aspect proximal shaft
MC5M13	Metacarpals	MC5	M	height tubercle on medial aspect proximal shaft
MC5M24	Metacarpals	MC5	M	proximo-distal length
MC5M25	Metacarpals	MC5	M	medio-lateral width shaft at midpoint
MC5M26	Metacarpals	MC5	M	palmo-dorsal width shaft at midpoint
CO1	Carpals	Capitate	O	presence of notch in midline of MC facet
				no (0), yes (1)
CO2	Carpals	Capitate	O	MC2/trapezoid facet divided or continuous
				Divided (0) continuous (1)
CO3	Carpals	Capitate	O	presence of palmar expansion of hamate facet
				no (0), yes (1)
CO4	Carpals	Capitate	O	does MC2 articulate with capitate above palmar trapezoid articulation
				no (0), yes (1)
CO5	Carpals	Capitate	O	hamate facet continuous or divided
				continuous (0), divided (1)
CS3	Carpals	Capitate	M	circumference capitate head
CS4	Carpals	Capitate	M	medio-lateral length along curvature dorsal border MC facet
CS5	Carpals	Capitate	M	dorso-palmar length along curvature in midline of MC facet
CM1	Carpals	Capitate	M	length palmar border MC facet
CM2	Carpals	Capitate	M	length dorsal border MC facet.
CM3	Carpals	Capitate	M	medio-lateral width MC facet in midline
CM4	Carpals	Capitate	M	length medial border MC facet
CM5	Carpals	Capitate	M	length lateral border MC facet
CM6	Carpals	Capitate	M	dorso palmar length MC3 facet in midline
CM7	Carpals	Capitate	M	narrowest point in midline of palmar surface
CM8	Carpals	Capitate	M	narrowest point in midline of dorsal surface
CM10	Carpals	Capitate	M	narrowest point in midline of lateral surface
CM11	Carpals	Capitate	M	width hamate facet at head
CM12	Carpals	Capitate	M	width hamate facet in midline

CM13	Carpals	Capitate	M	width hamate facet at MC3 border
CM14	Carpals	Capitate	M	proximo distal length hamate facet
CM15	Carpals	Capitate	M	proximo-distal length palmar aspect MC2 trapezoid facet
CM16	Carpals	Capitate	M	proximo-distal length dorsal aspect trapezoid facet
CM18	Carpals	Capitate	M	width dorsal aspect trapezoid facet
CM19	Carpals	Capitate	M	width palmar aspect trapezoid facet
CM20	Carpals	Capitate	M	length capitate head
CM21	Carpals	Capitate	M	width capitate head
CM22	Carpals	Capitate	M	proximo-distal height of capitate
HS3	Carpals	Hamate	M	medio-lateral length along curvature of dorsal border MC facet
HS4	Carpals	Hamate	M	dorso-palmar length along curvature of MC facet
HM1	Carpals	Hamate	M	proximo-distal height hamate with hamulus
HM2	Carpals	Hamate	M	proximo-distal height hamate without hamulus
HM3	Carpals	Hamate	M	medio-lateral width of hamulus at midpoint
HM4	Carpals	Hamate	M	palmo-dorsal width hamulus at midpoint
HM5	Carpals	Hamate	M	width of dorsal border of MC facet
HM6	Carpals	Hamate	M	medio-lateral width of medial aspect MC facet
HM7	Carpals	Hamate	M	medio-lateral width lateral aspect of MC facet
HM8	Carpals	Hamate	M	dorso-palmar breadth medial border MC facet
HM9	Carpals	Hamate	M	dorso-palmar breadth MC facet in midline
HM10	Carpals	Hamate	M	dorso-palmar breadth MC facet at lateral border
HM11	Carpals	Hamate	M	width capitate/MC3 facet
HM12	Carpals	Hamate	M	width capitate facet in midline
HM13	Carpals	Hamate	M	proximo-distal length distal arm of capitate/MC3 facet
HM14	Carpals	Hamate	M	proximo-distal length proximal segment of capitate facet
HM15	Carpals	Hamate	M	medio-lateral breadth hamate head
HM16	Carpals	Hamate	M	palmo-dorsal breadth hamate head
HM17	Carpals	Hamate	M	proximo-distal height of triquetral/scaphoid facet
HM18	Carpals	Hamate	M	width of triquetral facet in midline
HM19	Carpals	Hamate	M	medio-lateral breadth dorsal surface in midline
TQO1	Carpals	Triquetral	O	topography of pisiform facet concave
				concave (0), convex (1), flat (2)
TQO2	Carpals	Triquetral	O	topography margin of lunate and hamate facets
				flat (0), concave (1), convex (2)

TQO3	Carpals	Triquetral	O	presence of facet for ulna
				no (0) yes (1) present, divided (2)
TQO4	Carpals	Triquetral	O	shape hamate facet
				circular (0), oval (1), trapezoidal (2) triangular (3) extensive (4)
TQO5	Carpals	Triquetral	O	topography of hamate facet
				flat (0), curved (1)
TQO6	Carpals	Triquetral	O	orientation of main axis of pisiform facet
				proximo-distal (0), medio-lateral (1)
TQO7	Carpals	Triquetral	O	accessory facet on palmar aspect between facets for hamate and pisiform
				absent (0), present (1) tubercle (2)
TQO8	Carpals	Triquetral	O	topography of ulnar facet
				absent (0) convex (1) concave (2)
TQM1	Carpals	Triquetral	M	width of pisiform facet
TQM2	Carpals	Triquetral	M	breadth of pisiform facet
TQM3	Carpals	Triquetral	M	dorso palmar width proximal border of hamate facet
TQM4	Carpals	Triquetral	M	dorso-palmar width distal border of hamate facet
TQM5	Carpals	Triquetral	M	medio-lateral length hamate facet at palmar border
TQM6	Carpals	Triquetral	M	medio-lateral length hamate facet at dorsal border
TQM7	Carpals	Triquetral	M	width lunate facet in midline
TQM8	Carpals	Triquetral	M	triquetral length
TQM9	Carpals	Triquetral	M	length ulnar facet perpendicular to main axis
TQM10	Carpals	Triquetral	M	triquetral breadth
PO1	Carpals	Pisiform	O	articular surface divided or undivided
				no (0) yes (1)
PO2	Carpals	Pisiform	O	topography of ulnar facet
				concave (0), flat (1)
PO3	Carpals	Pisiform	O	triquetral facet shape
				circular (0), elongated (1) extensive (2)
PM1	Carpals	Pisiform	M	length of articular facet on triquetral surface
PM2	Carpals	Pisiform	M	length of articular facet on ulnar surface
PM3	Carpals	Pisiform	M	height of articular facet on triquetral surface
PM4	Carpals	Pisiform	M	height of articular facet on ulnar surface
PM5	Carpals	Pisiform	M	length pisiform
PM6	Carpals	Pisiform	M	width articular end through main axis
PM7	Carpals	Pisiform	M	width articular end perpendicular to main axis
PM8	Carpals	Pisiform	M	width pisiform head through main axis

PM9	Carpals	Pisiform	M	width pisiform head perpendicular to main axis
PM10	Carpals	Pisiform	M	narrowest midline width through main axis
PM11	Carpals	Pisiform	M	narrowest midline width pisiform perpendicular to main axis
SO1	Carpals	Scaphoid	O	os centrale fused or unfused
				no (0), yes (1)
SM1	Carpals	Scaphoid	M	palmo-dorsal length lunate facet
SM2	Carpals	Scaphoid	M	proximo-distal width lunate facet
SM3	Carpals	Scaphoid	M	proximo-distal length capitate facet
SM4	Carpals	Scaphoid	M	palmo-dorsal width capitate facet
SM5	Carpals	Scaphoid	M	length neck
SM6	Carpals	Scaphoid	M	width neck
SM7	Carpals	Scaphoid	M	palmo dorsal length radial facet
SM8	Carpals	Scaphoid	M	widest point radial facet
SM9	Carpals	Scaphoid	M	width where radial facet narrows
SM10	Carpals	Scaphoid	M	palmo-dorsal length trapezium/trapezoid facet
SM11	Carpals	Scaphoid	M	proximo-distal height trapezium/trapezoid facet
SM12	Carpals	Scaphoid	M	breadth from radial facet to border between capitate and lunate facet
SM15	Carpals	Scaphoid	M	proximo-distal height neck
SMS1	Carpals	Scaphoid	M	palmo-dorsal length along curvature of capitate facet
SMS2	Carpals	Scaphoid	M	medio-lateral length along curvature of capitate facet
TZDM1	Carpals	Trapezoid	M	length MC facet
TZDM2	Carpals	Trapezoid	M	medio-lateral width MC facet
TZDM3	Carpals	Trapezoid	M	medio-lateral width MC facet
TZDM4	Carpals	Trapezoid	M	palmo-dorsal length trapezium facet
TZDM5	Carpals	Trapezoid	M	proximo-distal height trapezium facet
TZDM7	Carpals	Trapezoid	M	length border between trapezium facet and scaphoid facet
TZDM8	Carpals	Trapezoid	M	length border between scaphoid facet and capitate facet
TZDM9	Carpals	Trapezoid	M	length dorsal border scaphoid facet
TZDM10	Carpals	Trapezoid	M	height capitate facet
TZDM11	Carpals	Trapezoid	M	width capitate facet
TZDM12	Carpals	Trapezoid	M	height of trapezoid
TZMO1	Carpals	Trapezium	O	morphology tubercle
				absent (0), present (1), hooked (2)
TZMO2	Carpals	Trapezium	O	presence separate facet for centrale
				absent (0), present but undivided (1) present

				(2) multiple (3)
TZMO3	Carpals	Trapezium	O	shape MC 1 facet
				circular (0), notched (1) elongated (2) L-shaped (3)
TZMO4	Carpals	Trapezium	O	topography of MC1 facet
				concave (0), convex (1)
TZMS1	Carpals	Trapezium	M	circumference MC1 facet
TZMM1	Carpals	Trapezium	M	length medial border MC1
TZMM2	Carpals	Trapezium	M	length dorsal border MC1
TZMM3	Carpals	Trapezium	M	length palmar border MC1
TZMM4	Carpals	Trapezium	M	length lateral border MC1
TZMM5	Carpals	Trapezium	M	dorso-palmar length MC2 facet
TZMM6	Carpals	Trapezium	M	proximo-distal width MC2 facet
TZMM7	Carpals	Trapezium	M	proximo-distal length trapezoid facet
TZMM8	Carpals	Trapezium	M	with trapezoid facet at midpoint
TZMM9	Carpals	Trapezium	M	width trapezoid facet at border with scaphoid facet
TZMM10	Carpals	Trapezium	M	length scaphoid facet
TZMM11	Carpals	Trapezium	M	width scaphoid facet at midpoint
TZMM15	Carpals	Trapezium	M	length between MC1 facet and scaphoid centrale facet
TZMM17	Carpals	Trapezium	M	length tubercle
TZMM19	Carpals	Trapezium	M	width tubercle
LO1	Carpals	Lunate	O	presence clearly divided accessory facet on palmar surface
				absent (0), reduced (1), present
LS5	Carpals	Lunate	M	length along curvature of capitate/hamate facet along border with scaphoid facet
LS6	Carpals	Lunate	M	length along curvature of capitate/hamate facet along border with triquetral facet
LS9	Carpals	Lunate	M	medio-lateral length along curvature of radial facet
LS10	Carpals	Lunate	M	palmo-dorsal length along curvature of radial facet
LM1	Carpals	Lunate	M	palmo-dorsal width capitate/hamate facet at margin of triquetral facet
LM2	Carpals	Lunate	M	palmo-dorsal width capitate/hamate facet at margin of scaphoid facet
LM3	Carpals	Lunate	M	medio-lateral width capitate/hamate facet at dorsal border
LM4	Carpals	Lunate	M	medio-lateral width capitate/hamate facet at palmar border

LM5	Carpals	Lunate	M	medio-lateral length triquetral facet at midpoint
LM6	Carpals	Lunate	M	palmo-dorsal width triquetral facet at midpoint
LM7	Carpals	Lunate	M	width border radial facet
LM8	Carpals	Lunate	M	width lateral border triquetral facet
LM9	Carpals	Lunate	M	width palmar border radial facet
LM10	Carpals	Lunate	M	height dorsal border radial facet
LM12	Carpals	Lunate	M	lunate medio-lateral width at palmar aspect
LM13	Carpals	Lunate	M	lunate medio-lateral width at dorsal aspect
LM14	Carpals	Lunate	M	lunate medio-lateral width at midpoint
LM15	Carpals	Lunate	M	palmo dorsal width proximal accessory facet on palmar surface
LM16	Carpals	Lunate	M	proximo distal width proximal accessory facet on palmar surface
MT1M1	Metatarsals	MT1	M	medio-lateral width proximal facet
MT1M2	Metatarsals	MT1	M	planto-dorsal width proximal facet
MT1M3	Metatarsals	MT1	M	medio-lateral width plantar border distal facet
MT1M4	Metatarsals	MT1	M	medio-lateral width dorsal border distal facet
MT1M5	Metatarsals	MT1	M	planto-dorsal width lateral border distal facet
MT1M6	Metatarsals	MT1	M	planto-dorsal width medial border distal facet
MT1M7	Metatarsals	MT1	M	planto-dorsal width midline distal facet
MT1M8	Metatarsals	MT1	M	proximo-distal height of head at medial edge
MT1M9	Metatarsals	MT1	M	proximo-distal height of head at lateral edge
MT1M10	Metatarsals	MT1	M	proximo-distal height of head at midpoint
MT1M11	Metatarsals	MT1	M	proximo-distal length
MT1M12	Metatarsals	MT1	M	medio-lateral width shaft at midpoint
MT1M13	Metatarsals	MT1	M	planto-dorsal width shaft at midpoint
MT1M14	Metatarsals	MT1	M	chord length on plantar surface from proximal border of distal facet to proximal termination of shaft
MT1S1	Metatarsals	MT1	M	circumference proximal articular facet
MT1S2	Metatarsals	MT1	M	curvature along length of plantar surface
MT1S3	Metatarsals	MT1	M	length along curvature of head
MT2O1	Metatarsals	MT2	O	plantar segment of MT3 facet articular
				yes (0), no (1)
MT2O2	Metatarsals	MT2	M	height cuneiform facet
MT2M1	Metatarsals	MT2	M	medio-lateral width dorsal border proximal facet
MT2M2	Metatarsals	MT2	M	medio-lateral width plantar border proximal facet
MT2M3	Metatarsals	MT2	M	medio-lateral width midline proximal facet
MT2M4	Metatarsals	MT2	M	planto-dorsal width dorsal aspect proximal

				facet
MT2M5	Metatarsals	MT2	M	planto-dorsal width plantar aspect proximal facet
MT2M6	Metatarsals	MT2	M	planto-dorsal height medial border proximal facet
MT2M7	Metatarsals	MT2	M	planto-dorsal height midline proximal facet
MT2M8	Metatarsals	MT2	M	planto-dorsal height lateral border proximal facet
MT2M11	Metatarsals	MT2	M	planto-dorsal width MT 3 facet
MT2M12	Metatarsals	MT2	M	proximo-distal height MT3 facet
MT2M13	Metatarsals	MT2	M	planto dorsal width dorsal segment lateral cuneiform facet
MT2M14	Metatarsals	MT2	M	proximo distal height dorsal segment lateral cuneiform facet
MT2M15	Metatarsals	MT2	M	width plantar segment lateral cuneiform facet
MT2M16	Metatarsals	MT2	M	height plantar segment lateral cuneiform facet
MT2M17	Metatarsals	MT2	M	medio-lateral width plantar border distal facet
MT2M18	Metatarsals	MT2	M	medio-lateral width dorsal border distal facet
MT2M19	Metatarsals	MT2	M	planto-dorsal width lateral border distal facet
MT2M20	Metatarsals	MT2	M	planto-dorsal width medial border distal facet
MT2M21	Metatarsals	MT2	M	planto-dorsal width midline distal facet at head
MT2M22	Metatarsals	MT2	M	planto-dorsal width midline distal facet at keel
MT2M23	Metatarsals	MT2	M	proximo-distal height of head at medial edge
MT2M24	Metatarsals	MT2	M	proximo-distal height of head at lateral edge
MT2M25	Metatarsals	MT2	M	proximo-distal height of head at midpoint
MT2M26	Metatarsals	MT2	M	proximo-distal length
MT2M27	Metatarsals	MT2	M	medio-lateral width shaft at midpoint
MT2M28	Metatarsals	MT2	M	planto-dorsal width shaft at midpoint
MT2M29	Metatarsals	MT2	M	chord length on plantar surface from proximal border of distal facet to proximal termination of shaft
MT2M30	Metatarsals	MT2	M	proximo-distal height facet on proximo-dorsal surface
MT2M31	Metatarsals	MT2	M	dorso-plantar height facet for m1
MT2S6	Metatarsals	MT2	M	length along curvature of plantar surface
MT2S7	Metatarsals	MT2	M	length along curvature of distal articular facet in midline
MT2S8	Metatarsals	MT2	M	length along curvature dorsal border proximal facet
MT2S12	Metatarsals	MT2	M	dorso-plantar length along curvature midline proximal facet
MT3O1	Metatarsals	MT3	O	plantar segment of MT4 facet articular or not
				yes (0), no (1)

MT3M12	Metatarsals	MT3	M	planto-dorsal width plantar aspect MT 4 facet or tubercle
MT3M13	Metatarsals	MT3	M	planto-dorsal width dorsal aspect MT 4 facet
MT3M14	Metatarsals	MT3	M	proximo-distal height plantar aspect MT 4 facet
MT3M15	Metatarsals	MT3	M	proximo-distal height dorsal aspect MT 4 facet
MT3M24	Metatarsals	MT3	M	proximo-distal length
MT3M25	Metatarsals	MT3	M	medio-lateral width shaft at midpoint
MT3M26	Metatarsals	MT3	M	planto-dorsal width shaft at midpoint
MT3M1	Metatarsals	MT3	M	medio-lateral width dorsal border proximal facet
MT3M2	Metatarsals	MT3	M	medio-lateral width plantar border proximal facet
MT3M3	Metatarsals	MT3	M	medio-lateral width midline proximal facet
MT3M4	Metatarsals	MT3	M	planto-dorsal width dorsal aspect proximal facet
MT3M5	Metatarsals	MT3	M	planto-dorsal width plantar aspect proximal facet
MT3M6	Metatarsals	MT3	M	medio-lateral width dorsal aspect of proximal articular facet
MT3M7	Metatarsals	MT3	M	medio-lateral width plantar aspect of proximal articular facet
MT3M8	Metatarsals	MT3	M	planto-dorsal height midline proximal facet
MT3S2	Metatarsals	MT3	M	length along curvature dorsal border proximal facet
MT3S3	Metatarsals	MT3	M	dorso-plantar length along curvature midline proximal facet
MT4O1	Metatarsals	MT4	O	facet for MT5 divided in midline or not
				Divided (0) continuous (1)
MT4M9	Metatarsals	MT4	M	planto-dorsal width MT 5 facet
MT4M10	Metatarsals	MT4	M	proximo-distal width plantar aspect MT 5 facet
MT4M11	Metatarsals	MT4	M	proximo-distal width dorsal aspect MT 5 facet
MT4M12	Metatarsals	MT4	M	planto-dorsal height dorsal aspect MT 5 facet
MT4M13	Metatarsals	MT4	M	planto-dorsal height plantar aspect MT 5 facet
MT4M22	Metatarsals	MT4	M	proximo-distal length
MT4M23	Metatarsals	MT4	M	medio-lateral width shaft at midpoint
MT4M24	Metatarsals	MT4	M	planto-dorsal width shaft at midpoint
MT4M25	Metatarsals	MT4	M	medio-lateral width dorsal border proximal facet
MT4M26	Metatarsals	MT4	M	medio-lateral width plantar border proximal facet
MT4M27	Metatarsals	MT4	M	planto-dorsal width medial border proximal facet
MT4M28	Metatarsals	MT4	M	planto-dorsal width lateral border proximal

				facet
MT4M29	Metatarsals	MT4	M	planto dorsal width in midline of proximal facet
MT4S1	Metatarsals	MT4	M	planto dorsal length along curvature in midline of proximal facet
MT4S2	Metatarsals	MT4	M	medio-lateral length along curvature of dorsal border of proximal facet
MT5O1	Metatarsals	MT5	O	facet for MT4 divided or continuous
				Divided (0) continuous (1)
MT5O2	Metatarsals	MT5	O	orientation of main axis of MT4 facet
				Medio-lateral (0), proximo-distal (1)
MT5O3	Metatarsals	MT5	O	MT4 facet divided from cuboid facet or continuous
				Divided (0) continuous (1)
MT5M8	Metatarsals	MT5	M	proximo-distal width tubercle
MT5M9	Metatarsals	MT5	M	planto-dorsal height tubercle
MT5M18	Metatarsals	MT5	M	proximo-distal length at medial extent
MT5M19	Metatarsals	MT5	M	proximo-distal length at lateral extent
MT5M20	Metatarsals	MT5	M	medio-lateral width shaft at midpoint
MT5M21	Metatarsals	MT5	M	planto-dorsal width shaft at midpoint
MT5M22	Metatarsals	MT5	M	medio-lateral width dorsal border proximal facet
MT5M23	Metatarsals	MT5	M	medio-lateral width plantar border proximal facet
MT5M24	Metatarsals	MT5	M	planto-dorsal width medial border proximal facet
MT5M25	Metatarsals	MT5	M	planto-dorsal width lateral border proximal facet
MT5M26	Metatarsals	MT5	M	width proximal facet
MT5s1	Metatarsals	MT5	M	length proximal facet
MT5S2	Metatarsals	MT5	M	planto-dorsal length along curvature of proximal facet
ccO1	Tarsals	Calcaneus	O	middle/anterior facet for talus continuous or divided
				continuous (0) divided (1)
ccO2	Tarsals	Calcaneus	O	presence of laterally facing flange of posterior talus facet
				absent (0) reduced (1) present (2) prominent (3)
ccM1	Tarsals	Calcaneus	M	proximo-distal length posterior Tali facet through midpoint
ccM2	Tarsals	Calcaneus	M	proximo-distal length posterior tali facet at medial border
ccM3	Tarsals	Calcaneus	M	proximo-distal length posterior tali facet at lateral border

ccM4	Tarsals	Calcaneus	M	medio-lateral width through posterior Tali facet at midpoint
ccM5	Tarsals	Calcaneus	M	medio-lateral width posterior border posterior Tali facet
ccM6	Tarsals	Calcaneus	M	medio-lateral width anterior border posterior Tali facet
ccM7	Tarsals	Calcaneus	M	length middle/anterior Tali facet
ccM8	Tarsals	Calcaneus	M	width middle Tali facet at midpoint
ccM9	Tarsals	Calcaneus	M	width anterior Tali facet at border with cuboid facet
ccM10	Tarsals	Calcaneus	M	medio-lateral width from lateral border posterior Tali facet to tip of sustentaculum
ccM15	Tarsals	Calcaneus	M	planto-dorsal height tuberosity
ccM16	Tarsals	Calcaneus	M	width tuberosity
ccM17	Tarsals	Calcaneus	M	planto-dorsal height of neck
ccM18	Tarsals	Calcaneus	M	width at narrowest point of neck at midpoint
ccM19	Tarsals	Calcaneus	M	medio-lateral width neck at trochlear process
ccM20	Tarsals	Calcaneus	M	proximo-distal length trochlear process
ccM21	Tarsals	Calcaneus	M	planto-dorsal height trochlear process
ccM22	Tarsals	Calcaneus	M	planto-dorsal height from highest point of posterior Tali facet to plantar surface
ccM23	Tarsals	Calcaneus	M	planto-dorsal height from distal posterior Tali facet to plantar surface
ccM24	Tarsals	Calcaneus	M	proximo-distal height sustentaculum
ccM25	Tarsals	Calcaneus	M	planto-dorsal height sustentaculum
ccM26	Tarsals	Calcaneus	M	length calcaneus from dorsal border cuboid facet to tuberosity
ccM27	Tarsals	Calcaneus	M	length calcaneus from most depressed point of cuboid facet to tuberosity
ccM28	Tarsals	Calcaneus	M	length from proximal border of posterior Tali facet to tuberosity
ccS8	Tarsals	Calcaneus	M	medio-lateral length along curvature posterior Tali facet
ccS11	Tarsals	Calcaneus	M	antero-posterior length along curvature posterior Tali facet
AO1	Tarsals	Talus	O	presence of attachment foramen on head of Talus
				absent (0) present (1)
AM1	Tarsals	Talus	M	medio-lateral width posterior border trochlea
AM2	Tarsals	Talus	M	medio-lateral width anterior border trochlea
AM3	Tarsals	Talus	M	antero-posterior length medial border trochlea
AM4	Tarsals	Talus	M	antero-posterior length lateral border trochlea

AM5	Tarsals	Talus	M	antero-posterior length trochlea
AM6	Tarsals	Talus	M	medio-lateral breadth at widest point
AM7	Tarsals	Talus	M	antero-posterior length facet for lateral malleolus on side of trochlea
AM8	Tarsals	Talus	M	antero-posterior length facet for lateral malleolus on extending flange
AM9	Tarsals	Talus	M	dorso-plantar height lateral malleolus facet at anterior aspect
AM10	Tarsals	Talus	M	dorso-palmar height lateral malleolus facet on side of trochlea at level of flange
AM11	Tarsals	Talus	M	length through main axis of posterior calcaneal facet
AM12	Tarsals	Talus	M	medio-lateral width posterior border posterior calcaneal facet
AM13	Tarsals	Talus	M	medio-lateral width post calcaneal facet
AM14	Tarsals	Talus	M	medio-lateral width at anterior border posterior calcaneal facet
AM15	Tarsals	Talus	M	medio-lateral length through main axis of Talus head
AM16	Tarsals	Talus	M	planto-dorsal width Talus head
AM17	Tarsals	Talus	M	length calcaneal facet on neck at lateral margin
AM18	Tarsals	Talus	M	length calcaneal facet on neck at midline
AM20	Tarsals	Talus	M	medio-lateral width calcaneal facet on neck at posterior extent
AM21	Tarsals	Talus	M	medio-lateral width at neck
AM22	Tarsals	Talus	M	planto-dorsal height of neck
AM23	Tarsals	Talus	M	length from head to medial tubercle
AM24	Tarsals	Talus	M	width across posterior tubercles
AM25	Tarsals	Talus	M	antero-posterior length facet for medial malleolus
AM26	Tarsals	Talus	M	planto-dorsal height facet for medial malleolus at anterior border
AM27	Tarsals	Talus	M	planto-dorsal height facet for medial malleolus at posterior border
AM28	Tarsals	Talus	M	planto-dorsal height through facet for medial malleolus at level of flange
AM29	Tarsals	Talus	M	distance from posterior most point of lateral malleolus facet to most projecting point of posterior calcaneal facet
AM30	Tarsals	Talus	M	dorsal projection of medial tubercle below trochlea
AM31	Tarsals	Talus	M	dorsal projection of tubercles below trochlea
AM32	Tarsals	Talus	M	dorsal projection of lateral tubercle below trochlea

AS5	Tarsals	Talus	M	length along curvature medial border of trochlea
AS8	Tarsals	Talus	M	length along curvature lateral border of trochlea
AS10	Tarsals	Talus	M	length along curvature trochlea in midline
CBO1	Tarsals	Cuboid	O	number of distinct facets on medial surface
				,
CBM7	Tarsals	Cuboid	M	medio-lateral width calcaneal facet in midline
CBM8	Tarsals	Cuboid	M	medio-lateral width calcaneal facet at dorsal border
CBM9	Tarsals	Cuboid	M	medio-lateral width calcaneal facet at plantar border
CBM10	Tarsals	Cuboid	M	dorso-plantar width medial border calcaneal facet
CBM11	Tarsals	Cuboid	M	dorso-plantar width midline calcaneal facet
CBM12	Tarsals	Cuboid	M	dorso-plantar width lateral border calcaneal facet
CBM13	Tarsals	Cuboid	M	proximo-distal length at medial border
CBM14	Tarsals	Cuboid	M	proximo-distal length at lateral border
CBM15	Tarsals	Cuboid	M	in plantar view proximo-distal length at lateral border
CBM16	Tarsals	Cuboid	M	in plantar view proximo-distal length at medial border
CBM17	Tarsals	Cuboid	M	proximo-distal height from dorsal border in midline
CBM18	Tarsals	Cuboid	M	proximo-distal height from plantar border in midline
CBM19	Tarsals	Cuboid	M	planto-dorsal width of neck at medial edge
CBM20	Tarsals	Cuboid	M	planto-dorsal width of neck at lateral edge
CBM21	Tarsals	Cuboid	M	medio-lateral width neck
CBM22	Tarsals	Cuboid	M	medio-lateral width at ridge proximal to neck
CBM23	Tarsals	Cuboid	M	planto-dorsal height ridge proximal to neck at medial border
CBM24	Tarsals	Cuboid	M	proximo-distal height navicular facet
CBS3	Tarsals	Cuboid	M	length along curvature of plantar border calcaneal facet
CBS6	Tarsals	Cuboid	M	planto-dorsal length along midpoint of calcaneal facet
NO1	Tarsals	Navicular	O	cuboid facet contacts Tali facet or lateral cuneiform
				neither (0) tali (1) cuneiform (2) both (3)
NO2	Tarsals	Navicular	O	presence of dorsal extension of tubercle
				no (0), yes (1)
NM1	Tarsals	Navicular	M	medio-lateral length through midpoint

NM2	Tarsals	Navicular	M	dorso-plantar height at lateral border
NM3	Tarsals	Navicular	M	dorso-plantar height of tuberosity
NM5	Tarsals	Navicular	M	proximo-distal height at middle of middle cuneiform facet
NM6	Tarsals	Navicular	M	proximo-distal height at middle of lateral cuneiform facet
NM7	Tarsals	Navicular	M	proximo-distal height at tubercle
NM8	Tarsals	Navicular	M	proximo-distal height at middle of medial cuneiform facet
NM13	Tarsals	Navicular	M	dorso-plantar width cuboid facet
NM14	Tarsals	Navicular	M	proximo distal width cuboid facet
NM15	Tarsals	Navicular	M	dorso plantar height at medial cuneiform facet
NM16	Tarsals	Navicular	M	dorso plantar height at middle cuneiform facet
NM17	Tarsals	Navicular	M	dorso plantar height at lateral cuneiform facet
NM18	Tarsals	Navicular	M	medio-lateral length astragular facet
NM19	Tarsals	Navicular	M	dorso plantar height astragular facet at medial border
NM20	Tarsals	Navicular	M	dorso plantar height astragular facet at lateral border
NM21	Tarsals	Navicular	M	dorso plantar height astragular facet in midline
NS2	Tarsals	Navicular	M	medio-lateral length along curvature of Tali facet
MCO1	Tarsals	Med. Cuneiform	O	number of facets for intermediate cuneiform
				none (0) only proximal (1) proximal and disto-medial (2) proximal and disto-lateral (3) all present (4)
MCO2	Tarsals	Med. Cuneiform	O	proximal and disto-lateral cuneiform facets divided or continuous
				divided (0) or continuous (1)
MCO3	Tarsals	Med. Cuneiform	O	presence of projection of medial cuneiform facet at lateral extent
				absent (0), present (1)
MCM1	Tarsals	Med. Cuneiform	M	length MT1 facet through main axis
MCM2	Tarsals	Med. Cuneiform	M	width perpendicular to main axis MT1 facet at dorsal border
MCM3	Tarsals	Med. Cuneiform	M	width MT1 facet perpendicular to main axis at midpoint
MCM4	Tarsals	Med. Cuneiform	M	width MT1 facet perpendicular to main axis at plantar border
MCM5	Tarsals	Med. Cuneiform	M	proximo distal length MT2 facet
MCM6	Tarsals	Med.	M	dorso plantar length MT2 facet

		Cuneiform		
MCM7	Tarsals	Med. Cuneiform	M	proximo distal length proximal segment of intermediate cuneiform facet
MCM8	Tarsals	Med. Cuneiform	M	dorso plantar length proximal segment of intermediate cuneiform facet
MCM9	Tarsals	Med. Cuneiform	M	proximo distal length disto-medial segment of intermediate cuneiform facet
MCM10	Tarsals	Med. Cuneiform	M	dorso plantar length disto-medial segment of intermediate cuneiform facet
MCM11	Tarsals	Med. Cuneiform	M	proximo distal length disto-later segment of intermediate cuneiform facet
MCM12	Tarsals	Med. Cuneiform	M	dorso plantar length disto-lateral segment of intermediate cuneiform facet
MCM13	Tarsals	Med. Cuneiform	M	dorso plantar length navicular facet
MCM14	Tarsals	Med. Cuneiform	M	medio-lateral length navicular facet through midpoint
MCM15	Tarsals	Med. Cuneiform	M	proximo distal length plantar border
MCM16	Tarsals	Med. Cuneiform	M	proximo-distal length lateral border
MCM17	Tarsals	Med. Cuneiform	M	dorso-plantar height
MCM18	Tarsals	Med. Cuneiform	M	proximo-distal height bone at lateral edge
MCS2	Tarsals	Med. Cuneiform	M	antero-posterior length along curvature of medial aspect MT1 facet
MCS3	Tarsals	Med. Cuneiform	M	antero-posterior length along curvature of midline MT1 facet
MCS4	Tarsals	Med. Cuneiform	M	antero-posterior length along curvature of lateral aspect MT1 facet
MCS6	Tarsals	Med. Cuneiform	M	medio-lateral width along curvature of midline MT1 facet
MCS8	Tarsals	Med. Cuneiform	M	length along curvature margin of navicular and intermediate cuneiform facet
ICM5	Tarsals	Int. cuneiform	M	medio-lateral length dorsal border of navicular facet
ICM6	Tarsals	Int. cuneiform	M	medio-lateral length plantar border of navicular facet
ICM7	Tarsals	Int. cuneiform	M	dorso-plantar height navicular facet through midline
ICM8	Tarsals	Int. cuneiform	M	medio-lateral length dorsal border of MT2 facet
ICM9	Tarsals	Int. cuneiform	M	medio-lateral length midpoint of MT2 facet
ICM10	Tarsals	Int. cuneiform	M	medio-lateral length plantar border of MT2

				facet
ICM11	Tarsals	Int. cuneiform	M	dorso plantar length MT2 facet
ICM12	Tarsals	Int. cuneiform	M	proximo-distal length dorsal border in midline
ICM13	Tarsals	Int. cuneiform	M	proximo-distal length plantar edge
ICS6	Tarsals	Int. cuneiform	M	dorso-plantar length along curvature through midline of navicular facet
LCO1	Tarsals	Lat. cuneiform	O	number of distinct facets on lateral surface.
				,
LC02	Tarsals	Lat. cuneiform	O	navicular facet angles medially or not
				no (0), yes (1)
LCM1	Tarsals	Lat. cuneiform	M	medio-lateral length dorsal border of navicular facet
LCM2	Tarsals	Lat. cuneiform	M	medio-lateral length plantar border of navicular facet
LCM3	Tarsals	Lat. cuneiform	M	dorso plantar length navicular facet at lateral border
LCM4	Tarsals	Lat. cuneiform	M	dorso plantar length navicular facet at medial border
LCM5	Tarsals	Lat. cuneiform	M	dorso-plantar length navicular facet in midline
LCM6	Tarsals	Lat. cuneiform	M	length non-articular area on lateral surface
LCM7	Tarsals	Lat. cuneiform	M	medio-lateral width plantar tubercle
LCM8	Tarsals	Lat. cuneiform	M	proximo distal length dorsal surface at medial edge
LCM14	Tarsals	Lat. cuneiform	M	proximo distal length dorsal surface at lateral edge
LCM15	Tarsals	Lat. cuneiform	M	dorso-plantar length MT2 facet in midline on medial surface
LCM16	Tarsals	Lat. cuneiform	M	dorso plantar length intermediate cuneiform facet
LCM17	Tarsals	Lat. cuneiform	M	proximo distal length intermediate cuneiform facet
LCM28	Tarsals	Lat. cuneiform	M	proximo distal length plantar tubercle
LCS3	Tarsals	Lat. cuneiform	M	length along curvature dorsal border of navicular facet
LCS5	Tarsals	Lat. cuneiform	M	dorso-plantar length along curvature in midline of navicular facet
LCR1	Tarsals	Lat. cuneiform	M	angle of navicular facet

Appendix B: Chapter 3 PCA loadings

	Separate Sexes		
	PC1	PC2	PC3
o19	-0.1590	-0.0974	-0.1626
UO8	-0.0881	-0.0516	-0.0045
o28	-0.0858	-0.0910	0.0257
o17	-0.0740	-0.0085	0.1293
huo4	-0.0721	-0.0125	0.0215
m2	-0.0718	-0.0473	0.0222
MM23	-0.0718	-0.0473	0.0222
CCO1	-0.0718	-0.0473	0.0222
RO4	-0.0650	-0.0602	0.0086
UO7	-0.0632	-0.0989	0.0155
o29	-0.0607	-0.0946	0.0555
MM21	-0.0603	-0.0380	0.0734
MM29	-0.0603	-0.0380	0.0734
TQO3	-0.0589	-0.0576	0.0206
o30	-0.0579	-0.1182	-0.0022
RO1	-0.0564	-0.0555	0.0407
PO3	-0.0554	-0.0577	0.0229
MT3M25	-0.0545	0.0351	0.0085
MT3M1	-0.0545	0.0351	0.0085
MT3M6	-0.0545	0.0351	0.0085
ICM7	-0.0545	0.0351	0.0085
o25	-0.0538	-0.0584	-0.0025
MM22	-0.0523	-0.0380	0.0845
o35	-0.0503	0.0211	-0.0035
o51	-0.0489	0.0890	0.1089
CCM7	-0.0489	0.0324	0.0418
MT3S3	-0.0465	0.0351	0.0196
o54	-0.0454	0.0068	0.0019
huo8	-0.0432	0.0017	-0.0337
m30	-0.0426	-0.0272	0.0711
huo9	-0.0426	-0.0670	0.0246
UM8	-0.0416	-0.0287	0.0297

	Separate Sexes		
	PC1	PC2	PC3
MT2M13	-0.0002	-0.0024	0.0023
PVO15	-0.0002	0.0175	-0.0011
hum56	-0.0001	-0.0002	0.0092
PM7	-0.0001	0.0011	0.0066
TZDM3	0.0000	-0.0003	0.0078
CM21	0.0000	0.0020	0.0046
o39	0.0000	0.0000	0.0000
o42	0.0000	0.0000	0.0000
huo1	0.0000	0.0000	0.0000
huo2	0.0000	0.0000	0.0000
PVM2	0.0000	0.0000	0.0000
LO1	0.0000	0.0000	0.0000
MC4O2	0.0000	0.0000	0.0000
CO4	0.0000	0.0000	0.0000
TZMO3	0.0000	0.0000	0.0000
MT4O1	0.0000	0.0000	0.0000
MT5O1	0.0000	0.0000	0.0000
AO1	0.0000	0.0000	0.0000
MCO1	0.0000	0.0000	0.0000
HM3	0.0000	0.0006	0.0037
HM19	0.0000	-0.0014	0.0077
CCM24	0.0000	0.0029	-0.0033
LCM16	0.0001	-0.0128	0.0088
PM10	0.0001	0.0016	0.0093
MT2M18	0.0001	-0.0058	0.0016
CCS8	0.0001	-0.0008	0.0043
MC3M33	0.0001	-0.0026	0.0044
MT4M24	0.0001	-0.0036	0.0007
CM18	0.0002	-0.0001	-0.0007
MC4M17	0.0002	-0.0011	0.0003
HM13	0.0002	0.0030	0.0054
NM18	0.0003	-0.0016	0.0022
LCM5	0.0003	-0.0060	0.0025

	Separate Sexes		
	PC1	PC2	PC3
MC1M10	0.0096	-0.0048	0.0042
MT2M14	0.0096	0.0108	-0.0135
CCM15	0.0097	-0.0021	-0.0075
HM14	0.0097	-0.0012	-0.0006
CM1	0.0098	0.0000	-0.0018
hum16	0.0098	0.0034	0.0168
hum37	0.0098	0.0013	0.0055
RM19	0.0100	0.0105	0.0003
RM3	0.0101	-0.0025	0.0053
hum33	0.0102	-0.0002	0.0081
o55	0.0102	0.0275	0.0152
RM15	0.0102	-0.0063	0.0127
UM11	0.0103	0.0021	0.0058
AS1	0.0105	0.0355	0.0487
SM3	0.0106	-0.0011	0.0071
MC2M11	0.0107	-0.0053	0.0037
MT2M22	0.0107	-0.0032	-0.0003
RS1	0.0107	-0.0099	0.0165
MT2M20	0.0108	-0.0032	-0.0030
MT2M19	0.0108	-0.0008	-0.0033
MC3O2	0.0110	0.0292	-0.0744
MC3M17	0.0110	0.0478	-0.0194
UM26	0.0110	0.0077	0.0125
HS4	0.0113	-0.0062	0.0079
PVO6	0.0113	-0.0428	0.0305
MCS3	0.0116	0.0438	0.0542
UM34	0.0118	-0.0018	0.0038
RM20	0.0118	-0.0018	0.0091
MM19	0.0119	-0.0624	0.0626
RM17	0.0120	0.0031	0.0124
PVO14	0.0122	0.0076	-0.0043
SM5	0.0122	-0.0001	0.0069
AM24	0.0123	0.0090	-0.0099

	Separate Sexes				Separate Sexes				Separate Sexes		
	PC1	PC2	PC3		PC1	PC2	PC3		PC1	PC2	PC3
m17	-0.0407	-0.0294	0.0861	hum44	0.0003	-0.0019	0.0139	RM22	0.0123	0.0093	-0.0039
m18	-0.0407	-0.0294	0.0861	MT3M14	0.0004	-0.0062	0.0074	hum31	0.0124	0.0056	0.0067
UO14	-0.0406	-0.0322	0.1631	MCM10	0.0004	-0.0025	-0.0015	MC1M2	0.0124	-0.0020	0.0046
UM10	-0.0401	-0.0273	0.0179	hum36	0.0004	-0.0064	0.0061	RM12	0.0124	-0.0028	0.0017
PVS11	-0.0393	-0.0176	0.0790	m42	0.0005	-0.0010	0.0033	RM27	0.0126	0.0055	0.0094
MM14	-0.0387	-0.0151	0.0489	AM14	0.0006	0.0042	0.0048	MT1M14	0.0126	0.0007	-0.0684
MO1	-0.0382	-0.0655	-0.0624	PVM5	0.0006	0.0033	0.0221	MCO3	0.0127	0.0553	-0.0062
o2	-0.0372	-0.0018	0.0465	CM2	0.0007	-0.0018	0.0046	UM41	0.0127	0.0195	0.0078
MT3M5	-0.0370	0.0445	0.0308	MT3M12	0.0007	-0.0022	0.0036	RM25	0.0127	0.0039	0.0019
o21	-0.0364	0.0057	-0.0373	CBM21	0.0007	0.0012	0.0000	SM10	0.0128	0.0092	0.0054
MT3M24	-0.0355	0.0555	-0.0259	AM26	0.0007	0.0014	0.0037	NM5	0.0129	0.0464	0.0453
UM7	-0.0352	-0.0234	0.0228	CS4	0.0007	-0.0059	0.0055	hum7	0.0130	0.0099	-0.0065
MT2M5	-0.0349	0.0445	0.0709	hum41	0.0008	-0.0014	0.0128	RM23	0.0131	-0.0008	0.0070
o44	-0.0348	-0.0146	-0.0350	MCM8	0.0008	-0.0044	-0.0058	MT2M23	0.0131	-0.0036	-0.0008
o46	-0.0346	0.1097	0.1941	LCM4	0.0008	-0.0080	0.0025	RM24	0.0132	0.0065	0.0012
o15	-0.0345	-0.0610	0.0847	MT5M23	0.0009	-0.0015	0.0026	CM22	0.0137	-0.0036	0.0095
UO13	-0.0341	0.0230	0.0324	ICM8	0.0009	-0.0033	0.0030	CO1	0.0137	0.0091	-0.0629
o36	-0.0331	0.0297	0.0300	MT3M7	0.0009	-0.0012	0.0031	PVM4	0.0137	-0.0216	0.0251
MO3	-0.0330	-0.0232	-0.1080	RM18	0.0009	-0.0074	0.0216	AM32	0.0138	0.0152	0.0003
PVO2	-0.0311	-0.0447	-0.0561	NM15	0.0010	-0.0002	-0.0007	m1	0.0138	-0.0645	0.0777
AS8	-0.0307	0.0040	0.0605	MC4M21	0.0010	-0.0025	0.0013	hum25	0.0141	0.0016	0.0056
PO1	-0.0297	-0.0726	0.0169	hum35	0.0011	-0.0003	0.0262	LCM28	0.0143	0.0407	0.0177
o37	-0.0296	-0.0420	0.0129	NM21	0.0011	-0.0040	0.0102	SMS1	0.0143	-0.0757	-0.0118
UM9	-0.0293	-0.0200	0.0111	SM6	0.0011	-0.0028	0.0052	TZDM4	0.0143	-0.0757	-0.0118
MT2M6	-0.0292	0.0151	0.0037	NM7	0.0011	-0.0149	0.0019	LCO1	0.0145	0.0227	0.0152
MT2M8	-0.0292	0.0151	0.0037	AM22	0.0011	-0.0033	0.0061	hum38	0.0147	-0.0054	0.0121
MT3S2	-0.0292	0.0151	0.0037	CBS6	0.0011	-0.0009	0.0040	UM5	0.0149	0.0049	0.0076
MT4S1	-0.0292	0.0151	0.0037	MT2M31	0.0011	-0.0001	-0.0055	ICM12	0.0150	-0.0186	0.0202
m26	-0.0273	-0.0232	0.0791	SM4	0.0011	-0.0012	0.0082	hum20	0.0150	0.0000	0.0133
CCM27	-0.0272	-0.0269	0.0241	TZMM10	0.0012	-0.0003	-0.0027	hum9	0.0151	0.0050	0.0096
m32	-0.0270	-0.0581	0.0798	MT3M2	0.0012	-0.0008	0.0009	hum55	0.0151	0.0183	0.0093
m33	-0.0270	-0.0581	0.0798	SM12	0.0013	-0.0009	0.0028	UM6	0.0152	0.0039	0.0025
AM13	-0.0270	-0.0581	0.0798	NM2	0.0014	-0.0011	0.0052	o52	0.0158	-0.0561	0.0188

	Separate Sexes				Separate Sexes				Separate Sexes		
	PC1	PC2	PC3		PC1	PC2	PC3		PC1	PC2	PC3
o40	-0.0268	-0.0517	0.0577	CBM12	0.0014	-0.0011	0.0018	MC2M10	0.0160	-0.0011	0.0023
MO5	-0.0265	0.0537	0.0318	CCM9	0.0014	-0.0017	0.0050	HM1.1	0.0161	0.0377	-0.0343
MT4M22	-0.0259	0.0663	-0.0394	UM35	0.0014	-0.0109	0.0109	hus10	0.0161	-0.0117	0.0403
MT5M18	-0.0259	0.0663	-0.0394	CM6	0.0015	0.0028	0.0054	hum4	0.0162	0.0229	0.0039
MT5M19	-0.0259	0.0663	-0.0394	LM6	0.0015	0.0016	-0.0009	MCS6	0.0163	-0.0010	0.0048
CCM26	-0.0258	-0.0263	0.0323	HM9	0.0015	-0.0016	0.0078	LS6	0.0165	-0.0095	0.0049
m38	-0.0244	-0.0237	-0.0076	CCM5	0.0015	-0.0019	0.0051	hum46	0.0166	0.0133	0.0106
TQM9	-0.0240	-0.0134	0.0124	SMS2	0.0016	-0.0052	0.0084	hum1	0.0170	0.0152	0.0044
MM15	-0.0231	-0.0531	0.0808	CCM10	0.0016	0.0028	0.0041	CCS11	0.0174	0.0825	-0.0137
MM30	-0.0231	-0.0531	0.0808	UM30	0.0016	-0.0056	0.0088	UM21	0.0174	0.0084	0.0212
o57	-0.0225	0.0898	0.0044	AM21	0.0016	0.0035	0.0007	m34	0.0176	-0.0314	0.0275
PVM8	-0.0220	-0.0159	0.0296	MCM13	0.0017	0.0037	0.0007	TZMS1	0.0177	-0.0114	0.0149
PM2	-0.0215	-0.0197	0.0192	MT2M29	0.0017	0.0404	-0.0185	MT2S7	0.0178	-0.0124	0.0116
CBM8	-0.0213	0.0673	0.0352	MT2S6	0.0017	0.0404	-0.0185	CM14	0.0179	-0.0084	0.0040
TQO7	-0.0208	-0.0182	0.0370	CBM10	0.0017	0.0014	0.0057	hum47	0.0179	0.0183	0.0136
MO6	-0.0193	0.0026	0.0973	CBM24	0.0017	-0.0051	0.0096	RM28	0.0187	0.0103	0.0049
m31	-0.0191	-0.0410	0.0587	CM13	0.0017	-0.0019	0.0010	AM27.1	0.0189	0.0204	-0.0344
RO6	-0.0187	0.0262	0.0112	LM7	0.0018	0.0048	0.0097	PVO5	0.0195	0.0489	0.0229
TQM2	-0.0186	0.0434	0.0756	hum42	0.0018	-0.0012	-0.0036	MT5s1	0.0196	0.0471	0.0058
UO2	-0.0186	0.0584	0.1594	MC5M26	0.0019	-0.0017	0.0041	SM1	0.0196	0.0086	0.0127
UM39	-0.0183	-0.0162	0.0361	MT2M15	0.0020	-0.0026	0.0106	TZMM19	0.0196	0.0015	-0.0061
m9	-0.0174	-0.0825	0.0137	CBM16	0.0020	0.0330	0.0677	UO12	0.0197	0.0636	-0.0296
m36	-0.0174	-0.0825	0.0137	m7	0.0020	-0.0189	0.0140	PVO10	0.0205	0.0119	-0.0110
PVO16	-0.0174	-0.0825	0.0137	LM10	0.0020	0.0043	0.0075	hus5	0.0206	-0.0037	0.0808
o43	-0.0169	-0.0380	0.1536	MC4M19	0.0020	-0.0005	0.0017	o31	0.0208	0.0115	-0.0661
CO2	-0.0166	-0.0180	0.0464	MT2M2	0.0021	-0.0017	0.0016	UM31	0.0209	0.0111	0.0019
o11	-0.0165	-0.0440	-0.0044	AM9	0.0022	-0.0014	0.0087	hum48	0.0211	0.0167	0.0110
o50	-0.0157	0.1016	0.0729	m11	0.0022	-0.0732	0.0761	MC1S1	0.0211	-0.0181	0.0257
o34	-0.0156	-0.0089	-0.0552	m20	0.0022	-0.0732	0.0761	o41	0.0213	-0.0678	-0.0982
CCM28	-0.0154	0.0046	0.0140	m22	0.0022	-0.0732	0.0761	CCM6	0.0216	0.0228	-0.0245
m3	-0.0154	-0.0494	0.0814	m23	0.0022	-0.0732	0.0761	o1	0.0228	-0.0414	0.1508
NM6	-0.0153	0.0531	0.0836	m41	0.0022	-0.0732	0.0761	UO6	0.0234	-0.0295	-0.1147
PVM3	-0.0151	-0.0273	0.0165	MM20	0.0022	-0.0732	0.0761	HM8	0.0236	0.0488	0.0664

	Separate Sexes				Separate Sexes				Separate Sexes		
	PC1	PC2	PC3		PC1	PC2	PC3		PC1	PC2	PC3
CBO1	-0.0145	0.0076	0.0026	MM28	0.0022	-0.0732	0.0761	hum10	0.0237	0.0166	0.0146
RO3	-0.0143	0.0110	0.0624	hum51	0.0022	-0.0039	0.0028	MC2M26	0.0240	-0.0649	-0.0253
AM20	-0.0140	-0.0139	0.0116	MC5M25	0.0022	0.0026	-0.0003	MC2S2	0.0240	-0.0649	-0.0253
PVS12	-0.0137	0.0639	0.0589	UM17	0.0023	-0.0044	0.0010	o16	0.0243	-0.0537	-0.0393
MT2M12	-0.0133	-0.0842	-0.0357	MM16	0.0023	0.0168	0.0187	TZMM17	0.0246	0.0057	-0.0072
MT3M26	-0.0133	-0.0842	-0.0357	huo6	0.0023	-0.1004	-0.0231	hum15	0.0251	0.0137	0.0265
RO5	-0.0133	-0.0134	0.1116	AM18	0.0023	0.0742	-0.0015	US13	0.0257	0.0215	0.0177
MT4M9	-0.0130	-0.0072	0.0116	CM4	0.0023	0.0059	-0.0003	huo3	0.0259	0.0135	0.0173
o18	-0.0126	0.0486	0.0687	AM8	0.0025	0.0006	0.0043	MCM15	0.0266	0.0169	-0.0107
o7	-0.0121	0.0031	-0.0181	CS5	0.0025	0.0015	-0.0002	hus7	0.0270	-0.0209	0.0880
MT4M29	-0.0117	-0.0099	0.0104	NM16	0.0025	0.0002	0.0061	hus6	0.0276	-0.0187	0.0426
MT4M28	-0.0116	-0.0101	0.0094	CCM18	0.0025	0.0081	0.0066	MC5O1	0.0280	0.0778	-0.0176
MT5S2	-0.0116	-0.0146	0.0135	AM7	0.0025	-0.0077	0.0091	MM17	0.0284	-0.0231	0.0441
AS5	-0.0114	0.0652	0.0615	TZMM8	0.0027	-0.0003	0.0014	MCM1	0.0293	0.0194	-0.0008
CBM13	-0.0114	0.0652	0.0615	MT4M25	0.0027	0.0005	0.0030	PVM23	0.0309	-0.0189	-0.0097
PM4	-0.0114	-0.0134	0.0059	US12	0.0028	-0.0081	0.0241	hus8	0.0309	-0.0033	0.0243
PM6	-0.0113	-0.0102	0.0134	NM13	0.0028	0.0013	-0.0031	CBM14	0.0312	0.0180	0.0640
TQM8	-0.0111	-0.0104	0.0108	MC3M20	0.0029	-0.0032	0.0103	CBM15	0.0312	0.0180	0.0640
UO11	-0.0110	-0.0892	-0.0449	MC2M7	0.0029	-0.0035	0.0073	CBM17	0.0312	0.0180	0.0640
m16	-0.0109	0.0165	0.0349	CCM8	0.0029	0.0036	0.0023	CBM18	0.0312	0.0180	0.0640
UM1	-0.0109	-0.0169	0.0202	CM7	0.0029	-0.0002	-0.0031	PVM18	0.0315	0.0214	0.0514
CCO2	-0.0109	-0.0172	0.0155	AM3	0.0030	-0.0083	0.0070	MT2S8	0.0315	0.0206	0.0018
PM9	-0.0108	-0.0087	0.0124	RM9	0.0030	-0.0071	0.0175	UM20	0.0316	0.0159	-0.0132
ICM13	-0.0103	0.0015	0.0249	ICM10	0.0030	-0.0021	0.0034	hum54	0.0322	0.0184	0.0117
o53	-0.0102	-0.0763	-0.0555	TZDM2	0.0031	0.0000	0.0093	MT1M8	0.0323	0.0093	-0.0556
m19	-0.0101	-0.0327	0.0753	US10	0.0031	-0.0076	0.0375	MT1S2	0.0323	0.0093	-0.0556
HS3	-0.0096	-0.0104	0.0179	HM18	0.0031	-0.0041	0.0037	MC2O1	0.0327	0.0294	-0.0973
LM5	-0.0095	-0.0041	0.0144	NM20	0.0031	0.0028	-0.0032	MT2M26	0.0329	0.0584	0.0455
PM1	-0.0094	-0.0098	0.0147	MCM7	0.0032	-0.0029	0.0029	MCS4	0.0331	0.0322	0.0268
MT4M27	-0.0094	-0.0055	0.0081	MC3M19	0.0032	0.0023	-0.0001	MCS2	0.0348	0.0167	0.0326
m8	-0.0093	-0.0825	0.0249	MC4M34	0.0033	-0.0002	0.0017	m4	0.0349	-0.0437	-0.0212
m24	-0.0093	-0.0825	0.0249	ICM5	0.0033	-0.0048	0.0046	RM11	0.0353	-0.0112	0.0264
m29	-0.0093	-0.0825	0.0249	US11	0.0033	-0.0339	0.0488	o47	0.0355	-0.0540	0.0628

	Separate Sexes				Separate Sexes				Separate Sexes		
	PC1	PC2	PC3		PC1	PC2	PC3		PC1	PC2	PC3
m40	-0.0093	-0.0825	0.0249	PVM6	0.0033	0.0188	0.0059	CM14.1	0.0355	-0.0555	0.0259
MT5M24	-0.0086	-0.0045	0.0127	MCM5	0.0033	-0.0016	-0.0041	MT1M2	0.0355	-0.0555	0.0259
CCM20	-0.0083	-0.0057	0.0058	SM11	0.0034	-0.0048	0.0137	HM1	0.0359	-0.0091	0.0084
UM15	-0.0079	-0.0126	0.0184	MT5M8	0.0034	-0.0018	0.0149	MC3M32	0.0359	-0.0528	-0.0363
TQM10	-0.0074	-0.0105	0.0129	AM29	0.0034	0.0059	-0.0108	m37	0.0378	-0.0542	0.0284
o38	-0.0074	0.0299	0.0587	TZMM4	0.0034	-0.0026	0.0020	US14	0.0382	0.0060	0.0169
LCM8	-0.0071	0.0176	0.0742	TQM5	0.0034	-0.0023	0.0055	LC02	0.0385	0.0297	0.0280
LCM6	-0.0071	-0.0028	0.0011	CCM2	0.0035	-0.0036	0.0037	UO10	0.0385	-0.0164	0.0123
US9	-0.0068	-0.0229	0.0270	LM12	0.0035	-0.0119	0.0085	RO7	0.0388	0.0237	-0.0576
MT3M8	-0.0068	-0.0085	0.0074	MCM3	0.0035	-0.0061	0.0040	UM12	0.0389	-0.0459	0.0339
o48	-0.0067	0.0765	0.1079	HM15	0.0036	-0.0036	0.0031	PVM20	0.0392	0.0179	0.0751
LM9	-0.0065	0.0058	0.0159	hum39	0.0036	0.0021	0.0097	MT1M7	0.0397	0.0204	0.0450
PM11	-0.0063	-0.0042	0.0121	UM37	0.0036	-0.0004	0.0098	MT1M1.1	0.0397	0.0204	0.0450
LCM15	-0.0063	-0.0095	0.0123	MO2	0.0036	-0.0118	-0.0688	UM35.1	0.0408	0.0288	0.0505
MT4M13	-0.0062	-0.0051	0.0082	CBM11	0.0036	0.0004	0.0007	LS5	0.0408	0.0288	0.0505
UM18	-0.0061	-0.0132	0.0277	NM8	0.0037	0.0734	0.0492	AM4	0.0408	0.0288	0.0505
PVM7	-0.0060	-0.0121	-0.0179	m25	0.0037	-0.0621	0.0193	AM5	0.0408	0.0288	0.0505
CBM7	-0.0058	-0.0070	0.0059	AM10	0.0037	-0.0014	0.0075	MCM12	0.0408	0.0288	0.0505
UM40	-0.0058	0.0055	0.0215	MC3M34	0.0038	0.0011	0.0009	MCM16	0.0408	0.0288	0.0505
m12	-0.0058	-0.0731	0.0649	o5	0.0038	-0.0299	-0.0343	MC4O3	0.0413	0.0723	-0.1246
MC2M12	-0.0058	-0.0038	0.0170	TZDM10	0.0038	0.0035	0.0019	AM1	0.0425	0.0692	0.0320
ICM11	-0.0057	-0.0072	0.0046	MC4M20	0.0038	-0.0039	0.0038	TQO1	0.0428	-0.0390	0.0356
o6	-0.0057	-0.0045	-0.0261	NM1	0.0039	0.0012	-0.0046	m15	0.0434	-0.0417	0.0644
LCM2	-0.0057	0.0287	0.0175	MO8	0.0039	-0.0133	0.0259	o26	0.0434	-0.0227	-0.0837
CCM21	-0.0056	-0.0009	0.0060	CM20	0.0039	0.0066	0.0060	PVO1	0.0438	0.0175	-0.0379
CCM23	-0.0056	-0.0074	0.0057	TZMM6	0.0039	0.0012	0.0024	MT1M11	0.0438	0.0187	-0.0044
UM3	-0.0055	-0.0068	0.0282	TQM6	0.0039	-0.0019	0.0015	UM19	0.0444	0.0279	-0.0187
NM14	-0.0053	-0.0099	0.0073	m43	0.0039	0.0015	-0.0073	UM22	0.0459	-0.0376	0.0105
hum8	-0.0053	-0.0085	0.0114	AM27	0.0040	-0.0171	-0.0072	TQO6	0.0466	0.0674	-0.0174
MT2M7	-0.0052	-0.0099	0.0108	MCM6	0.0040	-0.0007	-0.0071	MT1S3	0.0478	0.0203	0.0562
CM12	-0.0052	0.0020	0.0014	TZDM8	0.0040	-0.0036	0.0068	UM41.1	0.0485	-0.0351	0.0204
MT5M25	-0.0052	-0.0020	-0.0060	CM16	0.0040	0.0016	-0.0024	m14	0.0495	-0.0187	-0.0025
hus9	-0.0051	-0.0280	0.0330	MT2M16	0.0041	-0.0015	0.0137	RO2	0.0496	-0.0271	0.0037

	Separate Sexes				Separate Sexes				Separate Sexes		
	PC1	PC2	PC3		PC1	PC2	PC3		PC1	PC2	PC3
LCM1	-0.0048	-0.0074	0.0026	MC2M24	0.0041	0.0000	0.0049	CO5	0.0498	-0.0298	-0.0098
CBM19	-0.0047	-0.0026	0.0028	SM7	0.0041	-0.0087	0.0075	CCM17	0.0501	0.0383	0.0296
MC5M13	-0.0047	0.0018	0.0107	MC1M14	0.0041	0.0026	0.0038	UO4	0.0503	0.0111	-0.0640
m28	-0.0047	0.0097	-0.0032	UM2	0.0042	-0.0065	0.0165	NO1	0.0506	0.0780	0.0503
AM28	-0.0046	-0.0104	0.0055	MT2M28	0.0042	-0.0025	0.0010	MC1M13	0.0527	0.0408	0.0395
TQM7	-0.0045	-0.0044	0.0156	UM4	0.0042	-0.0095	0.0083	MC1M16	0.0527	0.0408	0.0395
TQM4	-0.0045	-0.0070	0.0089	SO1	0.0044	0.0621	-0.0082	HM2	0.0527	0.0408	0.0395
AM12	-0.0041	-0.0007	0.0103	TQM3	0.0044	-0.0040	-0.0012	TZDM7	0.0527	0.0408	0.0395
NO2	-0.0040	0.0005	-0.0040	TZMM1	0.0045	-0.0067	0.0056	TZMM7	0.0527	0.0408	0.0395
MT4M26	-0.0040	-0.0062	0.0061	LCM3	0.0045	0.0009	0.0030	MT2M17	0.0527	0.0408	0.0395
HM6	-0.0039	-0.0029	0.0074	MT2M30	0.0047	-0.0039	-0.0033	MCM2	0.0527	0.0408	0.0395
MC4M18	-0.0039	-0.0023	0.0018	HM12	0.0047	-0.0010	0.0045	MT1M9	0.0529	0.0270	0.0122
MT4M23	-0.0038	-0.0047	0.0015	AM6	0.0048	0.0046	0.0007	TZMO4	0.0545	-0.0351	-0.0085
MC3M18	-0.0036	-0.0034	0.0055	TZMM11	0.0050	0.0007	-0.0011	MT3O1	0.0549	0.0265	-0.0239
SM15	-0.0036	-0.0087	0.0184	SM9	0.0050	-0.0021	0.0031	o3	0.0551	-0.0074	-0.0199
MT5M9	-0.0035	-0.0028	0.0019	MCM11	0.0050	-0.0031	0.0044	RM21	0.0558	0.0370	0.0382
MT4M12	-0.0034	-0.0030	0.0033	MT1M4	0.0051	-0.0037	0.0023	MM18	0.0564	-0.0213	0.0589
MO4	-0.0033	-0.0335	-0.0517	LM1	0.0051	-0.0051	0.0046	MT2M24	0.0568	0.0391	-0.0099
CM8	-0.0033	-0.0012	0.0013	MC2M25	0.0051	-0.0017	0.0029	o22	0.0569	-0.0344	-0.0958
NM17	-0.0033	-0.0054	0.0074	LS9	0.0051	-0.0007	0.0085	TQO5	0.0581	0.0383	0.0408
CCM16	-0.0032	-0.0025	0.0139	CCM4	0.0052	0.0042	0.0036	TQO2	0.0581	0.0597	-0.0136
CBM20	-0.0032	-0.0027	0.0009	TZDM5	0.0052	-0.0086	0.0015	o45	0.0590	0.0122	-0.0272
UM28	-0.0031	-0.0071	0.0029	TZDM1	0.0052	-0.0003	0.0083	MC4M32	0.0598	0.0491	0.0161
MC5M12	-0.0029	-0.0004	0.0092	AM23	0.0053	0.0843	0.0246	ICM9	0.0598	0.0491	0.0161
UM38	-0.0029	0.0045	0.0292	MC1M3	0.0055	-0.0035	0.0079	MC1M12	0.0608	0.0408	0.0507
PM5	-0.0029	-0.0099	0.0105	UM25	0.0055	-0.0093	0.0118	MC1S2	0.0608	0.0408	0.0507
RM29	-0.0029	-0.0104	0.0184	MCM4	0.0055	-0.0045	0.0030	TZMM2	0.0608	0.0408	0.0507
TQM1	-0.0029	-0.0033	0.0061	MCM18	0.0055	-0.0032	0.0015	MT1S1	0.0608	0.0408	0.0507
MT2O1	-0.0029	0.0429	-0.0738	LM8	0.0056	-0.0033	0.0015	MT2M25	0.0608	0.0408	0.0507
CBM22	-0.0028	-0.0108	0.0074	RM4	0.0057	-0.0029	0.0056	UO5	0.0614	-0.0640	-0.0569
HM7	-0.0028	-0.0048	0.0051	RM10	0.0057	-0.0043	0.0012	AM17	0.0622	0.0365	-0.0087
MC4M16	-0.0027	-0.0011	0.0040	MT1M12	0.0058	-0.0027	0.0004	RM14	0.0638	0.0474	-0.0333
UM27	-0.0026	-0.0031	0.0033	MCM14	0.0058	-0.0015	0.0000	MT4S2	0.0638	0.0474	-0.0333

	Separate Sexes				Separate Sexes				Separate Sexes		
	PC1	PC2	PC3		PC1	PC2	PC3		PC1	PC2	PC3
PM3	-0.0026	-0.0018	0.0085	CCM3	0.0058	0.0010	0.0137	PVO17	0.0672	0.0201	-0.0147
MT4M10	-0.0025	-0.0061	0.0038	UM29	0.0059	-0.0063	0.0046	HM17	0.0678	0.0491	0.0273
LCM7	-0.0025	-0.0007	0.0041	MT2S12	0.0059	0.0381	0.0687	LS1	0.0678	0.0491	0.0273
TZMO2	-0.0025	0.0067	0.0500	AM25	0.0059	-0.0057	0.0021	PO2	0.0678	0.0479	-0.0261
MC2M8	-0.0024	-0.0030	0.0028	hum53	0.0060	0.0046	0.0077	o56	0.0705	0.0333	-0.0464
hum24	-0.0024	-0.0120	0.0124	RM5	0.0060	-0.0036	0.0016	o24	0.0725	0.0942	0.0117
hum45	-0.0024	-0.0027	0.0131	RM8	0.0061	-0.0059	-0.0006	MC3O3	0.0738	0.0957	-0.0277
AM31	-0.0024	0.0083	-0.0072	hum23	0.0062	-0.0030	0.0364	LCR1	0.0740	0.2370	0.0748
hum30	-0.0024	-0.0064	0.0104	hum62	0.0062	0.0031	0.0177	MC5M24	0.0766	-0.0442	-0.0167
MT5M26	-0.0024	0.0023	0.0011	MS1	0.0063	-0.0749	0.0267	o12	0.0868	-0.0007	0.0504
NM3	-0.0023	0.0001	0.0007	CBS3	0.0063	0.0759	0.0591	o10	0.0877	-0.0342	-0.0295
CCM19	-0.0023	-0.0094	0.0079	LM14	0.0063	-0.0086	0.0128	o4	0.0997	-0.0469	-0.0339
MCS8	-0.0023	-0.0079	-0.0002	AM11	0.0063	-0.0010	-0.0012	UO9	0.1065	0.0678	-0.0518
MT3M4	-0.0021	-0.0035	0.0025	MT1M5	0.0063	-0.0060	0.0004	o33	0.1122	-0.1069	-0.0359
MT5M21	-0.0021	-0.0037	0.0025	MT1M13	0.0063	-0.0021	-0.0012	UO3	0.1127	-0.0083	-0.0266
LCM14	-0.0020	-0.0149	0.0124	hum28	0.0064	-0.0115	0.0127	TZMO1	0.1133	-0.0082	-0.0251
MT5O2	-0.0020	-0.0007	0.0039	MT2M1	0.0065	-0.0037	0.0007	o20	0.1161	0.0403	-0.1528
MT3M13	-0.0020	-0.0018	0.0024	LM4	0.0066	0.0020	0.0039	TQO4	0.1166	0.1546	-0.0074
HM5	-0.0019	-0.0042	0.0089	MCO2	0.0067	0.0096	-0.0041	UO1	0.1338	0.0903	-0.0499
HM11	-0.0019	-0.0055	0.0008	hum11	0.0067	0.0054	0.0079	huo5	0.1961	0.1272	0.0383
CCM25	-0.0018	0.0018	0.0011	HM16	0.0067	-0.0007	0.0049	o23	0.2617	-0.0391	0.2856
MT4M11	-0.0018	-0.0057	0.0007	RM16	0.0067	-0.0035	0.0010	RM26	0.5614	-0.4069	-0.0122
MT5M20	-0.0017	-0.0019	0.0008	MC1M1	0.0068	-0.0064	0.0094				
MT2M4	-0.0017	-0.0021	0.0023	MM24	0.0068	0.0170	0.0303				
CM3	-0.0017	-0.0020	0.0095	CCM1	0.0069	0.0034	0.0006				
MC3M16	-0.0017	-0.0042	0.0013	hum26	0.0069	-0.0060	0.0161				
MT5M22	-0.0017	-0.0030	0.0035	LM13	0.0069	-0.0064	0.0130				
MCM17	-0.0016	0.0621	0.0207	hum13	0.0070	0.0107	-0.0025				
m1.1	-0.0015	-0.0302	0.0564	TZDM9	0.0070	-0.0033	0.0090				
m13	-0.0015	-0.0302	0.0564	CM10	0.0071	0.0056	0.0052				
m21	-0.0015	-0.0302	0.0564	m35	0.0072	-0.0527	0.0594				
MM31	-0.0015	-0.0302	0.0564	hum22	0.0072	-0.0007	0.0069				
MC2M9	-0.0014	-0.0018	0.0057	MT1M6	0.0073	-0.0041	-0.0002				

	Separate Sexes				Separate Sexes		
	PC1	PC2	PC3		PC1	PC2	PC3
TZMM15	-0.0014	-0.0008	0.0088	LM2	0.0073	-0.0026	0.0052
AM30	-0.0013	0.0042	-0.0077	HM4	0.0073	0.0060	0.0026
hum50	-0.0013	-0.0015	-0.0023	RM13	0.0074	-0.0081	0.0133
MCM9	-0.0013	-0.0023	-0.0008	MC1M11	0.0075	-0.0032	0.0021
AM15	-0.0013	0.0004	0.0009	RM2	0.0075	-0.0090	0.0059
MT2M11	-0.0012	-0.0088	0.0066	SM2	0.0075	-0.0087	0.0038
MC4M33	-0.0012	-0.0004	0.0036	MT2M3	0.0076	-0.0051	0.0032
LCM17	-0.0012	-0.0068	0.0133	hum27	0.0076	-0.0058	0.0180
CBM9	-0.0011	-0.0069	0.0038	hum57	0.0076	0.0030	0.0125
MC3M21	-0.0011	-0.0042	0.0109	CM11	0.0076	-0.0008	0.0009
TZDM11	-0.0011	-0.0038	0.0031	UM14	0.0076	0.0004	0.0247
CM19	-0.0010	-0.0007	0.0057	TZMM9	0.0077	0.0002	0.0010
hum60	-0.0010	0.0097	0.0153	MT1M1	0.0078	-0.0088	0.0025
MT3M3	-0.0010	-0.0039	0.0015	hum40	0.0078	0.0031	0.0004
PM8	-0.0009	-0.0037	0.0114	hum29	0.0079	0.0029	0.0226
m39	-0.0009	0.0000	0.0038	LM3	0.0079	-0.0012	-0.0023
ICM6	-0.0008	-0.0041	-0.0002	hum5	0.0080	0.0062	0.0084
NM19	-0.0008	0.0008	-0.0011	TZMM3	0.0080	-0.0026	0.0007
MT3M15	-0.0008	-0.0092	-0.0006	hum34	0.0082	-0.0117	0.0364
CCM22	-0.0008	-0.0069	0.0072	Rs2	0.0083	-0.0057	-0.0055
CBM23	-0.0008	-0.0021	0.0072	o32	0.0084	0.0338	-0.0103
AM16	-0.0007	-0.0064	0.0099	SM8	0.0084	-0.0048	0.0075
MT2M27	-0.0006	-0.0037	0.0038	CS3	0.0087	0.0101	0.0183
CO3	-0.0006	-0.0277	0.0114	RM7	0.0088	-0.0080	0.0032
UM16	-0.0006	-0.0098	0.0210	TZMM5	0.0088	-0.0018	-0.0016
o49	-0.0006	0.0232	0.0344	MT2M21	0.0088	-0.0035	0.0006
hum2	-0.0005	-0.0102	0.0031	RM6	0.0090	-0.0102	0.0037
NS2	-0.0004	-0.0093	-0.0031	CM5	0.0094	0.0035	0.0013
LM15	-0.0004	-0.0004	0.0002	huo7	0.0095	0.1194	0.0146
UM32	-0.0003	0.0002	-0.0020	hum32	0.0095	0.0014	0.0146
MO7	-0.0003	0.0348	-0.0007	hum14	0.0096	0.0012	0.0112
LM16	-0.0003	-0.0003	0.0002	MT1M3	0.0096	-0.0092	0.0023
m6	-0.0003	-0.0070	0.0059	TZDM12	0.0096	-0.0034	0.0086

	All characters				All characters				All characters		
	PC1	PC2	PC3		PC1	PC2	PC3		PC1	PC2	PC3
RM26	-0.5021	-0.4420	-0.0140	TZMM2	-0.0594	0.0354	0.0521	UM22	-0.0418	-0.0441	0.0130
o23	-0.2726	-0.0317	0.3352	MT1S1	-0.0594	0.0354	0.0521	o56	-0.0403	0.0756	-0.0458
TQO4	-0.1942	0.1159	-0.0019	MT2M25	-0.0594	0.0354	0.0521	MT1M11	-0.0403	0.0143	-0.0170
huo5	-0.1508	0.0799	0.0676	TQO5	-0.0580	0.0318	0.0347	LC02	-0.0399	0.0253	0.0295
o20	-0.1466	0.1210	-0.0979	MT3O1	-0.0579	0.0209	-0.0234	UM35.1	-0.0396	0.0255	0.0513
UO1	-0.1409	0.0828	0.0125	RO2	-0.0579	-0.0470	0.0094	LS5	-0.0396	0.0255	0.0513
UO3	-0.1365	-0.0122	-0.0120	TQO2	-0.0575	0.0798	0.0336	AM4	-0.0396	0.0255	0.0513
UO9	-0.1168	0.0685	-0.0754	RM21	-0.0572	0.0321	0.0448	AM5	-0.0396	0.0255	0.0513
TZMO1	-0.1080	-0.0185	-0.0303	MT2M24	-0.0544	0.0327	-0.0129	MCM12	-0.0396	0.0255	0.0513
MC4O3	-0.1047	0.0576	-0.1417	UO4	-0.0544	-0.0246	-0.0402	MCM16	-0.0396	0.0255	0.0513
o12	-0.1046	-0.0202	0.0401	MM18	-0.0516	-0.0248	0.0687	m15	-0.0374	-0.0432	0.0646
o4	-0.1001	-0.0441	0.0766	MC1M13	-0.0512	0.0369	0.0383	MT1M7	-0.0371	0.0185	0.0342
TQO1	-0.0988	-0.0562	0.1228	MC1M16	-0.0512	0.0369	0.0383	MT1M1.1	-0.0371	0.0185	0.0342
o33	-0.0981	-0.1247	-0.0407	HM2	-0.0512	0.0369	0.0383	PVM20	-0.0369	0.0122	0.0678
LCR1	-0.0860	0.2351	0.0738	TZDM7	-0.0512	0.0369	0.0383	US14	-0.0366	0.0034	0.0157
NO1	-0.0827	0.0701	-0.0113	TZMM7	-0.0512	0.0369	0.0383	CCO2	-0.0351	-0.0837	0.0743
MC3O3	-0.0799	0.0995	-0.0359	MT2M17	-0.0512	0.0369	0.0383	MCS2	-0.0349	0.0152	0.0270
o24	-0.0753	0.0835	-0.0234	MCM2	-0.0512	0.0369	0.0383	HM1	-0.0338	-0.0105	0.0047
PO2	-0.0721	0.0393	-0.0193	MT1M9	-0.0510	0.0197	0.0138	MT2M26	-0.0334	0.0532	0.0438
MC5M24	-0.0709	-0.0462	-0.0143	CO5	-0.0501	-0.0393	-0.0068	MCS4	-0.0331	0.0305	0.0331
UO5	-0.0691	-0.0772	-0.0575	CCM17	-0.0498	0.0333	0.0210	o39	-0.0324	0.0387	-0.0257
HM17	-0.0688	0.0435	0.0319	o3	-0.0482	-0.0116	-0.0327	UM12	-0.0323	-0.0522	0.0332
LS1	-0.0688	0.0435	0.0319	TQO6	-0.0475	0.0608	-0.0102	m4	-0.0320	-0.0458	-0.0120
o10	-0.0677	-0.0493	-0.0877	TZMO4	-0.0469	-0.0351	0.0444	UM20	-0.0317	0.0131	-0.0101
PVO17	-0.0657	0.0132	-0.0072	m14	-0.0456	-0.0249	-0.0161	RM11	-0.0315	-0.0145	0.0232
RM14	-0.0639	0.0408	-0.0331	o26	-0.0453	-0.0329	-0.0318	hum54	-0.0311	0.0165	0.0118
MT4S2	-0.0639	0.0408	-0.0331	MT1S3	-0.0452	0.0170	0.0480	PVM18	-0.0305	0.0172	0.0497
AM17	-0.0612	0.0276	-0.0165	UM19	-0.0450	0.0229	-0.0152	PVM23	-0.0300	-0.0244	-0.0043
MC4M32	-0.0607	0.0451	0.0181	o22	-0.0448	-0.0356	-0.1170	MC3M32	-0.0299	-0.0547	-0.0355
ICM9	-0.0607	0.0451	0.0181	AM1	-0.0442	0.0650	0.0410	m37	-0.0298	-0.0592	0.0162
o45	-0.0600	-0.0082	0.0013	RO7	-0.0438	0.0254	-0.0618	MT2S8	-0.0297	0.0179	-0.0078
MC1M12	-0.0594	0.0354	0.0521	UM41.1	-0.0432	-0.0405	0.0304	MT1M8	-0.0296	0.0070	-0.0659
MC1S2	-0.0594	0.0354	0.0521	UO6	-0.0424	-0.0939	-0.0708	MT1S2	-0.0296	0.0070	-0.0659

	All characters		
	PC1	PC2	PC3
CM14.1	-0.0290	-0.0589	0.0263
MT1M2	-0.0290	-0.0589	0.0263
MCM1	-0.0289	0.0182	0.0023
CBM14	-0.0288	0.0138	0.0541
CBM15	-0.0288	0.0138	0.0541
CBM17	-0.0288	0.0138	0.0541
CBM18	-0.0288	0.0138	0.0541
o41	-0.0287	-0.0539	-0.1047
PVO1	-0.0284	-0.0154	0.0160
MCM15	-0.0275	0.0146	-0.0150
hus8	-0.0272	-0.0057	0.0208
PVO5	-0.0258	0.0548	0.0360
MM17	-0.0257	-0.0236	0.0472
UO12	-0.0251	0.0606	-0.0206
US13	-0.0245	0.0186	0.0149
MC2O1	-0.0243	0.0153	-0.0843
TZMM17	-0.0242	0.0037	-0.0103
hum15	-0.0239	0.0117	0.0249
PVO6	-0.0235	-0.0269	0.0400
HM8	-0.0232	0.0454	0.0741
hus7	-0.0231	-0.0201	0.0886
hum10	-0.0226	0.0150	0.0129
CCM6	-0.0225	0.0232	-0.0158
CCS11	-0.0220	0.0786	-0.0125
hus6	-0.0220	-0.0202	0.0355
o16	-0.0213	-0.0531	-0.0609
o47	-0.0213	-0.0177	0.0622
AM27.1	-0.0211	0.0196	-0.0331
hum48	-0.0205	0.0134	0.0116
UM31	-0.0201	0.0091	0.0026
TZMM19	-0.0192	0.0000	-0.0081
MC2M26	-0.0183	-0.0662	-0.0226
MC2S2	-0.0183	-0.0662	-0.0226

	All characters		
	PC1	PC2	PC3
UO10	-0.0183	0.0203	-0.0298
MT5s1	-0.0182	0.0427	0.0092
SM1	-0.0181	0.0065	0.0052
MC1S1	-0.0180	-0.0169	0.0166
RM28	-0.0180	0.0090	0.0058
hum47	-0.0175	0.0160	0.0147
o52	-0.0169	-0.0698	-0.0400
hum1	-0.0168	0.0136	0.0046
hum4	-0.0167	0.0212	0.0013
hus5	-0.0166	-0.0043	0.0728
o5	-0.0165	-0.0217	-0.0410
CM14	-0.0165	-0.0091	0.0031
hum46	-0.0163	0.0116	0.0114
MO2	-0.0163	0.0089	-0.0511
UM21	-0.0161	0.0072	0.0191
MT2S7	-0.0158	-0.0115	0.0118
HM1.1	-0.0157	0.0339	-0.0260
MCO3	-0.0156	0.0525	-0.0004
TZMS1	-0.0156	-0.0109	0.0109
PVO10	-0.0156	0.0416	-0.0585
MC2M10	-0.0153	-0.0020	0.0037
LS6	-0.0150	-0.0098	0.0022
MCS6	-0.0148	-0.0002	-0.0017
hum55	-0.0147	0.0181	0.0085
UM6	-0.0145	0.0030	0.0021
MCS3	-0.0141	0.0434	0.0490
CO1	-0.0141	0.0075	-0.0540
hum9	-0.0141	0.0044	0.0108
hum20	-0.0141	-0.0019	0.0131
AM32	-0.0139	0.0137	0.0041
UM5	-0.0138	0.0045	0.0073
MC3M17	-0.0138	0.0478	-0.0087
UO2	-0.0137	0.0559	0.1199

	All characters		
	PC1	PC2	PC3
NM5	-0.0136	0.0433	0.0430
LCM28	-0.0133	0.0378	0.0151
UM41	-0.0130	0.0180	0.0103
RM24	-0.0129	0.0055	0.0014
hum7	-0.0129	0.0082	-0.0057
hum38	-0.0129	-0.0062	0.0128
CM22	-0.0129	-0.0036	0.0084
hus10	-0.0128	-0.0131	0.0371
hum25	-0.0128	0.0004	0.0057
SM10	-0.0126	0.0078	0.0032
MT2M23	-0.0123	-0.0045	0.0002
RM25	-0.0122	0.0027	0.0016
RM22	-0.0122	0.0082	-0.0035
RM23	-0.0120	-0.0006	0.0028
AM24	-0.0119	0.0076	-0.0092
ICM12	-0.0117	-0.0197	0.0173
RM27	-0.0117	0.0043	0.0091
AS1	-0.0116	0.0364	0.0319
MC1M2	-0.0116	-0.0025	0.0037
MT1M14	-0.0115	0.0005	-0.0711
RM12	-0.0115	-0.0034	0.0007
m34	-0.0115	-0.0350	0.0109
hum31	-0.0114	0.0045	0.0060
SM5	-0.0113	0.0000	0.0057
o32	-0.0112	0.0408	-0.0258
MT2M14	-0.0109	0.0117	-0.0028
RM20	-0.0108	-0.0024	0.0072
UM34	-0.0108	-0.0018	0.0041
RM17	-0.0106	0.0020	0.0100
AM23	-0.0106	0.0844	0.0249
HS4	-0.0105	-0.0058	0.0052
MT2M19	-0.0104	-0.0013	-0.0021
UM26	-0.0104	0.0065	0.0111

	All characters				All characters				All characters		
	PC1	PC2	PC3		PC1	PC2	PC3		PC1	PC2	PC3
PVM4	-0.0104	-0.0221	0.0235	SMS1	-0.0075	-0.0779	-0.0198	MC1M1	-0.0059	-0.0059	0.0078
MT2M20	-0.0102	-0.0035	-0.0017	TZDM4	-0.0075	-0.0779	-0.0198	RM2	-0.0059	-0.0088	0.0041
SM3	-0.0100	-0.0018	0.0057	TZMM3	-0.0075	-0.0030	0.0010	hum27	-0.0059	-0.0056	0.0164
MT2M22	-0.0100	-0.0036	0.0005	LM3	-0.0075	-0.0019	-0.0014	MT1M13	-0.0058	-0.0022	-0.0018
RM19	-0.0098	0.0096	-0.0007	TZMM9	-0.0074	0.0000	0.0008	AM11	-0.0058	-0.0009	-0.0017
MC2M11	-0.0098	-0.0061	0.0043	HM4	-0.0074	0.0054	0.0011	hum53	-0.0058	0.0045	0.0060
CM1	-0.0095	-0.0008	-0.0007	hum40	-0.0071	0.0021	0.0013	MT2M1	-0.0057	-0.0038	0.0000
UM11	-0.0094	0.0013	0.0061	CM11	-0.0071	-0.0012	0.0009	RM16	-0.0057	-0.0041	-0.0011
CM5	-0.0094	0.0032	0.0005	hum13	-0.0070	0.0102	-0.0022	hum34	-0.0057	-0.0112	0.0352
HM14	-0.0093	-0.0016	-0.0002	CM10	-0.0070	0.0054	0.0037	MT1M5	-0.0057	-0.0055	-0.0012
CBS3	-0.0093	0.0747	0.0589	UO11	-0.0070	-0.0853	-0.0300	LS9	-0.0056	0.0003	0.0069
RS1	-0.0091	-0.0104	0.0143	MM24	-0.0069	0.0155	0.0310	hum26	-0.0055	-0.0059	0.0152
hum16	-0.0090	0.0033	0.0158	MC1M11	-0.0069	-0.0034	0.0015	LM14	-0.0054	-0.0079	0.0120
hum14	-0.0089	0.0008	0.0109	LM2	-0.0068	-0.0029	0.0050	MCM14	-0.0054	-0.0016	-0.0012
TZDM12	-0.0089	-0.0031	0.0059	o48	-0.0068	0.1069	0.0964	hum62	-0.0053	0.0027	0.0165
MC1M10	-0.0089	-0.0053	0.0044	m1	-0.0068	-0.0649	0.0666	LM8	-0.0053	-0.0033	0.0013
hum37	-0.0089	0.0005	0.0050	LM4	-0.0067	0.0019	0.0039	MC1M3	-0.0052	-0.0032	0.0063
RM3	-0.0088	-0.0028	0.0037	MT2M3	-0.0067	-0.0056	0.0038	RM5	-0.0052	-0.0038	0.0003
RM15	-0.0088	-0.0067	0.0114	SM2	-0.0067	-0.0088	0.0037	RM8	-0.0051	-0.0064	-0.0019
CCM15	-0.0087	-0.0016	-0.0090	hum57	-0.0066	0.0024	0.0107	UM29	-0.0051	-0.0064	0.0037
hum33	-0.0087	-0.0005	0.0082	hum29	-0.0066	0.0026	0.0201	MT1M12	-0.0050	-0.0028	-0.0010
CS3	-0.0086	0.0116	0.0141	Rs2	-0.0066	-0.0061	-0.0072	MCM18	-0.0050	-0.0031	0.0010
MT1M3	-0.0084	-0.0092	-0.0002	MT1M6	-0.0066	-0.0042	-0.0014	AM25	-0.0049	-0.0066	0.0023
hum32	-0.0084	0.0007	0.0145	TZDM9	-0.0065	-0.0033	0.0068	RM10	-0.0049	-0.0045	0.0002
MT2M21	-0.0082	-0.0037	0.0017	CCM1	-0.0065	0.0029	-0.0001	CCM3	-0.0049	0.0012	0.0137
TZMM5	-0.0082	-0.0023	0.0017	MT1M1	-0.0065	-0.0088	0.0009	TZMM11	-0.0048	0.0006	-0.0005
NM8	-0.0079	0.0711	0.0415	hum11	-0.0064	0.0052	0.0075	huo7	-0.0048	0.0817	0.0453
SO1	-0.0078	0.0602	-0.0166	MC5O1	-0.0063	0.0261	-0.0121	CCM4	-0.0048	0.0043	0.0025
MM19	-0.0077	-0.0612	0.0723	HM16	-0.0063	-0.0008	0.0032	TZDM1	-0.0048	0.0002	0.0051
hum5	-0.0077	0.0057	0.0079	LM13	-0.0062	-0.0061	0.0128	MCM4	-0.0048	-0.0043	0.0005
SM8	-0.0076	-0.0047	0.0051	hum22	-0.0062	-0.0006	0.0074	SM9	-0.0047	-0.0018	0.0024
RM6	-0.0075	-0.0107	0.0021	UM14	-0.0061	0.0004	0.0216	LM1	-0.0047	-0.0042	0.0030
RM7	-0.0075	-0.0085	0.0016	RM13	-0.0059	-0.0080	0.0117	MC2M25	-0.0047	-0.0018	0.0024

	All characters		
	PC1	PC2	PC3
hum28	-0.0046	-0.0110	0.0116
MT2M29	-0.0046	0.0395	-0.0103
MT2S6	-0.0046	0.0395	-0.0103
RM4	-0.0046	-0.0029	0.0039
MCM11	-0.0046	-0.0034	0.0047
AM6	-0.0046	0.0036	-0.0013
TZDM5	-0.0045	-0.0082	0.0006
hum23	-0.0044	-0.0030	0.0333
LCM3	-0.0044	0.0011	0.0027
AM18	-0.0044	0.0721	-0.0060
HM12	-0.0043	-0.0012	0.0037
MT1M4	-0.0042	-0.0039	0.0001
MT2M30	-0.0042	-0.0044	-0.0031
MT2S12	-0.0041	0.0352	0.0632
CM16	-0.0041	0.0014	-0.0024
CM20	-0.0040	0.0069	0.0048
TQM3	-0.0039	-0.0044	-0.0023
MC1M14	-0.0039	0.0024	0.0025
m43	-0.0039	0.0012	-0.0055
TQM6	-0.0039	-0.0017	0.0017
UM25	-0.0038	-0.0089	0.0101
TZMM6	-0.0038	0.0011	0.0018
MCM6	-0.0038	-0.0009	-0.0060
TZMM1	-0.0038	-0.0065	0.0054
MT2M28	-0.0037	-0.0024	0.0002
MC2M24	-0.0037	0.0001	0.0037
MT2M16	-0.0037	-0.0021	0.0142
MC3M34	-0.0037	0.0012	0.0001
CBM11	-0.0037	0.0007	-0.0010
TZDM10	-0.0037	0.0035	0.0011
TQM5	-0.0035	-0.0015	0.0067
MC4M20	-0.0034	-0.0034	0.0033
TZDM8	-0.0034	-0.0031	0.0047

	All characters		
	PC1	PC2	PC3
SM7	-0.0034	-0.0079	0.0054
PVM6	-0.0034	0.0186	0.0068
MC3M19	-0.0034	0.0021	0.0020
NM1	-0.0033	0.0018	-0.0073
huo3	-0.0033	0.0067	0.0069
CBM16	-0.0033	0.0316	0.0518
HM15	-0.0033	-0.0032	0.0015
AM29	-0.0032	0.0056	-0.0101
MC4M34	-0.0031	-0.0001	0.0010
MCM3	-0.0031	-0.0058	0.0027
TZMM4	-0.0031	-0.0027	0.0021
UM37	-0.0031	-0.0007	0.0089
NM13	-0.0031	0.0015	-0.0021
MCM5	-0.0031	-0.0018	-0.0035
CM7	-0.0029	-0.0002	-0.0023
LM12	-0.0029	-0.0108	0.0066
hum39	-0.0029	0.0023	0.0107
MM16	-0.0029	0.0166	0.0197
MCM7	-0.0029	-0.0029	0.0031
TZDM2	-0.0029	0.0005	0.0079
m35	-0.0029	-0.0529	0.0655
UM4	-0.0029	-0.0092	0.0067
UM2	-0.0028	-0.0057	0.0167
NM20	-0.0028	0.0025	-0.0056
CS5	-0.0028	0.0021	-0.0007
CM4	-0.0028	0.0068	-0.0014
SM11	-0.0027	-0.0041	0.0113
AM10	-0.0027	-0.0016	0.0073
TZMM8	-0.0027	0.0000	0.0010
HM18	-0.0027	-0.0036	0.0024
ICM5	-0.0027	-0.0045	0.0033
ICM10	-0.0027	-0.0020	0.0040
MC2M7	-0.0026	-0.0023	0.0055

	All characters		
	PC1	PC2	PC3
AM27	-0.0026	-0.0168	-0.0057
CCM2	-0.0026	-0.0034	0.0023
MT5M8	-0.0025	-0.0013	0.0136
MC3M20	-0.0025	-0.0029	0.0092
CCM8	-0.0024	0.0034	0.0016
MT4M25	-0.0023	0.0005	0.0030
LM7	-0.0023	0.0061	0.0079
LM10	-0.0022	0.0045	0.0076
MC5M25	-0.0022	0.0028	-0.0008
NM16	-0.0021	0.0010	0.0020
CCM18	-0.0021	0.0090	0.0032
AM8	-0.0019	0.0001	0.0033
MC4M19	-0.0019	-0.0007	0.0022
RM9	-0.0019	-0.0068	0.0160
LM6	-0.0019	0.0017	0.0006
CBM10	-0.0018	0.0020	0.0049
MT2M2	-0.0018	-0.0017	0.0021
AM3	-0.0018	-0.0074	0.0046
MCM13	-0.0017	0.0042	-0.0018
CM6	-0.0017	0.0036	0.0042
CM13	-0.0017	-0.0020	0.0008
MC5M26	-0.0017	-0.0015	0.0036
UM17	-0.0016	-0.0043	0.0019
MT2M15	-0.0016	-0.0029	0.0108
PVO15	-0.0015	0.0341	-0.0045
AM7	-0.0014	-0.0071	0.0069
AM9	-0.0014	-0.0015	0.0074
AM21	-0.0014	0.0044	-0.0005
hum51	-0.0014	-0.0041	0.0006
HM9	-0.0014	-0.0012	0.0078
US10	-0.0013	-0.0076	0.0306
TZMM10	-0.0013	-0.0001	-0.0023
SM12	-0.0013	-0.0003	0.0010

	All characters		
	PC1	PC2	PC3
NM2	-0.0012	-0.0006	0.0052
MT2M31	-0.0012	0.0000	-0.0047
CBS6	-0.0011	-0.0003	0.0022
MT3M2	-0.0011	-0.0005	0.0019
hum42	-0.0011	-0.0010	-0.0014
m7	-0.0011	-0.0188	0.0120
CCM9	-0.0011	-0.0011	0.0035
CBM12	-0.0010	-0.0005	0.0013
UM30	-0.0010	-0.0053	0.0077
CBM24	-0.0010	-0.0045	0.0077
US12	-0.0009	-0.0089	0.0219
MCM17	-0.0009	0.0591	0.0206
SMS2	-0.0009	-0.0047	0.0048
SM4	-0.0009	-0.0007	0.0058
SM6	-0.0008	-0.0021	0.0042
MT3M7	-0.0008	-0.0011	0.0041
MC4M21	-0.0008	-0.0023	0.0014
CCM5	-0.0008	-0.0017	0.0044
CM2	-0.0008	-0.0010	0.0043
CCM10	-0.0007	0.0040	0.0011
MCM10	-0.0007	-0.0022	-0.0012
NM15	-0.0007	0.0001	-0.0022
AM14	-0.0007	0.0046	0.0032
MCM8	-0.0007	-0.0039	-0.0068
NM21	-0.0006	-0.0035	0.0090
MT5M23	-0.0006	-0.0018	0.0026
CS4	-0.0006	-0.0042	0.0027
CBM21	-0.0006	0.0020	-0.0017
m42	-0.0005	-0.0009	0.0036
MT3M12	-0.0005	-0.0023	0.0041
ICM8	-0.0004	-0.0030	0.0016
m25	-0.0004	-0.0617	0.0303
LCM4	-0.0004	-0.0073	0.0022

	All characters		
	PC1	PC2	PC3
AM26	-0.0003	0.0017	0.0033
CM18	-0.0003	-0.0003	0.0000
UM35	-0.0003	-0.0105	0.0100
MC4M17	-0.0002	-0.0010	0.0011
AM22	-0.0001	-0.0033	0.0034
HM3	-0.0001	0.0008	0.0026
o57	-0.0001	0.1015	0.0055
PM10	-0.0001	0.0019	0.0086
MS1	-0.0001	-0.0771	0.0240
NM7	-0.0001	-0.0144	-0.0003
PM7	0.0000	0.0017	0.0049
CCM24	0.0000	0.0034	-0.0058
NM18	0.0000	-0.0008	0.0000
o42	0.0000	0.0000	0.0000
MO7	0.0000	0.0000	0.0000
huo1	0.0000	0.0000	0.0000
huo2	0.0000	0.0000	0.0000
PVO14	0.0000	0.0000	0.0000
PVM2	0.0000	0.0000	0.0000
LO1	0.0000	0.0000	0.0000
MC4O2	0.0000	0.0000	0.0000
CO4	0.0000	0.0000	0.0000
TZMO2	0.0000	0.0000	0.0000
TZMO3	0.0000	0.0000	0.0000
MT4O1	0.0000	0.0000	0.0000
MT5O1	0.0000	0.0000	0.0000
AO1	0.0000	0.0000	0.0000
CBO1	0.0000	0.0000	0.0000
MCO1	0.0000	0.0000	0.0000
MCO2	0.0000	0.0000	0.0000
CM21	0.0000	0.0027	0.0032
HM13	0.0000	0.0032	0.0043
hum35	0.0001	0.0001	0.0234

	All characters		
	PC1	PC2	PC3
TZDM3	0.0001	0.0002	0.0069
LCM5	0.0001	-0.0054	0.0023
MC3M33	0.0002	-0.0021	0.0037
hum44	0.0003	-0.0017	0.0136
MT4M24	0.0003	-0.0030	-0.0001
LM16	0.0003	-0.0003	0.0003
UM32	0.0003	0.0005	-0.0015
hum41	0.0003	-0.0017	0.0104
MT3M14	0.0003	-0.0062	0.0071
HM19	0.0003	-0.0008	0.0066
LM15	0.0004	-0.0004	0.0004
MT2M13	0.0004	-0.0019	0.0012
hum36	0.0005	-0.0061	0.0051
MT2M18	0.0005	-0.0049	0.0012
RM18	0.0006	-0.0066	0.0184
CCS8	0.0006	-0.0003	0.0021
NM19	0.0007	0.0009	-0.0023
US11	0.0009	-0.0333	0.0362
MCM9	0.0009	-0.0020	-0.0001
NS2	0.0010	-0.0081	-0.0051
LCM16	0.0010	-0.0119	0.0044
m39	0.0010	0.0000	0.0021
m6	0.0010	-0.0067	0.0035
hum56	0.0010	0.0000	0.0059
MT2M27	0.0011	-0.0031	0.0026
CBM23	0.0011	-0.0013	0.0048
AM30	0.0011	0.0047	-0.0080
ICM6	0.0011	-0.0036	0.0001
CM19	0.0012	-0.0003	0.0041
MC4M33	0.0013	0.0001	0.0030
MC3M21	0.0013	-0.0038	0.0097
PM8	0.0013	-0.0028	0.0105
MT3M3	0.0013	-0.0034	0.0014

	All characters		
	PC1	PC2	PC3
hum60	0.0013	0.0104	0.0130
hum2	0.0014	-0.0096	0.0040
hum50	0.0014	-0.0005	-0.0018
TZMM15	0.0015	0.0001	0.0060
MC2M9	0.0015	-0.0009	0.0039
MT3M15	0.0015	-0.0086	-0.0012
MC3M16	0.0016	-0.0035	0.0014
TZDM11	0.0016	-0.0029	-0.0018
AM15	0.0016	0.0013	-0.0010
CM3	0.0017	-0.0011	0.0078
CBM9	0.0017	-0.0057	0.0027
o38	0.0017	0.0383	0.0467
HM11	0.0018	-0.0045	0.0000
AM31	0.0018	0.0096	-0.0099
CCM25	0.0018	0.0020	-0.0006
MT2M4	0.0018	-0.0015	0.0008
AM16	0.0018	-0.0061	0.0072
MT5M22	0.0019	-0.0025	0.0039
PVM5	0.0019	0.0038	0.0263
MT5M20	0.0019	-0.0014	0.0007
CCM22	0.0020	-0.0051	0.0050
MT3M13	0.0020	-0.0013	0.0022
MT5O2	0.0020	-0.0005	0.0034
LCM17	0.0020	-0.0063	0.0100
HM5	0.0021	-0.0032	0.0072
MT2M11	0.0022	-0.0080	0.0042
MT5M26	0.0022	0.0031	0.0012
NM3	0.0022	0.0005	0.0004
MT4M11	0.0023	-0.0051	0.0002
MT3M4	0.0023	-0.0027	0.0015
PM3	0.0024	-0.0014	0.0062
MC2M8	0.0024	-0.0024	0.0018
MT5M21	0.0025	-0.0029	0.0018

	All characters		
	PC1	PC2	PC3
UM16	0.0025	-0.0090	0.0166
MC4M16	0.0025	-0.0003	0.0043
LCM7	0.0026	0.0000	0.0021
MCS8	0.0027	-0.0072	-0.0009
HM7	0.0028	-0.0040	0.0055
MT4M10	0.0029	-0.0054	0.0033
UM27	0.0029	-0.0026	0.0027
TQM1	0.0030	-0.0028	0.0056
MC5M12	0.0030	0.0001	0.0090
hum45	0.0030	-0.0019	0.0118
m11	0.0031	-0.0729	0.0752
m20	0.0031	-0.0729	0.0752
m22	0.0031	-0.0729	0.0752
m23	0.0031	-0.0729	0.0752
m41	0.0031	-0.0729	0.0752
MM20	0.0031	-0.0729	0.0752
MM28	0.0031	-0.0729	0.0752
CCM19	0.0032	-0.0071	0.0030
LCM14	0.0033	-0.0137	0.0089
CM8	0.0033	-0.0005	0.0005
CBM20	0.0034	-0.0018	0.0006
hum30	0.0034	-0.0056	0.0089
MT4M12	0.0034	-0.0021	0.0027
MC3M18	0.0035	-0.0022	0.0048
NM17	0.0036	-0.0041	0.0058
UM28	0.0036	-0.0061	0.0022
MC4M18	0.0036	-0.0012	0.0022
PM5	0.0036	-0.0079	0.0074
MT5M9	0.0037	-0.0019	0.0013
hum24	0.0038	-0.0112	0.0114
CBM22	0.0039	-0.0094	0.0050
HM6	0.0039	-0.0021	0.0062
UM38	0.0040	0.0053	0.0248

	All characters		
	PC1	PC2	PC3
MT4M23	0.0040	-0.0038	0.0013
RM29	0.0041	-0.0096	0.0173
SM15	0.0041	-0.0068	0.0156
CCM16	0.0041	-0.0014	0.0094
CM12	0.0042	0.0023	0.0015
AM12	0.0043	0.0006	0.0086
o31	0.0043	0.0189	-0.0610
MT4M26	0.0044	-0.0054	0.0055
MC5M13	0.0045	0.0024	0.0102
PVM7	0.0047	-0.0103	-0.0243
CBM19	0.0047	-0.0013	0.0010
TQM4	0.0048	-0.0060	0.0069
TQM7	0.0048	-0.0037	0.0143
m28	0.0049	0.0082	-0.0068
MT5M25	0.0049	-0.0010	-0.0056
LCM1	0.0052	-0.0060	0.0017
m1.1	0.0053	-0.0283	0.0685
m13	0.0053	-0.0283	0.0685
m21	0.0053	-0.0283	0.0685
MM31	0.0053	-0.0283	0.0685
AM28	0.0054	-0.0094	0.0048
CCM21	0.0057	0.0005	0.0049
NM14	0.0058	-0.0083	0.0071
MT2M7	0.0059	-0.0087	0.0079
hum8	0.0059	-0.0074	0.0117
LM9	0.0059	0.0075	0.0122
UM40	0.0060	0.0063	0.0184
ICM11	0.0061	-0.0061	0.0021
CBM7	0.0062	-0.0051	0.0040
CCM23	0.0062	-0.0053	0.0034
MC2M12	0.0063	-0.0035	0.0148
MT4M13	0.0063	-0.0043	0.0079
CO3	0.0063	-0.0261	0.0121

	All characters				All characters				All characters		
	PC1	PC2	PC3		PC1	PC2	PC3		PC1	PC2	PC3
PM11	0.0064	-0.0032	0.0109	m16	0.0114	0.0133	0.0280	m3	0.0187	-0.0470	0.0643
LCM2	0.0065	0.0279	0.0143	TQM8	0.0115	-0.0080	0.0066	MT2M12	0.0188	-0.0828	-0.0387
o55	0.0067	0.0356	-0.0182	PM6	0.0115	-0.0085	0.0121	MT3M26	0.0188	-0.0828	-0.0387
UM3	0.0071	-0.0060	0.0240	PM4	0.0117	-0.0116	0.0056	TQO7	0.0189	-0.0162	0.0404
MT3M8	0.0071	-0.0071	0.0054	UM1	0.0119	-0.0143	0.0191	UM39	0.0199	-0.0132	0.0278
LCM6	0.0072	-0.0015	-0.0017	MT4M28	0.0119	-0.0083	0.0087	MO3	0.0214	-0.0146	-0.0978
LCO1	0.0074	0.0244	0.0029	MT4M29	0.0120	-0.0078	0.0090	m9	0.0220	-0.0786	0.0125
LCM15	0.0074	-0.0089	0.0098	MT5S2	0.0122	-0.0126	0.0113	m36	0.0220	-0.0786	0.0125
UM18	0.0076	-0.0120	0.0255	RO3	0.0127	-0.0261	-0.0509	PVO16	0.0220	-0.0786	0.0125
TQM10	0.0078	-0.0090	0.0117	ICM13	0.0129	0.0018	0.0265	PM2	0.0221	-0.0169	0.0178
o1	0.0079	-0.0127	0.1515	MT4M9	0.0131	-0.0054	0.0103	m38	0.0231	-0.0212	0.0000
NO2	0.0082	0.0015	-0.0137	NM6	0.0131	0.0515	0.0747	o44	0.0232	0.0006	-0.0678
hus9	0.0087	-0.0265	0.0297	RO6	0.0132	0.0406	0.0165	TQM9	0.0239	-0.0105	0.0082
MT5M24	0.0088	-0.0031	0.0113	m19	0.0136	-0.0330	0.0884	PVM8	0.0241	-0.0128	0.0202
CCM20	0.0088	-0.0033	0.0013	m8	0.0138	-0.0802	0.0262	m31	0.0243	-0.0385	0.0576
UO13	0.0091	0.0205	0.0649	m24	0.0138	-0.0802	0.0262	MT2M6	0.0255	0.0179	-0.0023
LM5	0.0091	-0.0022	0.0106	m29	0.0138	-0.0802	0.0262	MT2M8	0.0255	0.0179	-0.0023
MT4M27	0.0094	-0.0040	0.0073	m40	0.0138	-0.0802	0.0262	MT3S2	0.0255	0.0179	-0.0023
UM15	0.0096	-0.0116	0.0143	o34	0.0139	-0.0031	0.0023	MT4S1	0.0255	0.0179	-0.0023
HS3	0.0097	-0.0080	0.0140	MO8	0.0141	-0.0075	0.0540	MO5	0.0255	0.0497	0.0535
PM1	0.0097	-0.0083	0.0133	MO4	0.0142	-0.0184	-0.0041	o7	0.0263	-0.0049	-0.0189
AS5	0.0097	0.0645	0.0480	CO2	0.0148	-0.0072	0.0641	MO6	0.0267	-0.0114	0.1254
CBM13	0.0097	0.0645	0.0480	AM20	0.0150	-0.0116	0.0091	m26	0.0271	-0.0210	0.0684
US9	0.0099	-0.0215	0.0216	o53	0.0151	-0.0934	-0.0365	MM15	0.0277	-0.0514	0.0843
LCM8	0.0100	0.0168	0.0591	CCM28	0.0155	0.0067	0.0071	MM30	0.0277	-0.0514	0.0843
o49	0.0103	0.0343	0.0051	o18	0.0157	0.0445	0.0576	RO5	0.0277	-0.0085	0.0166
o2	0.0104	-0.0255	0.0519	TQM2	0.0164	0.0448	0.0677	o46	0.0278	0.1154	0.2197
PVS12	0.0105	0.0648	0.0581	CBM8	0.0169	0.0698	0.0400	o51	0.0283	0.1472	0.1574
MC3O2	0.0105	0.0290	-0.0449	huo6	0.0170	-0.1134	-0.0874	CCM26	0.0284	-0.0220	0.0254
o6	0.0107	-0.0073	-0.0489	PVM3	0.0176	-0.0246	0.0133	m32	0.0286	-0.0550	0.0729
PM9	0.0108	-0.0067	0.0099	MT4M22	0.0182	0.0706	-0.0291	m33	0.0286	-0.0550	0.0729
MT2O1	0.0110	0.0545	-0.0793	MT5M18	0.0182	0.0706	-0.0291	AM13	0.0286	-0.0550	0.0729
m12	0.0113	-0.0713	0.0614	MT5M19	0.0182	0.0706	-0.0291	AS8	0.0289	0.0067	0.0425

	All characters		
	PC1	PC2	PC3
MT3M24	0.0290	0.0589	-0.0263
CCM27	0.0292	-0.0223	0.0168
UM9	0.0295	-0.0168	0.0101
o36	0.0302	0.0181	0.0379
MT2M5	0.0312	0.0451	0.0695
o15	0.0324	-0.0044	0.0873
o37	0.0324	-0.0387	0.0257
MT3M5	0.0325	0.0477	0.0185
UM7	0.0355	-0.0191	0.0205
o43	0.0358	-0.0619	0.1491
UO14	0.0371	-0.0132	0.1044
o11	0.0389	-0.0107	0.0343
MM14	0.0389	-0.0088	0.0525
PVS11	0.0390	-0.0151	0.0861
huo8	0.0400	0.0058	-0.0598
UM10	0.0406	-0.0228	0.0149
o50	0.0418	0.0502	0.1113
MT3S3	0.0419	0.0378	0.0206
UM8	0.0422	-0.0240	0.0258
m30	0.0423	-0.0218	0.0792
m17	0.0433	-0.0255	0.0734
m18	0.0433	-0.0255	0.0734
CCM7	0.0441	0.0363	0.0315
o40	0.0468	-0.0168	0.0612
MO1	0.0487	-0.1024	-0.0373
MT3M25	0.0501	0.0393	0.0068
MT3M1	0.0501	0.0393	0.0068
MT3M6	0.0501	0.0393	0.0068
ICM7	0.0501	0.0393	0.0068
PVO2	0.0522	-0.0252	0.0272
MM22	0.0532	-0.0336	0.0820
o35	0.0532	0.0090	-0.0322
o21	0.0560	0.0424	-0.0178

	All characters		
	PC1	PC2	PC3
o54	0.0564	0.0132	0.0190
MM21	0.0614	-0.0320	0.0683
MM29	0.0614	-0.0320	0.0683
o25	0.0639	-0.0408	0.0331
PO3	0.0639	-0.0408	0.0331
RO1	0.0647	-0.0387	0.0613
o29	0.0687	-0.0848	0.0951
m2	0.0721	-0.0393	0.0193
MM23	0.0721	-0.0393	0.0193
huo4	0.0721	-0.0393	0.0193
huo9	0.0721	-0.0393	0.0193
TQO3	0.0721	-0.0393	0.0193
PO1	0.0721	-0.0393	0.0193
CCO1	0.0721	-0.0393	0.0193
RO4	0.0753	-0.0156	-0.0094
o17	0.0753	-0.0033	0.1263
o30	0.0832	-0.1062	0.0290
UO7	0.0883	-0.0641	0.0487
UO8	0.0901	-0.0458	0.0142
o28	0.0926	-0.0839	0.0274
o19	0.1556	-0.0796	-0.0746
	Cranial characters		
	PC1	PC2	PC3
o23	-0.4724	-0.5783	-0.1381
o20	-0.3484	0.1376	-0.0312
o12	-0.1946	-0.1214	0.0891
o24	-0.1737	0.0738	-0.0150
o4	-0.1481	-0.2007	0.0625
o56	-0.1475	0.0895	-0.0662
o33	-0.1247	-0.1152	0.2438
o45	-0.0953	-0.0563	0.0417
o3	-0.0808	-0.0006	0.0794
o26	-0.0795	-0.0270	0.0870

	All characters		
	PC1	PC2	PC3
o10	-0.0719	0.0027	0.1880
m14	-0.0717	-0.0328	0.0999
o39	-0.0647	0.0485	0.0157
o32	-0.0564	0.0481	-0.0285
o48	-0.0561	-0.0053	-0.2714
o22	-0.0498	0.0519	0.1315
o57	-0.0453	0.0958	-0.1381
o41	-0.0333	0.0185	0.1743
m15	-0.0251	-0.1292	0.0215
o5	-0.0227	0.0046	0.0813
m4	-0.0212	-0.0595	0.0652
o31	-0.0187	0.0738	0.0441
o47	-0.0181	-0.1024	-0.0195
o38	-0.0096	-0.0154	-0.0927
o51	-0.0093	0.0015	-0.4090
m43	-0.0085	0.0044	0.0025
o16	-0.0077	-0.0188	0.1117
m37	-0.0066	-0.0783	0.0913
m28	-0.0056	0.0371	-0.0138
o52	-0.0036	-0.0490	0.1568
m42	-0.0005	-0.0061	-0.0011
o55	-0.0003	0.0679	-0.0434
o42	0.0000	0.0000	0.0000
m39	0.0017	-0.0012	-0.0001
m6	0.0055	-0.0110	0.0078
m16	0.0058	0.0050	-0.0192
m7	0.0064	-0.0367	0.0257
o46	0.0068	-0.0666	-0.4758
o18	0.0117	0.0023	-0.0852
o6	0.0135	0.0407	0.0464
o49	0.0143	0.0367	-0.0653
m34	0.0154	-0.0341	0.0560
o34	0.0157	-0.0134	-0.0026

	Cranial characters		
	PC1	PC2	PC3
o44	0.0250	0.0852	0.0565
m1	0.0295	-0.1268	0.0507
m35	0.0306	-0.1125	-0.0004
o1	0.0307	-0.1840	-0.1264
m25	0.0325	-0.1010	0.0457
m1.1	0.0345	-0.1025	-0.0564
m13	0.0345	-0.1025	-0.0564
m21	0.0345	-0.1025	-0.0564
m19	0.0397	-0.1183	-0.0624
o36	0.0418	-0.0028	-0.0632
m38	0.0453	-0.0127	0.0169
o7	0.0506	0.0326	-0.0159
o2	0.0534	-0.0709	-0.0048
m11	0.0570	-0.1526	0.0341
m20	0.0570	-0.1526	0.0341
m22	0.0570	-0.1526	0.0341
m23	0.0570	-0.1526	0.0341
o37	0.0647	-0.0485	-0.0157
m31	0.0668	-0.0764	-0.0353
m12	0.0685	-0.1235	0.0345
o21	0.0685	0.1022	-0.0808
m3	0.0691	-0.0873	0.0309
m8	0.0704	-0.1120	0.0806
m24	0.0704	-0.1120	0.0806
m29	0.0704	-0.1120	0.0806
m40	0.0704	-0.1120	0.0806
o11	0.0720	-0.0350	-0.0565
o50	0.0733	-0.0427	-0.1918
o40	0.0793	-0.0878	-0.0598
m9	0.0820	-0.0828	0.0809
m36	0.0820	-0.0828	0.0809
m26	0.0846	-0.0744	-0.0293
o15	0.0885	-0.0638	-0.0429

	Cranial characters		
	PC1	PC2	PC3
m17	0.0897	-0.0640	-0.0308
m18	0.0897	-0.0640	-0.0308
o35	0.0901	0.0838	-0.0301
o53	0.0903	-0.0401	0.1768
o54	0.0924	0.0298	-0.0791
m30	0.0964	-0.0867	-0.0681
m32	0.0965	-0.1131	0.0144
m33	0.0965	-0.1131	0.0144
o43	0.1040	-0.1983	-0.0504
o25	0.1306	-0.0491	-0.0009
o17	0.1359	-0.0779	-0.1551
m2	0.1422	-0.0199	-0.0006
o29	0.1840	-0.1230	0.0326
o30	0.2034	-0.0997	0.0595
o28	0.2123	-0.0640	0.0366
o19	0.3173	0.0487	0.0203
	Mandible characters		
	PC1	PC2	PC3
MO3	-0.0947	-0.3246	0.2233
MO2	-0.0895	-0.2549	-0.0334
MM16	-0.0021	0.0534	-0.0513
MO7	0.0000	0.0000	0.0000
MM24	0.0110	0.0675	-0.0841
MO5	0.0358	0.3367	0.1725
MO4	0.0663	-0.0377	0.0432
MM18	0.0712	0.0166	-0.4473
MO8	0.0814	0.1921	0.0047
MM17	0.1446	-0.0180	-0.3848
MM14	0.1650	0.1247	0.1021
MM23	0.1935	0.0227	0.3918
MO6	0.2150	0.2810	-0.0745
MS1	0.2269	-0.0887	-0.1038
MM31	0.2296	-0.0502	-0.1812

	Mandible characters		
	PC1	PC2	PC3
MM21	0.2409	0.1850	0.2801
MM29	0.2409	0.1850	0.2801
MM19	0.2556	-0.0850	-0.2506
MM22	0.2781	0.1192	0.1500
MM20	0.2819	0.0092	-0.1748
MM28	0.2819	0.0092	-0.1748
MM15	0.3056	0.0101	-0.0031
MM30	0.3056	0.0101	-0.0031
MO1	0.3537	-0.6887	0.2076
	Forelimb characters		
	PC1	PC2	PC3
RO4	-0.0923	0.1365	-0.0232
UO8	-0.0868	0.1869	-0.0021
UO7	-0.0710	0.1852	-0.1713
huo4	-0.0688	0.1641	0.0112
huo9	-0.0688	0.1641	0.0112
RO1	-0.0687	0.1610	0.1372
huo8	-0.0517	0.0515	0.1358
RO6	-0.0463	-0.0761	0.0419
UO14	-0.0429	0.0923	-0.0555
UM8	-0.0401	0.0937	-0.0260
RO5	-0.0389	0.0341	-0.2050
UM10	-0.0387	0.0932	-0.0037
UM7	-0.0345	0.0780	-0.0072
UO13	-0.0341	-0.0429	0.0724
huo7	-0.0339	-0.1699	0.2219
UM9	-0.0279	0.0638	-0.0189
UM39	-0.0202	0.0516	-0.0105
UM40	-0.0115	-0.0080	-0.0145
UO2	-0.0102	-0.1379	0.0442
UM38	-0.0079	-0.0105	-0.0207
UM1	-0.0076	0.0384	0.0004
RO3	-0.0076	0.0994	0.0224

	Forelimb characters		
	PC1	PC2	PC3
hum60	-0.0074	-0.0196	-0.0229
UM3	-0.0059	0.0199	-0.0064
UM15	-0.0056	0.0351	-0.0159
hum8	-0.0032	0.0215	0.0085
hum45	-0.0030	0.0062	-0.0148
UM18	-0.0027	0.0295	-0.0006
hum50	-0.0025	0.0056	0.0182
UM27	-0.0017	0.0084	-0.0026
UM28	-0.0012	0.0169	0.0054
hum56	-0.0011	-0.0003	-0.0078
hum30	-0.0011	0.0169	-0.0026
US9	-0.0010	0.0563	-0.0041
hum41	-0.0002	0.0041	0.0053
UM32	-0.0001	0.0003	0.0049
huo1	0.0000	0.0000	0.0000
huo2	0.0000	0.0000	0.0000
hum35	0.0003	-0.0024	-0.0140
RM29	0.0004	0.0206	-0.0100
hum44	0.0009	0.0017	-0.0155
UM16	0.0015	0.0220	-0.0017
hum24	0.0019	0.0282	0.0066
hum39	0.0021	-0.0101	0.0026
hum42	0.0024	0.0005	0.0201
hum51	0.0028	0.0101	0.0142
hum36	0.0028	0.0147	-0.0014
UO10	0.0028	-0.0547	0.0451
RM18	0.0029	0.0150	-0.0029
UO12	0.0033	-0.1493	-0.1013
hum2	0.0035	0.0212	0.0161
UM30	0.0038	0.0095	0.0011
hus9	0.0040	0.0665	0.0141
hum13	0.0041	-0.0242	0.0098
UM37	0.0043	-0.0015	-0.0092

	Forelimb characters		
	PC1	PC2	PC3
US10	0.0047	0.0073	-0.0225
hum11	0.0050	-0.0193	-0.0052
UM17	0.0053	0.0057	0.0017
RM9	0.0054	0.0105	-0.0019
UM35	0.0054	0.0207	0.0130
hum62	0.0055	-0.0123	0.0004
US12	0.0057	0.0136	-0.0043
hum53	0.0058	-0.0152	-0.0062
hum5	0.0065	-0.0211	-0.0109
UM2	0.0067	0.0038	-0.0001
hum57	0.0069	-0.0127	-0.0074
hum29	0.0071	-0.0166	-0.0208
RM4	0.0071	0.0027	0.0081
UM14	0.0072	-0.0108	-0.0117
hum22	0.0074	-0.0081	-0.0076
hum23	0.0075	-0.0012	-0.0129
hum40	0.0076	-0.0128	0.0182
UM41	0.0077	-0.0555	-0.0046
UM4	0.0081	0.0138	-0.0098
RM5	0.0084	0.0035	0.0074
RM19	0.0084	-0.0288	0.0040
hum4	0.0086	-0.0618	-0.0188
RM10	0.0091	0.0060	0.0134
UM26	0.0092	-0.0253	-0.0008
hum16	0.0095	-0.0220	-0.0083
UM25	0.0096	0.0128	-0.0022
huo3	0.0096	-0.0236	-0.1640
RM8	0.0096	0.0090	0.0107
RM16	0.0098	0.0034	0.0047
UM29	0.0098	0.0062	-0.0082
hum26	0.0099	0.0051	0.0035
hum55	0.0100	-0.0517	0.0092
hum14	0.0101	-0.0117	0.0047

	Forelimb characters		
	PC1	PC2	PC3
hum32	0.0106	-0.0113	-0.0075
hum27	0.0107	0.0021	0.0027
RM13	0.0108	0.0085	-0.0001
UM11	0.0109	-0.0154	-0.0047
hum37	0.0112	-0.0099	0.0029
RM22	0.0118	-0.0306	0.0085
hum33	0.0118	-0.0101	0.0229
hum31	0.0119	-0.0196	-0.0016
hum34	0.0120	0.0147	0.0173
RM2	0.0120	0.0144	0.0152
RM27	0.0121	-0.0238	-0.0131
hum7	0.0121	-0.0303	0.0025
RM17	0.0123	-0.0152	-0.0175
RM3	0.0126	-0.0024	0.0049
hum28	0.0126	0.0145	-0.0042
Rs2	0.0132	0.0100	0.0202
RM24	0.0133	-0.0243	0.0056
RM7	0.0135	0.0096	0.0082
RM15	0.0136	0.0020	0.0035
hum1	0.0137	-0.0484	-0.0038
RM25	0.0138	-0.0195	-0.0018
RM23	0.0140	-0.0114	0.0014
hum47	0.0142	-0.0546	-0.0255
UM34	0.0145	-0.0104	0.0149
RM6	0.0147	0.0132	0.0082
UM5	0.0147	-0.0268	-0.0133
RM20	0.0152	-0.0068	-0.0129
hum46	0.0154	-0.0428	-0.0043
hum9	0.0155	-0.0254	0.0124
hum25	0.0156	-0.0140	0.0093
US11	0.0157	0.0591	0.0017
RM12	0.0162	-0.0053	0.0116
RS1	0.0166	0.0077	-0.0063

	Forelimb characters		
	PC1	PC2	PC3
UM6	0.0168	-0.0216	-0.0112
UM21	0.0175	-0.0345	-0.0230
hum20	0.0176	-0.0120	0.0095
RM28	0.0178	-0.0399	-0.0001
hum48	0.0185	-0.0547	-0.0261
hum38	0.0195	-0.0052	0.0157
hum10	0.0205	-0.0540	0.0022
UM31	0.0207	-0.0405	-0.0070
US13	0.0212	-0.0700	-0.0183
hus10	0.0218	0.0108	0.0083
hum15	0.0228	-0.0518	0.0008
hus5	0.0241	-0.0164	-0.0414
hum54	0.0309	-0.0738	-0.0050
UM35.1	0.0316	-0.0868	0.1059
UM20	0.0326	-0.0657	-0.0084
hus7	0.0365	0.0083	0.0577
hus8	0.0372	-0.0127	0.0203
hus6	0.0401	0.0158	0.0196
huo6	0.0421	0.2701	-0.4634
US14	0.0439	-0.0508	-0.0098
RO7	0.0439	-0.0828	0.1446
UM19	0.0442	-0.1035	-0.0104
RM11	0.0462	-0.0108	-0.0060
RM21	0.0467	-0.1414	-0.0119
UO11	0.0555	0.1601	0.0480
RM14	0.0608	-0.1296	0.0315
UM12	0.0708	0.0390	-0.1011
UM41.1	0.0746	0.0017	0.0295
UM22	0.0780	0.0189	-0.1762
UO4	0.0821	-0.0094	0.0259
RO2	0.1037	0.0095	-0.0051
UO9	0.1066	-0.2957	0.2080
UO6	0.1198	0.0714	-0.2276

	Forelimb characters		
	PC1	PC2	PC3
UO1	0.1287	-0.3303	0.0108
UO5	0.1371	0.0598	-0.1208
huo5	0.1556	-0.3607	-0.5701
UO3	0.1842	-0.1821	-0.0974
RM26	0.8694	0.2924	0.1769
	Manus characters		
	PC1	PC2	PC3
TQO4	-0.5186	-0.0444	0.1046
MC4O3	-0.2647	-0.1003	0.4307
MC3O3	-0.2456	-0.1843	0.0827
TZMO1	-0.2173	0.1757	0.2092
PO2	-0.1770	-0.0255	0.0769
HM17	-0.1748	-0.0088	-0.0758
LS1	-0.1748	-0.0088	-0.0758
TQO2	-0.1710	-0.1202	-0.1593
TQO1	-0.1611	0.3996	-0.1908
MC1M12	-0.1526	0.0544	-0.1362
MC1S2	-0.1526	0.0544	-0.1362
TZMM2	-0.1526	0.0544	-0.1362
MC4M32	-0.1513	-0.0437	-0.1124
TQO6	-0.1406	-0.1153	0.0281
TQO5	-0.1305	-0.0271	-0.0571
MC1M13	-0.1292	0.0195	-0.1729
MC1M16	-0.1292	0.0195	-0.1729
HM2	-0.1292	0.0195	-0.1729
TZDM7	-0.1292	0.0195	-0.1729
TZMM7	-0.1292	0.0195	-0.1729
MC5M24	-0.1079	0.2212	0.0855
LS5	-0.1035	0.0693	-0.1867
HM8	-0.0906	0.0144	-0.1988
CO5	-0.0743	0.1673	0.1017
TZMO4	-0.0721	0.1839	-0.0510
SO1	-0.0686	-0.1589	0.0058

	Manus characters		
	PC1	PC2	PC3
HM1.1	-0.0626	-0.0006	0.0629
HM1	-0.0612	0.0871	0.0124
MC3M17	-0.0591	-0.0821	-0.0660
TZMM17	-0.0561	0.0153	0.0484
MC2O1	-0.0501	-0.1296	0.2269
CO1	-0.0466	0.0016	0.1340
TZMM19	-0.0427	0.0190	0.0418
MC5O1	-0.0355	-0.0764	0.0011
SM10	-0.0333	0.0065	-0.0082
MC2M10	-0.0290	0.0298	-0.0030
SM1	-0.0290	0.0527	-0.0590
CM14.1	-0.0265	0.2802	0.0274
CS3	-0.0263	-0.0012	-0.0540
CM14	-0.0254	0.0540	-0.0002
MC1S1	-0.0234	0.1258	-0.0594
SM5	-0.0231	0.0256	-0.0170
CM22	-0.0227	0.0352	-0.0189
LS6	-0.0222	0.0621	-0.0015
TZMS1	-0.0222	0.0824	-0.0321
MC3M32	-0.0220	0.2321	0.1502
CM5	-0.0213	0.0109	-0.0029
MC1M2	-0.0211	0.0319	-0.0066
HM4	-0.0205	-0.0027	0.0030
CM1	-0.0186	0.0159	0.0024
TQM2	-0.0185	-0.0292	-0.2211
SM3	-0.0179	0.0286	-0.0124
CM10	-0.0177	0.0002	-0.0182
HM14	-0.0166	0.0165	0.0035
HS4	-0.0160	0.0416	-0.0073
MC2M11	-0.0156	0.0312	0.0015
TZDM12	-0.0154	0.0298	-0.0142
LM4	-0.0152	0.0105	-0.0112
TZMM5	-0.0141	0.0180	0.0026

	Manus characters		
	PC1	PC2	PC3
TZMM9	-0.0140	0.0128	-0.0066
MC1M10	-0.0138	0.0362	-0.0091
CM20	-0.0137	-0.0061	-0.0218
TZMM3	-0.0128	0.0238	-0.0045
LM3	-0.0126	0.0183	0.0013
CM11	-0.0121	0.0198	-0.0001
MC1M11	-0.0113	0.0267	-0.0041
HM16	-0.0110	0.0164	-0.0061
CM4	-0.0108	-0.0095	-0.0066
LM2	-0.0107	0.0256	-0.0151
TZDM9	-0.0107	0.0224	-0.0123
SM8	-0.0106	0.0290	-0.0147
TZMM11	-0.0104	0.0077	-0.0014
MC3O2	-0.0101	-0.0882	0.0852
TZDM1	-0.0096	0.0157	-0.0142
MC1M14	-0.0095	0.0064	-0.0110
CM16	-0.0094	-0.0013	0.0003
MC3M34	-0.0092	0.0023	0.0012
LS9	-0.0089	0.0091	-0.0187
TZMM6	-0.0088	0.0040	-0.0011
TZDM10	-0.0088	-0.0002	-0.0120
MC2M25	-0.0088	0.0142	-0.0022
MC2M24	-0.0082	0.0099	-0.0074
CS5	-0.0080	0.0018	0.0036
LM7	-0.0078	-0.0049	-0.0364
HM12	-0.0078	0.0145	-0.0050
SM9	-0.0078	0.0138	-0.0022
LM8	-0.0075	0.0168	-0.0029
MC3M19	-0.0071	0.0015	-0.0130
MC4M34	-0.0069	0.0053	-0.0004
MC1M3	-0.0069	0.0267	-0.0199
MC1M1	-0.0068	0.0400	-0.0225
TZDM2	-0.0065	0.0102	-0.0245

	Manus characters		
	PC1	PC2	PC3
MC5M25	-0.0065	-0.0046	-0.0005
TQM5	-0.0063	0.0104	-0.0143
LM6	-0.0063	0.0017	-0.0072
CM7	-0.0061	0.0037	0.0082
CM6	-0.0060	0.0016	-0.0178
LM13	-0.0058	0.0398	-0.0389
SM2	-0.0053	0.0381	-0.0051
TZMM8	-0.0053	0.0041	-0.0037
LM1	-0.0051	0.0237	-0.0091
TQM3	-0.0048	0.0190	0.0106
TQM6	-0.0047	0.0111	-0.0104
HM15	-0.0045	0.0154	0.0010
LM10	-0.0043	-0.0047	-0.0359
TZMM4	-0.0038	0.0157	-0.0087
TZDM8	-0.0038	0.0184	-0.0124
MC4M20	-0.0035	0.0130	-0.0030
MC2M7	-0.0032	0.0137	-0.0143
LM14	-0.0031	0.0396	-0.0269
HM9	-0.0031	0.0196	-0.0251
MC4M19	-0.0027	0.0092	-0.0086
MC3M20	-0.0027	0.0154	-0.0188
HM18	-0.0027	0.0162	-0.0028
MC5M26	-0.0025	0.0092	-0.0066
TZDM5	-0.0024	0.0304	0.0021
TZMM10	-0.0024	0.0058	-0.0068
CM21	-0.0022	0.0001	-0.0159
HM3	-0.0020	0.0014	-0.0104
HM13	-0.0020	-0.0008	-0.0150
SM12	-0.0019	0.0021	-0.0025
PM7	-0.0018	-0.0033	-0.0140
CM13	-0.0018	0.0091	-0.0008
SM11	-0.0018	0.0250	-0.0243
SM4	-0.0013	0.0101	-0.0177

	Manus characters		
	PC1	PC2	PC3
TZDM3	-0.0011	0.0085	-0.0183
TZMM1	-0.0011	0.0331	-0.0178
SM7	-0.0006	0.0330	-0.0140
SM6	-0.0003	0.0105	-0.0081
PM10	-0.0002	0.0010	-0.0264
CM18	-0.0001	0.0015	-0.0017
LO1	0.0000	0.0000	0.0000
MC4O2	0.0000	0.0000	0.0000
CO4	0.0000	0.0000	0.0000
TZMO2	0.0000	0.0000	0.0000
TZMO3	0.0000	0.0000	0.0000
CM2	0.0005	0.0058	-0.0197
LM16	0.0006	0.0011	-0.0003
LM15	0.0008	0.0016	-0.0004
MC4M21	0.0009	0.0102	-0.0040
MC4M17	0.0009	0.0051	-0.0057
HM19	0.0012	0.0107	-0.0214
SMS2	0.0015	0.0183	-0.0084
MC3M33	0.0016	0.0098	-0.0087
MC4M33	0.0020	0.0013	-0.0095
LM12	0.0029	0.0397	-0.0128
CM19	0.0031	0.0076	-0.0168
MC2M9	0.0034	0.0050	-0.0131
MC2M26	0.0037	0.2819	0.1364
MC2S2	0.0037	0.2819	0.1364
CM12	0.0039	-0.0144	0.0004
CM3	0.0043	0.0066	-0.0228
TZMM15	0.0043	0.0017	-0.0232
CS4	0.0044	0.0068	-0.0064
PM8	0.0052	0.0143	-0.0248
MC4M16	0.0053	0.0018	-0.0175
HM5	0.0053	0.0172	-0.0181
TZDM11	0.0054	0.0115	0.0011

Manus characters			
	PC1	PC2	PC3
PM3	0.0055	0.0027	-0.0194
MC3M16	0.0055	0.0085	-0.0061
MC3M21	0.0059	0.0158	-0.0214
HM7	0.0064	0.0145	-0.0083
CM8	0.0065	0.0005	-0.0082
TQM1	0.0072	0.0077	-0.0138
MC5M12	0.0073	0.0024	-0.0306
MC4M18	0.0075	0.0022	-0.0097
MC2M8	0.0077	0.0050	-0.0067
HM11	0.0078	0.0115	-0.0009
MC5M13	0.0083	-0.0047	-0.0345
MC3M18	0.0083	0.0051	-0.0142
LM9	0.0085	-0.0178	-0.0559
HM6	0.0094	0.0079	-0.0189
PM5	0.0097	0.0162	-0.0017
TQM7	0.0125	0.0164	-0.0419
TQM4	0.0132	0.0172	-0.0164
SM15	0.0148	0.0204	-0.0417
MC2M12	0.0152	0.0207	-0.0407
PM11	0.0156	0.0081	-0.0306
LM5	0.0215	0.0002	-0.0384
TQM10	0.0226	0.0251	-0.0311
HS3	0.0239	0.0219	-0.0353
PM1	0.0253	0.0192	-0.0314
PM9	0.0272	0.0095	-0.0271
CO2	0.0279	0.0664	-0.1665
TQM8	0.0291	0.0087	-0.0178
PM6	0.0303	0.0158	-0.0296
PM4	0.0323	0.0191	-0.0149
CO3	0.0355	0.0764	-0.0011
TQO7	0.0443	0.1264	-0.1209
SMS1	0.0480	0.2636	0.1551
TZDM4	0.0480	0.2636	0.1551

Manus characters			
	PC1	PC2	PC3
TQM9	0.0560	0.0040	-0.0338
PM2	0.0564	0.0277	-0.0452
PO3	0.1536	0.0603	-0.0402
TQO3	0.1770	0.0255	-0.0769
PO1	0.1770	0.0255	-0.0769
Pelvis characters			
	PC1	PC2	PC3
PVO1	-0.8101	0.2373	-0.1607
PVO2	-0.3260	-0.5623	0.1643
PVS11	-0.2205	-0.2053	-0.1113
PVM5	-0.1354	-0.0644	0.0347
PVS12	-0.1025	0.1375	0.3632
PVO5	-0.0950	0.3206	0.1809
PVM8	-0.0869	-0.0973	0.0641
PVM6	-0.0603	0.0798	0.0710
PVM18	-0.0405	0.1377	-0.3368
PVM4	-0.0183	-0.0330	-0.1865
PVM23	-0.0177	-0.0704	-0.5500
PVO14	0.0000	0.0000	0.0000
PVM2	0.0000	0.0000	0.0000
PVM3	0.0033	-0.1983	-0.0668
PVO16	0.0036	-0.2605	-0.0466
PVO17	0.0122	0.3514	-0.2978
PVM20	0.0124	0.1312	-0.2458
PVO10	0.0987	0.3296	0.1433
PVO15	0.1056	0.1792	0.0948
PVO6	0.2029	-0.1409	-0.3514
PVM7	0.2740	-0.1009	-0.0174
Pes characters			
	PC1	PC2	PC3
LCR1	-0.4519	0.2442	0.2385
NO1	-0.2270	-0.0936	-0.0701
AM1	-0.1537	0.0311	0.1051

Pes characters			
	PC1	PC2	PC3
ICM9	-0.1497	-0.0654	0.0768
AM23	-0.1486	0.0872	-0.0354
MT1S1	-0.1441	-0.0874	0.0570
MT2M25	-0.1441	-0.0874	0.0570
CBS3	-0.1431	0.0652	-0.0552
MT2M17	-0.1430	-0.1024	-0.0062
MCM2	-0.1430	-0.1024	-0.0062
CCS11	-0.1312	0.0716	0.0308
MT4S2	-0.1312	-0.0960	0.0797
MT2M26	-0.1298	0.0794	0.0772
NM8	-0.1258	0.1506	-0.0002
CCM17	-0.1258	-0.0170	0.0488
MT2M24	-0.1246	-0.1331	-0.0033
AM18	-0.1235	0.0195	-0.1155
AS5	-0.1181	0.0985	-0.1464
CBM13	-0.1181	0.0985	-0.1464
AM4	-0.1125	-0.1114	-0.0873
AM5	-0.1125	-0.1114	-0.0873
MCM12	-0.1125	-0.1114	-0.0873
MCM16	-0.1125	-0.1114	-0.0873
MT1S3	-0.1089	-0.1243	0.0296
AM17	-0.1085	-0.0326	0.1150
MCS3	-0.1085	-0.0402	-0.1646
MT1M7	-0.1078	-0.1394	-0.0337
MT1M1.1	-0.1078	-0.1394	-0.0337
AS1	-0.1038	-0.0682	-0.1110
NM5	-0.0982	0.0554	-0.0672
MT3O1	-0.0971	-0.1179	0.1155
MT5s1	-0.0969	-0.0607	-0.1193
MT1M9	-0.0951	-0.1270	-0.0211
MCM17	-0.0940	0.0256	-0.1333
MCS4	-0.0937	-0.0605	0.0616
CBM8	-0.0926	0.0921	-0.0506

	Pes characters				Pes characters				Pes characters		
	PC1	PC2	PC3		PC1	PC2	PC3		PC1	PC2	PC3
MT2S12	-0.0915	0.0183	-0.1502	MT2M14	-0.0238	-0.0483	0.0280	MCM14	-0.0048	-0.0183	0.0010
MT1M11	-0.0893	-0.1701	-0.0307	AM24	-0.0234	-0.0186	0.0084	AM11	-0.0047	-0.0148	0.0087
NM6	-0.0887	0.1046	-0.1643	CCM18	-0.0180	0.0106	-0.0018	CCM24	-0.0047	0.0001	-0.0071
CBM14	-0.0886	-0.0630	-0.1153	CCM4	-0.0145	-0.0076	-0.0042	AM10	-0.0047	-0.0114	-0.0112
CBM15	-0.0886	-0.0630	-0.1153	AM6	-0.0121	-0.0084	-0.0038	MT4M25	-0.0044	-0.0046	-0.0038
CBM17	-0.0886	-0.0630	-0.1153	CCM1	-0.0118	-0.0082	0.0025	NM13	-0.0044	0.0003	0.0105
CBM18	-0.0886	-0.0630	-0.1153	CCM3	-0.0113	-0.0024	-0.0082	CBM21	-0.0044	-0.0047	-0.0108
MCO3	-0.0880	0.0575	0.0464	AM31	-0.0104	0.0057	0.0021	NM2	-0.0040	-0.0148	-0.0115
CBM16	-0.0846	0.0082	-0.1926	CCM10	-0.0103	-0.0064	-0.0137	MT2M21	-0.0039	-0.0161	0.0110
LCM28	-0.0839	0.0635	0.0416	MCM13	-0.0102	-0.0060	-0.0038	MT1M13	-0.0038	-0.0200	0.0061
MCS2	-0.0838	-0.1113	-0.0318	AM14	-0.0099	-0.0025	-0.0132	MT1M12	-0.0038	-0.0226	-0.0024
MT2S8	-0.0799	-0.0330	0.0132	CCM8	-0.0095	-0.0017	-0.0060	AM9	-0.0033	-0.0047	-0.0121
LC02	-0.0776	0.0400	0.1799	CCM7	-0.0095	0.1316	-0.1041	MT1M6	-0.0031	-0.0286	0.0074
MCM1	-0.0732	-0.0903	-0.0399	ICM13	-0.0091	0.0253	-0.0872	MCM18	-0.0029	-0.0168	-0.0048
MT4M22	-0.0599	0.1503	0.0799	AM29	-0.0086	-0.0050	-0.0004	MT2M1	-0.0027	-0.0225	-0.0014
MT5M18	-0.0599	0.1503	0.0799	MT2M19	-0.0085	-0.0180	0.0170	MCM11	-0.0026	-0.0193	-0.0085
MT5M19	-0.0599	0.1503	0.0799	LCM3	-0.0084	-0.0097	0.0050	AM30	-0.0026	-0.0017	0.0064
LCM8	-0.0563	-0.0186	-0.1777	MT2M23	-0.0082	-0.0307	0.0161	CCS8	-0.0026	-0.0046	-0.0180
MCM15	-0.0560	-0.0049	0.0151	AM21	-0.0081	0.0024	0.0105	MCM4	-0.0023	-0.0253	-0.0098
MT2O1	-0.0556	0.0407	-0.0125	NM16	-0.0080	-0.0060	-0.0159	CBM12	-0.0021	-0.0015	-0.0065
CCM6	-0.0544	-0.0394	0.1091	NM20	-0.0077	-0.0134	-0.0094	CCM9	-0.0021	-0.0137	-0.0053
LCM2	-0.0523	0.0394	-0.1028	CBM10	-0.0070	0.0014	-0.0023	MT1M4	-0.0020	-0.0217	-0.0040
MT1M8	-0.0500	-0.1490	0.0167	MT5M8	-0.0064	-0.0044	-0.0095	NM15	-0.0019	-0.0071	-0.0083
MT1S2	-0.0500	-0.1490	0.0167	MT2M22	-0.0064	-0.0226	0.0129	ICM10	-0.0019	-0.0100	-0.0030
LCO1	-0.0454	0.0293	-0.1452	AM26	-0.0063	-0.0096	-0.0102	MT5M26	-0.0016	0.0076	-0.0084
MT2M29	-0.0412	0.1425	0.1925	ICM12	-0.0062	-0.0560	-0.0523	CCM25	-0.0015	0.0016	-0.0065
MT2S6	-0.0412	0.1425	0.1925	NM1	-0.0061	-0.0157	-0.0017	MCM6	-0.0013	-0.0113	0.0062
MT3M5	-0.0401	0.1405	-0.0230	CCM15	-0.0058	-0.0210	0.0055	AM15	-0.0011	0.0003	-0.0096
MT2M5	-0.0393	0.1465	-0.0964	MT2M20	-0.0057	-0.0220	0.0169	MT2M28	-0.0011	-0.0094	0.0070
MCS6	-0.0379	-0.1272	-0.0674	CBM11	-0.0052	-0.0023	0.0024	NM18	-0.0007	-0.0058	-0.0118
AM27.1	-0.0372	0.0460	0.1641	AM8	-0.0052	-0.0049	-0.0097	MT1M14	-0.0007	-0.1070	0.0846
MT3M24	-0.0361	0.1986	0.0519	MT2M16	-0.0050	-0.0097	-0.0081	CCM2	-0.0006	-0.0103	-0.0071
AM32	-0.0332	-0.0072	0.0310	MT2S7	-0.0050	-0.0425	0.0204	MT2M3	-0.0006	-0.0162	0.0084

	Pes characters		
	PC1	PC2	PC3
NM19	-0.0006	-0.0032	-0.0121
CBS6	-0.0004	0.0047	0.0023
MT3M2	-0.0003	-0.0047	-0.0008
MCM5	-0.0002	-0.0133	0.0021
CCM5	-0.0001	-0.0022	-0.0111
MT2M2	-0.0001	-0.0073	0.0004
MT2M15	-0.0001	0.0018	-0.0039
MCM7	-0.0001	-0.0066	-0.0023
MT3S3	0.0000	0.1676	-0.0489
CBM23	0.0000	-0.0010	-0.0162
LCM7	0.0000	0.0010	-0.0215
AS8	0.0000	0.0131	-0.1522
MT4O1	0.0000	0.0000	0.0000
MT5O1	0.0000	0.0000	0.0000
AO1	0.0000	0.0000	0.0000
CBO1	0.0000	0.0000	0.0000
MCO1	0.0000	0.0000	0.0000
MCO2	0.0000	0.0000	0.0000
MT1M5	0.0001	-0.0255	0.0048
MT5M23	0.0001	-0.0080	-0.0173
MT3M7	0.0002	-0.0029	-0.0010
NM21	0.0005	-0.0017	-0.0129
AM22	0.0007	-0.0101	-0.0130
AM25	0.0007	-0.0222	-0.0155
AM12	0.0008	0.0110	-0.0232
MT1M3	0.0008	-0.0386	0.0016
MT1M1	0.0009	-0.0378	-0.0042
MT2M31	0.0009	-0.0048	0.0039
MT3M25	0.0011	0.1526	-0.1122
MT3M1	0.0011	0.1526	-0.1122
MT3M6	0.0011	0.1526	-0.1122
ICM7	0.0011	0.1526	-0.1122
NO2	0.0011	-0.0151	-0.0633

	Pes characters		
	PC1	PC2	PC3
CCM16	0.0012	0.0037	-0.0183
ICM8	0.0014	-0.0118	-0.0154
ICM5	0.0014	-0.0122	-0.0063
CBM24	0.0015	-0.0062	-0.0144
MT3M12	0.0015	-0.0038	-0.0060
MT2M30	0.0018	-0.0190	-0.0003
MT5O2	0.0021	0.0037	-0.0079
MCM3	0.0022	-0.0168	-0.0096
NM3	0.0022	0.0048	-0.0064
MT2M13	0.0024	-0.0023	-0.0050
MT2M4	0.0030	-0.0022	-0.0076
CCM28	0.0031	0.0353	-0.0436
AM3	0.0035	-0.0177	-0.0243
MT3M13	0.0039	0.0051	-0.0032
MT2M6	0.0040	0.0712	-0.0773
MT2M8	0.0040	0.0712	-0.0773
MT3S2	0.0040	0.0712	-0.0773
MT4S1	0.0040	0.0712	-0.0773
MT2M27	0.0040	-0.0039	-0.0083
LCM17	0.0043	-0.0152	-0.0274
MT5M20	0.0043	0.0032	-0.0044
MCM10	0.0045	-0.0067	0.0034
MT4M24	0.0047	-0.0034	-0.0008
AM7	0.0047	-0.0145	-0.0156
MT5M22	0.0051	-0.0053	-0.0129
MT3M3	0.0054	-0.0021	-0.0073
CCM21	0.0054	0.0161	-0.0085
MT3M14	0.0056	-0.0110	-0.0167
MT3M4	0.0057	0.0026	-0.0069
AM16	0.0057	-0.0112	-0.0238
MCM9	0.0060	-0.0038	-0.0032
MT4M12	0.0061	0.0041	-0.0071
LCM5	0.0062	-0.0082	-0.0028

	Pes characters		
	PC1	PC2	PC3
CBM19	0.0063	0.0073	-0.0150
MCM8	0.0063	-0.0129	0.0011
MT5M9	0.0064	0.0061	-0.0106
ICM6	0.0064	-0.0041	-0.0039
MT5M21	0.0065	0.0012	-0.0044
MT2M18	0.0068	-0.0038	-0.0042
CBM20	0.0071	0.0094	-0.0048
NM17	0.0073	0.0015	-0.0204
CCM22	0.0074	0.0006	-0.0099
CBM9	0.0084	-0.0095	-0.0092
LCM4	0.0087	-0.0062	-0.0019
MT5M25	0.0088	0.0068	-0.0051
MT4M11	0.0095	0.0000	-0.0007
MT4M10	0.0098	-0.0010	-0.0099
LCM6	0.0100	0.0105	-0.0152
MT4M23	0.0104	0.0055	-0.0051
MT5M24	0.0108	0.0195	-0.0266
MT2M11	0.0108	-0.0008	-0.0085
MT4M13	0.0112	0.0093	-0.0251
CCM19	0.0116	-0.0033	-0.0108
MT4M26	0.0116	0.0022	-0.0150
CCM20	0.0126	0.0154	-0.0290
ICM11	0.0127	-0.0032	-0.0271
CCM23	0.0127	0.0065	-0.0125
LCM16	0.0130	-0.0202	-0.0126
CBM7	0.0130	0.0046	-0.0125
LCM1	0.0134	0.0022	-0.0144
MT3M15	0.0138	-0.0080	-0.0042
NS2	0.0140	-0.0110	-0.0046
LCM15	0.0142	-0.0183	-0.0478
MT4M27	0.0142	0.0158	-0.0238
MCS8	0.0145	-0.0094	0.0004
CBM22	0.0145	-0.0062	-0.0199

	Pes characters		
	PC1	PC2	PC3
NM14	0.0154	-0.0008	-0.0167
MT2M7	0.0155	-0.0002	-0.0256
MT3M8	0.0162	0.0076	-0.0221
AM28	0.0163	-0.0137	-0.0182
LCM14	0.0172	-0.0108	-0.0247
MT4M9	0.0198	0.0227	-0.0400
NM7	0.0200	-0.0210	0.0029
MT4M29	0.0225	0.0171	-0.0302
MT4M28	0.0235	0.0165	-0.0342
AM27	0.0236	-0.0232	0.0117
MT5S2	0.0285	0.0125	-0.0338
AM20	0.0291	0.0109	-0.0355
MT1M2	0.0361	-0.1986	-0.0519
CCM26	0.0541	0.0344	-0.0853
CCM27	0.0567	0.0232	-0.0856
CCO2	0.0913	-0.1414	0.2995
AM13	0.0949	-0.0065	-0.0923
CCO1	0.1323	0.0810	-0.1430
MT2M12	0.1497	-0.1023	-0.0278
MT3M26	0.1497	-0.1023	-0.0278

Appendix C: Chapter 3 distance matrices.

Separate sexes

	FCercop	MCercop	FColobus	MColobı	FGorilla	MGorill	FHyloba	MHyloba	FMacaca	MMaca	FNasalis	MNasalis	FPan_f	MPan_r	FPapio_f	MPapio	FPongo	MPong	FPresby
Cercopithecus_f	0	6.9652	11.45	12.54	17.026	16.659	18.044	17.9675	10.522	12.37	13.16	13.3469	15.91	16.35	14.005	13.51	16.88	17.25	13.02
Cercopithecus_m	6.965	0	12.099	12.7	17.042	16.514	18.014	17.4745	11.293	12.07	12.88	13.3409	16.25	16.09	13.203	13.35	16.39	16.76	13.85
Colobus_f	11.45	12.099	0	5.8301	17.044	16.949	20.246	20.0429	12.884	14.21	13.54	13.4782	16.32	16.65	15.519	14.75	18.01	18.2	11.88
Colobus_m	12.54	12.7	5.8301	0	17.14	16.99	20.424	20.1303	13.435	13.91	13.83	13.5084	17.03	16.96	15.416	14.83	18.87	18.74	12.41
Gorilla_f	17.03	17.042	17.044	17.14	0	4.6118	19.927	19.9591	15.719	16.74	15.18	14.2362	9.479	9.234	15.44	15.09	13.66	13.07	17.19
Gorilla_m	16.66	16.514	16.949	16.99	4.6118	0	19.707	19.8801	15.672	16.57	15.1	14.3546	9.347	9.139	15.189	14.58	13.08	12.4	17.25
Hylobates_f	18.04	18.014	20.246	20.424	19.927	19.707	0	5.94446	16.491	17.34	17.25	17.4037	17.58	17.58	17.99	18.05	17	17.45	18.31
Hylobates_m	17.97	17.475	20.043	20.13	19.959	19.88	5.9445	0	16.599	16.94	17.28	17.388	17.57	17.38	17.755	18.01	16.44	16.87	18.57
Macaca_f	10.52	11.293	12.884	13.435	15.719	15.672	16.491	16.5993	0	7.664	12.78	12.7829	15	14.92	13.012	12.5	16.58	16.48	14.2
Macaca_m	12.37	12.071	14.21	13.915	16.745	16.572	17.342	16.9447	7.6645	0	13.68	13.1744	16.26	15.33	12.997	13.2	16.99	16.96	15.53
Nasalis_f	13.16	12.877	13.541	13.831	15.177	15.097	17.248	17.2849	12.782	13.68	0	7.3313	14.1	14.37	14.571	14.62	15.5	16.08	12.52
Nasalis_m	13.35	13.341	13.478	13.508	14.236	14.355	17.404	17.388	12.783	13.17	7.331	0	14.18	13.9	13.765	14.35	16.18	16.42	13.26
Pan_f	15.91	16.252	16.322	17.031	9.4785	9.3466	17.577	17.5734	14.997	16.26	14.1	14.1802	0	5.69	15.217	15.3	12.19	12.64	16.32
Pan_m	16.35	16.091	16.65	16.959	9.2338	9.1394	17.579	17.3768	14.924	15.33	14.37	13.9006	5.69	0	15.099	15.42	12.16	12.34	16.64
Papio_f	14	13.203	15.519	15.416	15.44	15.189	17.99	17.7554	13.012	13	14.57	13.7655	15.22	15.1	0	6.345	15.95	15.77	17.38
Papio_m	13.51	13.348	14.754	14.825	15.086	14.577	18.046	18.0084	12.496	13.2	14.62	14.3522	15.3	15.42	6.3447	0	16.11	15.49	17
Pongo_f	16.88	16.386	18.005	18.866	13.664	13.083	16.995	16.4375	16.583	16.99	15.5	16.1803	12.19	12.16	15.946	16.11	0	5.634	17.01
Pongo_m	17.25	16.763	18.205	18.741	13.071	12.404	17.448	16.8723	16.476	16.96	16.08	16.4163	12.64	12.34	15.765	15.49	5.634	0	17.49
Presbytis_f	13.02	13.853	11.88	12.407	17.195	17.248	18.311	18.5675	14.2	15.53	12.52	13.2554	16.32	16.64	17.383	17	17.01	17.49	0
Presbytis_m	13.13	14.215	12.155	12.912	17.165	17.226	18.209	18.5882	14.54	16.14	12.79	13.5252	16.17	16.66	17.628	17.14	17.05	17.44	4.839
Symphalangus_f	18.89	18.236	20.484	20.861	19.897	19.749	11.851	10.4862	17.925	18.28	18.48	18.7415	17.6	17.85	18.145	18.46	15.25	15.94	19.12
Symphalangus_m	18.75	18.121	20.47	20.718	19.629	19.582	11.218	9.62325	17.744	18	18.56	18.4113	17.48	17.5	17.64	18.04	15.08	15.57	19.11
Erythrocebus_f	10.76	10.515	11.793	12.801	16.814	16.518	18.653	18.3637	12.55	13.85	12.54	13.4703	15.78	16.06	14.022	13.63	16.47	16.68	13.8
Erythrocebus_m	12.56	11.213	13.676	13.742	17.508	17.051	16.911	16.5154	13.438	13.14	13.92	13.6909	16.87	16.47	12.569	13.06	16.49	16.68	14.81
Allouatta_f	14.52	14.578	13.199	13.595	17.546	17.211	19.445	19.451	15.34	16.38	14.85	15.269	16.96	16.71	16.768	16.83	17.82	18.31	14.69
Allouatta_m	15.02	14.986	13.476	13.791	17.65	17.356	19.854	19.9241	15.59	16.65	15.48	15.6235	17.39	16.94	16.887	16.94	18.41	18.55	15.29
Aotus_f	15.22	15.887	15.526	15.763	18.045	17.483	19.035	19.2115	15.833	16.91	14.99	15.7904	16.22	15.92	18.205	18.04	17.99	18.34	15.1
Aotus_m	14.98	15.173	15	15.422	17.85	17.473	19.137	19.0409	15.794	16.72	14.43	15.4563	16.06	15.84	17.678	17.89	17.43	17.96	14.49
Ateles_f	14.45	14.726	13.505	13.623	17.519	17.319	19.505	19.1797	15.946	16.99	14.16	14.7016	16.39	16.47	18.079	18.14	17.49	17.92	13.83
Ateles_m	14.44	14.905	13.58	14.115	17.321	17.269	18.959	18.7408	15.793	16.97	13.9	14.4919	15.71	16.25	17.243	17.45	16.81	17.28	13.56
Cebus_f	12.97	13.542	14.624	15.215	17.602	17.522	18.475	18.5124	13.38	14.56	14.63	15.2053	15.85	16.06	15.093	15.84	16.91	17.63	15.64
Cebus_m	13.39	13.863	14.766	15.011	17.412	17.468	18.701	18.6642	13.408	14.17	14.57	14.9673	16.15	15.98	14.896	15.76	17.09	17.49	15.54
Saguinus_f	14.4	15.303	13.985	14.288	20.277	19.926	19.795	20.1055	15.188	16.14	16.73	17.3638	18.55	18.6	17.924	17.48	19.48	19.68	15.83
Saguinus_m	13.9	14.912	13.411	14.016	19.965	19.621	19.962	20.2307	14.91	15.88	16.38	16.9305	18.08	18.08	17.991	17.67	19	19.45	15.43
Saimiri_f	15.14	16.093	16.394	16.913	19.686	19.431	18.858	19.183	15.771	17.29	16.3	16.8509	17.23	17.68	18.263	18.3	18.95	19.44	15.75
Saimiri_m	15.23	16.038	16.322	16.887	19.598	19.382	19.339	19.5064	15.957	17.49	16.34	16.849	17.12	17.58	18.195	18.44	19.03	19.54	15.7
Pithecia_f	14.58	15.174	12.805	13.113	18.733	18.871	20.292	19.8929	14.718	15.82	15.27	15.5865	17.43	17.81	17.385	17.67	18.7	18.91	14.49
Pithecia_m	14.56	15.284	13.32	13.174	19.053	19.042	19.798	19.433	14.983	15.78	15.76	15.7542	17.78	17.66	17.588	17.95	18.75	18.89	14.53

Separate sexes

	MPresb	FSympha	MSymph	FErythro	MErythr	FAllouat	MAlloua	FAotus_f	MAotus_	FAteles	MAtele	FCebus_f	MCebu	FSaguin	MSaguin	FSaimir	MSaimi	FPithec	MPithe
Cercopithecus_f	13.13	18.889	18.751	10.762	12.562	14.523	15.015	15.2214	14.98	14.45	14.44	12.974	13.39	14.4	13.896	15.14	15.23	14.58	14.56
Cercopithecus_m	14.21	18.236	18.121	10.515	11.213	14.578	14.986	15.8874	15.173	14.73	14.9	13.5423	13.86	15.3	14.912	16.09	16.04	15.17	15.28
Colobus_f	12.16	20.484	20.47	11.793	13.676	13.199	13.476	15.5263	15	13.51	13.58	14.6242	14.77	13.99	13.411	16.39	16.32	12.8	13.32
Colobus_m	12.91	20.861	20.718	12.801	13.742	13.595	13.791	15.7629	15.422	13.62	14.12	15.215	15.01	14.29	14.016	16.91	16.89	13.11	13.17
Gorilla_f	17.16	19.897	19.629	16.814	17.508	17.546	17.65	18.0452	17.85	17.52	17.32	17.6016	17.41	20.28	19.965	19.69	19.6	18.73	19.05
Gorilla_m	17.23	19.749	19.582	16.518	17.051	17.211	17.356	17.4828	17.473	17.32	17.27	17.5225	17.47	19.93	19.621	19.43	19.38	18.87	19.04
Hylobates_f	18.21	11.851	11.218	18.653	16.911	19.445	19.854	19.0349	19.137	19.51	18.96	18.4755	18.7	19.8	19.962	18.86	19.34	20.29	19.8
Hylobates_m	18.59	10.486	9.6232	18.364	16.515	19.451	19.924	19.2115	19.041	19.18	18.74	18.5124	18.66	20.11	20.231	19.18	19.51	19.89	19.43
Macaca_f	14.54	17.925	17.744	12.55	13.438	15.34	15.59	15.8326	15.794	15.95	15.79	13.3797	13.41	15.19	14.91	15.77	15.96	14.72	14.98
Macaca_m	16.14	18.282	18	13.849	13.143	16.379	16.646	16.9127	16.718	16.99	16.97	14.5589	14.17	16.14	15.875	17.29	17.49	15.82	15.78
Nasalis_f	12.79	18.482	18.559	12.538	13.92	14.852	15.479	14.9922	14.426	14.16	13.9	14.6283	14.57	16.73	16.379	16.3	16.34	15.27	15.76
Nasalis_m	13.53	18.742	18.411	13.47	13.691	15.269	15.623	15.7904	15.456	14.7	14.49	15.2053	14.97	17.36	16.93	16.85	16.85	15.59	15.75
Pan_f	16.17	17.599	17.485	15.779	16.868	16.963	17.392	16.2174	16.065	16.39	15.71	15.8501	16.15	18.55	18.083	17.23	17.12	17.43	17.78
Pan_m	16.66	17.847	17.501	16.06	16.465	16.71	16.944	15.9201	15.837	16.47	16.25	16.064	15.98	18.6	18.075	17.68	17.58	17.81	17.66
Papio_f	17.63	18.145	17.64	14.022	12.569	16.768	16.887	18.2047	17.678	18.08	17.24	15.0928	14.9	17.92	17.991	18.26	18.19	17.39	17.59
Papio_m	17.14	18.463	18.037	13.634	13.056	16.83	16.939	18.035	17.893	18.14	17.45	15.8358	15.76	17.48	17.668	18.3	18.44	17.67	17.95
Pongo_f	17.05	15.247	15.078	16.469	16.486	17.817	18.411	17.9933	17.428	17.49	16.81	16.9059	17.09	19.48	19.004	18.95	19.03	18.7	18.75
Pongo_m	17.44	15.939	15.572	16.679	16.681	18.311	18.55	18.3437	17.961	17.92	17.28	17.6274	17.49	19.68	19.449	19.44	19.54	18.91	18.89
Presbytis_f	4.839	19.124	19.115	13.805	14.809	14.692	15.285	15.1027	14.487	13.83	13.56	15.6402	15.54	15.83	15.428	15.75	15.7	14.49	14.53
Presbytis_m	0	19.301	19.244	13.514	15.048	14.305	14.624	14.6537	14.238	13.71	13.28	15.1313	15.06	15.36	15.181	15.25	15.18	14.19	14.27
Symphalangus_f	19.3	0	5.1579	19.509	17.594	20.091	20.645	20.5513	20.3	20.53	19.77	19.1313	19.4	21.51	21.351	20.1	20.42	20.74	20.39
Symphalangus_m	19.24	5.1579	0	19.475	17.307	20.045	20.626	20.3836	20.136	20.24	19.7	19.2503	19.38	21.23	21.117	20.15	20.34	20.58	20.3
Erythrocebus_f	13.51	19.509	19.475	0	9.5782	13.606	14.12	14.8161	14.361	13.83	13.75	13.084	13.24	14.4	14.055	14.99	14.74	13.86	14.47
Erythrocebus_m	15.05	17.594	17.307	9.5782	0	15.344	15.545	15.9723	15.417	16.19	15.82	14.3725	14.49	16.12	15.939	15.74	15.96	15.92	15.75
Allouatta_f	14.3	20.091	20.045	13.606	15.344	0	4.5682	13.8604	13.623	11.17	10.57	12.7421	12.7	13.4	13.142	14.9	14.64	11.74	12.34
Allouatta_m	14.62	20.645	20.626	14.12	15.545	4.5682	0	13.9989	13.826	12.14	11.18	13.0071	12.77	13.26	13.138	15.23	14.9	11.82	12.24
Aotus_f	14.65	20.551	20.384	14.816	15.972	13.86	13.999	0	6.6182	13.53	13.5	13.905	14	13.55	13.055	12.44	12.57	14.03	13.58
Aotus_m	14.24	20.3	20.136	14.361	15.417	13.623	13.826	6.61823	0	13.88	13.42	13.3286	13.22	13.58	13.328	12.87	12.88	13.18	12.95
Ateles_f	13.71	20.529	20.24	13.831	16.188	11.173	12.144	13.5292	13.881	0	6.428	14.6316	14.84	13.94	13.374	15.28	14.91	12.66	12.7
Ateles_m	13.28	19.772	19.703	13.752	15.824	10.569	11.181	13.5009	13.421	6.428	0	13.7776	13.83	13.35	12.841	14.81	14.46	11.32	11.92
Cebus_f	15.13	19.131	19.25	13.084	14.372	12.742	13.007	13.905	13.329	14.63	13.78	0	4.815	13.71	13.54	13.35	13.4	12.4	12.76
Cebus_m	15.06	19.403	19.379	13.236	14.485	12.705	12.774	14.0038	13.219	14.84	13.83	4.81546	0	13.72	13.686	13.5	13.57	12.11	12.55
Saguinus_f	15.36	21.514	21.233	14.405	16.118	13.403	13.26	13.5545	13.582	13.94	13.35	13.7147	13.72	0	4.621	13.28	13.47	12.38	11.9
Saguinus_m	15.18	21.351	21.117	14.055	15.939	13.142	13.138	13.055	13.328	13.37	12.84	13.5396	13.69	4.621	0	13.18	13.26	12.06	11.64
Saimiri_f	15.25	20.1	20.155	14.992	15.738	14.905	15.228	12.4391	12.871	15.28	14.81	13.3454	13.5	13.28	13.175	0	3.224	13.85	13.71
Saimiri_m	15.18	20.417	20.338	14.738	15.965	14.639	14.905	12.5684	12.879	14.91	14.46	13.3982	13.57	13.47	13.257	3.224	0	13.59	13.56
Pithecia_f	14.19	20.737	20.578	13.862	15.92	11.741	11.817	14.0313	13.179	12.66	11.32	12.3975	12.11	12.38	12.061	13.85	13.59	0	5.371
Pithecia_m	14.27	20.386	20.303	14.466	15.746	12.341	12.236	13.5829	12.955	12.7	11.92	12.7583	12.55	11.9	11.635	13.71	13.56	5.371	0

All characters distance matrix

	Gorilla	Pan	Pongo	Hylobate	Symphal	Cercopit	Colobus	Macaca	Nasalis	Papio	Presbyti	Erythro	Allouatt	Aotus	Ateles	Cebus	Saguinus	Saimiri	Pithecia	Proconsul
Gorilla	---	9.78	14.09	20.03	19.59	17.02	17.10	16.47	14.59	15.11	17.24	17.72	18.33	18.20	17.79	17.76	20.05	19.74	18.75	15.81
Pan	9.78	---	13.56	17.64	17.49	16.33	17.17	16.20	14.46	15.79	16.85	16.86	17.42	16.31	16.89	15.97	18.31	17.40	17.85	14.21
Pongo	14.09	13.56	---	17.00	15.92	17.55	18.87	17.67	16.90	15.84	18.20	17.64	19.35	19.03	17.82	18.21	20.48	19.97	19.17	15.96
Hylobat	20.03	17.64	17.00	---	10.17	18.27	20.71	18.23	18.15	18.79	19.15	18.38	21.00	20.44	19.81	19.38	20.92	20.36	20.78	17.93
Sympha	19.59	17.49	15.92	10.17	---	18.31	20.48	17.99	18.53	17.71	19.33	18.99	20.49	20.72	19.72	19.76	21.38	20.65	20.46	16.69
Cercopi	17.02	16.33	17.55	18.27	18.31	---	12.07	11.33	13.04	13.41	13.99	11.35	14.98	15.47	14.63	13.33	14.62	15.75	14.71	15.31
Colobus	17.10	17.17	18.87	20.71	20.48	12.07	---	12.75	13.73	14.97	12.97	13.07	14.28	15.91	14.58	15.01	14.15	16.70	13.19	16.31
Macaca	16.47	16.20	17.67	18.23	17.99	11.33	12.75	---	12.91	13.07	14.89	13.93	16.27	16.33	16.70	14.42	15.65	16.70	14.79	14.50
Nasalis	14.59	14.46	16.90	18.15	18.53	13.04	13.73	12.91	---	14.87	13.64	13.07	15.52	15.97	15.07	15.15	17.04	16.92	15.72	15.44
Papio	15.11	15.79	15.84	18.79	17.71	13.41	14.97	13.07	14.87	---	17.71	15.00	17.96	18.73	17.99	16.24	18.28	18.85	17.75	15.54
Presbyti	17.24	16.85	18.20	19.15	19.33	13.99	12.97	14.89	13.64	17.71	---	14.82	15.44	15.15	13.98	15.98	16.06	15.36	14.70	17.28
Erythro	17.72	16.86	17.64	18.38	18.99	11.35	13.07	13.93	13.07	15.00	14.82	---	14.63	15.53	15.29	12.68	15.42	14.89	14.88	16.18
Allouatt	18.33	17.42	19.35	21.00	20.49	14.98	14.28	16.27	15.52	17.96	15.44	14.63	---	14.29	10.91	13.41	13.33	15.49	12.17	16.19
Aotus	18.20	16.31	19.03	20.44	20.72	15.47	15.91	16.33	15.97	18.73	15.15	15.53	14.29	---	13.80	14.57	13.27	12.41	13.56	15.69
Ateles	17.79	16.89	17.82	19.81	19.72	14.63	14.58	16.70	15.07	17.99	13.98	15.29	10.91	13.80	---	14.89	13.71	15.36	12.31	16.73
Cebus	17.76	15.97	18.21	19.38	19.76	13.33	15.01	14.42	15.15	16.24	15.98	12.68	13.41	14.57	14.89	---	14.12	13.25	13.07	15.14
Saguinu	20.05	18.31	20.48	20.92	21.38	14.62	14.15	15.65	17.04	18.28	16.06	15.42	13.33	13.27	13.71	14.12	---	13.48	11.78	16.28
Saimiri	19.74	17.40	19.97	20.36	20.65	15.75	16.70	16.70	16.92	18.85	15.36	14.89	15.49	12.41	15.36	13.25	13.48	---	13.45	16.68
Pithecia	18.75	17.85	19.17	20.78	20.46	14.71	13.19	14.79	15.72	17.75	14.70	14.88	12.17	13.56	12.31	13.07	11.78	13.45	---	15.31
Procons	15.81	14.21	15.96	17.93	16.69	15.31	16.31	14.50	15.44	15.54	17.28	16.18	16.19	15.69	16.73	15.14	16.28	16.68	15.31	---

Cranial distance matrix

	Gorilla	Pan	Pongo	Hylobate	Symphal	Cercopit	Colobus	Macaca	Nasalis	Papio	Presbyti	Erythro	Victoria	Allouatta	Aotus	Ateles	Cebus	Saguinu	Saimiri	Pitheci	Procons
Gorilla	---	7.27	8.83	10.72	10.57	9.91	9.50	9.07	7.67	9.87	10.25	9.59	8.87	9.49	9.66	8.36	9.91	11.19	11.42	9.29	9.00
Pan	7.27	---	8.65	8.98	9.16	9.96	10.51	10.06	9.16	11.31	10.26	9.91	10.65	9.66	8.23	8.10	9.12	9.49	9.80	9.21	8.52
Pongo	8.83	8.65	---	10.71	9.34	10.01	11.42	11.08	10.17	10.05	11.00	10.38	9.12	10.80	10.55	8.56	9.71	11.87	11.49	9.92	8.97
Hylobat	10.72	8.98	10.71	---	6.93	8.22	10.85	9.91	9.75	10.41	9.91	8.28	11.16	10.71	10.27	9.55	8.71	10.07	10.46	10.11	9.38
Sympha	10.57	9.16	9.34	6.93	---	9.54	11.46	10.26	10.51	9.12	11.58	10.32	11.01	11.03	11.62	10.23	9.96	11.46	11.79	10.56	8.05
Cercopi	9.91	9.96	10.01	8.22	9.54	---	7.11	5.90	8.16	7.86	9.39	6.00	8.89	9.59	10.26	8.31	7.97	8.79	10.36	9.16	9.93
Colobus	9.50	10.51	11.42	10.85	11.46	7.11	---	6.00	8.47	9.32	9.43	8.34	8.20	9.89	10.53	9.59	9.69	8.59	11.27	8.89	11.21
Macaca	9.07	10.06	11.08	9.91	10.26	5.90	6.00	---	8.52	8.10	9.38	6.94	7.81	9.60	10.56	9.33	9.06	8.54	10.06	8.09	10.02
Nasalis	7.67	9.16	10.17	9.75	10.51	8.16	8.47	8.52	---	10.66	9.43	7.16	8.39	8.77	10.01	8.10	9.23	10.33	10.60	9.54	9.97
Papio	9.87	11.31	10.05	10.41	9.12	7.86	9.32	8.10	10.66	---	12.30	9.85	9.42	11.10	13.24	10.65	10.74	11.92	13.30	11.18	10.11
Presbyti	10.25	10.26	11.00	9.91	11.58	9.39	9.43	9.38	9.43	12.30	---	9.64	10.32	11.09	9.22	9.43	9.41	10.56	8.99	9.81	11.79
Erythro	9.59	9.91	10.38	8.28	10.32	6.00	8.34	6.94	7.16	9.85	9.64	---	7.79	8.78	10.13	7.83	7.54	9.05	9.91	9.33	10.26
Victoria	8.87	10.65	9.12	11.16	11.01	8.89	8.20	7.81	8.39	9.42	10.32	7.79	---	9.66	10.91	9.47	9.33	10.50	10.92	9.36	10.64
Allouatt	9.49	9.66	10.80	10.71	11.03	9.59	9.89	9.60	8.77	11.10	11.09	8.78	9.66	---	8.88	7.27	8.34	8.91	10.56	8.82	9.52
Aotus	9.66	8.23	10.55	10.27	11.62	10.26	10.53	10.56	10.01	13.24	9.22	10.13	10.91	8.88	---	8.61	9.22	8.62	8.10	7.77	9.78
Ateles	8.36	8.10	8.56	9.55	10.23	8.31	9.59	9.33	8.10	10.65	9.43	7.83	9.47	7.27	8.61	---	7.82	8.46	10.02	8.29	9.10
Cebus	9.91	9.12	9.71	8.71	9.96	7.97	9.69	9.06	9.23	10.74	9.41	7.54	9.33	8.34	9.22	7.82	---	8.58	7.91	8.22	9.64
Saguinu	11.19	9.49	11.87	10.07	11.46	8.79	8.59	8.54	10.33	11.92	10.56	9.05	10.50	8.91	8.62	8.46	8.58	---	8.47	6.95	9.54
Saimiri	11.42	9.80	11.49	10.46	11.79	10.36	11.27	10.06	10.60	13.30	8.99	9.91	10.92	10.56	8.10	10.02	7.91	8.47	---	7.76	10.47
Pithecia	9.29	9.21	9.92	10.11	10.56	9.16	8.89	8.09	9.54	11.18	9.81	9.33	9.36	8.82	7.77	8.29	8.22	6.95	7.76	---	8.71
Procons	9.00	8.52	8.97	9.38	8.05	9.93	11.21	10.02	9.97	10.11	11.79	10.26	10.64	9.52	9.78	9.10	9.64	9.54	10.47	8.71	---
Aegypto	8.93	10.58	10.12	10.13	9.97	9.60	9.70	8.71	9.45	9.21	11.01	8.80	7.77	8.34	10.94	9.80	8.46	10.32	10.28	9.39	9.85

Mandible distance matrix

	Gorilla	Pan	Pongo	Hylobate	Symphal	Cercopit	Colobus	Macaca	Nasalis	Papio	Presbyti	Erythro	Allouatt	Aotus	Ateles	Cebus	Saguinus	Saimiri	Pithecia	Procon	Aegypto	Epiplio
Gorilla	---	1.48	1.81	2.96	3.90	4.04	4.42	4.66	2.35	4.66	3.78	3.61	4.78	2.81	2.96	3.91	4.67	4.19	4.17	3.75	3.76	2.12
Pan	1.48	---	1.80	2.59	3.90	4.05	4.18	4.42	2.38	4.42	4.07	3.62	4.78	3.20	3.32	3.93	4.68	4.21	4.18	3.46	3.78	2.61
Pongo	1.81	1.80	---	2.79	4.04	4.18	4.55	4.54	2.59	4.54	4.20	3.76	4.89	3.36	3.48	4.06	4.79	4.33	4.30	3.61	3.91	2.80
Hylobat	2.96	2.59	2.79	---	2.96	3.75	3.90	3.91	3.45	3.94	4.29	3.61	4.07	3.76	3.89	3.29	3.61	4.17	3.30	2.76	3.76	3.29
Sympha	3.90	3.90	4.04	2.96	---	3.13	2.95	2.95	4.54	4.18	4.05	4.16	2.77	3.49	3.61	3.30	3.62	3.91	3.29	2.76	3.76	3.62
Cercopi	4.04	4.05	4.18	3.75	3.13	---	1.81	2.35	3.61	4.06	4.42	2.76	3.63	3.91	4.03	3.12	4.03	4.77	3.46	2.95	3.90	4.03
Colobus	4.42	4.18	4.55	3.90	2.95	1.81	---	1.49	3.75	3.64	4.77	3.29	3.16	4.05	4.16	2.55	3.61	4.89	2.95	2.75	3.46	4.42
Macaca	4.66	4.42	4.54	3.91	2.95	2.35	1.49	---	4.05	2.95	5.01	3.30	3.14	4.33	4.43	2.58	3.63	4.45	2.95	2.76	3.47	4.68
Nasalis	2.35	2.38	2.59	3.45	4.54	3.61	3.75	4.05	---	4.07	4.16	3.13	4.91	3.30	3.45	3.45	4.29	4.77	3.76	3.90	3.30	3.13
Papio	4.66	4.42	4.54	3.94	4.18	4.06	3.64	2.95	4.07	---	5.45	2.97	4.30	4.84	4.91	3.00	3.01	4.47	2.58	3.77	3.16	4.70
Presbyti	3.78	4.07	4.20	4.29	4.05	4.42	4.77	5.01	4.16	5.45	---	5.00	4.93	2.95	3.13	5.21	4.99	3.76	5.01	4.66	4.67	3.13
Erythro	3.61	3.62	3.76	3.61	4.16	2.76	3.29	3.30	3.13	2.97	5.00	---	4.55	4.31	4.42	2.95	3.61	4.89	2.95	3.45	3.46	3.90
Allouatt	4.78	4.78	4.89	4.07	2.77	3.63	3.16	3.14	4.91	4.30	4.93	4.55	---	4.23	3.78	3.49	3.17	4.08	3.46	2.97	3.31	4.07
Aotus	2.81	3.20	3.36	3.76	3.49	3.91	4.05	4.33	3.30	4.84	2.95	4.31	4.23	---	1.08	4.54	4.54	3.46	4.32	4.19	4.19	1.82
Ateles	2.96	3.32	3.48	3.89	3.61	4.03	4.16	4.43	3.45	4.91	3.13	4.42	3.78	1.08	---	4.65	4.42	3.30	4.42	4.03	4.04	1.48
Cebus	3.91	3.93	4.06	3.29	3.30	3.12	2.55	2.58	3.45	3.00	5.21	2.95	3.49	4.54	4.65	---	2.55	5.10	1.49	2.76	2.34	4.42
Saguinu	4.67	4.68	4.79	3.61	3.62	4.03	3.61	3.63	4.29	3.01	4.99	3.61	3.17	4.54	4.42	2.55	---	4.66	1.50	3.46	2.34	4.16
Saimiri	4.19	4.21	4.33	4.17	3.91	4.77	4.89	4.45	4.77	4.47	3.76	4.89	4.08	3.46	3.30	5.10	4.66	---	4.90	4.30	4.30	3.29
Pithecia	4.17	4.18	4.30	3.30	3.29	3.46	2.95	2.95	3.76	2.58	5.01	2.95	3.46	4.32	4.42	1.49	1.50	4.90	---	3.13	2.33	4.17
Procons	3.75	3.46	3.61	2.76	2.76	2.95	2.75	2.76	3.90	3.77	4.66	3.45	2.97	4.19	4.03	2.76	3.46	4.30	3.13	---	3.30	3.76
Aegypto	3.76	3.78	3.91	3.76	3.76	3.90	3.46	3.47	3.30	3.16	4.67	3.46	3.31	4.19	4.04	2.34	2.34	4.30	2.33	3.30	---	3.76
Epiliop	2.12	2.61	2.80	3.29	3.62	4.03	4.42	4.68	3.13	4.70	3.13	3.90	4.07	1.82	1.48	4.42	4.16	3.29	4.17	3.76	3.76	---

Forelimb distance matrix

	Gorilla	Pan	Pongo	Hylobate	Symphal	Cercopit	Colobus	Macaca	Nasalis	Papio	Presbyti	Erythro	Victoria	Allouatta	Aotus	Ateles	Cebus	Saguinu	Saimiri	Pitheci	Procons
Gorilla	---	4.14	8.41	13.84	13.30	7.02	6.82	7.66	7.38	6.45	7.33	8.88	7.62	8.71	9.09	8.77	8.47	9.45	9.47	9.54	8.01
Pan	4.14	---	7.56	11.89	11.61	6.43	6.68	6.92	6.51	6.24	6.97	7.70	7.07	7.66	8.32	8.42	7.00	8.61	8.01	8.88	7.11
Pongo	8.41	7.56	---	8.87	8.67	9.06	9.36	8.54	9.19	8.23	8.68	8.84	8.35	9.91	9.91	9.65	9.89	10.25	10.27	10.41	7.86
Hylobat	13.84	11.89	8.87	---	3.66	12.52	13.44	11.51	11.36	11.86	12.03	11.43	11.62	13.51	12.73	12.90	13.24	14.03	12.68	14.05	11.69
Sympha	13.30	11.61	8.67	3.66	---	11.95	12.82	10.98	10.83	11.31	11.23	10.81	11.06	12.98	12.32	12.27	12.69	13.57	12.20	13.16	10.80
Cercopi	7.02	6.43	9.06	12.52	11.95	---	4.99	5.64	4.78	5.71	5.58	5.55	4.94	5.68	5.60	6.64	6.38	6.74	6.89	6.71	6.63
Colobus	6.82	6.68	9.36	13.44	12.82	4.99	---	5.59	5.34	6.10	4.29	6.20	5.31	4.99	5.33	5.71	5.90	6.26	6.64	5.31	5.72
Macaca	7.66	6.92	8.54	11.51	10.98	5.64	5.59	---	5.02	5.11	5.60	7.62	6.07	6.73	5.76	6.80	7.43	6.71	7.37	6.80	5.51
Nasalis	7.38	6.51	9.19	11.36	10.83	4.78	5.34	5.02	---	5.19	4.13	6.53	5.37	6.37	6.25	6.50	6.90	7.61	7.22	7.18	7.03
Papio	6.45	6.24	8.23	11.86	11.31	5.71	6.10	5.11	5.19	---	6.35	7.01	5.97	7.81	7.46	7.78	7.28	8.10	7.99	8.50	7.15
Presbyti	7.33	6.97	8.68	12.03	11.23	5.58	4.29	5.60	4.13	6.35	---	7.12	5.04	5.74	6.21	5.36	7.49	7.25	7.84	6.04	6.45
Erythro	8.88	7.70	8.84	11.43	10.81	5.55	6.20	7.62	6.53	7.01	7.12	---	6.30	6.81	6.90	8.21	5.47	8.03	6.29	7.73	7.16
Victoria	7.62	7.07	8.35	11.62	11.06	4.94	5.31	6.07	5.37	5.97	5.04	6.30	---	5.78	6.22	6.86	7.32	7.32	8.08	6.98	6.42
Allouatt	8.71	7.66	9.91	13.51	12.98	5.68	4.99	6.73	6.37	7.81	5.74	6.81	5.78	---	4.47	5.02	5.18	5.01	6.09	4.54	6.39
Aotus	9.09	8.32	9.91	12.73	12.32	5.60	5.33	5.76	6.25	7.46	6.21	6.90	6.22	4.47	---	4.96	5.95	3.85	5.21	4.69	6.50
Ateles	8.77	8.42	9.65	12.90	12.27	6.64	5.71	6.80	6.50	7.78	5.36	8.21	6.86	5.02	4.96	---	7.37	6.05	7.14	5.11	7.58
Cebus	8.47	7.00	9.89	13.24	12.69	6.38	5.90	7.43	6.90	7.28	7.49	5.47	7.32	5.18	5.95	7.37	---	6.09	3.93	6.39	7.00
Saguinu	9.45	8.61	10.25	14.03	13.57	6.74	6.26	6.71	7.61	8.10	7.25	8.03	7.32	5.01	3.85	6.05	6.09	---	5.90	5.48	7.12
Saimiri	9.47	8.01	10.27	12.68	12.20	6.89	6.64	7.37	7.22	7.99	7.84	6.29	8.08	6.09	5.21	7.14	3.93	5.90	---	5.66	7.30
Pithecia	9.54	8.88	10.41	14.05	13.16	6.71	5.31	6.80	7.18	8.50	6.04	7.73	6.98	4.54	4.69	5.11	6.39	5.48	5.66	---	5.98
Procons	8.01	7.11	7.86	11.69	10.80	6.63	5.72	5.51	7.03	7.15	6.45	7.16	6.42	6.39	6.50	7.58	7.00	7.12	7.30	5.98	---
Epipliop	9.03	8.09	9.55	12.33	11.83	7.01	6.03	6.36	6.64	8.11	5.45	8.47	6.39	4.79	5.23	5.41	7.29	5.68	7.50	5.76	6.34

Manus distance matrix

	Gorilla	Pan	Pongo	Hylobate	Symphal	Cercopit	Colobus	Macaca	Nasalis	Papio	Presbyti	Erythro	Victoria	Allouatta	Aotus	Ateles	Cebus	Saguinu	Saimiri	Pitheci	Procons
Gorilla	---	1.84	3.43	5.25	4.64	6.71	6.08	6.71	5.94	5.68	6.55	7.35	7.41	6.40	7.55	6.59	6.92	7.77	7.51	7.22	5.86
Pan	1.84	---	3.52	5.12	4.59	6.87	6.32	6.73	6.05	5.75	6.71	7.53	7.36	6.52	7.60	6.78	6.94	7.95	7.58	7.31	5.86
Pongo	3.43	3.52	---	4.60	4.24	6.38	6.26	6.83	5.98	4.92	6.65	7.49	7.02	6.78	7.31	6.38	7.18	7.54	7.15	7.55	6.14
Hylobat	5.25	5.12	4.60	---	2.58	6.80	7.01	6.76	6.79	5.87	6.86	7.75	7.61	7.54	7.41	6.90	7.11	7.19	6.95	7.94	6.67
Sympha	4.64	4.59	4.24	2.58	---	6.37	7.01	6.55	6.69	5.95	6.59	7.89	7.39	7.38	7.56	7.00	7.16	7.21	6.98	8.07	6.64
Cercopi	6.71	6.87	6.38	6.80	6.37	---	4.40	4.65	4.79	4.79	4.14	4.65	4.47	5.04	4.73	5.06	4.58	4.45	3.99	4.92	5.59
Colobus	6.08	6.32	6.26	7.01	7.01	4.40	---	5.44	3.67	5.49	3.27	3.44	5.38	3.32	4.81	3.87	4.98	4.95	5.00	3.83	5.93
Macaca	6.71	6.73	6.83	6.76	6.55	4.65	5.44	---	4.59	5.19	4.92	5.23	6.04	6.02	5.52	6.86	4.47	5.61	5.27	5.10	6.17
Nasalis	5.94	6.05	5.98	6.79	6.69	4.79	3.67	4.59	---	4.57	4.33	4.01	5.47	4.71	5.60	5.42	5.46	5.69	5.54	4.77	6.22
Papio	5.68	5.75	4.92	5.87	5.95	4.79	5.49	5.19	4.57	---	6.14	5.51	5.29	5.37	5.65	5.77	5.29	5.77	5.25	5.79	5.70
Presbyti	6.55	6.71	6.65	6.86	6.59	4.14	3.27	4.92	4.33	6.14	---	3.74	5.51	3.94	5.02	4.87	5.12	5.11	4.75	4.75	6.30
Erythro	7.35	7.53	7.49	7.75	7.89	4.65	3.44	5.23	4.01	5.51	3.74	---	5.03	4.01	4.42	5.25	4.75	5.01	4.38	3.62	6.41
Victoria	7.41	7.36	7.02	7.61	7.39	4.47	5.38	6.04	5.47	5.29	5.51	5.03	---	5.22	5.15	5.96	5.55	4.65	5.28	5.67	5.65
Allouatt	6.40	6.52	6.78	7.54	7.38	5.04	3.32	6.02	4.71	5.37	3.94	4.01	5.22	---	4.97	4.42	4.69	5.33	5.15	4.24	6.63
Aotus	7.55	7.60	7.31	7.41	7.56	4.73	4.81	5.52	5.60	5.65	5.02	4.42	5.15	4.97	---	5.12	4.76	4.02	4.04	4.84	6.48
Ateles	6.59	6.78	6.38	6.90	7.00	5.06	3.87	6.86	5.42	5.77	4.87	5.25	5.96	4.42	5.12	---	5.93	5.43	5.10	4.66	6.82
Cebus	6.92	6.94	7.18	7.11	7.16	4.58	4.98	4.47	5.46	5.29	5.12	4.75	5.55	4.69	4.76	5.93	---	5.08	4.18	3.73	5.60
Saguinu	7.77	7.95	7.54	7.19	7.21	4.45	4.95	5.61	5.69	5.77	5.11	5.01	4.65	5.33	4.02	5.43	5.08	---	3.88	5.13	6.55
Saimiri	7.51	7.58	7.15	6.95	6.98	3.99	5.00	5.27	5.54	5.25	4.75	4.38	5.28	5.15	4.04	5.10	4.18	3.88	---	4.51	6.25
Pithecia	7.22	7.31	7.55	7.94	8.07	4.92	3.83	5.10	4.77	5.79	4.75	3.62	5.67	4.24	4.84	4.66	3.73	5.13	4.51	---	6.30
Procons	5.86	5.86	6.14	6.67	6.64	5.59	5.93	6.17	6.22	5.70	6.30	6.41	5.65	6.63	6.48	6.82	5.60	6.55	6.25	6.30	---
Epipliop	6.58	6.65	6.46	7.15	6.73	4.61	4.46	5.38	5.46	5.35	4.42	4.75	5.39	3.66	4.73	4.57	4.39	4.82	4.39	4.46	6.51

Pelvis distance matrix

	Gorilla	Pan	Pongo	Hylobate	Symphal	Cercopit	Colobus	Macaca	Nasalis	Papio	Presbyti	Erythro	Allouatt	Aotus	Ateles	Cebus	Saguinus	Saimiri	Pithecia	Proconsul
Gorilla	---	3.21	4.49	2.86	3.73	3.87	4.17	4.07	3.97	3.91	3.70	4.35	4.40	4.45	4.08	4.14	3.98	4.57	3.96	4.25
Pan	3.21	---	3.79	3.07	2.39	2.16	2.61	3.20	3.18	2.14	2.80	2.87	3.71	3.39	3.07	3.00	4.05	3.30	2.87	2.86
Pongo	4.49	3.79	---	3.87	3.34	4.11	3.55	2.18	3.01	4.10	4.50	3.43	4.60	5.09	4.38	4.09	4.93	5.24	4.52	4.29
Hylobat	2.86	3.07	3.87	---	2.46	3.36	3.03	3.64	3.57	3.41	3.54	3.25	4.28	4.40	4.01	3.68	3.30	4.33	3.50	3.84
Sympha	3.73	2.39	3.34	2.46	---	2.42	1.91	3.05	3.07	2.81	2.65	2.24	3.50	3.77	3.58	3.15	3.82	3.73	3.07	3.11
Cercopi	3.87	2.16	4.11	3.36	2.42	---	2.10	3.21	3.20	2.12	2.39	2.36	3.43	3.28	3.47	3.01	3.36	2.42	2.46	2.87
Colobus	4.17	2.61	3.55	3.03	1.91	2.10	---	2.84	2.85	2.58	2.38	1.84	3.76	3.59	3.50	3.00	3.36	3.22	2.49	2.87
Macaca	4.07	3.20	2.18	3.64	3.05	3.21	2.84	---	2.18	2.80	3.42	2.64	3.64	4.15	3.71	2.88	4.25	4.35	3.54	3.53
Nasalis	3.97	3.18	3.01	3.57	3.07	3.20	2.85	2.18	---	3.21	2.66	3.06	3.62	4.68	3.29	3.57	4.28	4.07	3.11	3.43
Papio	3.91	2.14	4.10	3.41	2.81	2.12	2.58	2.80	3.21	---	2.83	2.37	3.43	2.96	3.18	2.15	3.99	2.90	2.53	2.92
Presbyti	3.70	2.80	4.50	3.54	2.65	2.39	2.38	3.42	2.66	2.83	---	2.66	2.50	3.20	2.49	2.83	3.26	2.71	2.17	2.59
Erythro	4.35	2.87	3.43	3.25	2.24	2.36	1.84	2.64	3.06	2.37	2.66	---	3.01	3.12	3.43	2.47	3.56	3.06	3.15	2.76
Allouatt	4.40	3.71	4.60	4.28	3.50	3.43	3.76	3.64	3.62	3.43	2.50	3.01	---	2.66	2.19	2.18	3.41	2.96	3.23	2.55
Aotus	4.45	3.39	5.09	4.40	3.77	3.28	3.59	4.15	4.68	2.96	3.20	3.12	2.66	---	2.81	2.02	3.33	2.61	3.18	2.90
Ateles	4.08	3.07	4.38	4.01	3.58	3.47	3.50	3.71	3.29	3.18	2.49	3.43	2.19	2.81	---	2.27	3.53	3.02	2.40	2.47
Cebus	4.14	3.00	4.09	3.68	3.15	3.01	3.00	2.88	3.57	2.15	2.83	2.47	2.18	2.02	2.27	---	3.31	2.86	2.44	2.48
Saguinu	3.98	4.05	4.93	3.30	3.82	3.36	3.36	4.25	4.28	3.99	3.26	3.56	3.41	3.33	3.53	3.31	---	3.04	3.21	3.29
Saimiri	4.57	3.30	5.24	4.33	3.73	2.42	3.22	4.35	4.07	2.90	2.71	3.06	2.96	2.61	3.02	2.86	3.04	---	2.68	2.31
Pithecia	3.96	2.87	4.52	3.50	3.07	2.46	2.49	3.54	3.11	2.53	2.17	3.15	3.23	3.18	2.40	2.44	3.21	2.68	---	2.99
Procons	4.25	2.86	4.29	3.84	3.11	2.87	2.87	3.53	3.43	2.92	2.59	2.76	2.55	2.90	2.47	2.48	3.29	2.31	2.99	---

Pes distance matrix

	Gorilla	Pan	Pongo	Hylobate	Symphal	Cercopit	Colobus	Macaca	Nasalis	Papio	Presbyti	Erythro	Allouatt	Aotus	Ateles	Cebus	Saguinus	Saimiri	Pithecia	Procon	Epiliop
Gorilla	---	3.46	4.35	7.48	7.15	8.44	9.35	7.27	6.85	5.06	8.53	7.94	9.66	8.74	10.29	8.42	9.83	9.06	9.75	6.59	9.05
Pan	3.46	---	5.04	7.16	7.08	7.89	8.97	6.61	5.84	5.50	8.09	7.33	8.84	7.38	9.31	7.41	8.71	7.86	9.00	5.29	7.88
Pongo	4.35	5.04	---	7.54	7.12	7.54	8.49	7.09	7.12	5.14	7.72	6.98	8.72	8.32	9.19	7.80	8.80	8.48	8.47	6.96	8.73
Hylobat	7.48	7.16	7.54	---	4.77	6.59	7.95	5.77	6.32	6.95	7.21	7.75	7.73	8.30	7.90	7.44	8.39	8.20	7.23	5.94	6.79
Sympha	7.15	7.08	7.12	4.77	---	7.10	8.23	6.48	6.84	6.88	7.25	7.63	7.84	8.12	8.04	8.00	8.31	8.24	7.39	6.34	7.13
Cercopi	8.44	7.89	7.54	6.59	7.10	---	6.73	5.17	6.17	6.71	6.17	5.42	7.36	7.68	7.17	6.09	6.95	7.34	7.00	6.92	7.16
Colobus	9.35	8.97	8.49	7.95	8.23	6.73	---	7.60	7.52	7.35	5.08	6.30	7.10	8.18	6.93	7.74	6.53	7.39	6.37	7.81	7.83
Macaca	7.27	6.61	7.09	5.77	6.48	5.17	7.60	---	5.49	6.22	6.82	6.78	8.53	7.85	8.39	6.26	8.32	7.94	7.97	5.06	7.20
Nasalis	6.85	5.84	7.12	6.32	6.84	6.17	7.52	5.49	---	6.15	6.41	6.72	8.33	7.56	8.43	6.82	7.92	7.62	7.91	5.35	7.65
Papio	5.06	5.50	5.14	6.95	6.88	6.71	7.35	6.22	6.15	---	7.29	6.13	9.22	7.92	9.40	7.61	8.62	8.07	8.72	6.13	8.76
Presbyti	8.53	8.09	7.72	7.21	7.25	6.17	5.08	6.82	6.41	7.29	---	5.89	6.46	8.11	6.44	7.40	6.16	7.34	5.99	7.45	7.09
Erythro	7.94	7.33	6.98	7.75	7.63	5.42	6.30	6.78	6.72	6.13	5.89	---	7.03	6.93	7.12	6.29	6.72	6.05	6.85	7.00	7.62
Allouatt	9.66	8.84	8.72	7.73	7.84	7.36	7.10	8.53	8.33	9.22	6.46	7.03	---	7.73	2.30	6.91	5.18	6.66	3.60	8.69	5.63
Aotus	8.74	7.38	8.32	8.30	8.12	7.68	8.18	7.85	7.56	7.92	8.11	6.93	7.73	---	7.69	6.99	6.59	5.42	7.31	6.74	6.96
Ateles	10.29	9.31	9.19	7.90	8.04	7.17	6.93	8.39	8.43	9.40	6.44	7.12	2.30	7.69	---	6.95	4.79	6.56	3.66	8.69	5.55
Cebus	8.42	7.41	7.80	7.44	8.00	6.09	7.74	6.26	6.82	7.61	7.40	6.29	6.91	6.99	6.95	---	6.99	7.08	6.54	6.78	6.88
Saguinu	9.83	8.71	8.80	8.39	8.31	6.95	6.53	8.32	7.92	8.62	6.16	6.72	5.18	6.59	4.79	6.99	---	5.77	4.91	7.89	6.49
Saimiri	9.06	7.86	8.48	8.20	8.24	7.34	7.39	7.94	7.62	8.07	7.34	6.05	6.66	5.42	6.56	7.08	5.77	---	6.43	7.56	6.82
Pithecia	9.75	9.00	8.47	7.23	7.39	7.00	6.37	7.97	7.91	8.72	5.99	6.85	3.60	7.31	3.66	6.54	4.91	6.43	---	8.26	5.82
Procons	6.59	5.29	6.96	5.94	6.34	6.92	7.81	5.06	5.35	6.13	7.45	7.00	8.69	6.74	8.69	6.78	7.89	7.56	8.26	---	7.20
Epiliop	9.05	7.88	8.73	6.79	7.13	7.16	7.83	7.20	7.65	8.76	7.09	7.62	5.63	6.96	5.55	6.88	6.49	6.82	5.82	7.20	---
Oeropit	8.75	7.69	8.12	7.17	7.79	8.03	7.69	7.64	7.28	8.38	7.01	7.67	6.43	7.45	6.28	7.14	6.32	7.17	5.93	7.06	6.57

Appendix D: Synapomorphies supporting each hypothesis. Steps indicate tansition cost across the tree.

Char.	Element	Description	Synapomorphy	H1: Steps	H2: Steps	H3: Steps	optimal
hum40	Humerus	height of olecranon fossa	H1: stem catarrhine	1.75	1.766	1.75	H1=H3
hum41	Humerus	length from proximal-most point of olecranon fossa to disto-medial corner of fossa	H1: stem catarrhine	1.22	1.317	1.22	H1=H3
TZMM9	Trapezium	width trapezoid facet at border with scaphoid facet	H1: stem catarrhine	0.5	0.507	0.5	H1=H3
AM12	Astragalus	medio-lateral width posterior border posterior calcaneal facet	H1: stem catarrhine	0.596	0.603	0.596	H1=H3
AM14	Astragalus	medio-lateral width at anterior border posterior calcaneal facet	H1: stem catarrhine	0.818	0.846	0.818	H1=H3
AM30	Astragalus	dorsal projection of medial tubercle below torchlea	H1: stem catarrhine	1.005	1.064	1.005	H1=H3
RM4	Radius	antero-posterior width across depression at center of head	H1: stem catarrhine	0.501	0.501	0.501	H1=H2=H3
RM12	Radius	medio-lateral width tubercle	H1: stem catarrhine	0.59	0.59	0.59	H1=H2=H3
hum15	Humerus	medio-lateral length trochlear and capitulum at distal border	H1: stem catarrhine	1.914	1.914	1.914	H1=H2=H3
hum39	Humerus	width olecranon fossa	H1: stem catarrhine	1.306	1.306	1.306	H1=H2=H3
PVM4	Pelvis	width obturator foramen	H1: stem catarrhine	1.86	1.86	1.86	H1=H2=H3
PVM6	Pelvis	medio-lateral width inferior pubic ramus at inferior aspect	H1: stem catarrhine	1.733	1.733	1.733	H1=H2=H3
PVM13	Pelvis	width ischial tuberosity at widest point	H1: stem catarrhine	2.208	2.208	2.208	H1=H2=H3
PVS9	Pelvis	height of lunate surface at infero-medial aspect	H1: stem catarrhine	0.541	0.541	0.541	H1=H2=H3
MC1S3	MC1	curvature along head in midline	H1: stem catarrhine	1.518	1.518	1.518	H1=H2=H3
CM2	Capitate	length dorsal border MC facet.	H1: stem catarrhine	0.612	0.612	0.612	H1=H2=H3
CM12	Capitate	width hamate facet in midline	H1: stem catarrhine	0.723	0.723	0.723	H1=H2=H3
SM12	Scaphoid	breadth from radial facet to border between capitate and lunate facet	H1: stem catarrhine	0.332	0.332	0.332	H1=H2=H3
TZMM3	Trapezium	length palmar border MC1	H1: stem catarrhine	1.05	1.05	1.05	H1=H2=H3
TZMM8	Trapezium	with trapezoid facet at midpoint	H1: stem catarrhine	0.2	0.2	0.2	H1=H2=H3
MT4M23	MT4	medio-lateral width shaft at midpoint	H1: stem catarrhine	0.295	0.295	0.295	H1=H2=H3
MT5M21	MT5	planto-dorsal width shaft at midpoint	H1: stem catarrhine	0.26	0.26	0.26	H1=H2=H3
MT5S2	MT5	planto-dorsal length along curvature of proximal facet	H1: stem catarrhine	1.214	1.214	1.214	H1=H2=H3
CCM2	Calcaneus	proximo-distal length posterior Astragali at medial border	H1: stem catarrhine	1.073	1.073	1.073	H1=H2=H3
CCM18	Calcaneus	width at narrowest point of neck at midpoint	H1: stem catarrhine	0.902	0.902	0.902	H1=H2=H3

MCM3	Med. Cuneiform	width MT1 facet perpendicular to main axis at midpoint	H1: stem catarrhine	0.628	0.628	0.628	H1=H2=H3
ICM6	Int. cuneiform	medio-lateral length plantar border of navicular facet	H1: stem catarrhine	0.407	0.407	0.407	H1=H2=H3
o4	Orbit	orbit width	H1: stem catarrhine	2	2	2	H1=H2=H3
o25	Maxilla	inferior margin of nasal aperture flat or tantero-posteriorering	H1: stem catarrhine	5	5	5	H1=H2=H3
UO10	Ulna	pressence tubercle at base of styloid	H1: stem catarrhine	4	4	4	H1=H2=H3
UO12	Ulna	outline of lateral border of trochlea	H1: stem catarrhine	3	3	3	H1=H2=H3
m27	Temporal	height narrowest point anterior to articular tubercle	H1: stem catarrhine	5	5	5	H1=H2=H3
hum4	Humerus	medio-lateral projection of lateral epicondyle	H1: stem catarrhine	0.557	0.521	0.557	H2
hum7	Humerus	medio-lateral length trochlear keel at proxiumal border	H1: stem catarrhine	0.782	0.763	0.782	H2
PVM11	Pelvis	width across acetabulum	H1: stem catarrhine	0.874	0.811	0.874	H2
MC2M11	MC2	height dorsal aspect MC 3/capitate facet	H1: stem catarrhine	0.704	0.663	0.704	H2
AM10	Astragalus	dorso-palmar height lat malleolus facet on side of trochlea at level of flange	H1: stem catarrhine	1.016	1.007	1.016	H2
MM16	Mandible	width across incisors	H2: hominoid	1.088	1.065	1.088	H2
US14	Ulna	length along curvature of anterior border distal carpal facet	H2: hominoid	1.824	1.724	1.824	H2
RM28	Radius	medio-lateral length anterior border distal carpal facet	H2: hominoid	1.059	0.894	1.059	H2
hum10	Humerus	medio-lateral length of trochlea and capitulum at disto-anterior surface	H2: hominoid	2.024	1.773	2.024	H2
hum13	Humerus	medio-lateral length trochlear keel at disto-anterior surface	H2: hominoid	0.823	0.81	0.823	H2
hum20	Humerus	medio-lateral length capitulum at midline of trochlea	H2: hominoid	1.047	1.019	1.047	H2
hum38	Humerus	proximo-distal height lateral trochlear keel on posterior aspect	H2: hominoid	1.416	1.285	1.416	H2
hum46	Humerus	projection of median trochlear keel distal to margin of medial epicondyle	H2: hominoid	0.741	0.726	0.741	H2
hum47	Humerus	wdiest point of coronoid fossa	H2: hominoid	1.07	0.968	1.07	H2
PVM10	Pelvis	height of acetabulum	H2: hominoid	0.981	0.969	0.981	H2
MC5M25	MC5	medio-lateral width shaft at midpoint	H2: hominoid	0.218	0.192	0.218	H2
HM4	Hamate	palmo-dorsal width hamulus at midpoint	H2: hominoid	0.641	0.593	0.641	H2
PM1	Pisiform	length of articular facet on triquetral surface	H2: hominoid	0.603	0.591	0.603	H2

TZDM2	Trapezoid	medio-lateral width MC facet	H2: hominoid	0.517	0.502	0.517	H2
TZMM5	Trapezium	dorso-palmar length MC2 facet	H2: hominoid	0.584	0.544	0.584	H2
CCM25	Calcaneus	planto-dorsal height sustentaculum	H2: hominoid	0.41	0.394	0.41	H2
NM7	Navicular	proximo-distal height at tubercle	H2: hominoid	1.227	1.167	1.227	H2
NM13	Navicular	dorso-plantar width cuboid facet	H2: hominoid	0.825	0.802	0.825	H2
NM17	Navicular	dorso plantar height at lateral cuneiform facet	H2: hominoid	0.788	0.761	0.788	H2
NM21	Navicular	dorso plantar height astragular facet in midline	H2: hominoid	0.698	0.677	0.698	H2
MM13	Mandible	antero-posterior width coronoid process at tip	H2: hominoid	0.435	0.435	0.435	H1=H2=H3
US11	Ulna	length along curvature of lateral edge of trochlear notch	H2: hominoid	3.523	3.523	3.523	H1=H2=H3
UM1	Ulna	height olecranon process at medial border	H2: hominoid	1.266	1.266	1.266	H1=H2=H3
UM4	Ulna	width olecranon process at anterior border	H2: hominoid	0.62	0.62	0.62	H1=H2=H3
UM6	Ulna	width olecranon process at posterior border	H2: hominoid	0.934	0.934	0.934	H1=H2=H3
UM7	Ulna	length olecranon process to proximal border of trochlear notch at medial border	H2: hominoid	2.03	2.03	2.03	H1=H2=H3
UM8	Ulna	length olecranon process to proximal border of trochlear notch in midline	H2: hominoid	2.072	2.072	2.072	H1=H2=H3
UM10	Ulna	width proximal to trochlear notch	H2: hominoid	0.759	0.759	0.759	H1=H2=H3
UM23	Ulna	length oblique line running	H2: hominoid	5.946	5.946	5.946	H1=H2=H3
UM24	Ulna	length ridge extending from posterior aspect of coronoid process	H2: hominoid	2.183	2.183	2.183	H1=H2=H3
UM28	Ulna	medio-lateral width ulnar styloid at midline	H2: hominoid	0.39	0.39	0.39	H1=H2=H3
UM32	Ulna	antero-posterior width of distal carpal articulation in midline	H2: hominoid	0.453	0.453	0.453	H1=H2=H3
UM37	Ulna	antero-posterior width shaft proximal to distal radial articulation	H2: hominoid	0.529	0.529	0.529	H1=H2=H3
UM39	Ulna	antero-posterior height from tip of olecranon process to bottom of shaft	H2: hominoid	2.015	2.015	2.015	H1=H2=H3
RM7	Radius	proximo-distal height radial head border on anterior aspect	H2: hominoid	0.515	0.515	0.515	H1=H2=H3
RM12	Radius	medio-lateral width tubercle	H2: hominoid	0.59	0.59	0.59	H1=H2=H3
RM22	Radius	antero-posterior length facet for ulna	H2: hominoid	0.585	0.585	0.585	H1=H2=H3
RS1	Radius	medio-lateral length along curvature in midline of carpal facet	H2: hominoid	1.333	1.333	1.333	H1=H2=H3
hum2	Humerus	medio-lateral distance from lateral border of capitulum to midline of median keel	H2: hominoid	0.821	0.821	0.821	H1=H2=H3

hum15	Humerus	medio-lateral length trochlear and capitulum at distal border	H2: hominoid	1.914	1.914	1.914	H1=H2=H3
hum43	Humerus	length medial epicondyle	H2: hominoid	0.915	0.915	0.915	H1=H2=H3
hum53	Humerus	proximo-distal height of lateral epicondyle	H2: hominoid	1.483	1.483	1.483	H1=H2=H3
hum62	Humerus	antero-posterior depth distal humerus at lateralmost point	H2: hominoid	1.182	1.182	1.182	H1=H2=H3
PVM3	Pelvis	height obturator foramen	H2: hominoid	2.488	2.488	2.488	H1=H2=H3
PVM13	Pelvis	width ischial tuberosity at widest point	H2: hominoid	2.208	2.208	2.208	H1=H2=H3
PVM21	Pelvis	height from posterior inferior illiac spine to superior most point of posterior illiac blade border	H2: hominoid	3.64	3.64	3.64	H1=H2=H3
PVM26	Pelvis	height auricular surface at posterior aspect	H2: hominoid	4.063	4.063	4.063	H1=H2=H3
PVS5	Pelvis	circumferecen ilium at greater sciatic notch	H2: hominoid	3.096	3.096	3.096	H1=H2=H3
PVS9	Pelvis	height of lunate surface at infero-medial aspect	H2: hominoid	0.541	0.541	0.541	H1=H2=H3
PVS13	Pelvis	width acetabulum not including lunate surface	H2: hominoid	0.935	0.935	0.935	H1=H2=H3
MC2M24	MC2	medio-lateral width shaft at midpoint	H2: hominoid	0.361	0.361	0.361	H1=H2=H3
MC2M25	MC2	palmo-dorsal width shaft at midpoint	H2: hominoid	0.433	0.433	0.433	H1=H2=H3
MC3M18	MC3	width dorsal aspect MC 4 facet	H2: hominoid	0.311	0.311	0.311	H1=H2=H3
MC3M21	MC3	height MC 4 facet in midline	H2: hominoid	0.487	0.487	0.487	H1=H2=H3
MC3M33	MC3	medio-lateral width shaft at midpoint	H2: hominoid	0.291	0.291	0.291	H1=H2=H3
MC3M34	MC3	palmo-dorsal width shaft at midpoint	H2: hominoid	0.41	0.41	0.41	H1=H2=H3
MC4M17	MC4	width palmar aspect MC 5 facet	H2: hominoid	0.346	0.346	0.346	H1=H2=H3
MC4M21	MC4	height MC 5 facet in midline	H2: hominoid	0.373	0.373	0.373	H1=H2=H3
MC4M33	MC4	medio-lateral width shaft at midpoint	H2: hominoid	0.265	0.265	0.265	H1=H2=H3
MC5M12	MC5	width tubercle on medial aspect proximal shaft	H2: hominoid	0.619	0.619	0.619	H1=H2=H3
MC5M13	MC5	height tubercle on medial aspect proximal shaft	H2: hominoid	0.436	0.436	0.436	H1=H2=H3
CM11	Capitate	width hamate facet at head	H2: hominoid	0.528	0.528	0.528	H1=H2=H3
HM3	Hamate	medio-lateral width of hamulus at midpoint	H2: hominoid	0.602	0.602	0.602	H1=H2=H3
HM6	Hamate	medio-lateral width of medial aspect MC facet	H2: hominoid	0.472	0.472	0.472	H1=H2=H3
TQM1	Triquetral	width of pisiform facet	H2: hominoid	0.434	0.434	0.434	H1=H2=H3
TQM10	Triquetral	triquetral breadth	H2: hominoid	0.239	0.239	0.239	H1=H2=H3
PM4	Pisiform	height of articular facet on ulnar surface	H2: hominoid	0.326	0.326	0.326	H1=H2=H3
PM5	Pisiform	length pisiform	H2: hominoid	1.141	1.141	1.141	H1=H2=H3
PM7	Pisiform	width articular end perpendicular to main axis	H2: hominoid	0.31	0.31	0.31	H1=H2=H3
TZDM10	Trapezoid	height capitate facet	H2: hominoid	0.609	0.609	0.609	H1=H2=H3
TZMM8	Trapezium	with trapezoid facet at midpoint	H2: hominoid	0.2	0.2	0.2	H1=H2=H3

LM16	Lunate	proximo distal width proximal acessory facet on palmar surface	H2: hominoid	0	0	0	H1=H2=H3
MT2M13	MT2	planto dorsal width dorsal segment lateral cuneiform facet	H2: hominoid	0.286	0.286	0.286	H1=H2=H3
MT2M15	MT2	width plantar segment lateral cuneiform facet	H2: hominoid	0.558	0.558	0.558	H1=H2=H3
MT2M16	MT2	height plantar segment lateral cuneiform facet	H2: hominoid	0.841	0.841	0.841	H1=H2=H3
MT2M27	MT2	medio-lateral width shaft at midpoint	H2: hominoid	0.309	0.309	0.309	H1=H2=H3
MT3M14	MT3	proximo-distal height plantar aspect MT 4 facet	H2: hominoid	0.517	0.517	0.517	H1=H2=H3
MT3M4	MT3	planto-dorsal width dorsal aspect proximal facet	H2: hominoid	0.289	0.289	0.289	H1=H2=H3
MT4M10	MT4	proximo-distal width plantar aspect MT 5 facet	H2: hominoid	0.636	0.636	0.636	H1=H2=H3
MT4M29	MT4	planto dorsal width in midline of proximal facet	H2: hominoid	0.926	0.926	0.926	H1=H2=H3
MT5M8	MT5	proximo-distal width tubercle	H2: hominoid	0.84	0.84	0.84	H1=H2=H3
MT5M24	MT5	planto-dorsal width medial border proximal facet	H2: hominoid	0.916	0.916	0.916	H1=H2=H3
CCM18	Calcaneus	width at narrowest point of neck at midpoint	H2: hominoid	0.902	0.902	0.902	H1=H2=H3
AM20	Astragalus	medio-lateral width clacaneal facet on neck at posterior extent	H2: hominoid	1.184	1.184	1.184	H1=H2=H3
AM31	Astragalus	dorsal projection of tubercles below torchlea	H2: hominoid	0.536	0.536	0.536	H1=H2=H3
CBM24	Cuboid	proximo-distal hieght navicular facet	H2: hominoid	0.776	0.776	0.776	H1=H2=H3
CBS6	Cuboid	planto-dorsal length along curvated through midpoint of calcaneal facet	H2: hominoid	0.722	0.722	0.722	H1=H2=H3
MCM5	Med. Cuneiform	proximo distal length MT2 facet	H2: hominoid	0.7	0.7	0.7	H1=H2=H3
MCM7	Med. Cuneiform	proximo distal length proximal segment of intermediate cuneiform facet	H2: hominoid	0.431	0.431	0.431	H1=H2=H3
ICM5	Int. cuneiform	medio-lateral length dorsal border of navicular facet	H2: hominoid	0.661	0.661	0.661	H1=H2=H3
ICM10	Int. cuneiform	medio-lateral length plantar border of MT2 facet	H2: hominoid	0.465	0.465	0.465	H1=H2=H3
ICM11	Int. cuneiform	dorso plantar length MT2 facet	H2: hominoid	0.791	0.791	0.791	H1=H2=H3
LCM3	Lat. cuneiform	dorso plantar length navicular facet at lateral border	H2: hominoid	0.443	0.443	0.443	H1=H2=H3
LCM4	Lat. cuneiform	dorso plantar length navicular facet at medial border	H2: hominoid	0.462	0.462	0.462	H1=H2=H3
LCR1	Lat. cuneiform	angle of navicular facet	H2: hominoid	8.337	8.337	8.337	H1=H2=H3
o31	Palatine	number of palatine foramina	H2: hominoid	5	5	5	H1=H2=H3

o49	Neurocranium	prominence of temporal lines	H2: hominoid	5	5	5	H1=H2=H3
LO1	Lunate	pressence clearly divided acessory facet on palmar surface	H2: hominoid	0	0	0	H1=H2=H3
UO12	Ulna	outline of lateral border of trochlea	H2: hominoid	3	3	3	H1=H2=H3
m9	Facial	width between superior zygomatic roots	H2: hominoid	5	5	5	H1=H2=H3
m1	Frontal	thickness of supra-orbital rim	H2: hominoid	6	6	6	H1=H2=H3
m19	Maxilla	palate depth (supero-inferior) at m3	H2: hominoid	6	6	6	H1=H2=H3
m20	Maxilla	palate length	H2: hominoid	5	5	5	H1=H2=H3
m21	Maxilla	palate width at first premolars	H2: hominoid	6	6	6	H1=H2=H3
m22	Maxilla	width across all incisors	H2: hominoid	4	4	4	H1=H2=H3
m40	Temporal	length ectotympanic ring/tube	H2: hominoid	4	4	4	H1=H2=H3
MM8	Mandible	thickness of gonial angle	H2: hominoid	2	2	2	H1=H2=H3
MM18	Mandible	width at p3s	H2: hominoid	5	5	5	H1=H2=H3
MM19	Mandible	width across molars at m2	H2: hominoid	6	6	6	H1=H2=H3
MM25	Mandible	antero-posterior width ramus at alveolar margin	H2: hominoid	5	5	5	H1=H2=H3
MM26	Mandible	antero-posterior width ramus inferior to condyle	H2: hominoid	5	5	5	H1=H2=H3
MM30	Mandible	height corpus at symphysis	H2: hominoid	7	7	7	H1=H2=H3
MM31	Mandible	medio-lateral width mandible corpus at m1	H2: hominoid	7	7	7	H1=H2=H3
PVM17	Pelvis	height of illium	H2: hominoid	4	4	4	H1=H2=H3
MT1S3	MT1	length along curvature of head	H2: hominoid	6	6	6	H1=H2=H3
hum42	Humerus	length from proximal-most point of olecranon fossa to disto-lateral corner of fossa	H2: hominoid	1.554	1.648	1.554	H1=H3
PVM12	Pelvis	length ischial tuberosity	H2: hominoid	2.907	3.093	2.907	H1=H3
CCM3	Calcaneus	proximo-distal length posterior Astragali at lateral border	H2: hominoid	1.062	1.082	1.062	H1=H3
AM14	Astragalus	medio-lateral width at anterior border posterior calcaneal facet	H2: hominoid	0.818	0.846	0.818	H1=H3
AM26	Astragalus	planto-dorsal height facet for medial malleolus at anterior border	H2: hominoid	0.77	0.786	0.77	H1=H3
AM30	Astragalus	dorsal projection of medial tubercle below torchlea	H2: hominoid	1.005	1.064	1.005	H1=H3
NM1	Navicular	medio-lateral length through midpoint	H2: hominoid	0.708	0.847	0.708	H1=H3
NM19	Navicular	dorso plantar height astragular facet at medial border	H2: hominoid	0.742	0.819	0.742	H1=H3
MCM4	Med. Cuneiform	width MT1 facet perpendicular to main axis at plantar border	H2: hominoid	1.102	1.114	1.102	H1=H3

m18	Facial	interdentale in midline to glabella	H2: hominoid	5	6	5	H1=H3
MT5M22	MT5	medio-lateral width dorsal border proximal facet	H3: hominid	0.702	0.734	0.702	H1=H3
CCM23	Calcaneus	planto-dorsal height from distal posterior Astragali facet to plantar surface	H3: hominid	0.694	0.72	0.694	H1=H3
MM13	Mandible	antero-posterior width coronoid process at tip	H3: hominid	0.435	0.435	0.435	H1=H2=H3
US12	Ulna	length along curvature of proximal border of trochlea	H3: hominid	2.48	2.48	2.48	H1=H2=H3
UM17	Ulna	length of radial notch	H3: hominid	0.819	0.819	0.819	H1=H2=H3
UM24	Ulna	length ridge extending from posterior aspect of coronoid process	H3: hominid	2.183	2.183	2.183	H1=H2=H3
UM25	Ulna	antero-posterior width shaft at termination of oblique line	H3: hominid	0.989	0.989	0.989	H1=H2=H3
RM7	Radius	proximo-distal height radial head border on anterior aspect	H3: hominid	0.515	0.515	0.515	H1=H2=H3
RM16	Radius	antero-posterior width across shaft distal to tubercle	H3: hominid	0.637	0.637	0.637	H1=H2=H3
RM18	Radius	antero-posterior breadth across distal radius in midline	H3: hominid	0.809	0.809	0.809	H1=H2=H3
hus5	Humerus	length along curvature between starting and ending point of trochlear at medial trochlear keel	H3: hominid	4.108	4.108	4.108	H1=H2=H3
hum34	Humerus	antero-posterior depth of lateral border capitulum	H3: hominid	1.595	1.595	1.595	H1=H2=H3
hum36	Humerus	proximo-distal height medial to median trochlear keel	H3: hominid	0.669	0.669	0.669	H1=H2=H3
MC1M2	MC1	palmo-dorsal width proximal facet	H3: hominid	0.811	0.811	0.811	H1=H2=H3
MC1M9	MC1	palmo-dorsal width midline head at keel	H3: hominid	0.54	0.54	0.54	H1=H2=H3
CS4	Capitate	medio-lateral length along curvature dorsal border MC facet	H3: hominid	0.569	0.569	0.569	H1=H2=H3
CM8	Capitate	narrowest point in midline of dorsal surface	H3: hominid	0.314	0.314	0.314	H1=H2=H3
CM18	Capitate	width dorsal aspect trapezoid facet	H3: hominid	0.339	0.339	0.339	H1=H2=H3
LM9	Lunate	width palmar border radial facet	H3: hominid	1.149	1.149	1.149	H1=H2=H3
MT3M14	MT3	proximo-distal height plantar aspect MT 4 facet	H3: hominid	0.517	0.517	0.517	H1=H2=H3
MT5M9	MT5	planto-dorsal height tubercle	H3: hominid	0.528	0.528	0.528	H1=H2=H3
MT5M25	MT5	planto-dorsal width lateral border proximal facet	H3: hominid	0.537	0.537	0.537	H1=H2=H3
CCM4	Calcaneus	medio-lateral width through posterior Astragali facet at midpoint	H3: hominid	0.801	0.801	0.801	H1=H2=H3
CCM15	Calcaneus	planto-dorsal height tuberosity	H3: hominid	1.248	1.248	1.248	H1=H2=H3

Appendix E: Chapter 5 PCA loadings

	All synapomorphies		
	PC1	PC2	PC3
UO12	-0.242	0.185	-0.194
o31	-0.112	-0.160	0.201
hum47	-0.036	0.147	-0.053
hum10	-0.035	0.155	0.010
hum13	-0.035	0.038	0.018
AM31	-0.032	-0.028	0.023
hum46	-0.031	0.125	-0.016
US14	-0.027	0.210	-0.041
o49	-0.020	0.041	0.594
UM6	-0.018	0.080	-0.005
HM4	-0.018	0.049	-0.012
CCM18	-0.017	0.001	-0.001
PVM10	-0.017	0.122	-0.005
AM30	-0.015	-0.014	0.034
hum53	-0.013	0.038	-0.020
hum15	-0.010	0.183	-0.016
MC5M25	-0.009	0.015	0.004
TZDM10	-0.007	0.015	0.027
MM16	-0.007	0.073	0.025
AM14	-0.007	-0.005	-0.002
MCM5	-0.005	0.012	0.012
MC3M34	-0.005	0.024	0.008
CM11	-0.004	0.040	-0.005
UM32	-0.004	-0.001	0.012
TZMM8	-0.003	0.015	-0.002
CCM25	-0.002	-0.015	0.008
LCM3	-0.002	0.022	0.018
hum42	-0.001	0.015	0.000
TZMM5	0.001	0.060	0.006
PM7	0.002	0.006	-0.013
MC4M17	0.003	0.006	0.004
HM3	0.003	-0.001	0.011
MC2M24	0.004	0.025	0.009
AM26	0.004	-0.005	0.039
MC2M25	0.005	0.030	0.006
MCM7	0.005	0.018	-0.020
MC4M21	0.005	0.003	-0.003
ICM10	0.007	0.019	-0.006
MC4M33	0.007	-0.002	0.006
CCM3	0.008	0.052	-0.052

	All synapomorphies		
	PC1	PC2	PC3
MCM4	0.008	0.009	0.012
MC5M13	0.009	0.003	-0.023
TZDM2	0.009	0.024	0.011
UM37	0.011	0.024	-0.014
hum62	0.011	0.058	-0.014
MC3M33	0.012	0.002	0.004
MC5M12	0.012	-0.001	-0.020
ICM5	0.013	0.010	-0.013
hum20	0.013	0.089	0.016
PVS13	0.014	0.036	0.014
MC3M18	0.015	-0.015	0.003
HM6	0.016	-0.019	-0.011
LCM4	0.018	-0.011	0.006
PVM17	0.018	0.072	-0.263
TQM1	0.019	-0.009	0.011
MT4M10	0.019	-0.016	-0.001
hum38	0.019	0.094	-0.010
MC3M21	0.023	-0.002	-0.017
UM28	0.023	-0.023	0.011
ICM11	0.023	-0.049	0.005
PVS9	0.025	0.027	-0.009
UM4	0.028	0.018	-0.024
hum2	0.029	-0.007	0.003
MT4M29	0.038	-0.061	-0.027
TQM10	0.045	-0.038	-0.003
PM5	0.046	-0.013	0.033
PM1	0.046	-0.036	-0.033
PM4	0.046	-0.068	0.003
AM20	0.054	-0.087	-0.008
UM1	0.071	-0.042	-0.043
PVM21	0.073	-0.072	0.231
PVS5	0.087	0.074	0.205
UM39	0.101	-0.114	0.006
PVM3	0.107	-0.079	0.001
UM7	0.107	-0.184	-0.013
UM10	0.109	-0.236	-0.036
MM18	0.115	0.445	0.103
PVM12	0.119	-0.059	0.148
US11	0.130	-0.002	-0.045
UM8	0.131	-0.216	-0.051
PVM13	0.158	-0.146	0.210

	All synapomorphies		
	PC1	PC2	PC3
m18	0.187	-0.272	-0.189
PVM26	0.187	-0.088	0.107
m19	0.223	0.179	-0.252
m21	0.233	0.206	0.244
MM31	0.233	0.206	0.244
m9	0.234	-0.189	0.059
m1	0.236	-0.043	-0.117
m40	0.259	-0.034	0.031
MM19	0.268	0.219	-0.010
MM30	0.301	0.027	-0.128
m20	0.302	0.112	-0.131
m22	0.302	0.112	-0.131
	Cranial synapomorphies		
	PC1	PC2	PC3
m20	-0.430	-0.022	0.164
m22	-0.430	-0.022	0.164
m40	-0.351	-0.179	0.105
m1	-0.347	0.174	-0.459
m19	-0.323	-0.003	0.334
m9	-0.311	-0.045	-0.211
m21	-0.264	-0.429	0.239
m18	-0.254	0.141	-0.628
o49	0.111	-0.849	-0.342
o31	0.197	-0.098	0.015
MM16	0.029	-0.086	0.295
MM18	0.380	-0.827	0.110
MM30	0.507	0.551	0.150
MM31	0.529	0.066	0.561
MM19	0.564	0.005	-0.751
	Forelimb synapomorphies		
	PC1	PC2	PC3
UO12	-0.541	0.579	0.497
US14	-0.227	-0.327	0.221
hum10	-0.174	-0.195	0.099
hum47	-0.170	-0.108	0.215
hum15	-0.164	-0.250	0.206
RM28	-0.143	-0.132	0.041
hum46	-0.139	-0.116	0.163
RM22	-0.104	-0.075	-0.045
UM6	-0.103	-0.087	0.065
hum13	-0.082	-0.010	-0.026

	Forelimb synapomorphies		
	PC1	PC2	PC3
hum20	-0.060	-0.162	0.104
RM12	-0.049	-0.132	-0.043
hum53	-0.046	-0.058	0.112
hum38	-0.046	-0.178	0.086
hum62	-0.023	-0.105	0.175
UM37	-0.009	-0.046	0.131
hum42	-0.007	-0.024	-0.100
RM7	-0.007	-0.110	-0.014
UM32	-0.001	0.016	-0.012
RS1	0.008	-0.196	0.139
UM4	0.013	-0.053	0.094
hum2	0.048	-0.029	-0.003
UM28	0.051	-0.008	0.003
UM1	0.143	-0.040	0.172
US11	0.199	-0.407	0.307
UM39	0.240	-0.082	0.242
UM7	0.316	0.153	0.291
UM10	0.356	0.176	0.202
UM8	0.376	0.164	0.379
	Manus synapomorphies		
	PC1	PC2	PC3
HM4	-0.258	-0.055	-0.263
CM11	-0.141	0.307	-0.227
TZMM5	-0.133	0.333	-0.247
MC3M34	-0.102	0.003	-0.178
MC5M25	-0.094	0.066	-0.050
TZDM10	-0.084	0.131	-0.234
MC2M25	-0.064	0.057	-0.302
MC2M24	-0.056	0.009	-0.289
TZMM8	-0.043	0.081	-0.059
TZDM2	0.016	0.120	-0.350
PM7	0.016	-0.015	-0.066
HM3	0.029	-0.089	-0.179
MC4M21	0.029	0.132	-0.034
MC4M17	0.035	0.196	-0.030
MC4M33	0.061	0.016	-0.104
MC3M33	0.073	0.026	-0.166
MC5M12	0.165	0.375	-0.056
TQM1	0.165	-0.049	-0.124
MC3M21	0.173	0.055	-0.197
MC5M13	0.175	0.435	0.043

Manus synapomorphies			
	PC1	PC2	PC3
MC3M18	0.176	0.019	-0.044
HM6	0.182	0.070	-0.086
PM5	0.244	-0.562	-0.490
TQM10	0.420	0.082	-0.107
PM1	0.438	0.127	-0.049
PM4	0.491	-0.047	0.173

Pelvis synapomorphies			
	PC1	PC2	PC3
PVM17	-0.365	-0.883	0.079
PVM10	-0.058	-0.055	0.244
PVS9	0.017	-0.022	-0.051
PVS13	0.058	0.044	0.120
PVM3	0.150	-0.277	-0.306
PVS5	0.278	-0.010	0.127
PVM12	0.318	-0.286	-0.046
PVM13	0.412	-0.113	-0.653
PVM21	0.426	-0.118	0.599
PVM26	0.554	-0.172	0.137

Pes synapomorphies			
	PC1	PC2	PC3
LCR1	-0.983	-0.146	0.049
MT1S3	-0.147	0.962	0.033
CCM18	-0.032	0.018	0.007
AM31	-0.023	0.006	-0.321
CCM3	-0.019	0.000	0.261
LCM3	-0.010	0.052	0.009
AM14	-0.009	0.039	-0.024
NM13	-0.008	-0.008	0.021
CBS6	-0.004	-0.014	0.072
MT2M16	-0.003	0.081	0.216
MT5M8	-0.003	0.056	0.244
MT2M15	-0.002	0.006	0.235
CCM25	-0.001	0.015	-0.047
AM30	0.000	0.020	-0.281
AM26	0.000	0.060	0.008
ICM10	0.002	0.017	0.071
MCM7	0.003	0.001	0.102
NM19	0.004	-0.009	-0.047
NM1	0.005	0.068	-0.203
MCM5	0.006	0.015	-0.055
NM21	0.006	0.024	0.232
MT2M13	0.008	0.004	0.038
ICM5	0.009	0.041	0.079
CBM24	0.010	0.040	0.189
MT3M4	0.011	-0.005	0.088
MT2M27	0.011	0.020	0.069
MCM4	0.012	0.096	-0.020
MT5M24	0.018	-0.061	0.329
MT3M14	0.019	0.035	0.176
NM17	0.020	-0.009	0.187

Pes synapomorphies			
	PC1	PC2	PC3
LCM4	0.020	0.003	0.151
MT4M10	0.020	-0.005	0.129
ICM11	0.032	0.015	0.106
MT4M29	0.039	-0.073	0.317
NM7	0.041	0.056	-0.012
AM20	0.051	-0.043	0.282

Appendix F: Chapter 5 distance matrices

All synapomorphies distance matrix

	Gorilla	Hylob	Sympł	Pongo	Pan	Cerco	Colobi	Macac	Nasali	Papio	Presby	Erythr	Victor	Phese	Platyr	Catarr	Cerco	Homir	Homir	Alloua	Aotus	Ateles	Cebus	Saguir	Saimir	Pithec	Epiplic
Gorilla	0	3.47	4.3	2.1	2.15	4.21	3.93	4.67	3.16	4.32	2.89	3.87	4.15	4.28	4.88	3.84	3.96	3.97	1.23	4.86	2.78	2.86	5.23	4.68	4.35	4.09	3.55
Hylobi	3.47	0	2.53	3.43	3.31	2.97	3.29	3.32	3.02	3.22	3.23	3.04	3.21	3.44	4.75	3.07	2.83	3.23	3.42	4.87	3.72	3.98	4.57	3.75	3.81	3.41	3.55
Sympł	4.3	2.53	0	4.19	3.87	3.31	2.57	2.63	3.57	2.59	3.98	3.09	3.57	3.04	4.57	2.65	2.62	2.85	3.92	4.87	4.42	4.94	4.25	3.69	4.16	3.54	4
Pongo	2.1	3.43	4.19	0	2.72	3.93	4.11	4.73	3.64	4.35	3.64	3.96	4.26	4.28	4.85	4.14	4.24	4.26	2.48	4.81	3.09	3.11	4.98	4.32	4.1	3.99	3.81
Pan	2.15	3.31	3.87	2.72	0	3.81	3.6	4.33	2.76	4.2	2.69	3.5	4.45	3.73	4.44	3.81	3.98	3.69	1.9	4.59	2.16	2.96	4.48	4.55	3.83	3.9	3.42
Cercop	4.21	2.97	3.31	3.93	3.81	0	2.62	3.18	3.14	3.04	3.81	1.76	3.23	3.57	4.65	3.6	3.04	3.73	4.16	4.79	3.6	4.11	3.96	3.4	3.81	3.28	3.73
Colobi	3.93	3.29	2.57	4.11	3.6	2.62	0	2.58	3.51	2.39	3.33	2.48	3.09	3.1	4.28	2.77	2.54	2.96	3.73	4.48	3.6	4.3	4.04	3.24	4.12	3.21	3.78
Macac	4.67	3.32	2.63	4.73	4.33	3.18	2.58	0	3.66	1.29	3.96	2.63	2.95	3	4.35	2.53	2.21	2.71	4.37	4.64	4.45	5.2	4.01	3.37	4.14	3.59	3.75
Nasali	3.16	3.02	3.57	3.64	2.76	3.14	3.51	3.66	0	3.6	2.52	2.72	3.65	4	4.91	3.49	3.04	3.64	2.81	4.91	3.02	3.43	4.86	4.18	3.62	3.95	2.52
Papio	4.32	3.22	2.59	4.35	4.2	3.04	2.39	1.29	3.6	0	3.86	2.43	2.67	2.88	4.19	2.38	2	2.58	4.05	4.45	4.3	5.05	3.92	3.39	3.96	3.45	3.91
Presby	2.89	3.23	3.98	3.64	2.69	3.81	3.33	3.96	2.52	3.86	0	3.29	3.54	4.05	4.2	3.47	3.3	3.33	2.83	4.07	2.6	2.75	4.48	4.19	3.58	3.6	2.68
Erythr	3.87	3.04	3.09	3.96	3.5	1.76	2.48	2.63	2.72	2.43	3.29	0	3.12	3.44	4.59	3.24	2.61	3.39	3.62	4.84	3.45	4.27	4.12	3.63	3.65	3.64	3.36
Victor	4.15	3.21	3.57	4.26	4.45	3.23	3.09	2.95	3.65	2.67	3.54	3.12	0	3.73	4.09	3.05	1.6	3.19	4.31	4.16	4.04	4.23	4.16	2.95	3.59	3.14	3.58
Phese	4.28	3.44	3.04	4.28	3.73	3.57	3.1	3	4	2.88	4.05	3.44	3.73	0	3.72	2.12	3.2	1.85	3.96	4.33	3.86	4.7	3.24	3.57	4.01	2.74	4.61
Platyr	4.88	4.75	4.57	4.85	4.44	4.65	4.28	4.35	4.91	4.19	4.2	4.59	4.09	3.72	0	3.76	4.08	2.99	4.97	1.72	4.03	4.13	2.23	3.69	3.02	2.77	4.79
Catarr	3.84	3.07	2.65	4.14	3.81	3.6	2.77	2.53	3.49	2.38	3.47	3.24	3.05	2.12	3.76	0	2.38	1.02	3.57	4.29	3.93	4.32	3.96	3.18	4.11	2.39	3.9
Cercop	3.96	2.83	2.62	4.24	3.98	3.04	2.54	2.21	3.04	2	3.3	2.61	1.6	3.2	4.08	2.38	0	2.57	3.78	4.32	3.99	4.42	4.05	3.25	3.6	3.24	3.28
Homir	3.97	3.23	2.85	4.26	3.69	3.73	2.96	2.71	3.64	2.58	3.33	3.39	3.19	1.85	2.99	1.02	2.57	0	3.71	3.64	3.78	4.21	3.23	3.32	3.7	2.15	4.03
Homir	1.23	3.42	3.92	2.48	1.9	4.16	3.73	4.37	2.81	4.05	2.83	3.62	4.31	3.96	4.97	3.57	3.78	3.71	0	5.11	2.76	3.43	5.17	4.85	4.43	4.24	3.45
Alloua	4.86	4.87	4.87	4.81	4.59	4.79	4.48	4.64	4.91	4.45	4.07	4.84	4.16	4.33	1.72	4.29	4.32	3.64	5.11	0	4.21	3.95	2.98	3.78	3.22	3.18	4.72
Aotus	2.78	3.72	4.42	3.09	2.16	3.6	3.6	4.45	3.02	4.3	2.6	3.45	4.04	3.86	4.03	3.93	3.99	3.78	2.76	4.21	0	2.48	4.06	3.94	3.26	3.45	3.25
Ateles	2.86	3.98	4.94	3.11	2.96	4.11	4.3	5.2	3.43	5.05	2.75	4.27	4.23	4.7	4.13	4.32	4.42	4.21	3.43	3.95	2.48	0	4.64	4.03	3.64	3.34	3.26
Cebus	5.23	4.57	4.25	4.98	4.48	3.96	4.04	4.01	4.86	3.92	4.48	4.12	4.16	3.24	2.23	3.96	4.05	3.23	5.17	2.98	4.06	4.64	0	4.12	3.21	2.89	5
Saguir	4.68	3.75	3.69	4.32	4.55	3.4	3.24	3.37	4.18	3.39	4.19	3.63	2.95	3.57	3.69	3.18	3.25	3.32	4.85	3.78	3.94	4.03	4.12	0	3.44	2.67	3.88
Saimir	4.35	3.81	4.16	4.1	3.83	3.81	4.12	4.14	3.62	3.96	3.58	3.65	3.59	4.01	3.02	4.11	3.6	3.7	4.43	3.22	3.26	3.64	3.21	3.44	0	3.35	3.78
Pithec	4.09	3.41	3.54	3.99	3.9	3.28	3.21	3.59	3.95	3.45	3.6	3.64	3.14	2.74	2.77	2.39	3.24	2.15	4.24	3.18	3.45	3.34	2.89	2.67	3.35	0	4.22
Epiplic	3.55	3.55	4	3.81	3.42	3.73	3.78	3.75	2.52	3.91	2.68	3.36	3.58	4.61	4.79	3.9	3.28	4.03	3.45	4.72	3.25	3.26	5	3.88	3.78	4.22	0

Cranial synapomorphies

	Gorilla	Hylob	Sympl	Pongo	Pan	Cerco	Colobi	Maca	Nasali	Papio	Presby	Erythr	Victor	Phese	Platyr	Catarr	Cerco	Homir	Homir	Alloua	Aotus	Ateles	Cebus	Saguir	Saimir	Pithec	Epiplic
Gorilla	0	2.68	3.1	1.55	1.55	3.63	2.9	3.1	2.19	3.1	1.9	3.1	3.1	2.9	4.1	2.45	3.1	2.68	0	4.1	1.55	1.55	4.52	2.9	3.63	2.9	1.9
Hylob	2.68	0	1.55	2.68	2.68	1.9	1.9	2.19	2.19	2.19	2.45	1.55	2.19	2.45	4.38	2.45	2.19	2.68	2.68	4.38	2.68	2.68	3.95	2.45	3.29	2.45	2.45
Sympl	3.1	1.55	0	2.68	3.1	1.9	1.1	1.55	2.68	1.55	2.9	1.55	1.55	2.45	4.1	2.45	1.55	2.68	3.1	4.1	3.1	3.1	3.63	1.9	2.9	2.45	2.45
Pongo	1.55	2.68	2.68	0	1.55	2.9	2.45	3.1	2.19	3.1	2.45	2.68	3.1	2.9	4.1	2.9	3.1	3.1	1.55	4.1	1.55	1.55	4.24	2.45	3.29	2.9	1.9
Pan	1.55	2.68	3.1	1.55	0	3.29	2.9	3.46	2.19	3.46	1.9	3.1	3.46	2.45	3.46	2.9	3.46	2.68	1.55	3.46	0	0	3.63	2.9	2.9	2.45	2.45
Cercop	3.63	1.9	1.9	2.9	3.29	0	2.19	2.45	2.45	2.45	3.46	1.1	2.45	2.68	4.52	3.1	2.45	3.29	3.63	4.52	3.29	3.29	3.79	2.19	3.1	2.68	3.1
Colobi	2.9	1.9	1.1	2.45	2.9	2.19	0	1.9	2.9	1.9	2.68	1.9	1.9	2.19	3.95	2.19	1.9	2.45	2.9	3.95	2.9	2.9	3.79	1.55	3.1	2.19	2.68
Macac	3.1	2.19	1.55	3.1	3.46	2.45	1.9	0	2.68	0	2.9	1.55	0	2.45	3.79	1.9	0	2.19	3.1	3.79	3.46	3.46	3.63	1.9	2.9	2.45	2.45
Nasali	2.19	2.19	2.68	2.19	2.19	2.45	2.9	2.68	0	2.68	2.45	2.19	2.68	2.9	4.38	2.9	2.68	3.1	2.19	4.1	2.19	2.19	4.24	2.45	2.9	2.9	1.9
Papio	3.1	2.19	1.55	3.1	3.46	2.45	1.9	0	2.68	0	2.9	1.55	0	2.45	3.79	1.9	0	2.19	3.1	3.79	3.46	3.46	3.63	1.9	2.9	2.45	2.45
Presby	1.9	2.45	2.9	2.45	1.9	3.46	2.68	2.9	2.45	2.9	0	2.9	2.9	2.68	3.63	2.68	2.9	2.45	1.9	3.29	1.9	1.9	3.79	3.1	3.1	2.68	2.19
Erythr	3.1	1.55	1.55	2.68	3.1	1.1	1.9	1.55	2.19	1.55	2.9	0	1.55	2.45	4.1	2.45	1.55	2.68	3.1	4.1	3.1	3.1	3.63	1.9	2.9	2.45	2.45
Victor	3.1	2.19	1.55	3.1	3.46	2.45	1.9	0	2.68	0	2.9	1.55	0	2.45	3.79	1.9	0	2.19	3.1	3.79	3.46	3.46	3.63	1.9	2.9	2.45	2.45
Phese	2.9	2.45	2.45	2.9	2.45	2.68	2.19	2.45	2.9	2.45	2.68	2.45	2.45	0	2.9	1.55	2.45	1.1	2.9	3.29	2.45	2.45	2.68	2.19	2.68	0	3.46
Platyr	4.1	4.38	4.1	4.1	3.46	4.52	3.95	3.79	4.38	3.79	3.63	4.1	3.79	2.9	0	3.63	3.79	2.68	4.1	1.55	3.46	3.46	1.9	3.63	2.45	2.9	4.24
Catarr	2.45	2.45	2.45	2.9	2.9	3.1	2.19	1.9	2.9	1.9	2.68	2.45	1.9	1.55	3.63	0	1.9	1.1	2.45	3.95	2.9	2.9	3.79	2.19	3.46	1.55	3.1
Cercop	3.1	2.19	1.55	3.1	3.46	2.45	1.9	0	2.68	0	2.9	1.55	0	2.45	3.79	1.9	0	2.19	3.1	3.79	3.46	3.46	3.63	1.9	2.9	2.45	2.45
Homir	2.68	2.68	2.68	3.1	2.68	3.29	2.45	2.19	3.1	2.19	2.45	2.68	2.19	1.1	2.68	1.1	2.19	0	2.68	3.1	2.68	2.68	2.9	2.45	2.9	1.1	3.29
Homir	0	2.68	3.1	1.55	1.55	3.63	2.9	3.1	2.19	3.1	1.9	3.1	3.1	2.9	4.1	2.45	3.1	2.68	0	4.1	1.55	1.55	4.52	2.9	3.63	2.9	1.9
Alloua	4.1	4.38	4.1	4.1	3.46	4.52	3.95	3.79	4.1	3.79	3.29	4.1	3.79	3.29	1.55	3.95	3.79	3.1	4.1	0	3.46	3.46	2.45	3.63	2.45	3.29	3.95
Aotus	1.55	2.68	3.1	1.55	0	3.29	2.9	3.46	2.19	3.46	1.9	3.1	3.46	2.45	3.46	2.9	3.46	2.68	1.55	3.46	0	0	3.63	2.9	2.9	2.45	2.45
Ateles	1.55	2.68	3.1	1.55	0	3.29	2.9	3.46	2.19	3.46	1.9	3.1	3.46	2.45	3.46	2.9	3.46	2.68	1.55	3.46	0	0	3.63	2.9	2.9	2.45	2.45
Cebus	4.52	3.95	3.63	4.24	3.63	3.79	3.79	3.63	4.24	3.63	3.79	3.63	3.63	2.68	1.9	3.79	3.63	2.9	4.52	2.45	3.63	3.63	0	3.79	2.19	2.68	4.38
Saguir	2.9	2.45	1.9	2.45	2.9	2.19	1.55	1.9	2.45	1.9	3.1	1.9	1.9	2.19	3.63	2.19	1.9	2.45	2.9	3.63	2.9	2.9	3.79	0	2.68	2.19	2.68
Saimir	3.63	3.29	2.9	3.29	2.9	3.1	3.1	2.9	2.9	2.9	3.1	2.9	2.9	2.68	2.45	3.46	2.9	2.9	3.63	2.45	2.9	2.9	2.19	2.68	0	2.68	3.1
Pithec	2.9	2.45	2.45	2.9	2.45	2.68	2.19	2.45	2.9	2.45	2.68	2.45	2.45	0	2.9	1.55	2.45	1.1	2.9	3.29	2.45	2.45	2.68	2.19	2.68	0	3.46
Epiplic	1.9	2.45	2.45	1.9	2.45	3.1	2.68	2.45	1.9	2.45	2.19	2.45	2.45	3.46	4.24	3.1	2.45	3.29	1.9	3.95	2.45	2.45	4.38	2.68	3.1	3.46	0

Mandibular synapomorphies

	Gorilla	Hylob	Sympl	Pongo	Pan	Cercop	Colobi	Macac	Nasali	Papio	Presby	Erythr	Victor	Phese	Platyr	Catarr	Cercop	Homir	Homir	Alloua	Aotus	Ateles	Cebus	Saguir	Saimir	Pithec	Epiplic
Gorilla	0	1.69	2.37	1.19	0.17	1.69	2.05	2.37	0.2	2.37	0.23	1.19	1.68	2.37	2.38	2.37	1.68	2.37	0.02	2.37	0.37	0.22	2.38	2.38	1.24	2.37	0.36
Hylob	1.69	0	1.68	1.23	1.72	1.67	2.05	1.7	1.67	1.73	1.67	2.05	1.67	1.68	1.67	1.68	1.68	1.68	1.69	1.67	1.68	1.67	1.67	1.67	1.19	1.67	1.68
Sympl	2.37	1.68	0	2.06	2.38	1.68	1.18	0.17	2.37	0.29	2.37	2.05	1.68	0.03	0.16	0.03	1.67	0.03	2.37	0.07	2.38	2.37	0.16	0.16	2.07	0.1	2.38
Pongo	1.19	1.23	2.06	0	1.18	2.08	2.38	2.05	1.22	2.05	1.23	1.69	2.07	2.06	2.08	2.06	2.06	2.06	1.19	2.07	1.28	1.23	2.08	2.08	0.49	2.07	1.27
Pan	0.17	1.72	2.38	1.18	0	1.72	2.07	2.37	0.38	2.37	0.41	1.22	1.71	2.38	2.4	2.39	1.7	2.38	0.15	2.39	0.55	0.39	2.41	2.4	1.31	2.4	0.53
Cercop	1.69	1.67	1.68	2.08	1.72	0	1.19	1.7	1.67	1.72	1.67	1.19	1.67	1.68	1.67	1.68	1.68	1.68	1.69	1.67	1.68	1.67	1.67	1.67	2.06	1.67	1.68
Colobi	2.05	2.05	1.18	2.38	2.07	1.19	0	1.2	2.05	1.22	2.05	1.67	1.18	1.18	1.19	1.18	1.18	1.18	2.05	1.18	2.06	2.05	1.19	1.19	2.38	1.19	2.06
Macac	2.37	1.7	0.17	2.05	2.37	1.7	1.2	0	2.38	0.12	2.39	2.06	1.69	0.14	0.33	0.2	1.69	0.2	2.37	0.24	2.41	2.38	0.33	0.33	2.1	0.27	2.41
Nasali	0.2	1.67	2.37	1.22	0.38	1.67	2.05	2.38	0	2.4	0.03	1.19	1.67	2.37	2.37	2.37	1.67	2.37	0.22	2.37	0.17	0.02	2.37	2.37	1.2	2.37	0.16
Papio	2.37	1.73	0.29	2.05	2.37	1.72	1.22	0.12	2.4	0	2.4	2.07	1.72	0.26	0.45	0.32	1.71	0.32	2.37	0.36	2.43	2.4	0.45	0.45	2.13	0.39	2.43
Presby	0.23	1.67	2.37	1.23	0.41	1.67	2.05	2.39	0.03	2.4	0	1.19	1.67	2.37	2.37	2.37	1.68	2.37	0.25	2.37	0.14	0.02	2.37	2.37	1.19	2.37	0.13
Erythr	1.19	2.05	2.05	1.69	1.22	1.19	1.67	2.06	1.19	2.07	1.19	0	2.05	2.05	2.05	2.05	2.05	2.05	1.19	2.05	1.21	1.19	2.05	2.05	1.69	2.05	1.21
Victor	1.68	1.67	1.68	2.07	1.71	1.67	1.18	1.69	1.67	1.72	1.67	2.05	0	1.68	1.67	1.67	0.04	1.67	1.69	1.67	1.68	1.67	1.68	1.67	2.06	1.67	1.68
Phese	2.37	1.68	0.03	2.06	2.38	1.68	1.18	0.14	2.37	0.26	2.37	2.05	1.68	0	0.19	0.07	1.68	0.06	2.37	0.11	2.39	2.37	0.2	0.19	2.07	0.14	2.39
Platyr	2.38	1.67	0.16	2.08	2.4	1.67	1.19	0.33	2.37	0.45	2.37	2.05	1.67	0.19	0	0.13	1.68	0.13	2.38	0.08	2.37	2.37	0.01	0	2.05	0.05	2.37
Catarr	2.37	1.68	0.03	2.06	2.39	1.68	1.18	0.2	2.37	0.32	2.37	2.05	1.67	0.07	0.13	0	1.67	0	2.37	0.04	2.38	2.37	0.13	0.13	2.06	0.07	2.38
Cercop	1.68	1.68	1.67	2.06	1.7	1.68	1.18	1.69	1.67	1.71	1.68	2.05	0.04	1.68	1.68	1.67	0	1.67	1.68	1.67	1.69	1.68	1.68	1.68	2.06	1.67	1.69
Homir	2.37	1.68	0.03	2.06	2.38	1.68	1.18	0.2	2.37	0.32	2.37	2.05	1.67	0.06	0.13	0	1.67	0	2.37	0.05	2.38	2.37	0.14	0.13	2.07	0.08	2.38
Homir	0.02	1.69	2.37	1.19	0.15	1.69	2.05	2.37	0.22	2.37	0.25	1.19	1.69	2.37	2.38	2.37	1.68	2.37	0	2.37	0.39	0.24	2.38	2.38	1.25	2.38	0.38
Alloua	2.37	1.67	0.07	2.07	2.39	1.67	1.18	0.24	2.37	0.36	2.37	2.05	1.67	0.11	0.08	0.04	1.67	0.05	2.37	0	2.38	2.37	0.09	0.09	2.06	0.03	2.37
Aotus	0.37	1.68	2.38	1.28	0.55	1.68	2.06	2.41	0.17	2.43	0.14	1.21	1.68	2.39	2.37	2.38	1.69	2.38	0.39	2.38	0	0.16	2.37	2.37	1.18	2.37	0.01
Ateles	0.22	1.67	2.37	1.23	0.39	1.67	2.05	2.38	0.02	2.4	0.02	1.19	1.67	2.37	2.37	2.37	1.68	2.37	0.24	2.37	0.16	0	2.37	2.37	1.19	2.37	0.14
Cebus	2.38	1.67	0.16	2.08	2.41	1.67	1.19	0.33	2.37	0.45	2.37	2.05	1.68	0.2	0.01	0.13	1.68	0.14	2.38	0.09	2.37	2.37	0	0	2.05	0.06	2.37
Saguir	2.38	1.67	0.16	2.08	2.4	1.67	1.19	0.33	2.37	0.45	2.37	2.05	1.67	0.19	0	0.13	1.68	0.13	2.38	0.09	2.37	2.37	0	0	2.05	0.06	2.37
Saimir	1.24	1.19	2.07	0.49	1.31	2.06	2.38	2.1	1.2	2.13	1.19	1.69	2.06	2.07	2.05	2.06	2.06	2.07	1.25	2.06	1.18	1.19	2.05	2.05	0	2.06	1.18
Pithec	2.37	1.67	0.1	2.07	2.4	1.67	1.19	0.27	2.37	0.39	2.37	2.05	1.67	0.14	0.05	0.07	1.67	0.08	2.38	0.03	2.37	2.37	0.06	0.06	2.06	0	2.37
Epiplic	0.36	1.68	2.38	1.27	0.53	1.68	2.06	2.41	0.16	2.43	0.13	1.21	1.68	2.39	2.37	2.38	1.69	2.38	0.38	2.37	0.01	0.14	2.37	2.37	1.18	2.37	0

Forelimb synapomorphies

	Gorilla	Hylob	Sympl	Pongo	Pan	Cerco	Colobi	Macac	Nasali	Papio	Presby	Erythr	Victor	Phese	Platyr	Catarr	Cerco	Homir	Homir	Alloua	Aotus	Ateles	Cebus	Saguir	Saimir	Pithec	Epiplic
Gorilla	0	1.48	1.27	0.74	1.17	1.77	1.77	2.57	1.55	1.89	1.71	1.89	1.92	1.85	1.91	1.47	1.71	1.52	0.45	1.8	1.92	1.87	2.01	2.67	2.14	1.71	2.52
Hylob	1.48	0	0.59	1.45	0.93	1.45	1.74	1.64	1.35	1.43	1.72	1.51	1.55	1.43	1.76	1.25	1.31	1.24	1.4	1.78	1.76	2.21	1.73	2.03	1.7	1.64	2.16
Sympl	1.27	0.59	0	1.25	0.64	1.45	1.65	1.71	1.27	1.43	1.63	1.55	1.61	1.24	1.68	1.07	1.3	1.09	1.15	1.66	1.71	2.02	1.68	1.96	1.77	1.55	2
Pongo	0.74	1.45	1.25	0	1.29	2	2.1	2.64	1.8	2	2.05	2.09	2.11	1.78	2.15	1.64	1.87	1.66	0.51	2.12	2.13	2.34	2.15	2.81	2.28	2.01	2.75
Pan	1.17	0.93	0.64	1.29	0	1.41	1.47	1.73	1.17	1.41	1.45	1.48	1.57	1.34	1.62	1.01	1.29	1.06	1.15	1.55	1.66	1.8	1.67	1.97	1.81	1.43	1.86
Cercop	1.77	1.45	1.45	2	1.41	0	0.58	1.17	0.52	0.72	0.76	0.48	0.44	1.4	0.64	0.71	0.48	0.71	1.75	0.74	0.66	1.41	0.7	1.35	0.88	0.63	1.45
Colobi	1.77	1.74	1.65	2.1	1.47	0.58	0	1.44	0.52	1.05	0.45	0.81	0.79	1.66	0.61	0.83	0.83	0.88	1.81	0.56	0.68	0.98	0.82	1.42	1.15	0.39	1.27
Macac	2.57	1.64	1.71	2.64	1.73	1.17	1.44	0	1.3	1.19	1.55	1.18	1.19	1.62	1.42	1.32	1.13	1.29	2.5	1.57	1.41	2.12	1.35	1.1	1.44	1.47	1.35
Nasali	1.55	1.35	1.27	1.8	1.17	0.52	0.52	1.3	0	0.92	0.55	0.79	0.75	1.35	0.75	0.53	0.61	0.59	1.54	0.75	0.76	1.22	0.79	1.44	1.15	0.51	1.32
Papio	1.89	1.43	1.43	2	1.41	0.72	1.05	1.19	0.92	0	1.29	0.49	0.65	1.21	0.86	0.85	0.52	0.8	1.79	1.09	0.92	1.84	0.94	1.39	0.95	1.1	1.73
Presby	1.71	1.72	1.63	2.05	1.45	0.76	0.45	1.55	0.55	1.29	0	1.03	0.98	1.8	0.9	0.95	1.02	1.02	1.77	0.71	0.92	0.88	1.06	1.59	1.36	0.55	1.3
Erythr	1.89	1.51	1.55	2.09	1.48	0.48	0.81	1.18	0.79	0.49	1.03	0	0.42	1.43	0.7	0.86	0.49	0.84	1.86	0.87	0.78	1.6	0.86	1.37	0.86	0.88	1.6
Victor	1.92	1.55	1.61	2.11	1.57	0.44	0.79	1.19	0.75	0.65	0.98	0.42	0	1.49	0.69	0.87	0.44	0.85	1.89	0.89	0.67	1.61	0.79	1.4	0.86	0.82	1.58
Phese	1.85	1.43	1.24	1.78	1.34	1.4	1.66	1.62	1.35	1.21	1.8	1.43	1.49	0	1.49	0.92	1.12	0.86	1.6	1.68	1.61	2.25	1.35	1.74	1.55	1.57	1.96
Platyr	1.91	1.76	1.68	2.15	1.62	0.64	0.61	1.42	0.75	0.86	0.9	0.7	0.69	1.49	0	0.78	0.75	0.77	1.88	0.47	0.45	1.27	0.59	1.14	0.71	0.53	1.33
Catarr	1.47	1.25	1.07	1.64	1.01	0.71	0.83	1.32	0.53	0.85	0.95	0.86	0.87	0.92	0.78	0	0.56	0.11	1.38	0.87	0.9	1.42	0.84	1.35	1.09	0.73	1.37
Cercop	1.71	1.31	1.3	1.87	1.29	0.48	0.83	1.13	0.61	0.52	1.02	0.49	0.44	1.12	0.75	0.56	0	0.53	1.64	0.94	0.78	1.64	0.75	1.39	0.97	0.83	1.54
Homir	1.52	1.24	1.09	1.66	1.06	0.71	0.88	1.29	0.59	0.8	1.02	0.84	0.85	0.86	0.77	0.11	0.53	0	1.41	0.91	0.9	1.51	0.8	1.33	1.03	0.78	1.4
Homir	0.45	1.4	1.15	0.51	1.15	1.75	1.81	2.5	1.54	1.79	1.77	1.86	1.89	1.6	1.88	1.38	1.64	1.41	0	1.84	1.91	2.05	1.91	2.61	2.06	1.73	2.54
Alloua	1.8	1.78	1.66	2.12	1.55	0.74	0.56	1.57	0.75	1.09	0.71	0.87	0.89	1.68	0.47	0.87	0.94	0.91	1.84	0	0.71	0.92	0.88	1.26	1	0.44	1.34
Aotus	1.92	1.76	1.71	2.13	1.66	0.66	0.68	1.41	0.76	0.92	0.92	0.78	0.67	1.61	0.45	0.9	0.78	0.9	1.91	0.71	0	1.36	0.65	1.31	0.88	0.65	1.36
Ateles	1.87	2.21	2.02	2.34	1.8	1.41	0.98	2.12	1.22	1.84	0.88	1.6	1.61	2.25	1.27	1.42	1.64	1.51	2.05	0.92	1.36	0	1.61	1.83	1.81	0.98	1.46
Cebus	2.01	1.73	1.68	2.15	1.67	0.7	0.82	1.35	0.79	0.94	1.06	0.86	0.79	1.35	0.59	0.84	0.75	0.8	1.91	0.88	0.65	1.61	0	1.31	0.87	0.75	1.45
Saguir	2.67	2.03	1.96	2.81	1.97	1.35	1.42	1.1	1.44	1.39	1.59	1.37	1.4	1.74	1.14	1.35	1.39	1.33	2.61	1.26	1.31	1.83	1.31	0	1.22	1.34	1.1
Saimir	2.14	1.7	1.77	2.28	1.81	0.88	1.15	1.44	1.15	0.95	1.36	0.86	0.86	1.55	0.71	1.09	0.97	1.03	2.06	1	0.88	1.81	0.87	1.22	0	1.02	1.67
Pithec	1.71	1.64	1.55	2.01	1.43	0.63	0.39	1.47	0.51	1.1	0.55	0.88	0.82	1.57	0.53	0.73	0.83	0.78	1.73	0.44	0.65	0.98	0.75	1.34	1.02	0	1.26
Epiplic	2.52	2.16	2	2.75	1.86	1.45	1.27	1.35	1.32	1.73	1.3	1.6	1.58	1.96	1.33	1.37	1.54	1.4	2.54	1.34	1.36	1.46	1.45	1.1	1.67	1.26	0

Manus synapomorphies

	Gorilla	Cercop	Colobi	Hylobat	Macac	Pan	Pongo	Sympl	Nasali	Papio	Erythr	Presby	Saguir	Epiplic	Saimir	Pithec	Phese	Cebus	Victor	Platyr	Catarr	Cercop	Homir	Homir	Alloua	Aotus	Ateles
Gorilla	0	0.51	0.5	0.29	0.57	0.26	0.43	0.41	0.43	0.68	0.47	0.43	0.58	0.51	0.51	0.57	0.64	0.61	0.66	0.43	0.44	0.5	0.44	0.33	0.51	0.64	0.49
Cercop	0.51	0	0.23	0.38	0.22	0.48	0.53	0.47	0.24	0.29	0.12	0.28	0.43	0.43	0.43	0.23	0.43	0.23	0.42	0.24	0.36	0.31	0.36	0.37	0.18	0.41	0.59
Colobi	0.5	0.23	0	0.42	0.34	0.46	0.59	0.45	0.26	0.37	0.22	0.27	0.39	0.4	0.37	0.23	0.52	0.28	0.47	0.25	0.43	0.4	0.43	0.36	0.22	0.36	0.59
Hylobat	0.29	0.38	0.42	0	0.39	0.25	0.4	0.26	0.34	0.52	0.38	0.38	0.59	0.47	0.56	0.48	0.5	0.46	0.54	0.4	0.35	0.39	0.35	0.21	0.41	0.58	0.6
Macac	0.57	0.22	0.34	0.39	0	0.47	0.51	0.46	0.3	0.22	0.26	0.37	0.58	0.49	0.58	0.35	0.37	0.32	0.35	0.39	0.36	0.31	0.36	0.37	0.32	0.5	0.71
Pan	0.26	0.48	0.46	0.25	0.47	0	0.46	0.3	0.42	0.59	0.45	0.43	0.66	0.54	0.57	0.54	0.57	0.57	0.59	0.46	0.45	0.49	0.44	0.21	0.5	0.6	0.64
Pongo	0.43	0.53	0.59	0.4	0.51	0.46	0	0.47	0.45	0.66	0.52	0.47	0.67	0.59	0.74	0.61	0.59	0.6	0.58	0.55	0.38	0.42	0.37	0.46	0.58	0.78	0.57
Sympl	0.41	0.47	0.45	0.26	0.46	0.3	0.47	0	0.41	0.59	0.46	0.4	0.62	0.57	0.64	0.5	0.58	0.53	0.64	0.47	0.49	0.53	0.49	0.28	0.5	0.6	0.65
Nasali	0.43	0.24	0.26	0.34	0.3	0.42	0.45	0.41	0	0.39	0.23	0.16	0.39	0.31	0.44	0.3	0.46	0.31	0.46	0.25	0.29	0.27	0.3	0.36	0.26	0.5	0.46
Papio	0.68	0.29	0.37	0.52	0.22	0.59	0.66	0.59	0.39	0	0.32	0.46	0.61	0.49	0.59	0.39	0.34	0.33	0.38	0.46	0.43	0.37	0.43	0.48	0.36	0.51	0.78
Erythr	0.47	0.12	0.22	0.38	0.26	0.45	0.52	0.46	0.23	0.32	0	0.24	0.37	0.42	0.36	0.2	0.43	0.27	0.43	0.18	0.35	0.31	0.36	0.35	0.18	0.38	0.53
Presby	0.43	0.28	0.27	0.38	0.37	0.43	0.47	0.4	0.16	0.46	0.24	0	0.35	0.43	0.43	0.3	0.55	0.37	0.5	0.23	0.38	0.34	0.38	0.39	0.3	0.5	0.42
Saguir	0.58	0.43	0.39	0.59	0.58	0.66	0.67	0.62	0.39	0.61	0.37	0.35	0	0.51	0.36	0.36	0.68	0.46	0.69	0.28	0.57	0.54	0.57	0.57	0.39	0.46	0.4
Epiplic	0.51	0.43	0.4	0.47	0.49	0.54	0.59	0.57	0.31	0.49	0.42	0.43	0.51	0	0.51	0.48	0.47	0.43	0.54	0.44	0.32	0.36	0.33	0.48	0.41	0.63	0.55
Saimir	0.51	0.43	0.37	0.56	0.58	0.57	0.74	0.64	0.44	0.59	0.36	0.43	0.36	0.51	0	0.37	0.68	0.48	0.63	0.28	0.57	0.56	0.58	0.51	0.38	0.37	0.54
Pithec	0.57	0.23	0.23	0.48	0.35	0.54	0.61	0.5	0.3	0.39	0.2	0.3	0.36	0.48	0.37	0	0.53	0.24	0.48	0.2	0.45	0.42	0.46	0.45	0.2	0.37	0.56
Phese	0.64	0.43	0.52	0.5	0.37	0.57	0.59	0.58	0.46	0.34	0.43	0.55	0.68	0.47	0.68	0.53	0	0.44	0.45	0.54	0.36	0.39	0.36	0.46	0.48	0.61	0.78
Cebus	0.61	0.23	0.28	0.46	0.32	0.57	0.6	0.53	0.31	0.33	0.27	0.37	0.46	0.43	0.48	0.24	0.44	0	0.44	0.32	0.39	0.36	0.39	0.45	0.21	0.46	0.63
Victor	0.66	0.42	0.47	0.54	0.35	0.59	0.58	0.64	0.46	0.38	0.43	0.5	0.69	0.54	0.63	0.48	0.45	0.44	0	0.5	0.36	0.3	0.36	0.51	0.48	0.62	0.79
Platyr	0.43	0.24	0.25	0.4	0.39	0.46	0.55	0.47	0.25	0.46	0.18	0.23	0.28	0.44	0.28	0.2	0.54	0.32	0.5	0	0.41	0.38	0.41	0.38	0.21	0.35	0.45
Catarr	0.44	0.36	0.43	0.35	0.36	0.45	0.38	0.49	0.29	0.43	0.35	0.38	0.57	0.32	0.57	0.45	0.36	0.39	0.36	0.41	0	0.13	0.02	0.4	0.39	0.64	0.55
Cercop	0.5	0.31	0.4	0.39	0.31	0.49	0.42	0.53	0.27	0.37	0.31	0.34	0.54	0.36	0.56	0.42	0.39	0.36	0.3	0.38	0.13	0	0.13	0.44	0.36	0.62	0.56
Homir	0.44	0.36	0.43	0.35	0.36	0.44	0.37	0.49	0.3	0.43	0.36	0.38	0.57	0.33	0.58	0.46	0.36	0.39	0.36	0.41	0.02	0.13	0	0.4	0.39	0.65	0.56
Homir	0.33	0.37	0.36	0.21	0.37	0.21	0.46	0.28	0.36	0.48	0.35	0.39	0.57	0.48	0.51	0.45	0.46	0.45	0.51	0.38	0.4	0.44	0.4	0	0.41	0.45	0.66
Alloua	0.51	0.18	0.22	0.41	0.32	0.5	0.58	0.5	0.26	0.36	0.18	0.3	0.39	0.41	0.38	0.2	0.48	0.21	0.48	0.21	0.39	0.36	0.39	0.41	0	0.41	0.55
Aotus	0.64	0.41	0.36	0.58	0.5	0.6	0.78	0.6	0.5	0.51	0.38	0.5	0.46	0.63	0.37	0.37	0.61	0.46	0.62	0.35	0.64	0.62	0.65	0.45	0.41	0	0.75
Ateles	0.49	0.59	0.59	0.6	0.71	0.64	0.57	0.65	0.46	0.78	0.53	0.42	0.4	0.55	0.54	0.56	0.78	0.63	0.79	0.45	0.55	0.56	0.56	0.66	0.55	0.75	0

Pelvis synapomorphies

	Gorilla	Hylob	Sympl	Pongo	Pan	Cercop	Colobi	Macac	Nasali	Papio	Presby	Erythr	Victor	Phese	Platyr	Catarr	Cercop	Homir	Homir	Alloua	Aotus	Ateles	Cebus	Saguir	Saimir	Pithec	Epiplic
Gorilla	0	1.41	2.3	0.81	1.18	1.08	1.49	1.79	1.94	1.63	1.57	1.51	1.55	1.94	1.41	1.89	1.62	1.85	1.18	1.45	1.24	1.71	1.33	1.93	1.42	1.58	1.85
Hylob	1.41	0	1.48	1.68	1.42	1.39	1.46	1.55	1.13	1.44	0.73	1.44	1.12	1.67	1.19	0.85	0.48	0.83	1.38	1.62	1.68	1.91	1.71	1.69	1.07	1.47	1.06
Sympl	2.3	1.48	0	2.79	1.58	2.05	1.48	1.44	0.96	1.62	1.51	1.5	2.45	1.62	2.1	0.82	1.05	0.85	1.44	2.79	2.19	3.11	2.12	2.72	2.01	2.43	1.81
Pongo	0.81	1.68	2.79	0	1.66	1.13	1.97	2.21	2.36	2.02	1.83	1.9	1.45	2.32	1.42	2.23	1.97	2.2	1.74	1.3	1.33	1.39	1.38	1.73	1.53	1.42	1.86
Pan	1.18	1.42	1.58	1.66	0	1	0.66	1.11	1.45	1.01	1.44	0.77	2.13	1.63	1.73	1.45	1.36	1.44	0.47	2.17	1.18	2.51	1.34	2.37	1.7	2.05	1.78
Cercop	1.08	1.39	2.05	1.13	1	0	1.25	1.35	1.66	1.26	1.36	0.96	1.73	1.72	1.42	1.56	1.45	1.54	1.04	1.84	1.07	1.99	0.98	1.97	1.57	1.57	1.33
Colobi	1.49	1.46	1.48	1.97	0.66	1.25	0	0.74	1.42	0.61	1.38	0.6	2.19	1.4	2.03	1.37	1.31	1.37	0.72	2.5	1.45	2.85	1.64	2.48	1.91	2.37	1.91
Macac	1.79	1.55	1.44	2.21	1.11	1.35	0.74	0	1.26	0.46	1.52	0.59	2.36	1.21	2.28	1.28	1.32	1.3	0.88	2.81	1.91	3.05	1.85	2.76	2.21	2.54	1.77
Nasali	1.94	1.13	0.96	2.36	1.45	1.66	1.42	1.26	0	1.37	1.03	1.34	2.16	1.82	1.85	0.74	0.84	0.73	1.25	2.4	2.16	2.63	2.04	2.6	1.92	2.12	1.22
Papio	1.63	1.44	1.62	2.02	1.01	1.26	0.61	0.46	1.37	0	1.41	0.6	2.19	1.34	2.2	1.36	1.31	1.37	0.91	2.65	1.8	2.91	1.86	2.61	2.08	2.48	1.78
Presby	1.57	0.73	1.51	1.83	1.44	1.36	1.38	1.52	1.03	1.41	0	1.35	1.39	1.8	1.27	0.88	0.76	0.85	1.43	1.74	1.66	2.02	1.71	1.75	1.3	1.58	1.1
Erythr	1.51	1.44	1.5	1.9	0.77	0.96	0.6	0.59	1.34	0.6	1.35	0	2.13	1.31	1.9	1.27	1.26	1.27	0.71	2.46	1.43	2.72	1.45	2.4	1.85	2.19	1.66
Victor	1.55	1.12	2.45	1.45	2.13	1.73	2.19	2.36	2.16	2.19	1.39	2.13	0	2.15	1.11	1.77	1.47	1.75	2.15	1.18	1.75	1.37	1.82	0.9	0.96	1.18	1.6
Phese	1.94	1.67	1.62	2.32	1.63	1.72	1.4	1.21	1.82	1.34	1.8	1.31	2.15	0	2.24	1.36	1.47	1.38	1.41	2.81	1.86	3.03	1.66	2.43	2.1	2.42	1.95
Platyr	1.41	1.19	2.1	1.42	1.73	1.42	2.03	2.28	1.85	2.2	1.27	1.9	1.11	2.24	0	1.58	1.38	1.54	1.81	0.85	1.29	1.16	1.28	1.1	0.61	0.48	1.4
Catarr	1.89	0.85	0.82	2.23	1.45	1.56	1.37	1.28	0.74	1.36	0.88	1.27	1.77	1.36	1.58	0	0.46	0.05	1.31	2.24	1.86	2.5	1.73	2.12	1.55	1.85	1.1
Cercop	1.62	0.48	1.05	1.97	1.36	1.45	1.31	1.32	0.84	1.31	0.76	1.26	1.47	1.47	1.38	0.46	0	0.45	1.25	1.96	1.74	2.25	1.71	1.93	1.26	1.68	1.13
Homir	1.85	0.83	0.85	2.2	1.44	1.54	1.37	1.3	0.73	1.37	0.85	1.27	1.75	1.38	1.54	0.05	0.45	0	1.3	2.2	1.83	2.46	1.7	2.09	1.52	1.81	1.07
Homir	1.18	1.38	1.44	1.74	0.47	1.04	0.72	0.88	1.25	0.91	1.43	0.71	2.15	1.41	1.81	1.31	1.25	1.3	0	2.28	1.42	2.56	1.38	2.48	1.8	2.09	1.69
Alloua	1.45	1.62	2.79	1.3	2.17	1.84	2.5	2.81	2.4	2.65	1.74	2.46	1.18	2.81	0.85	2.24	1.96	2.2	2.28	0	1.72	0.59	1.82	1.27	1.08	0.86	1.9
Aotus	1.24	1.68	2.19	1.33	1.18	1.07	1.45	1.91	2.16	1.8	1.66	1.43	1.75	1.86	1.29	1.86	1.74	1.83	1.42	1.72	0	2.06	0.73	1.59	1.31	1.53	1.96
Ateles	1.71	1.91	3.11	1.39	2.51	1.99	2.85	3.05	2.63	2.91	2.02	2.72	1.37	3.03	1.16	2.5	2.25	2.46	2.56	0.59	2.06	0	2	1.51	1.49	0.92	1.93
Cebus	1.33	1.71	2.12	1.38	1.34	0.98	1.64	1.85	2.04	1.86	1.71	1.45	1.82	1.66	1.28	1.73	1.71	1.7	1.38	1.82	0.73	2	0	1.72	1.46	1.36	1.69
Saguir	1.93	1.69	2.72	1.73	2.37	1.97	2.48	2.76	2.6	2.61	1.75	2.4	0.9	2.43	1.1	2.12	1.93	2.09	2.48	1.27	1.59	1.51	1.72	0	0.99	1.15	2.02
Saimir	1.42	1.07	2.01	1.53	1.7	1.57	1.91	2.21	1.92	2.08	1.3	1.85	0.96	2.1	0.61	1.55	1.26	1.52	1.8	1.08	1.31	1.49	1.46	0.99	0	0.97	1.66
Pithec	1.58	1.47	2.43	1.42	2.05	1.57	2.37	2.54	2.12	2.48	1.58	2.19	1.18	2.42	0.48	1.85	1.68	1.81	2.09	0.86	1.53	0.92	1.36	1.15	0.97	0	1.43
Epiplic	1.85	1.06	1.81	1.86	1.78	1.33	1.91	1.77	1.22	1.78	1.1	1.66	1.6	1.95	1.4	1.1	1.13	1.07	1.69	1.9	1.96	1.93	1.69	2.02	1.66	1.43	0

Pes synapomorphies

	Gorilla	Hylob	Sympl	Pongo	Pan	Cerco	Colobi	Maca	Nasali	Papio	Presby	Erythr	Victor	Phese	Platyr	Catarr	Cerco	Homir	Homir	Alloua	Aotus	Ateles	Cebus	Saguir	Saimir	Pithec	Epiplic
Gorilla	0	3.83	3.43	1.62	2.08	4.67	4.3	4.47	4.55	2.14	4.36	3.87	4.66	4.46	4.37	3.87	4.23	3.87	1.95	3.51	4.72	4.66	4.34	4.92	4.58	4.01	3.88
Hylob	3.83	0	0.52	2.94	1.82	1.33	1.19	0.79	1.29	1.9	1.22	1.19	1.51	0.85	1.22	0.48	1.13	0.47	1.91	1.28	1.13	1.47	1.17	1.6	1.09	1.13	0.46
Sympl	3.43	0.52	0	2.59	1.44	1.58	1.37	1.15	1.53	1.52	1.41	1.2	1.75	1.17	1.37	0.64	1.29	0.64	1.52	1.17	1.42	1.66	1.36	1.82	1.31	1.22	0.64
Pongo	1.62	2.94	2.59	0	1.53	3.48	3.12	3.53	3.39	1.49	3.19	2.66	3.46	3.52	3.17	2.97	3.01	2.97	1.38	2.31	3.8	3.5	3.13	3.72	3.66	2.77	2.96
Pan	2.08	1.82	1.44	1.53	0	2.76	2.42	2.47	2.65	0.7	2.49	2.06	2.8	2.49	2.49	1.91	2.34	1.91	0.39	1.8	2.75	2.81	2.43	3.04	2.63	2.16	1.89
Cerco	4.67	1.33	1.58	3.48	2.76	0	0.54	1.07	0.4	2.76	0.54	0.89	0.7	1.12	0.54	1.29	0.51	1.29	2.83	1.34	1.2	0.8	0.49	0.68	1.29	0.83	1.34
Colobi	4.3	1.19	1.37	3.12	2.42	0.54	0	1.15	0.46	2.47	0.34	0.66	0.86	1.23	0.44	1.18	0.43	1.18	2.49	0.96	1.38	0.74	0.5	0.9	1.34	0.61	1.22
Macac	4.47	0.79	1.15	3.53	2.47	1.07	1.15	0	1.1	2.47	1.15	1.35	1.24	0.44	1.17	0.74	1.12	0.73	2.54	1.63	0.78	1.33	1.12	1.29	0.83	1.29	0.82
Nasali	4.55	1.29	1.53	3.39	2.65	0.4	0.46	1.1	0	2.68	0.41	0.89	0.77	1.18	0.6	1.28	0.5	1.27	2.73	1.26	1.31	0.83	0.53	0.9	1.34	0.82	1.34
Papio	2.14	1.9	1.52	1.49	0.7	2.76	2.47	2.47	2.68	0	2.53	2.01	2.73	2.48	2.54	1.92	2.34	1.92	0.62	1.86	2.76	2.9	2.45	3.05	2.7	2.19	1.96
Presby	4.36	1.22	1.41	3.19	2.49	0.54	0.34	1.15	0.41	2.53	0	0.75	0.86	1.22	0.49	1.21	0.48	1.21	2.55	1.04	1.38	0.74	0.56	0.92	1.35	0.7	1.26
Erythr	3.87	1.19	1.2	2.66	2.06	0.89	0.66	1.35	0.89	2.01	0.75	0	1.05	1.37	0.74	1.16	0.54	1.15	2.1	0.72	1.57	1.19	0.67	1.23	1.57	0.58	1.22
Victor	4.66	1.51	1.75	3.46	2.8	0.7	0.86	1.24	0.77	2.73	0.86	1.05	0	1.35	0.95	1.46	0.78	1.46	2.86	1.52	1.43	1.22	0.82	1.03	1.53	1.05	1.52
Phese	4.46	0.85	1.17	3.52	2.49	1.12	1.23	0.44	1.18	2.48	1.22	1.37	1.35	0	1.19	0.65	1.14	0.65	2.54	1.63	0.66	1.35	1.15	1.32	0.81	1.28	0.78
Platyr	4.37	1.22	1.37	3.17	2.49	0.54	0.44	1.17	0.6	2.54	0.49	0.74	0.95	1.19	0	1.16	0.48	1.16	2.54	0.95	1.26	0.54	0.48	0.68	1.18	0.5	1.18
Catarr	3.87	0.48	0.64	2.97	1.91	1.29	1.18	0.74	1.28	1.92	1.21	1.16	1.46	0.65	1.16	0	1.1	0.03	1.95	1.23	0.98	1.39	1.17	1.52	0.93	1.08	0.33
Cerco	4.23	1.13	1.29	3.01	2.34	0.51	0.43	1.12	0.5	2.34	0.48	0.54	0.78	1.14	0.48	1.1	0	1.1	2.4	0.94	1.34	0.91	0.33	0.98	1.36	0.46	1.14
Homir	3.87	0.47	0.64	2.97	1.91	1.29	1.18	0.73	1.27	1.92	1.21	1.15	1.46	0.65	1.16	0.03	1.1	0	1.95	1.23	0.98	1.39	1.17	1.52	0.93	1.09	0.34
Homir	1.95	1.91	1.52	1.38	0.39	2.83	2.49	2.54	2.73	0.62	2.55	2.1	2.86	2.54	2.54	1.95	2.4	1.95	0	1.79	2.82	2.85	2.5	3.08	2.68	2.2	1.95
Alloua	3.51	1.28	1.17	2.31	1.8	1.34	0.96	1.63	1.26	1.86	1.04	0.72	1.52	1.63	0.95	1.23	0.94	1.23	1.79	0	1.85	1.23	1.07	1.54	1.7	0.67	1.27
Aotus	4.72	1.13	1.42	3.8	2.75	1.2	1.38	0.78	1.31	2.76	1.38	1.57	1.43	0.66	1.26	0.98	1.34	0.98	2.82	1.85	0	1.41	1.27	1.3	0.69	1.45	1.02
Ateles	4.66	1.47	1.66	3.5	2.81	0.8	0.74	1.33	0.83	2.9	0.74	1.19	1.22	1.35	0.54	1.39	0.91	1.39	2.85	1.23	1.41	0	0.93	0.72	1.23	0.9	1.39
Cebus	4.34	1.17	1.36	3.13	2.43	0.49	0.5	1.12	0.53	2.45	0.56	0.67	0.82	1.15	0.48	1.17	0.33	1.17	2.5	1.07	1.27	0.93	0	0.92	1.33	0.57	1.21
Saguir	4.92	1.6	1.82	3.72	3.04	0.68	0.9	1.29	0.9	3.05	0.92	1.23	1.03	1.32	0.68	1.52	0.98	1.52	3.08	1.54	1.3	0.72	0.92	0	1.22	1.08	1.53
Saimir	4.58	1.09	1.31	3.66	2.63	1.29	1.34	0.83	1.34	2.7	1.35	1.57	1.53	0.81	1.18	0.93	1.36	0.93	2.68	1.7	0.69	1.23	1.33	1.22	0	1.41	0.89
Pithec	4.01	1.13	1.22	2.77	2.16	0.83	0.61	1.29	0.82	2.19	0.7	0.58	1.05	1.28	0.5	1.08	0.46	1.09	2.2	0.67	1.45	0.9	0.57	1.08	1.41	0	1.09
Epiplic	3.88	0.46	0.64	2.96	1.89	1.34	1.22	0.82	1.34	1.96	1.26	1.22	1.52	0.78	1.18	0.33	1.14	0.34	1.95	1.27	1.02	1.39	1.21	1.53	0.89	1.09	0

References

Agustí J., Cabrera L., Garcés M. and Parés J.M. (1997) The Vallesian mammal succession in the Vallès-Penedès basin (northeast Spain): paleomagnetic calibration and correlation with global events. Palaeogeography Palaeoclimatology Palaeoecology 133(3-4):149–180.

Agustí J., Köhler M., Moyà-Solà S., Cabrera L., Garcés M. and Pares JM (1996) Can Llobateres: the pattern and timing of the Vallesian hominoid radiation reconsidered. Journal of Human Evolution 31(2):143–155.

Alba DM, Almecija S, Móya-Solá S (2010) Locomotor inferences in *Pierolapithecus* and *Hispanopithecus*: Reply to Deane and Begun (2008) J Hum Evol 59: 143–149.

Alba DM, Móya-Solá S, Almecija S (2011) A partial hominoid humerus from the middle Miocene of Castell de Barberà (Vallès-Penedès Basin, Catalonia, Spain) Am J Phys Anthropol 144: 365–381.

Alba DM, Almécija S, Casanovas-Vilar I, Méndez JM, Moyà-Solà S (2012) A partial skeleton of *Hispanopithecus laietanus* from Can Feu and the mosaic evolution of crown-hominoid positional behaviors. PLoS ONE 7: e39617.

Alba, DM. Almecija, S, et al. (2015) Miocene small-bodied ape from Eurasia sheds light on hominoid evolution. Science. 350(6260): aab2625.

Almecija S, Alba DM, Móya-Solá, Kohler M. (2007) Orang-like manual adaptations in the fossil hominoid *Hispanopithecus laietanus*: first steps towards great ape suspensory behaviours. Proc R Soc B 274:2375–2384.

Almecija S, Alba DM, Móya-Solá. (2009) *Pierolapithecus* and the functional morphology of Miocene ape hand phalanges: paleobiological and evolutionary implications. J Hum Evol 57:284–297.

Almécija, S., Smaers, J. B. and Jungers, W. L. (2015) The evolution of human and ape hand proportions. Nat. Commun. 6, 7717.

Andrews P. (1978) A revision of the Miocene Hominoidea of East Africa. Bull Brit Museum Nat Hist Geol Ser 30:58-224.

Andrews P. (1985) Family group systematics and evolution among catarrhine primates. In Delson E (ed): *Ancestors: The Hard Evidence*. New York: Alan R. Liss. 14-22.

Andrews P (1992) Evolution and environment in the Hominoidea. Nature 360:641–646.

Andrews, P. (1996) Palaeoecology and hominoid paleoenvironments. Biol. Rev. 71, 257–300.

Andrews. P and Groves, C (1975) Gibbons and brachiation. In D.M. Rumbaugh (ed): *Gibbon and Siamang*. Basel: Karger. pp. lfi7~218.

Andrews, P., Harrison, T., Martin, L., Pickford, M., (1981) Hominoid primates from a new Miocene locality named Meswa Bridge in Kenya. J. Hum. Evol. 10, 123–128.

Andrews P., Martin L. (1987) Cladistic relationships of extant and fossil hominoids. Journal of Human Evolution. 16:101–118.

Ankel, F., (1972) Vertebral morphology of fossil and extant primates, in: Tuttle, R., Ed. The functional and evolutionary biology of primates. Aldine-Atherton, Chicago, pp. 223-240.

Archie JW (1985) Methods for coding variable morphological features for numerical taxonomic analysis. Systematic Biology 34, 326–45.

Arcila, D., Pyron, R.A., Tyler, J.C., Ortí, G., Betancur R., R. (2015) An evaluation of fossil tip-dating versus node-age calibrations in tetraodontiform fishes (Teleostei: Percomorphaceae) Molecular Phylogenetics and Evolution, 82: 131-145

Argot, C., (2003) Functional-adaptive anatomy of the axial skeleton of some extant marsupials and the paleobiology of the paleocene marsupials Mayulestes ferox and Pucadelphys andinus. J. Morphol. 255, 279e300.

Ashton E.H. and Oxnard C.E. (1963) The musculature of the primate shoulder. Trans. Zool. SOC. Lond. 29:553-650.

Ashton E.H., Oxnard C.E. (1964) Functional adaptations in the primate shoulder girdle. Proceedings of the Zoological Society of London 142:49–66.

Barnett C.H, Napier J.A. (1953) The axis of rotation at the ankle joint. J. Anat. 86:1-9.

Barrett, M., Donoghue, M., and Sober, E. (1991). Against consensus. Syst. Zool. 40, 486–493.

Beard K.C. (2002) Basal anthropoids. In: Hartwig W.C. (ed.), The Primate Fossil Record. Cambridge University Press, Cambridge, pp. 133–149.

Beard KC., Teaford MF. and Walker AC (1986) New wrist bones of *Proconsul* africanus and P. nyanzae from Rusinga Island, Kenya. Folia Primatologica 47:97–118.

Beard, K.C., Teaford, M.F., Walker, A., (1993) New hand bones of the early Miocene hominoid *Proconsul* and their implications for the evolution of the hominoid wrist. In: Preuschoft, H., Chivers, D.J. (Eds.), Hands of Primates. Springer-Verlag, Berlin, pp. 21e30.

Begun D.R. (1994) Relations among the great apes and humans: new interpretations based on the fossil great ape Dryopithecus. Yearbook of Physical Anthropology, 37: 11–63.

Begun D.R. (2001) African and Eurasian Miocene hominoids and the origins of the Hominidae. In: de Bonis L., Koufos G. and Andrews P. (eds.), *Hominoid Evolution and Environmental Change in the Neogene of Europe, Volume 2: Phylogeny of the Neogene Hominoid Primates of Eurasia.* Cambridge University Press, Cambridge, pp. 231–253.

Begun D.R. (2002) European Hominoids. In: Hartwig W. (ed.), *The Primate Fossil Record.* Cambridge University Press, Cambridge, pp. 339–368.

Begun D.R. (2004) The earliest hominins—is less more? Science, 303: 1478–1480.

Begun, D.R., (2007) Fossil record of Miocene hominoids. In: Henke, W., Tattersall, I. (Eds.), *Handbook of Paleoanthropology*. Springer Verlag, Heidelberg, pp. 921–977.

Begun D and Kordos L. (1997) Phyletic affinities and functional convergence in Dryopithecus and other Miocene and living hominids. In Begun DR, Ward CV and Rose MD (eds): *Function, phylogeny and fossils. Miocene hominoid evolution and adaptations*. p 291–316.

Begun, D.R., Nargolwalla, M.C., Kordos, L., (2012) European Miocene hominids and the origin of the African ape and human clade. Evol. Anthropol. 21, 10e23.

Begun, D.R., Ward, C.V., (2005) Comment on "*Pierolapithecus catalaunicus*, a new Middle Miocene great ape from Spain". Science 308, 203c.

Benefit B.R. and McCrossin M.L. (1991) Ancestral facial morphology of Old World higher primates. Proc. Natl. Acad. Sci. U.S.A. 88t5267-5271.

Benefit B.R., McCrossin M.L. (1993) New *Kenyapithecus* postcrania and other primate fossils from Maboko Island, Kenya. American Journal of Physical Anthropology 16: 55–56.

Benefit B.R., McCrossin M.L. (1995) Miocene hominoids and hominid origins. Annual Review of Anthropology 24:237–256.

Benefit B.R., McCrossin M.L.. (1997) Earliest known Old World monkey skull. Nature 388:368–371.

Benefit B.R.. (1999) *Victoriapithecus*: The key to Old World monkey and catarrhine origins. Evolutionary Anthropology: Issues, News and Reviews 7:155-174.

Benefit B.R., McCrossin M.L. (2002) The Victoriapithecidae, Cercopithecoidea. In Hartwig WC, (ed.) *The Primate Fossil Record.* Cambridge, Cambridge University Press.

Benton RS (1976) Structural patterns in the Pongidae and Cercopithecidae. Yrbk Phys Anthropol 18: 65–88.

Bernor, R. L. (1983) Geochronology and zoogeographic relationships of Miocene Hominoidea. In: R. L. Ciochon and R. S. Corruccini (eds.), *New Interpretations of Ape and Human Ancestry*. Academic Press, New York.

Bjarnason, A., Chamberlain, A.T., Lockwood, C.A. (2011) A methodological investigation of hominoid craniodental morphology and phylogenetics. J. Hum. Evol., 60 pp. 47–57

Bouckaert R., Heled J., Kühnert D., Vaughan T., Wu C.-H., Xie D., Suchard M. A., Rambaut A., Drummond A. J. (2014) BEAST2: a software platform for Bayesian evolutionary analysis. PLoS Comput. Biol. 10:e1003537.

Cameron D.W. (1997) A revised systematic scheme for the Eurasian Miocene fossil Hominidae. Journal of Human Evolution. 33:449-477.

Cant J. (1987) Positional behavior of female Bornean orangutans (*Pongo pygmaeus*) Am J Phys Anthropol 12:71-90.

Cartmill, M. and Milton, K. (1977) The lorisiform wrist joint and the evolution of "brachiating" adaptations in the Hominoidea. Phys. Anthropol. 47: 249-272.

Cartmill, M., MacPhee, R. D. E. and Simons, E. L. (1981) Anatomy of the temporal bone in early anthropoids, with remarks on the problem of anthropoid affinities. Am.]. Phys. Anthropol. 56:3-21.

Cartmill, M. (1985) Climbing. In M. Hildebrand, D. Bramble, K. F. Leim & D. B. Wake, (eds.) *Functional Vertebrate Morphology*. Cambridge: Belknap Press.

Casanovas-Vilar I, Alba D.M., Móya-Solá S, Galindo J, Cabrera L, Garces M, Furio M, Robles J.M., Kohler M, Angelone C. (2008) Biochronological, taphonomical and paleoenvironmental background of the fossil great ape *Pierolapithecus catalaunicus* (Primates. Hominidae) J Hum Evol 55:589–603.

Casanovas-Vilar I, Alba D.M., Garces M, Robles J.M., Móya-Solá S (2011) An updated chronology for the Miocene hominoid radiation in Western Eurasia. Proc Natl Acad Sci USA 108: 5554–5559.

Cave M.E., Haines R.W. (1940) The paranasal sinuses of the anthropoid apes. J. Anat. 72:493-523.

Ciochon, R. L., Corruccini, R. S. (1977) The phenetic position of Pliopithecus and its phylogenetic relationship to the Hominoidea. Syst. Zool. 26(3), 290-299.

Clutton-Brock, T. H., P. H. Harvey. (1979) Comparison and adaptation. Proc. R. Soc. Lond. B 205:547-565.

Collard, M., Wood, B., (2001) Homoplasy and the early hominid masticatory system: inferences from analyses of extant hominoids and papionins. J. Hum. Evol. 41, 167e194.

Conroy, G. C. (1976) Primate postcranial remains from the Oligocene of Egypt. Contrib. Primatol. 8:1-134.

Conroy. G. C. & Fleagle, J. G. (1972) Locomotor behaviour of living and fossil pongids. Nature (London) 237, 103-104.

Corruccini, R. S. (1975) Morphometric affinities in the forelimb of anthropoid primates. Z. Morph. Anthrop. 67, 19-31.

Corruccini, R. S. (1978) Comparative osteometries of the hominoid wrist joint, with special reference to knuckle-walking.]. Hum. Evol. 7:307-321.

Corruccini, R. S Ciochon. R. L McHenry. H. M. (1976) The postcranium of Miocene liomino~ds: Were Dryopithecines merely 'dental apes'? Primates 17(2) 205-223.

Daver, G., Nakatsukasa, M. (2015) *Proconsul heseloni* distal radial and ulnar epiphyses from the Kaswanga Primate Site, Rusinga Island, Kenya. Journal of Human Evolution 80: 17-30.

Day. M. H., Napier. J. (1963). The functional significance of the deep head of flexor pollicis brevis in primates. Folia Primatol. 1, 122-134.

DeBry, R.W. (2005) The systematic component of phylogenetic error as a function of taxonomic sampling under parsimony. Sys. Bio. 54(3): 432-440

Delson. E., Andrews, P. J. (1975) Evolution and interrelationships of the catarrhine primates. Phylogeny of the Primates: A Multidisciplinary Approach (W. P. Lucket & F. S. Szalay, eds.) pp 405-446. Plenum. New York.

Dembo M, Matzke N.J., Mooers A.Ø., Collard M. (2015) Bayesian analysis of a morphological supermatrix sheds light on controversial fossil hominin relationships. Proc. R. Soc. B 282: 20150943.

Drake, R.E., Van Couvering, J.A., Pickford, M.H., Curtis, G.H., Harris, J.A., (1988) New chronology for the early Miocene mammalian faunas of Kisingiri, Western Kenya. J. Geol. Soc. Lond. 145, 479–492.

Drapeau M.S.M. (2004) Functional anatomy of the olecranon process in hominoids and Plio-Pleistocene hominins. American Journal of Physical Anthropology. 124:297-314.

Drapeau M.S.M. (2008) Articular morphology of the proximal ulna in extant and fossil hominoids and hominins. J Hum Evol 55:86–102.

Dunsworth, H (2006) *Proconsul* heseloni feet from rusinga island, kenya. PhD Thesis. Pennsylvania State University.

Elton, S. (2007) Environmental correlates of the cercopithecoid radiations. Folia Primatologica 78:344–364.

Eernisse, D. J., Kluge, A. G. (1993). Taxonomic congruence versus total evidence and amniote phylogeny inferred from fossils, molecules and morphology. Molecular Biology and Evolution, 10, 1170–1195.

Egge, J.J.D., Simons, A.M. (2009) Molecules, morphology, missing data and the phylogenetic position of a recently extinct madtom catfish (Actinopterygii: Ictaluridae). Zoological Journal of the Linnean Society, 155, 60–75.

Evans, F. G., Krahl, V. E. (1945) The torsion of the humerus: A phylogenetic study from fish to man. Am. J Anat. 76:303-337.

Farris, J. (1990) Phenetics in camouflage. Cladistics 6: 91-100.

Felsenstein, J., (1985) Confidence limits on phylogenies: an approach using the bootstrap. Evolution 39, 783–791.

Felsenstein, J., (1988) Phylogenies and quantitative characters. Annual Review of Ecology and Systematics 19:445–471.

Felsenstein, J., (2002) Quantitative characters, phylogenies, andmorphometrics. In: N. MacLeod and P.L. Forey (eds.) Morphology, Shape & Phylogeny, pp. 27–44, Francis & Taylor, London.

Finarelli, J.A. & Clyde, W.C. (2004) Reassessing hominoid phylogeny: evaluating congruence in the morphological and temporal data. Paleobiology, 30, 614–651.

Fleagle J.G., Kay R.F. (1983) New interpretations of the phyletic position of Oligocene hominoids. In Ciochon RL, Corruccini RS, (eds): New Interpretations of Ape and Human Ancestry. Plenum. p 181-210.

Fleagle J.G., Kay R.F. (1987) The phyletic position of the Parapithecidae. J. Hum. Evol. 16:483–532.

Fleagle J.G. and Meldrum D.J. (1988) Locomotor behavior and skeletal morphology of two sympatric pitheciine monkeys, Pithecia pithecia and Chiropotes satanas. Am. J. Primatol. 16:227–249.

Fleagle J.G., Simons E.L. (1982) The humerus of *Aegyptopithecus zeuxis*: A primitive anthropoid. Am. J. Phys.Anthropol. 59:175-193.

Fleagle, J.G. (1983) Locomotor adaptations of Oligocene and Miocene hominoids and their phylogenetic implications. In R. L. Ciochon and R. S. Corruccini, (eds.), *New Interpretations of Ape and Human Ancestry.* New York: Plenum. Pp. 301-324.

Fleagle, J.G. (1998) Primate Adaptation and Evolution, 2nd edn. Academic Press, New York.

Fleagle, J. G., Gilbert, C. C., & Baden, A. L. (2010) Primate cranial diversity. American Journal of Physical Anthropology, 142, 565–578.

Forsyth Major, C.I. (1880) Beitrage zur Geschichte del' fossilen Pferde insbesondere Italiens. Abh. Schweiz. Palaont, Ges. 7:1-154.

Gamarra B, Nova Delgado M, Romero A, Galbany J, Pérez-Pérez A. (2016) Phylogenetic signal in molar dental shape of extant and fossil catarrhine primates. Journal of Human Evolution 94:13-27.

Gao, K., Norell, M. A. (1998) Taxonomic revision of Carusia (Reptilia: Squamata) fromthe Late Cretaceous of the Gobi Desert and phylogenetic relationships of anguimorphan lizards. Am. Mus. Novit. 3230:1–51.

Garcés m., Agustí j., Cabrera l. and Parés J.M. (1996) Magnetostratigraphy of the Vallesian (lateMiocene) in the Vallès-Penedès Basin (northeastern Spain). Earth and Planetary Science Letters 142:381–396.

Garland T, Jr. (1992) Rate tests for phenotypic evolution using phylogenetically independent contrasts. American Naturalist. 140:509-519.

Garland, T., Jr. and R. B. Huey. (1987) Testing symmorphosis: Does structure match functional requirements? Evolution 41:1404-1409.

Garland T, Jr. and Ives AR. (2000) Using the past to predict the present: confidence intervals for regression equations in phylogenetic comparative methods. The American Naturalist. 155:346-364.

Gauthier, J. (1986) Saurischian monophyly and the origin of birds. Mem. Calif. Acad. Sci. 8:1–47.

Gebo, DL, (1988) Foot morphology and locomotor adaptation in Eocene primates. Folia Primatol. 50, 3-41.

Gebo DL (1989) Locomotor and phylogenetic considerations in anthropoid evolution. J. Hum. Evol. 18:201-233.

Gebo DL (1992) Plantigrady and foot adaptation in African apes: implications for hominid evolution. Am. J. Phys. Anthropol. 89:29-58.

Gebo DL (1993) Postcranial anatomy andlocomotor adaptation in early African anthropoids. In DL Gebo (ed.): *Postcranial Adaptation in Nonhuman Primates*. Northen Illinois University Press, DeKalb.

Gebo D.L. (1996) Climbing, brachiation and terrestrial quadrupedalism: historical precursors of hominid bipedalism. Am J Phys Anthropol 101, 55–92.

Gebo , D., MacLatchy, L., Kityo, R., Deino, A., Kingston, J., Pilbeam, D. (1997) A Hominoid Genus from the Early Miocene of Uganda . Science 276 : 401 – 404.

Gebo D.L., Sargis E.J. (1994) Terrestrial adaptations in the postcranial skeleton of guenons. Am J Phys Anthropol 93:341–371.

Gebo, D.L., Malit, N.R., Nengo, I.O. (2009) New Proconsuloid postcranials from the early Miocene of Kenya. Primates 50:311–319.

Gervais, P. (1872) Sur un singe fossile, d'espece non encore decrite, qui a ete dtcouvert au Monte-Ban1boli (ltahe). Comptes rendus de J'Acadfmie des sciences de Paris, LXXIV, 1 217- J 223.

Gingerich, P. D. (1977) Radiation of Eocene Adapidae in Europe. Geobios, Mbn. Spec. 1: 165-U32.

Ginsburg L. (1986) Chronology of the European pliopithecids. In: Else JG, Lee PC, editors. Primate evolution. Cambridge: Cambridge University Press. p 47–57.

Goloboff, P., Farris, J., Nixon, K., (2003) T.N.T. Tree Analysis Using New Technology. Program and documentation, available at http://www.zmuc.dk/public/phylogeny/tnt

Goloboff P.A., Mattoni C.I. (2006) Cladistics Continuous characters analyzed as such. Cladistics 22:589-601.

Gomberg O.N. (1981) Form and Function of the Hominoid Foot. Ph.D. Thesis, University of Massachusetts.

Grand, T.I.(1968) The functional anatomy of the lower limb of the howler monkey (Alouatta curaya), Am. J. phys. Anthrop. 28: 163- 182.

Graybeal, A. (1998) Is it better to add taxa or characters to a difficult phylogenetic problem? Syst. Biol. 48:9-17.

Gregory, W.K. (1920) On the structure and relation of *Notharctus*, an American Eocene primate. Mem. Amer. Mus. Nat. Hist., n.s. 351.243.

Gregory, W. K. (1922) *The Origin and Evolution of the Human Dentition,* Williams and Wilkins, Baltimore.

Gregory, W. K. & M. Hellman, (1926) The dentition of *Dryopithecus* and the origin of man. Anthrop. Papers Amer. Mus. Nat. Hist., 28 : 1-123.

Gregory W.K. (1934) Man's place among the anthropoids. Oxford: Clarendon Press.

Gregory, W. K. & M. Hellman, & G. E. Lewis, (1938) Fossil anthropoids of the Yale-Cambridge Indian expedition of 1935. Carnegie Institution, Washington, 495: 1-27.

Grimm G.W., Kapli P., Bomfleur B., McLoughlin S., Renner S.S. (2015) Using more than the oldest fossils: Dating osmundaceae with three Bayesian clock approaches. Syst. Biol. 64:396–405.

Groves, C. P. (1968) The classification of the gibbons (Primates, Pongidae) Z. Saugetierkde. 33, 239-246.

Groves, C. P. (l972) Systematics and phylogeny of gibbons. Gibbon and Siamang 1, 1-89.

Gundling, T., Hill, A. (2000) Geological context of fossil Cercopithecoidea from eastern Africa; pp. 180-213 in P. L. Whitehead and C. J. Jolly (eds.), *Old World Monkeys*. Cambridge University Press, Cambridge.

Harrison T. (1982) Small-bodied apes from the Miocene of East Africa. Ph.D. thesis, University of London.

Harrison, T. (1986) New fossil anthropoids from the middle Miocene of East Africa and their bearing on the origin of the Oreopithecidae. Am.J. Phys. Anthropol. 71:265-284.

Harrison T. (1987) The phylogenetic relationships of the early catarrhine primates: a review of the current evidence. Journal of Hum. Evol. 16:41–80.

Harrison, T. (1988) A taxonomic revision of the small catarrhine primates from the early Miocene of East Africa. Folia Primatol. 50:59-108.

Harrison , T. , (1989) A New Species of *Micropithecus* from the Middle Miocene of Kenya. Journal of Human Evolution 18 : 537 – 557.

Harrison, T. (1991) The implications of *Oreopithecus* for the origins of bipedalism. In Y. Coppens and B. Senut, (eds.) *Origine(s) de la Bipédie Chez les Hominidés,* Cahiers de Paléoanthropologie, CNRS, Paris.

Harrison T. (1993) Cladistic concepts and the species problem in hominoid evolution. In Kimbel WH, Martin LB (eds): Species, Species Concepts and Primate Evolution. Plenum Press. p 346–371.

Harrison, T. (1998) Evidence for a tail in *Proconsul* heseloni. American Journal of Physical Anthropology, suppl. 26:93–94.

Harrison T. (2002) Late Oligocene to middle Miocene catarrhines from Afro-Arabia. In: W.C. HARTWIG (ed.) The Primate Fossil Record, pp. 311–338, Cambridge University Press, Cambridge.

Harrison T. (2005) The zoogeographic and phylogenetic relationships of early catarrhine primates in Asia. Anthropological Science 113(1):43–51.

Harrison T. (2010) Apes among the tangled branches of human origins. Science 327:532.

Harrison, T., (2013) Catarrhine Origins. In: Begun, D. R. (Ed.), A Companion to Paleoanthropology. Wiley-Blackwell, Hoboken, pp. 376-396.

Harrison, T., Gu, Y. (1999) Taxonomy and phylogenetic relationships of early Miocene catarrhines from Sihong, China. J. Hum. Evol. 37:225–277.

Harrison, T., Rook, L. (1997) Enigmatic anthropoid or misunderstood ape? The phylogenetic status of *Oreopithecus bambolii* reconsidered. In D. R. Begun, C. V. Ward and M. D. Rose, (eds.) *Function, Phylogeny and Fossils: Miocene Hominoid Evolution and Adaptations*, Plenum Press, New York.

Harrison, T., Sanders, W. (1999) Scaling of lumbar vertebrae in anthropoid primates: its implications for positional behavior and phylogenetic affinities of *Proconsul*. American Journal of Physical Anthropology 28(Suppl.):146.

Harvey, P. H. & Pagel, M. D. (1991) The Comparative Method in Evolutionary Biology. Oxford univ. press, Vol. 239.

Hennig, W. 1966. Phylogenetic Systematics. University of Illinois Press, Urbana, IL.

Hershckhowitz., P. (1977) Living New World Monkeys (Platyrrhini), Vol. I. University of Chicago Press.

Hillis, D. M. (1996) Inferring complex phylogenies. Nature 383:140-141.

Hillis, D. M. (1998) Taxonomic sampling, phylogenetic accuracy and investigator bias. Syst. Biol. 47:3-8.

Hillis, D. M. and J. J. Wiens. (2000) Molecules versus morphology in systematics. Pages 1-19 in Phylogenetic analysis of morphological data (J. J. Wiens, ed.) Smithsonian Institution Press, Washington, D.C.

Hillis, D.M., Pollock, J. A. McGuire and. J. Zwickl. (2003) Is sparse taxon sampling a problem for phylogenetic inference? Syst. Biol. 52:124-126.

Hofmann, A. (1893) Die Fauna von Goriach Abhandhmgen K-K. geologie, Reichsanstalt 6: 1-87.

Hopwood A.T. (1933) Miocene primates from Kenya. J. Linn. Soc. London, Zool. 38:437-464.

Huelsenbeck, J., Ronquist, F. (2001) MrBayes: Bayesian inference of phylogeny. Bioinformatics 17, 754–755.

Hurzelcr, J. (1954) Contribution l' odontologie et a la phvlogenese du genre Pliopithecus Gervais. Annales de Paleontologie 40: 1-63.

Hurzelcr, J. (1958) Oreopithecus bambolii Gervais: a preliminary report. Verhandlungen der Naturforschenden Gesellschaft in Basel 69(1):1–48.

Hürzeler J. (1960) The significance of *Oreopithecus* in the genealogy of man. Triangle 4:164–174.

Jablonski N., Frost S. (2010) Cercopithecoidea. In: Werdelin L and Sanders W, editors. Cenozoic Mammals of Africa. Berkeley: University of California Press. p 393-428.

Jenkins F. (1973) The functional anatomy and evolution of the mammalian humero-ulnar articulation Am J Anat 137:281-298.

Jenkins Jr., F.A., (1974) Tree shrew locomotion and the origins of primate arborealism. In: Jenkins Jr., F.A. (Ed.), *Primate Locomotion.* Academic Press, London, pp. 85e115.

Johnson, S.E., Shapiro, L.J., (1998) Positional behavior and vertebral morphology in atelines and cebines. Am. J. Phys. Anthropol. 105, 333e354.

Jolly C. (1967) The evolution of the baboons. In: Vagtborg H, editor. The Baboon in Medical Research. Austin: University of Texas Press. p 23-50.

Jolly, C.J. (1972) The classification and natural history of *Theropithecus* (*Simopithecus*)(Andrews, 1916), baboons of the African Plio-Pleistocene. Bulletin of the British Museum (Natural History), Geology 22:1–123.

Jouffroy F (1991) La "Main Sans Talon" du Primate Bipede. In Y Coppens and B Senut (eds.): Origine(s) de la Bipedie Chez les Hominides. Paris: CNRS, pp. 21-35.

Jungers, W.L., (1984) Scaling of the hominoid locomotor skeleton with special reference to lesser apes. In: Preuschoft, H., Chivers, D.J., Brockelman, W.Y., Creel, N. (eds.), *The Lesser Apes: Evolutionary and Behavioural Biology.* Edinburgh University Press, Edinburgh, pp. 146e169.

Jungers W.L. (1988) Relative joint size and hominoid locomotor adaptations with implications for the evolution of hominid bipedalism. J Hum Evol 17:247–265.

Jungers, W.L., (1990) Problems and methods in reconstructing body size in fossil primates, in: Damuth, J., MacFadden, B.J., (eds.) *Body size in mammalian paleobiology: Estimation and biological implications.* Cambridge: Cambridge University Press, pp. 103-118.

Jungers W.L, et al. (1995) Shape, relative size and size adjustments in morphometrics. American Journal of Physical Anthropology 38:137–161.

Kay R.F. (1981) The nut-crackers—a theory of the adaptations of the Ramapithecinae. American Journal of Physical Anthropology, 55: 141–1151.

Kay RF, Ross CF, Williams BA. (1997) Anthropoid Origins. Science 275:797–804.

Kay, R.F., Williams, B.A., Ross, C.F., Takai, M., Shigehara, N., (2004) Anthropoid origins: a phylogenetic analysis. In: Ross, C.F., Kay, R.F. (Eds.), *Anthropoid Origins: New Visions*. Kluwer Academic/Plenum Publishers, New York, pp. 91e135.

Keith, A. (1915) The relationship of the gibbon to the primitive human stock. Br. Med. J. April 6th, pp. 788–790.

Kelley, J., Pilbeam, D. R. (1986) The dryopithecines: taxonomy, comparative anatomy and phylogeny of Miocene large hominids. In Swinder DR & Irwin J, (eds): Comparative Primate Biology. Vol. I: Systematics, Evolution and Anatomy. New York: Alan R. Liss, Inc. pp. 361–411.

Kelley, J. (1997) Paleobiological and phylogenetic significan ce of life history in Miocene hominoids. In Function, phylogeny and fossils: miocene hominoid evolution and adaptation (eds D. R. Begun, C. V. Ward & M. D. Rose), pp. 173–208. New York, NY: Plenum Press.

Kim, J. (1996) General inconsistency conditions for maximum parsimony: Effects of branch lengths and increasing numbers of taxa. Syst. Biol. 45:363-374.

Kim J. (1998) Large-scale phylogenies and measuring the performance of phylogenetic estimators. Syst. Biol.47:43-60.

Kivell, T.L., (2007) Ontogeny of the hominoid midcarpal joint and implications for the origin of human bipedalism. Ph.D. Dissertation, University of Toronto.

Kivell, T.L., Begun, D.R., (2009) New primate carpal bones from Rudabánya (late Miocene, Hungary): taxonomic and functional implications. J. Hum. Evol. 57, 697e709.

Kluge, A. G. (1989). A concern for evidence and a phylogenetic hypothesis of relationships among Epicrates (Boidae, Serpentes). Syst. Zool. 38, 7–25.

Kluge, A. G. (1998). Total evidence or taxonomic congruence: cladistics or consensus classification. Cladistics, 14, 151–158.

Kluge A.G. and Wolf A.J. (1993) Cladistics: what's in a word? Cladistics. 9:183–199.

Köhler, M., Moyà-Solà, S., Alba, D.M., (2001) Eurasian hominoid evolution in the light of recent *Dryopithecus* findings. In: de Bonis, L., Koufos, G.D. andrews, P. (Eds.), *Phylogeny of the Neogene Hominoid Primates of Eurasia.* Cambridge University Press, Cambridge, pp. 192e212.

Kunimatsu, Y. (1992) New finds of small anthropoid primate from Nachola, northern Kenya. African Study Monographs 14:237–249.

Kunimatsu, Y. (1997) New species of *Nyanzapithecus* from Nachola, northern Kenya. Anthropological Science 105:117–141.

Langdon, J. (1984) A comparative functional study of the Miocene hominoid foot remains. PhD Dissertation. Yale University.

Larson, S. G. (1988) Subscapularis function in gibbons and chimpanzees: implications for interpretation of humeral head torsion in hominoids. Am. J. phys. Anthropol. 76, 449–462.

Larson, S. G. (1998) Parallel evolution in the hominoid trunk and forelimb. Evol. Anthropol. 6, 87–99.

Larson, S.G., Stern, J.T., (2006) Maintenance of above-branch balance during primate arboreal quadrupedalism: coordinated use of forearm rotators and tail motion. Am. J. Phys. Anthropol. 129, 71e81.

Le Gros Clark W.E. (1934) *The Early Forerunners of Man. A Morphological Study of the Evolutionary Origin of the Primates.* London: Baillere, Tindall and Cox.

Le Gros Clark, W. E. (1959) *The Antecedents of Man*, Edinburgh University Press, Edinburgh.

Le Gros Clark W.E. and Leakey L.S.B.\. (1950) Diagnoses of East African Miocene Hominoidea. Quarterly J. Geo. Soc. London 105:260-263.

Le Gros Clark W.E., Leakey L.S.B. (1951) The Miocene Hominoidea of East Africa: Fossil Mammals of East Africa., pp. 1-117.

Leakey R.E.F., Leakey M.G. (1986) A new Miocene hominoid from Kenya. Nature 324:143–148.

Leakey R.E.F, Leakey M.G.,Walker A.C. (1988) Morphology of *Turkanapithecus kalakolensis* from Kenya. Am. J. Phys.Anthropol. 76:277–288.

Leakey MG, Leakey RE, Richtsmeier JT, Simons EL, Walker AC. (1991) Similarities in Aegyptopithecus and Afropithecus facial morphology. Folia Primatol 56:65–85.

Leakey M.G., Teaford M.F. and Ward C.V. (2003) Cercopithecidae from Lothagam. In: Leakey M.G. and Harris J.M. (eds.), Lothagam: *The Dawn of Humanity in Eastern Africa.* Columbia University Press, New York, pp. 201–248.

Lemelin P. (1999) Morphological correlates of substrate use in didelphid marsupials: implications for primate origins. J Zool Lond 247:165–175.

Lewis O.J. (1970) The development of the human wrist joint during the fetal period. Anat Rec 166:499-516.

Lewis, O. J. (1965) Evolutionary changes in the primate wrist and inferior radio-ulnar joint. Anat. Rec. 151, 275-286.

Lewis, O.J. (1969) The hominoid wrist joint. Am. J. Phys. Anthropol. 30, 251e267.

Lewis, O. J. (1971) Brachiation and the early evolution of the Hominoidea. Nature (London) 230, 577-578.

Lewis, O. J. (1972a) Osteological features characterizing the wrists of monkeys and apes, with a reconsideration of this region in *Dryopithecus* (*Proconsul*) *africanus*. Amer. J. Phys. Anthropol. 36, 45-58.

Lewis, O. J. (1972b) The evolution of the hallucial tarsometatarsal joint in the Anthropoidea. Amer. J. Phys. Anthronol. 37, 13-34.

Lewis O.J. (1974) The wrist articulations of the Anthropoidea. In FA Jenkins Jr (ed.): Primate Locomotion. New York: Academic, pp. 143-169.

Lewis, O. J. (1977) Joint remodelling and the evolution of the human hand. J. Anat. 123, 157–201.

Lewis O.J. (1989) Functional morphology of the evolving hand and foot. Clarendon Press, Oxford.

Lopardo L., Giribet G., Hormiga G. (2011) Morphology to the rescue: molecular data and the signal of morphological characters in combined phylogenetic analyses—a case study from mysmenid spiders (Araneae, Mysmenidae), with comments on the evolution of web architecture. Cladistics 27, 278–330.

Lycett, S.J., Collard, M., (2005) Do homoiologies impede phylogenetic analyses of the fossil hominids? An assessment based on extant papionin craniodental morphology. J. Hum. Evol. 49, 618e642.

MacLatchy, L., Bossert, W. H. (1996) An analysis of the articular surface distribution of the femoral head and acetabulum in anthropoids, with implications for hip function in Miocene hominoids. Journal of Human Evolution 31:425–453.

MacLatchy, L., Gebo, D., Kityo, R., Pilbeam, D., (2000) Postcranial functional morphology of *Morotopithecus bishopi*, with implications for the evolution of modern ape locomotion. J. Hum. Evol. 39, 159e183.

MacLatchy L. (2004) The oldest ape. Evol Anthropol 13:90–103.

Maddison, W.P., (1993) Missing data versus missing characters in phylogenetic analysis. Syst. Biol. 42, 576–581.

Magallón, S. (2010) Using fossils to break long branches in molecular dating: a comparison of relaxed clocks applied to the origin of angiosperms. Syst.Biol. 59, 384–399.

Martin, R. D. (1990) Primate Origins and Evolution: A Phylogenetic Reconstruction. Princeton University Press, Princeton.

Marzke M.W. (1997) Precision grips, hand morphology and tools. Am J Phys Anthropol 102:91–110.

Matsui A, Rakotondraparany F, Munechika I, Hasegawa M, Horai S (2009) Molecular phylogeny and evolution of prosimians based on complete sequences of mitochondrial DNAs. Gene 441: 53–66.

McCrossin, M. L. (1992) An oreopithecid proximal humerus from the middle Miocene of Maboko Island, Kenya. International Journal of Primatology 13:659–677.

McCrossin M.L., Benefit B.R. (1992) Comparative assessment of the ischial morphology of Victoriapithecus macinnesi. Am. J. Phys. Anthropol. 87t277-290.

McCrossin M.L., Benefit B.R. (1994) Maboko Island and the evolutionary history of Old World monkeys and apes; pp. 95–121 in R. S. Corruccini and R. L. Ciochon (eds.), Integrative Paths to the Past: Paleoanthropological Advances in Honor of F. Clark Howell. Prentice Hall, Englewood Cliffs, N.J.

McCrossin M.L., Benefit B.R., Gitau S.N., Palmer A.K., Blue K.T. (1998) Fossil evidence for the origins of terrestriality among Old World higher primates. In: Strasser EL, Fleagle JG, Rosenberger AL, McHenry HM, editors. Primate locomotion. New York: Plenum. p 353–396.

McCollum, M.S., Peppe, D.J., McNulty, K.P., Dunsworth, H.M., Harcourt-Smith, W.E.H., Andrews, A.L., (2013) Magnetostratigraphy of the early Miocene Hiwegi Formation (Rusinga Island, Lake Victoria, Kenya). Geological Society of America Abstracts with Programs 45, p. 12.

McHenry, H. M. & Corruccini, R. S. (1983) The wrist of *Proconsul* africanus and the origin of hominoid postcranial adaptations. In (R. L. Ciochon & R. S. Corruccini, Eds) New Interpretations of Ape and Human Ancestry, pp. 252-367. New York: Plenum.

McNulty K.P., Begun D.R., Kelley J., Manthi F.K., Mbua E.N. (2015) A systematic revision of *Proconsul* with the description of a new genus of early Miocene hominoid. Journal of Human Evolution 84:42-61

Mendel F.C. (1979) The wrist joint of two-toed sloths and its relevance to brachiating adaptations in the Hominoidea. J. Morphol. 162:413-424.

Mickevich, M.F. and M.F. Johnson. (1976) Congruence between morphological and allozyme data in evolutionary inference and character evolution. Syst. Zool., 260-270.

Miller, R.A., (1945) The ischial callosities of primates. Am. J. Anat. 76, 67-91.

Miller, J.A., Griswold, C., Yin, C., (2009) The symphytognathoid spiders of the Gaoligongshan, Yunnan, China (Araneae: Araneoidea): systematics and diversity of micro-orbweavers. ZooKeys 11, 9–195.

Morbeck, M.E. (1972) A re-examination of the forelimb of the Miocene Hominoidea. Ph.D. dissertation, University of California, Berkeley.

Morbeck M.E. (1975) Dryopithecus africanus forelimb. J. Hum. Evol. 4:39-46.

Morbeck M.E. (1977) Positional behavior, selective use of habitat substrate and associated non-positional behavior in free-ranging Colobusguereza (Ruppel, 1835) Primates 18:35-58.

Móya-Solá, S. & Kohler, M. (1993) Recent discoveries of *Dryopithecus* shed new light on evolution of great apes. Nature 365, 543–545.

Moya Sola S and Köhler M. (1995) New partial cranium of Dryopithecus Lartet, 1863 (Hominoidea, Primates) from the upper Miocene of Can Llobateres, Barcelona, Spain. Journal of Human Evolution 29:101–101.

Móya-Solá, S. & Kohler, M. (1996) A *Dryopithecus* skeleton and the origins of great-ape locomotion. Nature 379, 156–159.

Móya-Solá, S., Kohler, M. & Rook, L. (1999) Evidence of hominid-like precision grip capability in the hand of the Miocene ape *Oreopithecus*. Proc. Natl Acad. Sci. USA 96, 313–317.

Móya-Solá, S., Kohler, M., Alba, D. M., Casanovas-Vilar, I. & Galindo, J. (2004) *Pierolapithecus catalaunicus*, a new Middle Miocene great ape from Spain. Science 306, 1339–1344.

Moyà-Solà, S. et al. (2009) A unique Middle Miocene European hominoid and the origins of the great ape and human clade. Proc. Natl. Acad. Sci. 106:9601–9606.

Nakatsukasa, M., (2008) Comparative study of Moroto vertebral specimens. J. Hum. Evol. 55, 581e588.

Nakatsukasa M, et al. (2012) Hind limb of the *Nacholapithecus kerioi* holotype and implications for its positional behavior. Anthropol Sci 120(3):235–250.

Nakatsukasa, M., Y. Kunimatsu, Y. Nakano and H. Ishida. (2002) Functional morphology of Nacholapithecus pedal phalanges. Anthropological Science 110:107-107.

Nakatsukasa M, Kunimatsu Y, Nakano Y, Takano T, Ishida H. (2003) Comparative and functional anatomy of phalanges in Nacholapithecus kerioi, a Middle Miocene hominoid from northern Kenya. Primates 44:371–412.

Nakatsukasa M, Kunimatsu Y, Nakano Y, Ishida H. (2007) Vertebral morphology of Nacholapithecus kerioi based on KNM-BG 35250. J Hum Evol 52:347–369.

Nakatsukasa, M., Kunimatsu, Y., (2009) *Nacholapithecus* and its importance for understanding hominoid evolution. Evol. Anthropol. 18, 103e119.

Nakatsukasa M, Ward CV, Walker A, Teaford MF, Kunimatsu Y, Ogihara N. (2004) Tail loss in *Proconsul* heseloni. J Hum Evol 46:777–784.

Nakatsukasa M, Yamanaka A, Kunimatsu Y, Shimizu D, Ishida H. (1998) A newly discovered Kenyapithecus skeleton and its implications for the evolution of positional behavior in Miocene East African hominoids. J HumEvol 34:657–664.

Napier J.A., Davis P.R. (1959) The forelimb skeleton and associated remains of *Proconsul* africanus. Fossil Mammals of Africa 16:1-70.

Napier, J.R., (1961) Prehensility and opposability in the hands of primates. Symposia of the Zoological Society of London 5:115-32.

Napier, J.R., (1962) Fossil hand bones from Olduvai Gorge. Nature 196, 409e 411.

Napier J.R. (1964) The evolution of bipedal walking in the hominids. Arch. de Biol. (Liege) ~: Suppl. 673-708.

Napier, J.R., (1967) Evolutionary aspects of primate locomotion. Am. J. Phys. Anthropol. 27, 333–341.

Napier, J. (1993) Hands. Princeton, NJ: Princeton University Press. (Revised by Russell H. Tuttle)

Nixon, K.C., Davis, J.I., (1991) Polymorphic taxa, missing values and cladistic analysis. Cladistics 7, 233–241.

Nixon, K.C., Wheeler, Q.D., (1992) Extinction and the origin of species. in: Novacek, M.J., Wheeler, Q.D., (Eds.), Extinction and Phylogeny. Columbia University Press, New York, pp. 119–143.

Novacek, M.J., (1992) Fossils, topologies, missing data and the higher complete level phylogeny of eutherian mammals. Syst. Biol. 41, 58–73.

Nylander, A.A.; Ronquist, F; Huelsenbeck, JP; et al. (2004) Bayesian phylogenetic analysis of combined data. Syst. Bio. 53(1): 47-67.

Nylander A.A., Wilgenbusch J.C., Warren D.L., Swofford D.L. (2008) AWTY (are we there yet?): a system for graphical exploration of MCMC convergence in Bayesian phylogenetics. Bioinformatics. 24:581–583.

O'Connor, B.L.(1975) The functional morphology of the cercopithecoid wrist and inferior radioulnar joints and their bearing on some problems in the evolution of the Hominoidea Am. J. phys. Anthrop. 43: 113- 122.

O'Connor, B.L.(1976) Dryopithecus (*Proconsul*) africanus: quadruped or non-quadruped? J. hum. Evol. 5: 279-283.

O'Connor, B. L.; Rarey, K.E. (1979) Normal amplitudes of radioulnar pronation and supi nation in several genera of anthropoid primates. Am. J. phys. Anthrop. 5 1: 39-44.

Oxnard, C. E. (1967) The Functional morphology of the primate shoulder as revealed by compararive anatomical osteometric and discriminant function techniques. Am.}. phys. An/hrop. 26, 219-2W.

Oxnard, C. E. (1969) Evolution of the human shoulder- Some possible pathways. Am.}. ph)·s. Allthrop. :50, 319-331.

Page, R. D. M. 1996. On consensus, confidence, and "total evidence." Cladistics 12: 83–92.

Pagel, M. (1997) Inferring evolutionary processes from phylogenies. Zool. Scripta 26:331-348.

Pagel, M. D., (1999) Inferring the historical patterns of biological evolution. Nature 401:877-884.

Pagel, M. D. and P. H. Harvey. (1988) The taxon- level problem in the evolution of mammalian brain size: Facts and artifacts. Am. Nat. 132:344-359.

Pagel, M. D. and P. H. Harvey. (1989) Taxonomic differences in the scaling of brain on body weight among mammals. Science 244:1589-1593.

Pagel M, Meade A. (2011) BayesTraits v1. 0. School of Biological Sciences. Reading, U.K: University of Reading.

Paradis E., Claude J. & Strimmer K. (2004) APE: analyses of phylogenetics and evolution in R language. Bioinformatics 20: 289–290. doi:10.1093/bioinformatics/btg412.

Penny, D. and M. Hendy. (1985) Testing methods of evolutionary tree construction. Cladistics 1: 266-278.

Peppe, D.J., McNulty, K.P., Cote, S.M., Harcourt-Smith, W.E.H., Dunsworth, H.M., Van Couvering, J.A., (2009) Stratigraphic interpretation of the Kulu Formation (Early Miocene, Rusinga Island, Kenya) and its implications for primate evolution. J. Hum. Evol. 56, 447e461.

Perelman P, et al. (2011) A molecular phylogeny of living primates. PLOS Genet. 7, e1001342.

Pérez de los Ríos, M., Moyà-Solà, S., Alba, D.M., (2012) The nasal and paranasal architecture of the Middle Miocene ape *Pierolapithecus catalaunicus* (Primates: Hominidae): phylogenetic implications. J. Hum. Evol., 497e506.

Pickford, M., (1981) Preliminary Miocene mammalian biostratigraphy for western Kenya. J. Hum. Evol. 10, 73e97.

Pickford, M., (1982) The tectonics, volcanics and sediments of the Nyanza Rift Valley, Kenya. Zeitschrift der Geomorphologie, N. F. 42 : 1-33.

Pickford, M., Kunimatsu, Y., (2005) Catarrhines from the middle Miocene (ca. 14.5 Ma) of Kipsaraman, Tugen Hills, Kenya. Anthropol. Sci. 113, 189–224.

Pickford, M., S. Musalizi, B. Senut, D. Gommery, and E. Musiime, (2010) Small Apes from the Early Miocene of Napak, Uganda. Geo-Pal Uganda 3:1–111.

Pickford, M., Y. Sawada, R. Tayama, Y. Matsuda, T. Itaya, H. Hyodo, and B. Senut. (2006) Refinement of the age of the Middle Miocene Fort Ternan Beds, Western Kenya, and its implications for Old World biochronology. Comptes Rendus Geoscience 338:545–555.

Pickford, M., Senut, B., Gommery, D., Musiime, E., (2009) Distinctiveness of *Ugandapithecus* from *Proconsul*. Estudios Geol. 65, 183e241.

Pilbeam D.R. (1969) Tertiary Pongidae of East Africa: Evolutionary Relationships and Taxonomy. Bulletin Peabody Museum Nat. Hist. 31: 1-185.

Pilbeam, D. R. (1972) The Ascent of Man, pp. 49-61, Macmillan, New York.

Pilbeam D.R. (1996) Genetic and morphological records of the Hominoidea and hominid origins: A synthesis. Molecular Phylogenetics and Evolution 5:155–168.

Pilbeam, D., Rose, M.D., Barry, J.C., Shah, S.M.I., (1990) New *Sivapithecus* humeri from Pakistan and the relationship of *Sivapithecus* and *Pongo*. Nature 348, 237–238.

Pilgrim, G. E., (1915) New Siwalik primates and their bearing on the question of the evolution of man and the Anthropoidea. Records of the Geological Survey of India, 45 :1-74.

Platnick, N., Coddington, J., Forster, R., Griswold, C., (1991) Spinneret morphology and the phylogeny of haplogyne spiders (Araneae, Araneomorphae). Am. Mus. Novit. 3016, 1–73.

Pocock, R. I. (1925) External characters of the catarrhinr monkeys and apes. Proc. Zool. Soc. Lond. 1479-1.579.

Poe, S. (1998) Sensitivity of phylogeny estimation to taxonomic sampling. Syst. Biol 47:18-31.

Poe S. and Wiens J.J. (2000) Character selection and the methodology of morphological phylogenetics. In: J.J. Wiens (ed.) Phylogenetic Analysis of Morphological Data, pp. 20–36, Smithsonian Institution Press,Washington, D.C.

Poux C, Douzery EJ (2004) Primate phylogeny, evolutionary rate variations and divergence times: a contribution from the nuclear gene IRBP. American Journal of Physical Anthropology 124: 1–16.

Preuschoft H. (1973) Body posture and locomotion in some East African Miocene Dryopithecinae. In: Day M, (ed.) *Human evolution.* New York: Barnes and Noble. p 13–43.

Preuschoft, H. (1979) Motor behavior and shape of the locomotor apparatus. In M.E. Morbeck, H. Preuschoft and N. Gomberg, (eds.) *Environment, Behavior and Morphology: Dynamic Interactions in Primates.* Gustav Fischer, N.Y.

Prevosti, F.J. & Chemisquy, M.A. (2010) The impact of missing data on real morphological phylogenies: influence of the number and distribution of missing entries. Cladistics, 26, 326–339.

Pyron, R.A. (2011) Divergence-time estimation using fossils as terminal taxa and the origins of Lissamphibia. Syst.Biol. 60, 466–481.

Rae T.C. (1993) Early Miocene hominoid evolution: phylogenetic considerations. American Journal of Physical Anthropology suppl 16:161-161.

Rae T.C. (1997) The early evolution of the hominoid face. In DR Begun, CV Ward and MD Rose (eds.): Function, Phylogeny and Fossils: Miocene Hominoid Evolution and Adaptations. New York: Plenum Press, pp. 59-78.

Rae T.C. (1999) Mosaic Evolution in the Origin of the Hominoidea. Folia Primatologica 70:125–135.

Rae T.C., Koppe T., Spoor F., Benefit B., McCrossin M. (2002) Ancestral Loss of the Maxillary Sinus in Old World Monkeys and Independent Acquisition in Macaca. Am J Phys Anthropol 117:293-296.

Rae T.C., Koppe T. (2004) Holes in the head: Evolutionary interpretations of the paranasal sinuses in catarrhines. Evol. Anth.: 13:211-223.

Rafferty K.L., Walker A., Ruff C.B., Rose M.D., Andrews P.J. (1995) Postcranial estimates of body weight in *Proconsul*, with a note on a distal tibia of *P. major* from Napak, Uganda. Am J Phys Anthropol 97:391–402.

Rasmussen , D. T. , (2002) Early Catarrhines of the African Eocene and Oligocene . In W. C. Hartwig , (ed.) *The Primate Fossil Record.* Cambridge : Cambridge University Press .

Rasmussen D.T., Simons E.L. (1988) New specimens of *Oligopithecus sauagei*, early Oligocene primate from Egypt. Folia Primatol. 51 :182-208.

Rein T.R., Harrison T., Zollikofer C.P.E. (2011) Skeletal correlates of quadrupedalism and climbing in the anthropoid forelimb: implications for inferring locomotion in Miocene catarrhines. J Hum Evol 61: 564–574.

Reippel, O. (2009) ‘Total evidence’ in phylogenetic systematics. Biol. Philos. (2009) 24:607–622.

Reyment, R. A. (1991). *Multidimensional Paleobiology*. Oxford: Pergamon Press.

Richmond, B.G., (1998) Ontogeny and Biomechanics of Phalangeal Form in Primates. Ph.D. Dissertation, State University of New York at Stony Brook.

Richmond, B.G., (2006) Functional morphology of the midcarpal joint in knucklewalkers and terrestrial quadrupeds. In: Ishida, H., Tuttle, R., Pickford, M.,Ogihara, N., Nakatsukasa, M. (Eds.), Human Origins and Environmental Backgrounds. Springer, Chicago, pp. 105–122.

Richmond B.G., Strait D.S. (2000) Evidence that humans evolved from a knuckle-walking ancestor. Nature 404: 382-285.

Riesenfeld A. (1975) Volumetric determination of metatarsal robusticity in a few living primates and in the foot of Oreopithecus, Primates, 16, 9-15.

Robertson, M.L.(1984) The carpus of *Proconsul* africanus: functional analysis and comparison with selected nonhuman primates; PhD diss. University of Michigan.

Rögl, F. (1999) Circum-Mediterranean Miocene Paleogeography . In The Miocene Land Mammals of Europe . G. E. Rössner and K. Heissig K . , eds. pp. 39 – 48 . Munich : Verlag Dr. Friedrich Pfeil .

Rollinson, J., Martin, R.D. (1981) Comparative aspects of primate locomotion with special reference to arboreal cercopithecines. · Zool. Soc. Land.: 377-427.

Ronquist F, Klopfstein S, Vilhelmsen L, Schulmeister S, Murray DL, Rasnitsyn AP. (2012) A total-evidence approach to dating with fossils, applied to the early radiation of the Hymenoptera. Syst Biol. 61:973–99.

Rose, M. D. (1973) Quadrupedalism in primates. Primates 14, 337-357.

Rose, M.D., (1974) Ischial tubersosities and ischial callosities. Am. J. Phys. Anthropol. 40, 375-384.

Rose, M.D., (1975) Functional proportions of primate lumbar vertebral bodies. J. Hum. Evol. 4, 21-38.

Rose, M.D., (1983) Miocene hominoid postcranial morphology: monkey-like, ape-like, neither, or both? In: Ciochon, R.L., Corruccini, R.S. (Eds.), New Interpretations of Ape and Human Ancestry. Plenum Press, New York, pp. 405e417.

Rose, M. D. (1986). Further hominoid postcranial specimens from the Late Miocene Nagri Formation of Pakistan. J. hum. Evol. 15, 333-367.

Rose, M. D. (1987) New postcranial specimens of catarrhines from the middle Miocene Chin-ii Formation, Pakistan. J. hum. Euol.

Rose, M.D., (1988) Another look at the anthropoid elbow. J. Hum. Evol. 17, 193e224.

Rose, M. D. (1992). Kinematics of the trapezium-I st mecacarpaljoim in extant anthropoids and Miocene hominoids.]. hum. Evo!. 22, 255-266.

Rose, M. D. (1993) Locomotor anatomy of Miocene hominoids. In (D. Gebo, Ed.) Postcranial Adaptation in Nonhuman Primates, pp. 252-272. DeKalb: Northern Illinois University Press.

Rose, M.D., (1994) Quadrupedalism in some Miocene catarrhines. J. Hum. Evol. 26, 387e411.

Rose, M.D., (1996) Functional morphological similarities in the locomotor skeleton of Miocene catarrhines and platyrrhine monkeys. Folia Primatol. 66, 7e14.

Rose M.D. (1997) Functional and phylogenetic features of the forelimb in Miocene hominoids. In: Begun D.R., Ward C.V. and Rose M.D. (eds.), Function, Phylogeny and Fossils: Miocene Hominoid Evolution and Adaptations. Plenum Press, New York, pp. 79–100.

Rosenberg, M . S., Kumar, S. (2001) Incomplete taxon sampling is not a problem for phylogenetic inference. Proc. Natl. Acad. Sci. USA 98:10751-10756.

Rosenberg M. S., Kumar S. (2003) Taxon sampling, bioinformatics, and phylogenomics. Syst. Biol. 52:119-124.

Rosenberger, A. L., Delson, E. (1985) The dentition of *Oreopithecus bainbolii*: Systematic and paleobiological implications. American Journal of Physical Anthropology 66:222-23.

Ross , C. F., Williams, B., Kay, R.F. (1998) Phylogenetic Analysis of Anthropoid Relationships . Journal of Human Evolution 35 : 221 – 306 .

Rossie J.B, et al. (2002) Paranasal sinus anatomy of Aegyptopithecus: implications for hominoid origins. Proc. Natl. Acad. Sci. 99:8454-6.

Rossie, J.B., (2005) Anatomy of the nasal cavity and paranasal sinuses in Aegyptopithecus and early Miocene African catarrhines. Am. J. Phys. Anthropol. 126, 250e267.

Rossie, J.B., (2008) The phylogenetic significance of anthropoid paranasal sinuses. Anat. Rec. 291, 1485e1498.

Ruff, C.B., (2003) Long bone articular and diaphyseal structure in Old World monkeys and apes II: estimation of body mass. Am. J. Phys. Anthropol. 120, 16e37.

Ruff, C. B., Walker, A. & Teaford, M. K. (1989) Body mass, sexual dimorphism and femoral proportions of *Proconsul* from Rusinga and Mfangano Islands, Kenya. J. hum. Evol. 18, 515–536.

Russo, G.A. (2016) Comparative sacral morphology and the reconstructed tail lengths of five extinct primates: *Proconsul* heseloni, *Epipliopithecus vindobonensis*, *Archaeolemur edwardsi*, *Megaladapis grandidieri* and *Palaeopropithecus kelyus* J. Hum. Evol., 90, pp. 135–162.

Sanders, W.J., Bodenbender, B.E., (1994) Morphometric analysis of lumbar vertebra UMP 67–28: implications for spinal function and phylogeny of the Miocene Moroto hominoid. J. Hum. Evol. 26, 203–237.

Sarmiento, E.E., (1985) Functional differences in the skeleton of wild and captive orangutans and their adaptative significance. Ph.D. Dissertation, NewYork University.

Sarmiento, E.E., (1987) The phylogenetic position of Oreopithecus and its significance in the origin of the Hominoidea. Am. Mus. Novit. 2881, 1e44.

Sarmiento, E.E., (1988) Anatomy of the hominoid wrist joint: its evolutionary and functional implications. Int. J. Primatol. 9, 281–345.

Sarmiento, E.E., (1995) Cautious climbing and folivory: a model of hominoid differentiation. Hum. Evol. 10, 289–321.

Sarmiento, E.E., (2002) Forearm rotation and the “origin of the hominoid lifestyle”: a reply to Stern and Larson (2001) Am. J. Phys. Anthropol. 119, 92e94.

Schlosser M, von Zittel K.A.. (1923) Grundzuge der Palaontologie. 4 Aufl. Munchen and Berlin: Oldenbourg.

Schmitt, D., (2003) Mediolateral reaction forces and forelimb anatomy in quadrupedal primates: implications for interpreting locomotor behavior in fossil primates. J. Hum. Evol. 44, 47e58.

Schon, M.A., Ziemer, L.K., (1973) Wrist mechanism and locomotor behavior of Dryopithecus (*Proconsul*) africanus. Folia Primatol. 20, 1e11.

Schuind, F., Cooney, W.P., Linscheid, R.L., An, K.N., Chao, E.Y.S., (1995) Force and pressure transmission through the normal wrist: A theoretical two-dimensional study in the posteroanterior plane. J. Biomech. 28, 587e601.

Schultz, A.H. (1930) The skeleton of the trunk and limbs of higher primates. Hum. Biol. 2: 303-438.

Schultz, A.H., (1936) Characters common to higher primates and characters specific for man. Quart. Rev. Biol. 11, 259-283.

Schultz, A.H. (1938) The relative length of the regions of the spinal column in Old World primates. Am. I. Phys. Anthrop. 24: 1-22.

Schultz A.H. (1960) Einige Beobachtungen und Masse am Skelett von *Oreopithecus*. Z. Morphol. Anthropol. 50:136-149.

Schultz, A.H., (1961) Vertebral column and thorax. Primatologia 4, 1-66.

Schultz, A.H. (1969) The skeleton of the chimpanzee. In The Chimpanzee. Edited by G. H. Bourne. 50-103. Basel: Karger.

Schultz, A., Straus Jr.,W., (1945) The numbers of vertebrae in primates. Proc. Am. Phil.Soc. 89 (4), 601e626.

Schwalbe, G (1915) Uber den fossilen Affen *Oreopithecus bambolii*. Z. Morphol. Anthropol. 19:149-254.

Scotland, R.W., Olmstead, R.G. and Bennett, J.R. (2003) Phylogeny Reconstruction: The Role of Morphology. Syst. Bio. 52(4):539-548.

Seiffert E.R, Kappelman J. (2001) Morphometric variation in the hominoid orbital aperture: A case study with implications for the use of variable characters in Miocene catarrhine systematics. J Hum Evol 40:301- 318.

Seiffert E.R. (2006) Revised age estimates for the later Paleogene mammal faunas of Egypt and Oman. Proceedings National Academy of Sciences USA 103(13):5000-5005.

Seiffert, E. (2007) A new estimate of afrotherian phylogeny based on simultaneous analysis of genomic, morphological and fossil evidence. BMC Evol. Biol. 7: 13.

Seiffert E.R., Simons E.L., Fleagle J.G. and Godinot M. (2010) Paleogene Anthropoids. In: Werdelin L. and Sanders W.J., (eds.) *Cenozoic Mammals of Africa.* Berkeley, California: University of California Press.

Senut, B. (1986). New data on Miocene hominoid humeri from Pakistan and Kenya. In U. G. Else & P. E. Lee, (eds.) *Primate Evolution*. Cambridge: Cambridge University Press.

Senut, B., (1989) Le coude des primates hominoïdes, anatomie, fonction, taxonomie, evolution. Cahiers de Paleoanthropologie. CNRS, Paris.

Senut B, Pickford M, Gommery D, Kunimatsu Y. (2000) Un nouveau genre d'hominoide du Miocene inferieur d'Afrique orientale: *Ugandapithecus major* (Le Gros Clark and Leakey, 1950). Comptes Rendus de l'Academie des Sciences Paris 331:227- 233.

Shaffer, H., Meylan, P. and McKnight, M. (1997). Tests of turtle phylogeny: Molecular, morphological and paleontological ap- stracts 17, 80A.

Shapiro, L., (1993) Evaluation of “unique” aspects of human vertebral bodies and pedicles with a consideration of Australopithecus africanus. J. Hum. Evol. 25, 433e470.

Shea BT. (1983) Allometry and heterochrony in the African apes. Am J Phys Anthropol 62:275-289.

Shea BT. (1984) An Allometric Perspective on the Morphological and Evolutionary Relationships between Pygmy (Pan paniscus) and Common (Pan troglodytes) Chimpanzees. In: Susman RL, (ed.) *The Pygmy Chimpanzee: Evolutionary Biology and Behavior.* New York: Plenum Press.

Shea B.T. (1985) On aspects of skull form in African apes and orangutans, with implications for Hominoid evolution. Am J Phys Anthropol 68:329-342.

Shea B.T. (1986) Scapular form and locomotion in chimpanzee evolution. American Journal of Physical Anthropology. 70:475-488.

Simon, C. M. (1983). A new coding procedure for morphometric data with an example from period- ical cicada wing veins. In J. Felsenstein (ed.), *Numerical taxonomy.* Proceedings of the NATO Advanced Study Institute. NATO Adv. Study Institute Ser. G (Ecological Sciences), No. 1. Springer-Verlag, New York.

Simons, E. L. (1962). Fossil evidence relating to the early evolution of primate behavior. Ann. New York Acad. Sci. 102:282-295.

Simons E. L. (1967) The earliest apes. Sci.Am. 217:28–35.

Simons, E. L. (1972) Primate Evolution:An Introduction to Man's Place in Nature. New York: Macmillan.

Simons E. L. (1992) Diversity in the early tertiary anthropoidean radiation in Africa. Proceedings National Academy of Sciences USA 89(22):10743-10747.

Simons E. L and Bown TM. (1984) A new species of Paratherium (Didelphidae: Poliprotodonta): the first African marsupial. Journal of Mammalogy 65:539-548.

Simons E. L and Bown TM. (1985). Afrotarsius chatrathi, first tarsiiform primate (?Tarsiidae) from Africa. Nature 313(6002):475-477.

Simons E. L, Bown TM, Rasmussen DT (1987). Discovery of two additional prosimian primate families (Omomyidae, Lorisidae) in the African Oligocene. Journal of Human Evolution 15: 431–437.

Simons, E. L and. G. Fleagle. (1973) The history of extinct gibbon-like primates. Gibbon and Siamang 2:121-48.

Simons, E. L. & Pilbeam, D. R. (1965) Preliminary revision of the *Dryopithecinae* (Pongidae, Anthropoidea) Folia Primatol. 3:81-152.

Simons , E. L. and D. T. Rasmussen , (1996) Skull of *Catopithecus browni* , an Early Tertiary Catarrhine . American Journal of Physical Anthropology 100 : 261 – 292 .

Simons E. L, Seiffert ER, Chatrath PS and Attia Y. (2001). Earliest record of a parapithecid anthropoid from the Jebel Qatrani formation, Northern Egypt. Folia Primatol (Basel) 72(6):316-331.

Simons, E. L., E. R. Seiffert, T. M. Ryan, and Y. Attia, (2007) A Remarkable Female Cranium of the Early Oligocene Anthropoid *Aegyptopithecus zeuxis* (Catarrhini, Propliopithecidae). Proceedings of the National Academy of Sciences of the USA 104:8731–8736.

Singleton M. (2000) The phylogenetic affinities of *Otavipithecus namibiensis*. J Hum Evol 38:537-573.

Sokal RR, Rohlf J.F. (2012). *Biometry*. 4th Ed. New York: W.H. Freeman and Co.

Springer, M., Teeling, E., Madsen, O., Stanhope, M., deJong, W.W., (2001). Integrated fossil and molecular data reconstruct bat echolocation. Proc. Natl. Acad. Sci. U.S.A. 98, 6241e6246.

Stern, JR and Jungers, WL (1985) Body size and proportions of the locomotor skeleton in *Oreopitheeus bambolii*. Am. J. Phys. Anthropol. 66:233.

Stevens N, Seiffert E, O'Connor P, Roberts E, Schmitz M, Krause C, Gorscak E, Ngasala S, Hieronymus T and Temu J. (2013). Palaeontological revidence for an Oligocene divergence between Old World monkeys and apes. Nature 497:611-614.

Strasser, E. (1988). Pedal evidence for the origin and diversification of cercopithecid clades. In The Primate Postcranium: Studies in Adaptation and Evolution. Edited by E. Strasser and M. Dagosto. 225-245. New York: Academic Press.

Strasser, E. and E. Delsou. (1987). Cladistic analysis of cercopithecid relationships. JournalofHuman Evolution 16:81-99.

Straus, W. L. (1963). The classification of Oreopithecus. In S. L. Washburn.(ed.), *Classification and Human Evolution.* New York: Viking Press.

Susman R.L. (1985). Functional morphology of the Oreopithecus hand. Am J Phys Anthropol S66:235.

Susman R.L. (2005). *Oreopithecus*: still apelike after all these years. J Hum Evol 49:405-411.

Szalay F.S. (1970) *Amphipithecus* and the origin of catarrhine primates. Nature 227:355-357.

Szalay F and Delson E. (1979) Evolutionary History of the Primates. New York: Academic Press.

Szalay. F. S. and Langdon, J. H. (1985). Evolutionary morphology of1he foot in *Oreopithecus*. Am. J. Phys. Anthropol. 66:237.

Teaford M.F., Beard K.C., Leakey R.E.F. and Walker A.C. (1988) New hominoid facial skeleton from the early Miocene of Rusinga Island, Kenya and it's bearing on the relationship between *Proconsul* nyanzae and *Proconsul* africanus. Journal of Human Evolution 17(5):461–477.

Temerin LA and Cant JGH (1983) The evolutionary divergence of Old World monkeys and apes. Am. Nat. 122:335-351.

Thiele, K. (1993). The holy grail of the perfect character: the cladistic treatment of morphometric data. Cladistics 9, 275–304.

Tuttle, R.H., (1967) Knuckle-walking and the evolution of hominoid hands. Am. J. Phys. Anthropol. 26, 171e206.

Tuttle R.H., (1977) Naturalistic Positional Behaviour of Apes and Models of Hominid Evolution, 1929-1976. In G Bourne (ed.): *Progress in APE Research.* New York: Academic Press, pp. 277-296.

Tuttle RH and Basmajian JV. (1974). Electromyography of brachial muscles in Pan gorilla and hominoid evolution. American Journal of Physical Anthropology. 41:71-90.

Van der Made J (1999) The Miocene Land Mammals of Europe, In eds Rossner GE, Heissig K (Friedrich Pfeil Verlag, Mu¨ nchen), pp 457–472.

Vogel C (1966) Morphologische studien am gesichtschadel Catarrhiner primaten. Biblio. Primatol. 4tl- 226.

Vogel C (1968) The phylogenetical evaluation of some characters and some morphological trends in the evolution of the skull in catarrhine primates. In B Chiarelli (ed.): *Taxonomy and Phylogeny of Old World Primates with Reference to the Origin of Man.* Turin: Rosenberg and Sellier, pp. 21-55.

Von Koenigswald, G. H. R. (1968) The phylogenetical position of the Hylobatinae. In Taxonomy and phylogeny of Old World Primates with special reference to the origin of Man. Rosenburg and Sellier, Torino. pp. 271- 276.

Von Koenigswald, G. H. R. (1969) Miocene Cercopithecoidea and Oreopithecoidea from the Miocene of East Africa. Fossil Vertebrates of Africa 1: 39-51.

Walker A. (1997) *Proconsul* Function and Phylogeny. In DR Begun, CV Ward and MD Rose (eds): Function, *Phylogeny and Fossils: Miocene Hominoid Evolution and Adaptations.* Plenum Press. p 209–224.

Walker, A., Pickford, M., (1983) New postcranial fossils of *Proconsul* africanus and *Proconsul* nyanzae. In: Ciochon, R.L., Corruccini, R.S. (eds.), *New Interpretations of Ape and Human Ancestry.* Plenum Press, New York, pp. 325e351.

Walker A and Rose MD (1968) Fossil hominoid vertebra from the Miocene of Uganda. Nature 217: 980–981

Walker A. and Teaford, M. (1989) The hunt for *Proconsul*. Scientific American. 260: 76-82.

Walker, A., Teaford, M. F.. Martin, L and Andrews, P. (1993) A new species *Proconsul* from the early Miocene of Rusinga/Mfangano Islands, Kenya. I Hum. Evol. 25:43-56.

Ward, C.V., (1992) Hip joints of *Proconsul* nyanzae and P. africanus. Am. J. phys. Anthrop. (Suppl. 14), 171.

Ward, C.V., (1993) Torso morphology and locomotion in *Proconsul* nyanzae. Am. J. phys. Anthrop. 92, 291e328.

Ward, C.V., (1997) Hominoid trunk and hindlimb evolution. In: Begun, D., Ward, C.V., Rose, M.D. (eds.), *Function, phylogeny and fossils: Miocene hominoids and great ape and human origins.* Plenum Press, New York, pp. 101e130.

Ward CV (1998) *Afropithecus*, *Proconsul* and the primitive hominoid postcranium. In: Strasser E, Fleagle J, Rosenberger AL, McHenry HM (eds) *Primate locomotion: recent advances.* Plenum Press, New York, pp 337–352

Ward, C.V., (2007). Postcranial and locomotor adaptations of hominoids. Handbook of Paleoanthropology 2, 1011e1030.

Ward, S. and D. L. Duren (2002) Middle and late Miocene African hominoids. In W. C. Hartwig (ed.), *The Primate Fossil Record.* Cambridge University Press, Cambridge.

Ward, S. C. and D. R. Pilbeam (1983) Maxillofacial morphology of Miocene hominoids from Africa and Indo-Pakistan. In R. L. Ciochon and R. S. Corruccini, (eds.). *New Interpretations of Ape and Human Ancestry*. Plenum Press, New York.

Ward, C.V., Walker, A., Teaford, M.F., (1991) *Proconsul* did not have a tail. J. Hum. Evol. 21, 215e220.

Ward, C.V., Walker, A., Teaford, M.F., (1999) Still no evidence for a tail in *Proconsul* heseloni. Am. J. Phys. Anthropol. Suppl. 28, 273.

Warren, D., Geneva, A., Lanfear, R., (2016) rwty: R We There Yet? Visualizing MCMC Convergence in Phylogenetics. https://CRAN.R-project.org/package=rwty

Washburn, S. L. (1957). Ischial callosities as sleeping adaptations. Am. I. Phys. Anthrop. 15 : 269-276.

Washburn, S. L. and Moore, R. (1974). Ape into Man: A Study of Human Evolution. Boston: Little Brown and Company.

Wheeler, W.C., (1992). Extinction, sampling and molecular phylogenetics. In: Novacek, M.J., Wheeler, Q.D. (Eds.), Extinction and Phylogeny. Columbia University Press, New York, pp. 205e215.

Wheeler, W.C., Pickett, K.M., (2008). Topology-Bayes versus Clade–Bayes in phylogenetic analysis. Mol. Biol. Evol. 25, 447–453.

Wickham, H (2009) ggplot2: Elegant Graphics for Data Analysis. Springer-Verlag New York.

Wiens J.J. (1998). Does adding characters with missing data increase or decrease phylogenetic accuracy? Syst. Biol. 47:625–640.

Wiens, J. J. (2001). Character analysis in morphological phylogenetics: Problems and solutions. Syst. Biol. 50:688-699.

Wiens, J. J. (2003a). Incomplete taxa, incomplete characters and phylogenetic accuracy: What is the missing data problem? J. Vert. Paleontol. 23:297-310.

Wiens J.J. (2003b). Missing data, incomplete taxa and phylogenetic accuracy. Syst. Biol. 52:528–538.

Wiens J.J. (2005). Can incomplete taxa rescue phylogenetic analyses from long-branch attraction? Syst. Biol. 54:731–742.

Wiens J.J., Brandley M.C., Reeder T.W. (2006). Why does a trait evolve multiple times within a clade? Repeated evolution of snake-like body form in squamate reptiles. Evolution. 60:123–141.

Wiens J.J., Kuczynski C.A., Townsend T., Reeder T.W., Mulcahy D.G., et al. (2010) Combining phylogenomics and fossils in higher-level squamate reptile phylogeny: molecular data change the placement of fossil taxa. Syst Biol 59: 674–688.

Wiens J.J., Moen D.S. (2008) Missing data and the accuracy of Bayesian phylogenetics. J. Syst. Evol. 46:307–314.

Wiens J.J., Tiu J (2012) Highly Incomplete Taxa Can Rescue Phylogenetic Analyses from the Negative Impacts of Limited Taxon Sampling. PLoS ONE 7(8): e42925.

Wilkinson, M. and M. J. Benton. (1995). Missing data and rhynchosaur phylogeny. Hist. Biol. 10:137–150.

Williams, S.A., Russo, G.A., (2015). Evolution of the hominoid vertebral column: The long and the short of it. Evolutionary Anthropology: Issues, News and Reviews 24, 15e32.

Wilson D.R. (1970) A functional anatomy of the tail, ischial callosities and pelvocaudal musculature in Macaca. Ph.D. Thesis, University of Chicago.

Wilson D.R. (1972) Tail reduction in Macaca. In: Tuttle R, (ed.). *The functional and evolutionary biology of primates.* New York: Aldine. p 241–261.

Wood H.M., Matzke N.J., Gillespie R.G., Griswold C.E. (2013). Treating fossils as terminal taxa in divergence time estimation reveals ancient vicariance patterns in the palpimanoid spiders. Syst. Biol. 62:264–284.

Wood-Jones F. (1929) Man's place among the mammals. New York: Longman's Green and Co.

Worthington, S., (2012). New Approaches to Late Miocene Hominoid Systematics: Ranking Morphological Characters by Phylogenetic Signal. Ph.D. Dissertation, New York University.

Youlatos, D., (1996) Atelines, apes and wrist joints. Folia Primatol. 67, 193e198.

Youlatos D. (2003) Calcaneal features of the Greek Miocene primate Mesopithecus pentelicus (Cercopithecoidea: Colobinae) Geobios 36:229-239.

Youlatos D, Meldrum J. (2011). Locomotor diversification in New World monkeys: running, climbing, or clawing along evolutionary branches. Anat Rec 294: 1991–2012.

Young N.M. and MacLatchy L. (2004) The phylogenetic position of Morotopithecus. Journal of human evolution 46:163-84.

Young N.M. (2003) A reassessment of living hominoid postcranial variability: implications for ape evolution. Journal of Human Evolution 45:441–464.

Young N.M. (2008) A comparison of the ontogeny of shape variation in the anthropoid scapula: functional and phylogenetic signal. American Journal of Physical Anthropology 136(3):247–264.

Zalmout I. S., et al. (2010) New Oligocene primate from Saudi Arabia and the divergence of apes and Old World monkeys. Nature 466:360-4.

Zapfe H. (1958) The skeleton of Pliopithecus (Epipliopithecus) vindobonensis Zapfe and Hürzeler. American Journal of Physical Anthropology 16:441–455.

Zapfe H. (1960) Die Primatenfunde aus der miozänen Spaltenfüllung von Neudorf an derMarch (Dˇevínská Nová Ves), Tschechoslowakei. Mit Anhang: Der Primatenfund aus demMiozän von Klein Hadersdorf in Niederösterreich. Schweizerische Palaeontologische Abhandlungen 78:1–293.

Zapfe, H., Hürzeler, J., (1957). Die Fauna der mioz€anen Spaltenfüllung von Neudorf ad March (C SR). Sitz-Ber Osterr Akad Wiss math-nat Kl 166, 113e123.

Zhang C, Stadler T, Klopfstein S, Heath TA, Ronquist F. (2015) Total-evidence dating under the fossilized birth–death process. Syst. Biol. 65, 228–249.

Zykstra, M., (1999) Functional morphology of the hominoid forelimb: implications for knuckle-walking and origin of hominid bipedalism. Ph.D. Dissertation, University of Toronto.